






Universitat Autònoma de Barcelona

ADVERTIMENT. L'accés als continguts d'aquesta tesi queda condicionat a l'acceptació de les condicions d'ús establertes per la següent llicència Creative Commons:  http://cat.creativecommons.org/?page_id=184

ADVERTENCIA. El acceso a los contenidos de esta tesis queda condicionado a la aceptación de las condiciones de uso establecidas por la siguiente licencia Creative Commons:  <http://es.creativecommons.org/blog/licencias/>

WARNING. The access to the contents of this doctoral thesis it is limited to the acceptance of the use conditions set by the following Creative Commons license:  <https://creativecommons.org/licenses/?lang=en>

Departament de Biologia Cel·lular, Fisiologia i d'Immunologia Facultat de Medicina
Universitat Autònoma de Barcelona

Doctoral thesis 2021

Systems Biology for the identification of epigenetic biomarkers and host factors associated with HIV-1 control

Bruna Oriol Tordera

Institut de Recerca de la Sida (IrsiCaixa), Hospital Germans Trias i Pujol i Institut d'Investigació en Ciències de la Salut Germans Trias i Pujol (IGTP)

Memòria de la tesi doctoral presentada per obtenir el grau de Doctora en Immunologia Avançada per la Universitat Autònoma de Barcelona, 2021

Directors de tesi:

Dr. Christian Brander i Dra. Marta Ruiz-Riol

UAB
Universitat Autònoma de Barcelona

IrsiCaixa
Institut de Recerca de la Sida

IGTP
Germans Trias i Pujol Research Institute


Germans Trias i Pujol
Hospital
Institut Català de la Salut

Cover Illustration by Óscar Blanch

The content of this thesis was partially funded by a grant from the Ministerio de Ciencia e Innovación (SAF2017_89726_R), the European Union Horizon 2020 Framework Programme for Research and Innovation under Grant N°681137-EAVI2020 and N° 847943-MISTRAL, and the National Institutes of Health, National Institute of Allergy and Infectious Diseases Program Grant P01-AI131568.

The printing of this thesis was made possible with the financial aid of the Universitat Autònoma de Barcelona.

Certificate of direction

IrsiCaixa

Institut de Recerca de la Sida

El Dr. Christian Brander (Director i Tutor) i la Dra. Marta Ruiz-Riol (Directora), investigadors de l'Institut de Recerca de la Sida (IrsiCaixa), de l'Hospital Germans Trias i Pujol,

Fan constar:

Que el treball experimental, les anàlisis de dades i la redacció de la memòria de la Tesi doctoral titulada "Systems Biology in the identification of epigenetically regulated host factors associated with HIV-1 control" ha estat realitzada per na Bruna Oriol Tordera sota llur direcció i tutoria i consideren que és apta per ser presentada per optar al grau de Doctora en Immunologia per la Universitat Autònoma de Barcelona.

I per tal que quedi constància, signen aquest document a Badalona, a 19 d'octubre del 2021

Dr. Christian Brander

Dra. Marta Ruiz-Riol

Als meus pares,

Acknowledgments

M'agrada pensar que els mèrits individuals son de fet, mèrits col·lectius. Així que, aquesta tesis també és vostra G R À C I E S.

Vull començar agraint als incondicionals. Gràcies a la meva mare i al meu pare per ser-hi sempre des de la distància justa, la que em permet ser jo mateixa i fer la meva, però aparèixer quan més ho necessito. Gràcies per alimentar-me amb la vostra filosofia de vida i per riure-us de mi (i amb mi) tantes vegades.

Gràcies als meus germans, Narcís i Aniol, els "solets" de la meva vida. Gràcies per brillar tant, per totes les estones compartides tan a casa com el pis de BCN, i per les petites baralles del dia a dia, que també donen vida ;)

Gràcies Albert, per tot, per estar tan a punt per celebrar els meus petits èxits com per tancar-te a casa mirant una peli (amb auriculars) mentre jo escrivia aquesta tesis o acabava qualsevol anàlisi o presentació. Gràcies pels silencis còmplices, per les abraçades, pels viatges a París i pels xuixos de crema que m'has comprat d'urgència per pujar l'ànim.

Moving now to my scientific "family", thank you Christian for giving me the opportunity to go ahead with this thesis and to grow both professionally and personally. I'd had never imagined to attend so many conferences with the occasion to present our results as well as visiting great places. I also want to thank you for all your efforts to make sure everything is up and running and for the leisure time like the fondues at your place.

Muchísimas gracias Marta por la confianza y el apoyo, pero sobretodo, gracias por tu forma de dirigir tan humana, por tu esfuerzo continuo para hacerlo cada vez mejor, enseñándome y motivándome a ser una buena científica, pero también cuidándome en lo personal: " Lo importante es que tu estés bien".

Acknowledgements

També vull donar les gràcies a l'Alex, la meua història a IrsCaixa i al grup de immunitat cel·lular i genètica de l'hoste comença amb el TFM que ell em va dirigir, així que gràcies per obrir-me les portes, però també per totes les sessions de "coaching" abans i durant la tesi.

Gràcies Miriam per ser la meua "germana gran" científica, per ser-hi sempre, pels nostres cafès de divendres a la tarda quan ja gairebé no quedava ningú i omplíem el tanc de nitrogen, pels cursos de EAVI a Suècia, París i BCN, o per la setmana a San Francisco ;).

Gràcies Clara, m'emporto molts records però sobretot de fer el préssec per Davos.

Luis muchas gracias por tu ímpetu, por tus ganas de llegar a todo y por todos los momentos compartidos.

Muchas gracias Anuska por formar parte de mi red de soporte durante estos años y espero que muchos más, por estar siempre dispuesta a ayudar y escuchar a cualquier nivel, eres una fuente inagotable de auto-motivación e inspiración.

Gracias Samandhy por tu soporte, por todas las charlas,comidas, cafés, etc. por compartir tu forma de ver la vida.

Gràcies Bea per treure temps de sota les pedres per mirar-te qualsevol abstract, presentació o article i fer-nos unes aportacions fantàstiques. També moltes gràcies per donar un cop de mà quan fa falta en qualsevol cosa, també a nivell personal.

Gracias Sandra por tu apoyo, por las charlas, y por los libros que me has dejado o recomendado.

Merci Tuixent per estar sempre a punt per ajudar els altres, per compartir les alegries, per la força que desprens i per regalar-nos un somriure cada dia malgrat no tinguis temps de sortir ni de p3 (o p2)!

Gràcies Cris per la teva visió positiva de la vida, pels teus consells i per la teva confiança: "segur que ho faràs molt bé".

Gràcies al Ventura per dirigir IrsiCaixa amb tant d'entusiasme i fer que tots ens en sentim part.

Gràcies a totes les persones que feu que IrsiCaixa sigui un lloc ple de vida i que treballau perquè tot plegat tingui sentit. Moltes gràcies a totes i tots pel dia a dia, pel suport rebut i la confiança, per les estones compartides, les reunions de resultats, els journal clubs, les calçotades i les festes de nadal. Esperem poder-ho recuperar ben aviat.

Vull donar també gràcies a la Julia per donar-nos suport i motivar-nos en la organització d'un PhD Day a Can Ruti. Gràcies a l'Ana Jordan també que a través d'aquesta "moguda" vam establir una bona amistat. Gràcies també a en Julià per portar-me amunt i avall, sobretot quan no tenia cotxe. Gràcies també a la Mariona pels viatges compartits. Vull agrair també als estudiants de doctorat d'IrsiCaixa, per les trobades després de treballar i per la xarxa de suport creada, sobretot amb els que vam començar al mateix any i que mica en mica anem tancant/obrint etapes noves. I evidentment, gràcies Óscar per aquesta bonica portada.

I appreciate the help and the collaboration of the co-authors of the articles included in this thesis. I also want to thank the different researchers and PhD students I have met in EAVI2020 or RETIRE-HIV meetings. Special thanks to Behazine Combadière who hosted me in her laboratory in Paris and showed me a different way of thinking, and with whom I enjoyed lively scientific discussions. Thank you as well to all the researchers in Behazine's laboratory. I also want to thank Dennis the scientific discussions about the present thesis and his help.

Agrair també a l'Alex Sánchez i la Malu Calle pel seu mentoratge en el mon de l'estadística, així com també a la Lupe Gómez i els membres del GRBIO per haver-me acollit tan bé a les seves reunions.

Acknowledgements

Tornant al meu cercle familiar i d'amistats, gràcies als meus avis, i a tots els familiars que avui s'alegren de que presenti aquesta tesis. Gràcies també a l'Anna, en Raül, en Pau, en Joan i la Maria.

Gràcies a...

l'Anna que mai falla i amb qui ens uneix per sempre l'essència de la Lydia

A la Clàudia, l'amiga de sempre

A la Laia, per assaborir tots els gustos de la vida

A la Duna, per sentir-la sempre a prop tot i la distància

A la Sílvia, per trobar-nos a Seva, Barcelona o Amsterdam.

A Erika, per ser mi primera mentora científica

Als amics del "comitè gastronòmic", a la colla de Seva, a les persones amb qui vaig coincidir a Paris i amb qui vaig compartir molts divendres de pizza, i a tothom qui m'ha donat suport.

Per acabar, vull donar les gràcies a les amigues de la uni, les que son per sempre i que aporten el seu granet de sorra sempre que poden. Gràcies a totes i cada una de vosaltres, per tots els moments i per seguir celebrant la vida.

En essència, la CIÈNCIA és VIDA.

GRÀCIES, GRACIAS, THANK YOU, MERCI.

Abbreviations

ADCC	Antibody-dependent cell mediated toxicity
ADCP	Antibody-dependent phagocytosis
AIDS	Acquired Immunodeficiency Syndrome
APC	Antigen presenting cell
ART	Antiretroviral treatment
ATI	Analytical treatment interruption
bNAbs	Broadly neutralizing antibodies
CA-RNA	Cell-associated RNA
cART	Combined antiretroviral treatment
CCR2	C-C Motif Chemokine Receptor 2
CCR5	C-C Motif Chemokine Receptor 5
CEF	CMV, EBV, and influenza virus
cGAS	Cyclic GMP-AMP Synthase
CMV	Cytomegalovirus
CNS	Central nervous system
cRNA	Complementary RNA
CTL	Cytotoxic T lymphocyte
CXCR4	C-X-C Motif Chemokine Receptor 4
DcR3	Decoy receptor 3
DCs	Dendritic cells
DEGs	Differentially expressed genes
DMPs	Differentially methylated positions
DNA	Deoxyribonucleic acid
DNMT	DNA Methyltransferases
dNTPs	Deoxynucleotide triphosphatases
DR3	Death receptor 3
dsRNA	Double-stranded RNA viruses
EBV	Epstein-Barr virus
EC	Elite controller
ELISA	Enzyme-Linked ImmunoSorbent Assay
ELISpot	Enzyme-linked Immunosorbent Spot
Fab	Antigen binding domain
Fc	Fragment crystallizable region
FDA	Food and Drug Administration
FDR	False Discovery Rate
GO	Gene Ontology
GSEA	Gene Set Enrichment Analysis
GWAS	Genome-wide association studies
HDACi	Histone deacetylase inhibitors
HDACs	Histone deacetylases
HIV	Human Immunodeficiency virus type
HIV-1	Human Immunodeficiency virus type 1
HLA	Human leukocyte antigen
HMTs	Histone methyl transferases

Abbreviations

HTI	HIVACAT T-cell immunogen
IC	Immune-concordant
ID	Immune-discordant
IFI16	Interferon inducible protein 16
IFN	Interferon
Ig	Immunoglobulin
IgG	Immunoglobulin G
IgM	Immunoglobulin M
IRF	Interferon regulatory factors
ISGs	Interferon stimulated genes
KEGG	Kyoto Encyclopedia of Genes and Genomes
KIR	Immunoglobulin-like receptors
LRA	Latency reversing agent
LTNP	Long-term nonprogressor
LTR	Long terminal repeats
MAP	Monitored antiretroviral pause
MAVS	Mitochondrial Antiviral Signaling Protein
MBD	Methyl-CpG-binding domain
MDA-5	Melanoma differentiation-associated gene 5
MHC	Major histocompatibility complex
mRNA	Messenger RNA
MSP	Methylation specific PCR
MVA	Modified Vaccinia Ankara
Nabs	Neutralizing antibodies
Nef	Negative Regulatory Factor
NES	Normalized enrichment score
NF-kB	Nuclear factor kappa-light-chain-enhancer of activated B cells
NGS	Next generation sequencing
NK	Natural Killer
NMR	Nuclear magnetic resonance
OLP	Overlapping peptide
PAMPs	Pathogen associated molecular patterns
PBMCs	Peripheral blood mononuclear cells
PCA	Principal component analysis
PCR	Polymerase chain reaction
PEA	Proximity extension assay
PEP	Post-exposure prophylaxis
PLS-DA	Partial least square discriminant analysis
PLWH	People living with HIV
PrEP	Pre-exposure prophylaxis
PRRs	Pathogen-recognition receptors
PTCs	Post-treatment controllers
pVL	Plasma viral load
qRT-PCR	Quantitative real-time PCR
RIG-I	Retinoic acid-inducible gene I

RMD	Romidepsin
RNA	Ribonucleic acid
RNA Pol II	RNA Polymerase II
rRNA	Ribosomal RNA
RT	Retro transcriptase
SCA	Single Copy Assay
sDR3	Soluble death receptor 3
SIV	Simian Immunodeficiency virus
SLE	Systemic Lupus Erythematosus
ssRNA	Single-stranded RNA
STING	Stimulator of interferon genes (STING)
sTL1A	Soluble TL1A
TB	Tuberculosis
TCR	T-cell receptor
TF	Transcription factor
TFBS	Transcription factor binding site
TFH	T follicular helper
TIV	Inactivated influenza vaccine
TL1A	TNF Ligand-Related Molecule 1
TLR	Toll-like receptor
TNFRSF25	TNF Receptor Superfamily Member 25
TNFSF15	Tumor Necrosis Factor Ligand Superfamily Member 15
Treg	Regulatory T cell
UNAIDS	Joint United Nations Programme on HIV/AIDS
VL	Viral Load
VP	Viremic progressors

Table of contents

CERTIFICATE OF DIRECTION	5
ACKNOWLEDGMENTS.....	9
ABBREVIATIONS.....	15
TABLE OF CONTENTS.....	21
ABSTRACT / RESUM / RESUMEN	25
ABSTRACT.....	27
RESUM	¡ERROR! MARCADOR NO DEFINIDO.
RESUMEN	29
INTRODUCTION	31
1. OVERVIEW HIV-1 INFECTION AND AIDS.....	33
2. CLINICAL COURSE OF HIV INFECTION AND IMMUNE RESPONSE	37
3. THE NEED OF AN HIV CURE.....	45
4. SYSTEMS BIOLOGY AND OMICS STUDIES TO GUIDE FUTURE HIV CURE INTERVENTIONS.....	56
HYPOTHESIS AND OBJECTIVES	69
CHAPTER I.....	73
METHYLATION REGULATION OF ANTIVIRAL HOST FACTORS, INTERFERON STIMULATED GENES (ISGS) AND T-CELL RESPONSES ASSOCIATED WITH NATURAL HIV CONTROL	75
ABSTRACT.....	77
AUTHOR SUMMARY.....	77
INTRODUCTION	78
RESULTS.....	80
DISCUSSION	93
METHODS	97
ACKNOWLEDGMENTS	102
FUNDING STATEMENT.....	102
DATA AVAILABILITY	103
REFERENCES.....	103
SUPPORTING INFORMATION	111
CHAPTER II.....	119
TL1A-DR3 PLASMA LEVELS ARE PREDICTIVE OF HIV-1 DISEASE CONTROL, AND DR3 COSTIMULATION BOOSTS HIV-1-SPECIFIC T CELL RESPONSES.....	121
ABSTRACT.....	124
KEY POINTS	124

Table of contents

INTRODUCTION	125
MATERIALS AND METHODS.....	126
RESULTS.....	131
DISCUSSION	140
DISCLOSURES.....	144
ACKNOWLEDGMENTS	144
FUNDING.....	144
REFERENCES.....	144
SUPPLEMENTARY INFORMATION.....	150
CHAPTER III.....	153
HOST DNA METHYLATION IS ASSOCIATED WITH ATI OUTCOME IN THE KICK-AND-KILL THERAPEUTIC VACCINE BCN02 CLINICAL TRIAL.....	155
ABSTRACT.....	158
INTRODUCTION	159
RESULTS.....	161
DISCUSSION	174
MATERIAL AND METHODS.....	178
REFERENCES.....	184
SUPPLEMENTARY METHODS.....	189
SUPPLEMENTARY FIGURES	190
SUPPLEMENTARY TABLES.....	194
DISCUSSION.....	217
CONCLUSIONS.....	229
PUBLICATIONS.....	233
ARTICLES PUBLISHED DURING THE PHD	235
BIBLIOGRAPHY.....	237

Abstract / Resum / Resumen

Abstract

An effective HIV-1 cure is still one of the major scientific challenges, and a global solution is not yet available beyond the administration of antiretroviral drugs, which maintain undetectable viral load and pause the progression of HIV associated disease. Albeit the evident benefits of antiretroviral therapy, it is not available worldwide, it requires life-long medication and, if stopped, a rapid viral rebound is observed due to HIV-1's capacity to establish latency and form an HIV-1 reservoir.

In the development of current HIV-1 strategies, the study of a small subset of individuals with the capacity to spontaneously control HIV-1 infection has been relevant. However, the mechanisms of this control are not fully understood. In the present thesis, we have applied different omics-based analyses to gain insight into host factors and biological mechanisms associated with natural HIV-1 control. In parallel, these analyses are also applied in the context of the BCN02 clinical trial, designed to achieve a functional HIV-1 cure, in order to identify mechanisms of post-treatment control, which might be different from the ones observed in natural control.

Chapter I describes the identification of epigenetically regulated host factors associated with spontaneous control of HIV-1. In brief, the genome-wide DNA methylation of PBMCs was studied in individuals with different levels of relative in vivo control of HIV-1 replication. Results indicated that differential DNA methylation on genes involved in the antiviral immune response and T-cell activation were associated with the capacity of natural control. Additionally, these methylation imprints were strongly associated with viral load, proviral DNA levels, markers of the T-cell response against HIV-1 and neutralizing antibody capacity. These observations indicate a crucial role of epigenetic imprints and have the potential to guide future HIV eradication and cure strategies.

The objective of Chapter II was to identify plasma biomarkers predictive of HIV-1 disease control. Specifically, soluble forms of TL1A and DR3 were found to be associated with virus control but also with parameters of T-cell mediated immunity. These results, coupled with validation analysis and in vitro experiments, showed that DR3 stimulation enhances HIV-1 specific T cell-responses, providing a potential tool for boosting HIV- specific T-cell responses in therapeutic vaccination strategies.

Finally, an integrated systems biology analysis was conducted in the setting of the kick-and-kill intervention applied in the BCN02 clinical trial, to understand the biological mechanisms impacted by the intervention and to identify potential drivers of post-treatment control (Chapter III). Participants from the BCN02 study were treated with romidepsin to disrupt HIV-1 latency, and vaccinated with HIVconsv immunogen to elicit T-cell responses against conserved regions of HIV-1. Subsequently, individuals interrupted their antiretroviral treatment in a "monitored antiretroviral pause" (MAP) during which 4 individuals showed a delayed viral rebound and maintained viral replication below 2,000 HIV RNA copies/ml for, at least, 8 weeks. This exploratory study demonstrated how the intervention impacted the host PBMCs' transcriptional and DNA methylation programs, especially after HIVconsv vaccination and romidepsin administration. Importantly multiple biological pathways, including the ones involved in HIV-1 infection and T-cell immunity, were modulated at both the epigenetic and transcriptional level. Additionally, individuals with an early or late rebound during MAP showed differential epigenetic signatures prior to treatment interruption, suggesting the use of DNA methylation-based biomarkers as a surrogate of post-treatment control.

Overall, omics-based systems biology analyses enabled the study of human plasma and PBMC samples to unveil different genes and pathways that are differentially modulated in natural and post-treatment HIV-1 control, thus providing new potential biomarkers and therapeutic targets.

Resum

La cura del VIH-1 és un dels majors reptes científics i l'únic tractament és l'administració de fàrmacs antiretrovirals per mantenir una càrrega viral indetectable, i bloquejar el progrés de la malaltia associada a la infecció. Malgrat els múltiples beneficis dels antiretrovirals, aquests fàrmacs no arriben a tota la població mundial i requereixen una adherència al tractament a llarg termini, ja que per la capacitat del VIH-1 d'induir latència, si s'interromp el tractament, la càrrega viral augmenta ràpidament.

L'estudi d'individus capaços de controlar la infecció del VIH-1 en absència de tractament antiretroviral ha estat rellevant en el disseny de les estratègies curatives del VIH-1, però encara es desconeixen tots els mecanismes que indueixen aquest control. En aquesta tesi, hem aplicat anàlisis de dades òmiques per identificar els factors de l'hoste i els mecanismes biològics associats al control natural de la infecció per VIH-1, o bé involucrats en el control induït per una teràpia *kick-and-kill*.

En el primer capítol de la tesi, es descriuen els factors de l'hoste regulats epigenèticament associats al control del VIH-1. Breument, l'estudi de la metilació de l'ADN en PBMCs d'individus amb diferent capacitat de controlar la replicació viral, ha demostrat que la metilació en gens involucrats en la resposta antiviral i en la resposta de cèl·lula T, s'associa a la capacitat de controlar espontàniament la infecció. A més, els nivells de metilació d'aquests gens correlacionen amb la càrrega viral, els nivells de proviral, els marcadors de resposta T, i la capacitat neutralitzant d'anticossos. Aquestes observacions indiquen que les marques epigenètiques s'han de tenir en compte en futures estratègies d'eradicació i/o curació del VIH-1.

L'objectiu del segon capítol de la tesi és la identificació de biomarcadors en plasma predictius del control del VIH-1. En aquest estudi, els nivells de les formes solubles del TL1A i el DR3 es troben associats al control del VIH-1 i a la resposta immune mediada per cèl·lules T. Aquests resultats, conjuntament amb experiments *in vitro*, han demostrat que la co-estimulació del DR3 millora la resposta T específica contra el VIH-1, i ofereixen una possible eina per millorar la resposta immune cel·lular en futurs assaigs clínics.

Finalment, el tercer capítol inclou una anàlisi de biologia de sistemes en els participants de l'assaig clínic BCN02 per identificar els desencadenants de control viral després d'una estratègia *kick-and-kill*. Als participants del BCN02 se'ls va administrar romidepsina per reactivar la latència del VIH-1, i se'ls va vacunar amb l'immunogen HIVconsv per induir una resposta cel·lular contra el VIH-1. Seguidament, en la fase MAP (de l'anglès, *Monitored Antiretroviral Pause*), es va interrompre el tractament antiretroviral i es va observar que 4 d'ells mostraven un rebot viral retardat amb una càrrega viral inferior a les 2,000 còpies d'ARN viral/ml durant, al menys, 8 setmanes. En l'estudi exploratori de la metilació de l'ADN i l'expressió gènica global en PBMCs dels participants del BCN02, s'ha observat com la intervenció clínica, impactava tan els patrons epigenètics com d'expressió gènica de l'hoste, incloent gens implicats en vies de senyalització relacionades amb la infecció del VIH-1 i la resposta immune cel·lular. També s'ha identificat una petjada epigenètica prèvia a la interrupció del tractament antiretroviral, que s'associa al rebot viral temprà o tardà. Aquests resultats suggereixen que els biomarcadors basats en la metilació de l'ADN podrien utilitzar-se com a variable subrogada del control viral post-tractament.

Globalment, aquestes anàlisis han permès identificar gens i vies de senyalització diferencialment regulades tant en el control natural de la infecció del VIH-1, com en el control post-tractament. Per tant, els estudis inclosos en aquesta tesi han permès identificar nous candidats a biomarcadors de control viral i possibles dianes terapèutiques.

Resumen

La cura del VIH-1 es uno de los mayores retos científicos y el único tratamiento son los fármacos antirretrovirales que mantienen una carga viral indetectable y bloquean el progreso de la enfermedad asociada a la infección. A pesar de los múltiples beneficios de los antirretrovirales, éstos no llegan a toda la población mundial y requieren la adherencia al tratamiento a largo plazo, ya por la capacidad del VIH de establecer latencia, la interrupción del tratamiento desencadena un rápido rebote viral.

El estudio de individuos capaces de controlar la infección del VIH-1 sin tratamiento antirretroviral, ha sido de especial relevancia en el diseño de estrategias curativas. Sin embargo, se desconocen todos los mecanismos asociados al control viral. En la presente tesis, aplicamos un análisis de datos ómicos para identificar factores del huésped y mecanismos biológicos asociados al control natural de la, o al control inducido después de la terapia *kick-and-kill*.

En el primer capítulo de la tesis, describimos factores del huésped regulados epigenéticamente y asociados al control espontáneo del VIH. Brevemente, el estudio de la metilación del ADN en PBMCs de individuos con diferente capacidad de controlar la replicación viral, ha demostrado que la metilación de genes de respuesta antiviral y de respuesta celular, se asocia al control natural de la infección. Además, los niveles de metilación de estos genes correlacionan con la carga viral, los niveles de proviral, marcadores de respuesta celular T, y la capacidad neutralizante de los anticuerpos. Estas observaciones indican que la regulación epigenética de la respuesta inmune debería considerarse en futuras estrategias de curación y/o erradicación del VIH.

El objetivo del segundo capítulo es la identificación de biomarcadores en plasma predictivos del control natural del VIH-1. En este estudio, los niveles de las formas solubles del TLA y el DR3 se asociaron al control viral y a la respuesta celular T. Estos resultados y los de experimentación *in vitro*, han demostrado que la co-estimulación del DR3 mejora la respuesta T específica contra el VIH-1, y ofrecen una posible herramienta terapéutica para mejorar la respuesta inmune celular contra el virus.

Finalmente, el tercer capítulo incluye un análisis de biología de sistemas en PBMCs de los participantes del ensayo clínico BCN02 para identificar los desencadenantes del control viral después de la estrategia *kick-and-kill*. A los participantes del BCN02 se les administró romidepsina para reactivar la latencia del VIH, y se los vacunó con el inmunógeno HIVconsv para inducir una respuesta inmune celular contra el VIH. En fase MAP (del inglés, *Monitored Antiretroviral Pause*), se interrumpió el tratamiento antirretroviral y se observó que 4 de ellos mostraban un rebote viral tardío, siendo capaces de mantener una carga viral por debajo las 2,000 copias de ARN viral/ml durante, al menos, 8 semanas. Mediante el estudio exploratorio de la metilación del ADN y la expresión génica global en PBMCs de los participantes, se observó que la intervención, tenía un gran impacto en los patrones transcripcionales y epigenéticos del huésped, incluyendo genes de vías de señalización involucradas en la replicación del VIH-1 y en la respuesta inmune. También se identificó una impronta epigenética, previa a la interrupción del tratamiento, que se asocia al rebote viral temprano o tardío durante la MAP. Estos resultados sugieren un posible uso de biomarcadores basados en la metilación del ADN como variables subrogadas del control viral post-tratamiento.

Globalmente, estos análisis han permitido la identificación de genes y vías de señalización diferencialmente reguladas tanto en el control natural de la infección como en el control inducido post-tratamiento. Por lo tanto, los estudios incluidos en esta tesis permiten identificar nuevos candidatos a biomarcadores y posibles dianas terapéuticas.

Introduction

1. Overview HIV-1 infection and AIDS

1.1. HIV-1 virus introduction, transmission and epidemiology

The Human Immunodeficiency virus-1 (HIV-1) is a single-stranded positive-sense RNA virus from the Retroviridae family and the Lentivirus genus, which targets the immune cells, mainly CD4 T cells and macrophages, and compromises the whole immune system [1]. HIV-1 was identified in 1984 as the etiological agent of AIDS (Acquired Immunodeficiency Syndrome), a devastating disease with a life expectancy between 6 and 12 months [2–4]. HIV-1 is transmitted by the exchange of body fluids (blood, vaginal secretion, semen, and breast milk), so the major transmission routes have been sexual transmission, injection drug use and maternal-infant infection. In this regard, raising awareness to avoid HIV-1 transmission and implementing specific actions such as needle supply or advocate for condom use have been essential, albeit absolutely not enough, in the fight against AIDS [5–9].

It is estimated that since the beginning of the HIV/AIDS pandemics and until 2019, more than 75.5 million people have been infected with the virus and 32.7 million, have died of AIDS-related illness, according UNAIDS fact sheet 2020 [10]. In 2019 1.7M people became newly infected with HIV-1, and 690,000 died of AIDS-related illnesses, indicating HIV-1 infection is still a major health concern [10]. Fortunately, the current life-expectancy is near to normal thanks to the antiretroviral therapy (ART) that blocks viral replication, maintains undetectable viral load and avoids HIV-1 disease progression as well as forward HIV-1 transmission. However, ART is still not available worldwide, in 2019, 67% of HIV-1-infected and diagnosed people had access to treatment and 59%, were virally suppressed [10]. Nevertheless, ART is not enough to achieve viral clearance and treatment is required lifelong, hence resulting in high health care costs and being associated with comorbidities that can be consequence of this long-term treatment.

1.2. HIV-1 virus structure and genome

The HIV-1 genome (size of 9.2 kb approximately) is flanked by long terminal repeats (LTR), required for the initiation of viral gene expression, integration and replication. The

Introduction

genome contains nine genes encoding for the essential proteins to constitute the HIV virions (encoded in *gag*, *env* and *pol*) and the accessory and regulatory proteins (*vif*, *vpr*, *tat*, *vpu*, *rev*, *nef*) (Figure 1) [1,11] .

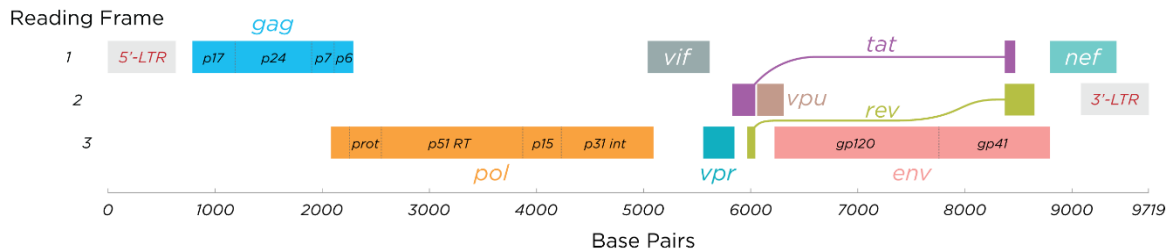


Figure 1. HIV-1 Genome. The different HIV-1 genes are shown in different color (*gag*, *pol*, *vif*, *vpr*, *vpu*, *tat*, *rev*, *env* and *nef*) and splicing is indicated by a line connecting to portions of gene coding regions. *Gag* gene encodes for p17 protein matrix and nucleocapsid proteins (p24, p7 and p6). *Pol* gene encodes for protease (prot), reverse transcriptase (p51 RT), and integrase (p31 int) and RNaseH (p15). Finally, *env* gene encodes the gp120 glycoprotein and the transmembrane protein gp41. For accessory proteins each gene encodes for one protein. Image from Wikipedia (https://en.wikipedia.org/wiki/Structure_and_genome_of_HIV) by Thomas Spletstoesser (www.scistyle.com) under Creative commons CC BY-SA 3.0 license.

The HIV-1 virions (Figure 2) contain two identical copies of the RNA viral genome and the viral enzymes necessary for viral replication: reverse transcriptase, integrase and protease, the three of them encoded by *pol* gene. The genome and the enzymes are inside a p24 nucleocapsid protein that is covered with a p17 protein matrix (encoded in *gag*), which is in turn inside the HIV-1 envelope, a lipidic bilayer embedding the proteins gp120 and gp41 (encoded in *env*) that are essential to bind and infect host cells. Each of the remaining 6 genes encode for one regulatory (*tat*, *rev*) or accessory protein (*vif*, *vpr*, *vpu*, *nef*). The regulatory proteins are indispensable for viral replication: while Tat (Transactivator protein) is required for efficient elongation of HIV-1 transcripts, Rev (Regulator of expression of viral proteins) is necessary for the export of partially spliced viral RNAs that will be translated into structural proteins. Likewise, accessory proteins promote viral replication, but they also act by evading the host antiviral immune response through the interaction with specific host factors. In particular, Vif (Viral infectivity factor) promotes viral replication by inhibiting the host restriction factor APOBEC3G, Vpr (Viral protein P) aids the process of HIV-1 integration and binds to the promoter of HIV to recruit transcription factors. Vpr is also associated with the induction of cell cycle arrest (G2) to promote virus production. Finally, Vpu and Nef downregulate CD4 expression to avoid antibody-dependent cell mediated toxicity

(ADCC). Additionally, Vpu contributes to the viral release and neutralizes the host restriction factor tetherin. In parallel, Nef downregulates HLA molecules to avoid antigen presentation and CTL-mediated killing of infected cells [1,11,12].

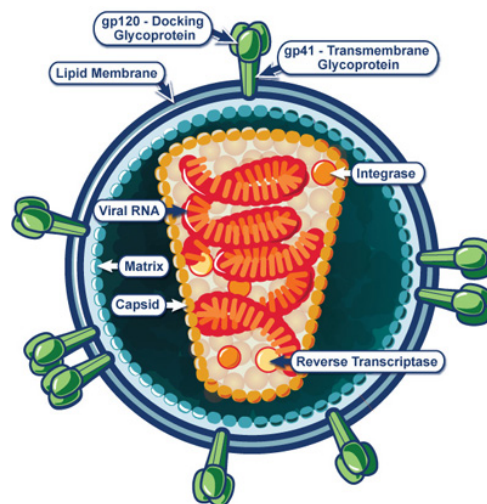


Figure 2. HIV-1 Virion structure. HIV-1 virions contain two identical strands of RNA and the associated enzymes like integrase and reverse transcriptase which are packed in the cone-shaped capsid which is in turn inside a protein matrix. Surrounding it, there is the lipid bilayer from host cells with the trimers of membrane proteins (gp120 and gp41) bound. Image from NIAID's HIV/AIDS Flickr Album <https://www.flickr.com/photos/niaid/albums/72157625994990013> under Creative commons CC-BY 2.0 license.

1.3. HIV-1 virus life cycle

The envelope glycoprotein complex (gp120 and gp41) interacts with the CD4 receptors and the co-receptors CCR5 or CXCR4, and triggers the fusion of the virion envelope with the target host cell. HIV-1 isolates can be divided in R5- or X4-tropic strains according to their use of CCR5 or CXCR4 as co-receptor, albeit some HIV-1 variants can use both receptors. Once the HIV-1 genome is inside the cell, the reverse transcriptase (RT) converts the RNA into a double-stranded DNA and a pre-integration complex is formed, which is then imported to the nucleus and gets integrated into the host genome. This integrated HIV-1 DNA (provirus) can be maintained transcriptionally inactive (HIV latency), or it can be expressed to produce the viral proteins to ultimately build new virions. In the early stage of the virus life cycle, the regulatory genes are exported to the cytoplasm and translated into proteins (Tat, Rev and Nef). Once Rev protein is expressed, it promotes the nuclear export of partially spliced or unspliced HIV-1 RNA which encodes for the structural proteins. When the different viral proteins have been produced, these

particles are assembled, released from the cell and matured to infect new host cells (Figure 3) [1,5,6,11].

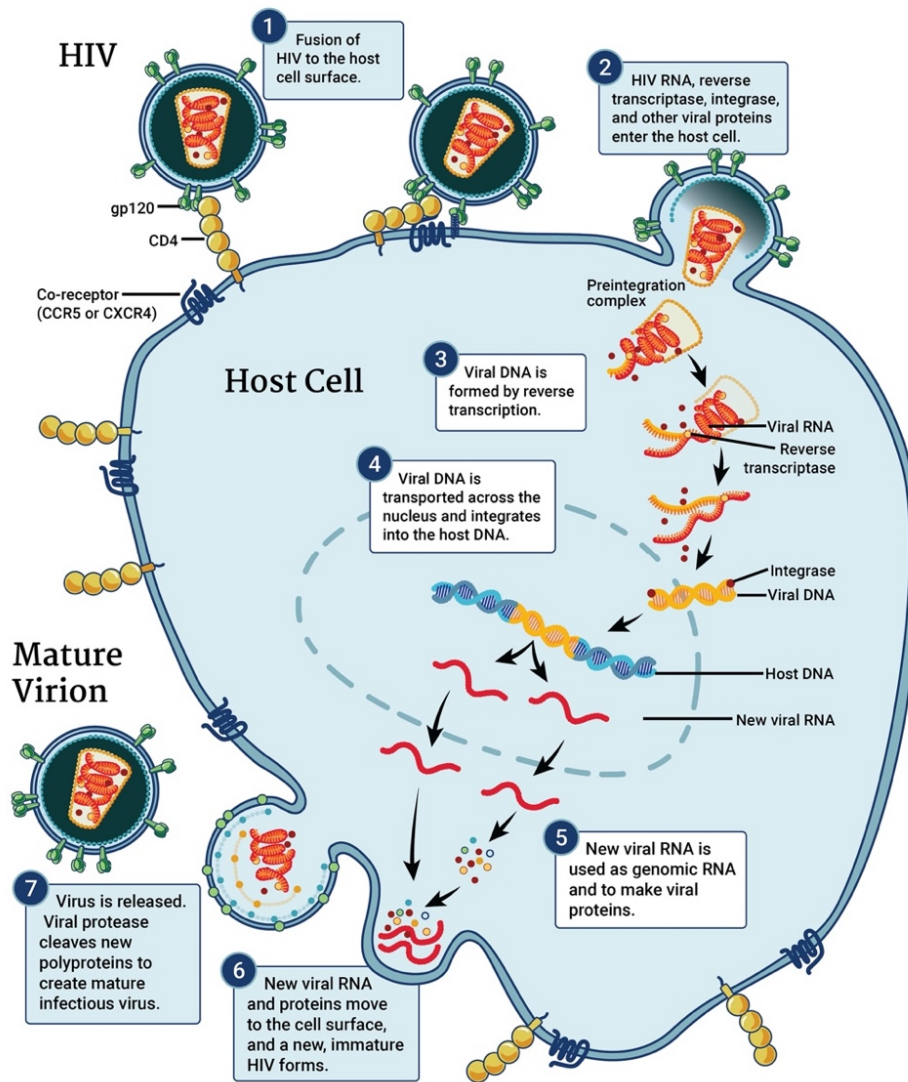


Figure 3. HIV-1 life cycle. Upon the recognition of CD4 by viral gp120 the HIV-1 virion also contacts through co-receptor (CCR5 or CXCR4) and enters the host cell. In the cytoplasm, the viral RNA is retro-transcribed by the viral retro-transcriptase. The HIV-1 DNA is then transported to the nucleus and with the help of the host integrase it is integrated in host DNA. At this point, the integrated HIV-1 DNA (HIV-1 provirus) can be induced to a latent state or be transcribed into new viral RNA molecules. The viral RNA is then transported to the cytoplasm where it is translated into viral proteins that can form new HIV-1 virions, which are ultimately released to the extracellular environment to infect new cells. Image from <https://www.niaid.nih.gov/diseases-conditions/hiv-replication-cycle> under Creative commons CC-BY 2.0 license.

The different stages of the virus life cycle are potential targets of ART and different drugs that interfere with them have been approved. The majority of FDA approved drugs block reverse transcription, while the others impede viral entry, integration or virions

maturation. Research to improve ART regimens and drug combinations have significantly improved the life span and quality of life of HIV-infected people [13,14], even though ART is not a curative strategy and treatment is chronically needed.

2. Clinical course of HIV infection and immune response

2.1. Clinical course of HIV infection

The clinical course of HIV-1 infection can be divided in three parts: Acute phase, chronic phase and AIDS (Figure 4). Upon HIV-1 infection in mucosal tissues, viral particles spread to lymphoid organs, and become detectable in blood roughly 10 days post infection. During this acute infection phase, there is an active viral replication that leads to a rapid increase of viral load followed by a decrease in CD4 T cells and which can be accompanied by flu-like symptoms in some individuals. Then, the immune response, mainly mediated by CTLs, is capable of reducing the viral loads around 100-fold where it remains stable at the so-called viral set point, which is a predictor of the likelihood of HIV-1 disease progression. In this steady state of virus replication, the CD4 T cells are also recovered to almost normal levels and the individuals enter the chronic phase of the infection, characterized by a clinical latency that can last years. However, unless individuals are treated, this equilibrium is eventually disrupted due to the appearance of viral mutants that escape the immune response, and a proinflammatory state that ultimately drives a dysfunctional and weak adaptive immunity. At this point, the individuals progress to AIDS, a period characterized by the appearance of clinical symptoms and a high susceptibility of opportunistic infections [5,6].

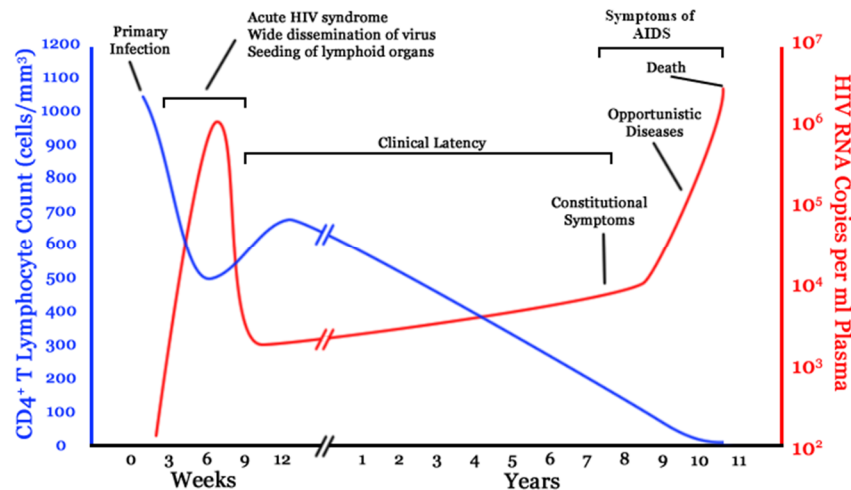


Figure 4. HIV-1 infection course. The x axis show the time upon HIV-1 infection. The left y axis, in blue, show the number of CD4 counts, and the right y axis the viral load in red. The first part of the plot show the primary infection during which there is a quick increase of viral load followed by a decrease of CD4 counts. About 9 weeks post-infection viral load is diminished until the viral set point and CD4 counts are partially recovered. Then HIV-1 infected individuals enter a phase of chronic infection during which there is a progressive loss of CD4 counts until the immune system is unable to control HIV-1 viral infection and viral load increase and individuals progress to AIDS. Figure from Jurema Oliveira Wikimedia Commons (<https://commons.wikimedia.org/wiki/File:Hiv-timecourse.png>), CC BY-SA 3.0.

2.2. The host response to HIV-1

The innate immune system confers the first line of defense against any infection. Generally, the pathogen-recognition receptors (PRRs) of host cells recognize the different pathogen associated molecular patterns (PAMPs) (Figure 5). In the case of HIV-1, the viral RNA can be detected either by the endosomal toll-like receptors TLR7 and TLR8 or RIG-I (retinoic acid-inducible gene I) receptor. In parallel, the product of retro transcription can be recognized by the cytosolic DNA sensors IFI16 (interferon inducible protein 16) and cGAS (cyclic GMP-AMP Synthase). Upon the onset of HIV-1 infection, the signaling through these receptors induce the activation of IRF (Interferon regulatory factor) and NF- κ B (Nuclear factor kappa-light-chain-enhancer of activated B cells) transcription factors that lead to the expression of inflammatory cytokines, type I interferon and HIV-1 restriction factors. Plasmacytoid dendritic cells are the major producers of type I interferon (IFN) at this step, when a positive loop is activated with an increase in the expression of interferon stimulated genes (ISGs) that further contribute to the induction of an antiviral state. Macrophages, which express CD4 and the co-receptors CXCR4 and/or CCR5, are susceptible to HIV-1 infection (mainly R5

viruses) and are among the first cell types to produce proinflammatory cytokines and restriction factors [1,15–17].

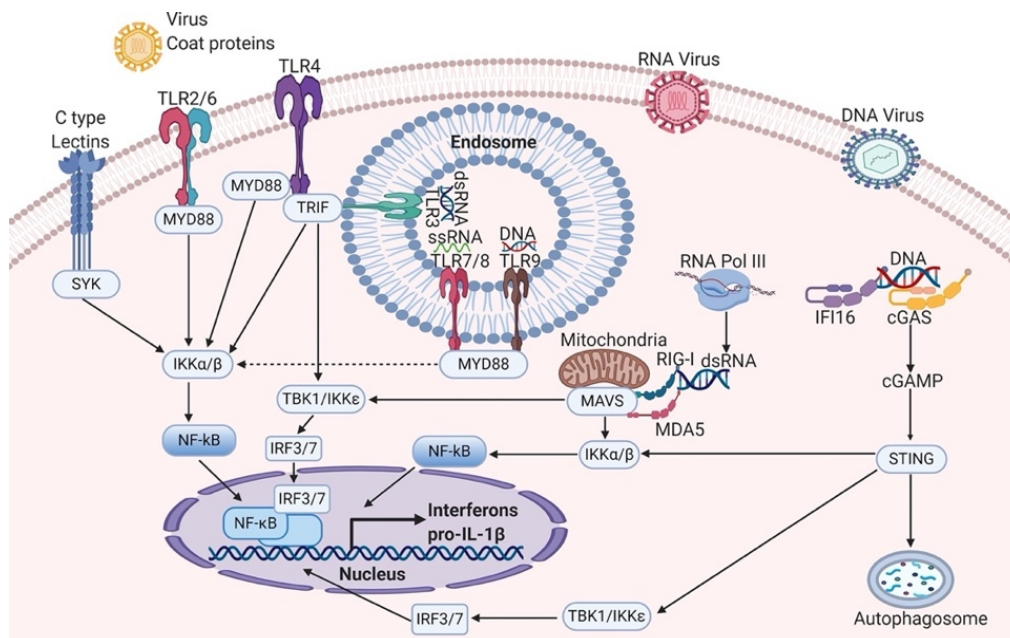


Figure 5. Innate immune response to viral infections. This image shows the different innate immune responses to viral infections. While the extracellular toll-like receptors (TLR) TLR3/6 and TLR4 recognize viral coating proteins, the endosomal TLR3, TLR7/8 and TLR9 preferentially recognize nucleic acids, specifically dsRNA, ssRNA and DNA respectively. dsRNA can also be recognized at the cytosolic level by RIG-I receptors, and DNA by the cGAS-STING system. TLRs signal mainly through MYD88 or TRIF, which leads to the translocation of NF-κB to the nucleus. TRIF signaling can also activate TBK1 that triggers IRF3/7 translocation to the nucleus. Also, RIG-I/MDA-5 signaling through MAVS, and cGAS-STING signaling ultimately stimulate NF-κB and IRF3/7 nucleus translocation to stimulate interferon and IL-1β transcription. Image from Carty M, Guy C, Bowie AG. Detection of Viral Infections by Innate Immunity. *Biochem Pharmacol.* 2021 <https://doi.org/10.1016/j.bcp.2020.114316> under Creative Commons CC-BY license.

The HIV-1 restriction factors APOBEC, SAMHD1, TRIM5α and Tetherin are regulated by IRF transcription factors. Additionally, different ISGs like *MX2*, *SLFN11* or *IFTIMs* also impair different steps of the virus life cycle. However, HIV-1 can circumvent these host defenses, in some cases directly antagonizing the action of the restriction factors (Table 1) [16,18].

Overall, the pro-inflammatory environment, produced by the innate immune system, promotes the migration of natural killers, macrophages and dendritic cells to the site of infection. This can then prime the antigen-presentation to adaptive immune cells, mainly CTLs, CD4 T helper lymphocytes and B cells to eliminate HIV-1 infected cells [16,19].

Table 1. HIV-1 host restriction factors

Restriction factor	Mechanism	HIV antagonism
SAMHD1	Deplete dNTPs pool to impede retro-transcription	Vpx protein in HIV-2 (not present in HIV-1).
TRIM5α	Premature capsid fragmentation	Unknown
APOBEC3	G-to-A hypermutation on cDNA that leads to defective viral particles	Vif
Tetherin	Transmembrane protein that impairs HIV budding	Vpu
MX2	MX2 expression inhibits nuclear entry	Unknown
SLFN11	Suppresses HIV protein translation	Unknown
IFTIMs	Inhibit HIV entry	Unknown

Information from this table is from references [16,18].

Natural killer cells (NKs), which are in the interface between innate and adaptive immunity, also have an active role in eliminating the virus-infected cells. NK cells contain different activation and inhibition receptors, and the balance among them drives the responses. In the acute phase of HIV-1 infection, NKs with an inhibitory KIR (Immunoglobulin-like receptors) interacting with self HLA class I molecules, trigger a rapid expansion of NK cell to eliminate the virus [16].

All this first line of defense against HIV-1 occurs between the date of infection and 1-2 weeks post-infection, by when the HIV-1-specific CD8 T cells start expanding. HIV-1-infected cells present HIV-1-derived peptides through HLA class I molecules that are recognized by the TCR of cytotoxic CD8 T cell, which eliminate the infected cell (Figure 6). This activation of the cellular arm of the adaptive immune system largely contributes to the establishment and the maintenance of a viral set point as well as to a partial recovery of CD4 cells during the early phase of infection [19,20]. Although CD4 T cells are the main target of HIV-1, the majority of these cells remain uninfected. Uninfected CD4 T cells are activated upon recognition of HIV peptides presented by antigen presenting cells (APCs) through HLA class II molecules and provide CD8 T cells with the signaling to be fully functional, thus enhancing CD8-mediated T-cell responses. Also, CD4 T cells have shown to be able to directly eliminate HIV-infected cells [19,21].

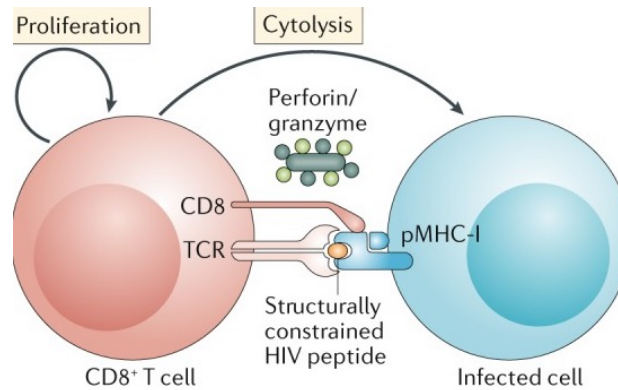


Figure 6. CD8 T cell function. The Infected cell (in blue, on the right) present the HIV-1 peptide through their HLA-I molecule. The CD8 T cell (in red, on the left) recognizes through its TCR the complex formed by the HIV-1 peptide and the host HLA-I (pMHC-I). Therefore, CD8 T cells start proliferating and to induce the cytolysis of infected cells by secretion of perforin and granzyme. Although not shown in the image, after TCR stimulation with an antigen there is progressively an increase of IFN γ production by CD8 T cells. Image adapted by permission of Springer Nature Customer Service Centre GmbH: Springer Nature. Nature Reviews Immunology. Collins DR, Gaiha GD, Walker BD. CD8 T cells in HIV control, cure and prevention. 2020;20(8):471-482 <https://doi.org/10.1038/s41577-020-0274-9>. Copyright © Springer Nature Limited 2020.

B cells are also activated upon HIV-1 infection which are converted into plasma cells to generate antibodies. IgM are the first type of produced antibodies, which show high avidity but low affinity [1]. Actually, CD4 T helper cells are indispensable to generate high affinity IgG antibodies as well as long-lived plasma cells [1]. However, the generated antibodies in acute infection lack the capacity to effectively neutralize the autologous virus and to block the infection of new cells [22]. Additionally, when the first Nabs emerge these are directed against HIV-1 envelope, and due to the high variability of the *env* gene, viral neutralization escape variants rapidly arise [22,23]. Nonetheless, beyond neutralizing activity, the Fc effector functions of the antibodies including antibody-dependent cellular cytotoxicity (ADCC) and antibody-dependent phagocytosis (ADCP), contribute in antiviral immunity and can reduce viral loads [23]. In particular, Fab region binds the Env protein in the surface of HIV-1-infected cells, while Fc is recognized by NK cells that release cytotoxic granules to lyse the infected cell (ADCC), or by macrophages that phagocyte the infected cell (ADCP). Finally, the classical complement activation through antibodies can also lead to phagocytosis of HIV-infected cells [22–25].

The immune system is thus not able to resolve HIV-1 infection and the immune pressure, especially the one exerted through HIV-specific T cells and antibodies, leads to HIV-1 escape variants that are present in chronic infection [26–31]. Consequently, during the chronic phase of the HIV-1 infection, the innate immune system is maintained active and

the negative regulation feedback mechanisms are disrupted, leading to a general chronic state of dysfunctional immune activation that can benefit HIV-1 replication [31–33]. Taking for example NF- κ B transcription factor, when it is translocated to the nucleus, it stimulates the antiviral gene expression but also promotes HIV-1 transcription [34,35]. In parallel, interferon signaling and ISGs gene expression are maintained during the chronic infection, and while it can be beneficial to stop the virus burden upon infection, it has been shown to have deleterious effects during the chronic stages of the infection and to contribute to the exhaustion of the immune system [36,37]. In fact, studies in natural hosts of SIV (Simian Immunodeficiency virus), in which SIV viral load is high but CD4 T-cell function is preserved, have shown that 1 month post-infection, the innate immune system is silenced, indicating that the lack of an effective negative regulation of IFN and proinflammatory cytokines in humans may drive the dysfunctional immune response in chronic stages of HIV-1 infection [38,39]. Moreover, other factors like microbial translocation or reactivation of viruses such as CMV contribute to the generalized immune activation [40,41]. As a consequence, large portions of adaptive immune cells become dysfunctional and, although they can identify HIV-1-infected cells, cannot exert their fully functional response to control the virus [32,42,43]. In recent years, several markers of T-cell exhaustion like PD-1, CTLA-4, TIGIT or TIM3, among others, have been identified, and strategies to block these molecules and restore T-cell function have been designed [44–46]. In summary, although the immune system is fully activated after HIV-infection, the virus has mechanisms to attenuate the immune response and hijack its functioning to persist in the host until the immune control is completely lost and HIV-infected individuals progress to HIV-associated disease, and to AIDS if they are left untreated.

2.3. Establishment of the HIV reservoir

One of the major hurdles of HIV-1 infection resolution is the virus capacity to establish latency and escape immune surveillance. Importantly, this occurs a few days after HIV infection, and to date, only prophylactic (PrEP) and post exposure (PEP) antiretroviral treatment have proven effective to avoid it [47–50]. Actually, in rhesus macaques, SIV

reservoirs are established as early as day 3 post infection and thus, even before viral particles become detectable in the peripheral blood [51].

The HIV-1 reservoir is heterogeneous and regulated at different levels by the anatomic location, the cell type and the different molecular mechanisms regulating latency. Tissue reservoirs are established early upon infection and even early antiretroviral treatment does not succeed in eliminating it [52,53], partially due to the limited penetration of ART into different tissues. Recent studies also show that upon treatment interruption, the viral rebound originates from multiple cellular and tissue reservoirs, especially blood, gut and lymph nodes [54,55]. Additionally, in the immune-privileged CNS, an exchange of viruses between CNS and blood has been observed, although the contribution to the viral rebound is still undetermined [54].

At cellular level, memory CD4 T cells, as a long-lived resting cell type, are one of the major cellular contributors to the latent HIV reservoir. These cells can harbor HIV-DNA and maintain it silenced, or low-level transcribed, so that negligible levels of HIV-1 viral particles are being produced. Other cell types harboring HIV-1 are CD4 naïve cells or T follicular helper (TFH) [56]. In the latter case, TFH are associated with low-levels of HIV-1 transcription in cART treated individuals and can contribute to HIV-1 persistence [56]. Something similar may occur in HIV-1-infected tissue-resident macrophage as macrophage-tropic HIV-1 variants have been detected upon interruption of antiretroviral treatment [57].

Although the precise process of HIV-1 latency induction remains incompletely understood, some important insights have been described and point to a multifactorial process [47,58–65]. Among them, epigenetic regulation is considered one of the major drivers of HIV latency. In particular, the HIV-1 promoter regions (5' LTR) contain two nucleosomes (Nuc-0 and Nuc-1) susceptible to remodeling and to histone modifications that dictate the condensation state of the chromatin (Figure 7). In HIV-latency, HIV-1 proviral DNA is found in heterochromatin (closed conformation of chromatin), therefore impeding the access of transcriptional machinery to the HIV-1 promoter. Such a state is

maintained by active HDACs (Histone deacetylases), to avoid histone acetylation which would induce chromatin relaxation, and HMTs (Histone Methyl transferases) that maintain trimethylation in lysine 27 of histone 3 (H3K27me3) and di- or trimethylation in lysine 9 of histone 3 (H3K9me2/ H3K9me3) [58,59,63,64]. Also, higher levels of DNA methylation have been found in the promoter of HIV-1 5'LTR, although this process is associated with antiretroviral treatment and the role in establishing latency remains unknown [64]. Regardless, it appears that closed chromatin landscapes hinder the binding of the RNA pol II as well as transcription factors either involved in transcription initiation (e.g. NF- κ B, NFAT, AP-1 or STAT5) or elongation (e.g. pTEFb). At the same time, the quiescent state of CD4 memory T cells further contributes to this state since resting cells have a decreased availability of such transcriptional factors [64]. Especially in HIV-1 elongation, the HIV-1 Tat protein plays an essential role, but basal levels of HIV-1 transcription are needed to produce it, therefore its levels are limited in latently HIV infected cells [59,64]. The integration sense of the HIV-1 provirus in the genome can further favor HIV latency: when it is inserted in the opposite direction of a host gene, the RNA Pol II complexes in two directions can collide impeding the complete transcription of host genes and HIV-1 provirus; whereas if provirus insertion takes place in introns of actively transcribed host genes, RNA Pol II can displace the TFs from host genes to HIV-1 promoter, favoring HIV-1 transcription. Indeed, it has been reported that in active CD4 T cells, where the NF- κ B signaling is active, transcription of HIV-1 is ensured rather than that of host gene [59,63]. In addition, post-transcriptional blocks also contribute to latency, such as low levels of Rev protein that hinders the export of HIV-1 transcripts [59,63,64]. Finally, homeostatic proliferation of latently infected cells is also contributing to the maintenance of the viral reservoir [60–63,66]. Overall, latency is a highly complex process regulated at multiple level.

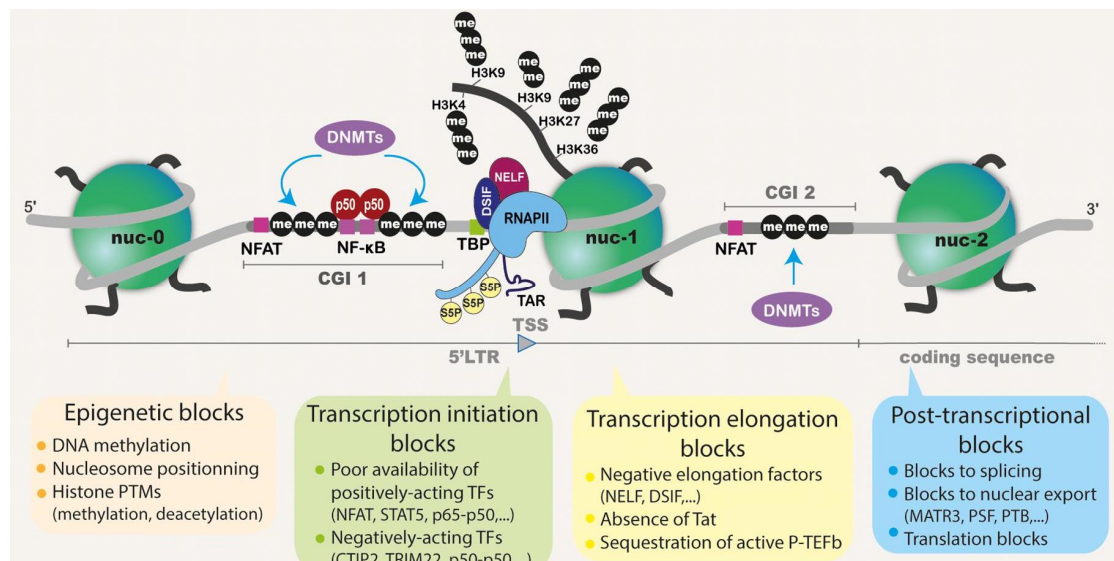


Figure 7. HIV-1 provirus latency. Image show the different mechanisms that contribute in the induction and maintenance of HIV-1 latency In the 5'LTR we observe high methylation levels induced by DNMTs Also, the binding sites for NF-kB are occupied by the homodimer p50p50 blocking HIV-1 transcription. We also see the nuc-1 nucleosome in the TSS with repressive histone modifications. The RNA Pol-II also shows phosphorylation of the C-terminal domain and is bound to the negative elongation factors NELF and DSIF. Each of the globes explain the different mechanisms to induce and maintain HIV-1 latency. Image adapted from Ait-Ammar A, Kula A, et al. C. Current Status of Latency Reversing Agents Facing the Heterogeneity of HIV-1 Cellular and Tissue Reservoirs. Front Microbiol. 2020 <https://doi.org/10.3389/fmicb.2019.03060> under Creative commons CC-BY license.

3. The need of an HIV cure

With the advent of antiretroviral treatment and the progress made to improve tolerability and safety in the latest years, people living with HIV (PLWH) have nowadays a good quality of life and a close to normal life expectancy. However, access to antiretroviral treatment is not ensured worldwide and, when available, it is not exempt of side-effects. Finally, PLWH need to be committed to lifelong therapy as when therapy is interrupted, the viral load increases exponentially. This is mainly due to the presence of a latent HIV reservoir which is established early after infection and is not eliminated by antiretroviral treatment, albeit it can reduce it over extensive period of times. Therefore, the search for an HIV cure is still a major challenge among the scientific community, and it could benefit the infected individuals but also it would allow to reduce the pressure on public health systems [67,68].

3.1. Lessons learned from the natural control of HIV infection

A small group of HIV-infected individuals is able to remain clinically stable in the chronic phase of infection for decades and does not progress to AIDS even without being on

Introduction

antiretroviral treatment. These individuals are estimated to account for the 5-8% of HIV-infected population and are known as long-term non-progressors (LTNP) [69]. LTNPs have normal levels of CD4 counts (>500 cells/mm³) and pVL $< 2,000 - 10,000$ HIV RNA copies/ml depending on the studied cohort. Among these LTNP, for individuals with pVL $< 2,000$ HIV RNA copies/ml the term viremic controllers (VC) has also been used. In addition, a small subset of PLWH ($< 1\%$) are elite controllers (EC), individuals able to maintain undetectable viral load (pVL < 50 HIV RNA copies/ml) and normal CD4 counts during long periods of time without the need for antiretroviral treatment [69,70]. While the mechanisms of virus control in these individuals are not fully elucidated, the study of these individuals has contributed to a better understanding of the antiviral immune response and has paved the way for current and future HIV-1 eradication strategies.

Different mechanisms have been identified that can partially explain the spontaneous virus control in LTNPs and ECs. This includes infection with attenuated or defective viruses, although this has only been well documented in few individuals. In addition, replication-competent HIV-1 variants have been isolated from ECs as well, suggesting that other mechanisms than impaired viral fitness support viral control in these individuals [71]. In addition to viral characteristics, several host gene polymorphisms have been identified in LTNPs, and about one third of this population is estimated to contain a variant genotype for CCR2 (V64I substitution, CCR2-V64I) or CCR5 (32 base pair deletion, CCR5- Δ 32) [69]. This has given rise to therapeutic strategies in which cells are *ex-vivo* modified to express a mutant CCR5 gene and then reinfused. The observation was also employed for the treatment of the first individual who has been cured of HIV infection, known as the "Berlin patient", after being transplanted with stem cells from a donor expressing the mutant CCR5 gene [72]. In parallel, host polymorphisms in HLA genes have been consistently related to the spontaneous control of HIV-1 infection [69]. These major histocompatibility complex (MHC) encoded molecules are found on the surface of host cells where they present viral antigens to be recognized by CD8 or CD4 T cells. In humans, the HLA class I genes (HLA-A, HLA-B and HLA-C) are expressed in all nucleated cells and preferentially present antigens to CD8 T cells. In contrast, HLA class II genes (HLA-DP, HLA-DQ, HLA-DR) are expressed by professional antigen presenting

cells (APCs), dendritic cells (DCs), macrophages and to a lesser extent, B cells and activated T cells; and they mainly present foreign antigens to CD4 T cells via their T cell receptor (TCR). When TCR on CD4 or CD8 T cells recognize the viral peptide and part of the presenting HLA molecule, the cells are activated and execute an effector function program, including lysis of the infected cells. The HLA genes are the most polymorphic genes in the human genome, and for the HLA-B locus alone, more than 8,000 alleles have been described [73]. It is postulated that this high variability is to ensure the survival of the species from emerging infections that can pose a threat to human life [1]. This heterogeneity has allowed to identify some beneficial and detrimental associations between HLA-class I and HLA-class II alleles and HIV-1 disease progression [69,70,72,74–77]. The best characterized associations are in the case of the beneficial alleles HLA-B*57 and HLA-B*27, which are expressed in higher proportions in elite controllers [69,70,72]. On the contrary, HLA-B*3502, HLA-B*3503 and HLA-B*3504 have been associated with accelerated disease progression [69]. In parallel, Killer cell immunoglobulin-like receptors (KIRs), that are expressed by NK cells and interact with HLA-class I molecules, have also been associated with differential disease progression [69]. Finally, genome-wide association studies (GWAS) have identified some SNPs, the majority of them in the HLA locus, that are associated with HIV-1 control [74]. Nevertheless, not all the ECs and LTNPs contain such protective host polymorphisms in HLA alleles or other loci, indicating that other parameters can drive virus control.

Generally, it is well accepted that a potent immune response soon after infection can mediate, at least partially, the control of the infection. In particular, it has been shown that an early and potent HIV-1 immune response, especially the one mediated by HIV-1 specific CD8 T cells, not only reduces the HIV-1 viral set point, but also limits the viral reservoir, especially in cellular CD4 T cells [20,71]. This may be especially pronounced in ECs, whose immune system may be able to eliminate the replication-competent HIV-1 infected cells. Additionally, in ECs, a high percentage of CD4 T cells that are clonally expanded contain replication-competent provirus inserted in regions of heterochromatin rather than regions of active transcription. Thus, ECs appear able to efficiently eliminate HIV-1 infected cells containing replication-competent proviruses

integrated in transcriptionally active regions, while the pool of HIV-1 infected cells that enter into a deep latency state is increased [71].

HIV-specific CD8 T-cell responses of high functional avidity and polyfunctional CD8 responses have been widely associated with viral control [20]. Also, CD8 responses targeting specific epitopes, especially in HIV Gag, have been linked with better immune control [20,78,79]. Notwithstanding, other HIV-1 epitopes beyond Gag have also been observed to be preferentially targeted in HIV-1 controllers [80,81]. In addition, loss of HIV-1 control has been linked to the exhaustion of CD8 T cells, which are reduced in HIV-1 controllers [82–84]. Other mechanisms including ADCC can further contribute to natural control of HIV-1 infection [82–84]. Similarly, some host restriction factors like SAMHD1 or Schlafen-11 are overexpressed in some ECs [85,86]. Overall, these select studies indicate the multifactorial nature of the mechanisms that drive virus control in ECs and/or LTNPs, involving genetic determinants but also immunologic factors. These insights on the immune mechanisms mediating HIV-1 control, independent of individual genetic background, may critically guide the development of strategies designed to improve the immune response against HIV-1, among others, by therapeutic vaccination approaches.

3.2. Strategies to achieve an HIV Cure

Several strategies have been designed to achieve either an sterilizing cure, understood as completely eliminating the virus from the body, or a functional HIV-1 cure that consist in inducing a state of undetectable levels of viral load and normal CD4 counts without the need of ART [68].

3.2.1. Early antiretroviral treatment

Early antiretroviral treatment initiation has been proposed to mimic the early control of the HIV-1 infection achieved in spontaneous HIV controllers, which harbor low viral reservoirs and maintain a functional immune response. Nevertheless, the HIV-1 reservoir is seeded rapidly after infection and the majority of the individuals rebound

once ART is interrupted [52,67,68]. However, a proportion of 5-10% of early-treated individuals will be able to control the viral rebound [67,87,88]. Generally, current knowledge suggests that, while it is beneficial to start early treatment to limit HIV-1 reservoir seeding and maintain a strong immune system, it is not sufficient to eliminate HIV-1 despite the long-term treatment. Nevertheless, early treatment may be beneficial to the individuals' health and to limit HIV-1 transmission, and, in combination with other curative strategies, may increase the possibilities of establishing effective cure interventions [68,89].

3.2.2. Gene therapy

To date, the only cases of HIV-1 cure have been reported as the consequences of CCR5 Δ 32/ Δ 32 allogeneic stem-cell transplantation. In both cases reported to date, the individuals had a blood malignancy that required stem cell transplantation, for which a CCR5 Δ 32 donor was selected that led to the replacement of the host cells by the mutated CCR5 Δ 32 donor cells [90,91]. Although these studies are not scalable, they point to the possibility to use gene therapy to induce mutations in CCR5 should these technologies demonstrate to be safe in other medical fields. Nevertheless, other gene therapies directed to HIV-1 provirus might be required since there are some individuals with X4-tropic viruses that are independent of the CCR5 co-receptor. All in all, the advances of *in vivo* genetic modifications in other medical settings, may be available in the future for HIV eradication strategies [67,68].

3.2.3. T-cell based vaccination and other immunotherapies

The study of HIV-1 controllers has manifested the importance of fully functional HIV-1-specific CD8 T-cell responses directed against vulnerable HIV-1 regions, in which mutations have been reported to impact viral replication fitness. More recently, preserved CD4 T-cell function has also been linked to *in-vivo* control of HIV-1. In the light of these observations, different T-cell immunogens have been designed to induce a long-term T-cell based immune control of the infection in PLWH. One of the first strategies was the design of immunogens against well-conserved regions of the HIV-1, as viral-escape mutations in these regions may severely impact viral fitness [92,93]. One of these

Introduction

immunogens is *HIVconsv*, a mosaic immunogen that contains conserved regions in HIV Gag, Pol, Env, and Vif protein (Figure 8) and which, in the BCN01 and BCN02 clinical trials, has shown the ability to re-direct the HIV-1 specific immune responses towards more conserved regions [94–96]. Another approach has been the bioinformatic optimization of mosaic antigens to elicit a broad humoral and cellular response. Indeed, vaccination of individuals with Ad26.Mos.HIV trivalent vaccine (Ad26.Mos.1.Gag-Pol, Ad26.Mos2.Gag-Pol, Ad26.Mos1.Env) and MVA-Mosaic vaccine (MVA-Mosaic1 and MVA-Mosaic2, both containing Gag, Pol and Env proteins) have shown the induction of greater T-cell breadth and a delayed viral rebound in contrast to placebo recipients [97,98]. An alternative approach was the one used in the design of the HTI immunogen, which was based on the identification of HIV-1 segments that elicited a beneficial T-cell immunity in HIV-1 controllers or individuals with low viral loads independently of their HLA genotype [68,80,99]. Many of the beneficial responses mapped to Gag and Pol peptides, while none was identified in Env, which has been described to be associated with ineffective control of HIV [100]. The final sequence of HTI contains peptides in Gag, Pol, Vif and Nef [68,80]. The recent placebo-controlled clinical trial Aelix-002, in which early-treated individuals were vaccinated with placebo or HTI, showed that while among vaccinees, 40% maintained a VL < 10,000 HIV RNA copies/ml for 22 weeks post-ATI, only 8% of the placebo individuals remained off treatment at that time point [101]. These results clearly support a central role of T-cell responses towards vulnerable epitopes to partially control the HIV-1 replication.

Different strategies have been employed to enhance HIV-specific T-cell immune response, including vaccination with heterologous prime-boost strategies that improve the breadth, magnitude and polyfunctionality of T-cell immune responses. In addition, the integration of immune checkpoints inhibitors (e.g. anti-PD-L1) to rescue immune-exhaustion and improve the quality of HIV-1 specific T-cell responses has been explored [102]. Also, the use of adjuvants like TLR agonists or T-cell costimulatory molecules are under study to improve such responses in a similar manner that has been observed in immunotherapies against tumor cells [68,103].

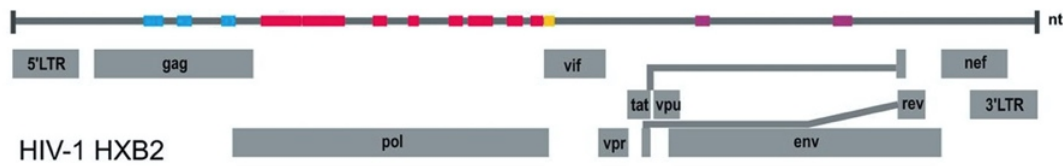


Figure 8. HIVconsv immunogen. The HIV-1 genome is indicated along with colored sections marking the the sequences included in the HIV-1consv immunogen. Blue indicates the Gag peptides, pink Pol peptides, yellow Vif peptide and purple the Env peptides. Image from Mothe B, Manzardo C, et al. Therapeutic Vaccination Refocuses T-cell Responses Towards Conserved Regions of HIV-1 in Early Treated Individuals (BCN 01 study). *EclinicalMedicine*. 2019. <https://doi.org/10.1016/j.eclinm.2019.05.009> under Creative commons CC-BY license.

The extent to which HIV-1-specific T-cell responses can mediate the protection against HIV-1 acquisition remains unknown. To date, the RV144 study have yielded the most promising results in the context of preventive vaccination, which after 3 years of vaccination showed a 31.2% reduction in HIV-1 acquisition amongst vaccinated individuals compared to placebo group. In this trial, CD4 T-cell polyfunctionality was related to lower risk of acquisition. In parallel, the levels of IgG that recognized specific envelope regions (V2 loop) were associated with the protection against HIV-1 acquisition, while the contrary was observed with the levels of IgA that recognized Env [104,105]. Overall, it is widely accepted that a successful HIV vaccine should be able to induce both the cellular and the humoral response, especially in the context of a preventive vaccine.

Over the last years, great efforts have been dedicated towards the identification and the clinical development of broadly neutralizing antibodies (bNAbs) against HIV-1. These bNAb, do not only allow to block the infection of new cells, but they also exert Fc-mediated functions like ADCC or ADCP and they induce the formation of immune-complexes that can boost HLA-I and HLA-II antigen presentation by APCs and enhance CD8 and CD4 T-cell responses [23]. To date, the passive administration of bNAbs have been shown to be safe in uninfected HIV-1 population as well as in PLWH, where effective and at least transient suppression of viral loads have been observed [23]. The induction of such bNAbs by vaccination using B cell immunogen is however complicated, partially due to the huge mutability capacity of Env, the structural form of Env trimers and the Env glycan shield that complicates the recognition of Env conserved regions

[106]. Therefore, different immunogens based on Native-like Env trimers (such as BG505 SOSIP.GT.1.1 gp140 and many other) have been designed to induce bNABs and are now in a Phase I human clinical trial (IAVI C101, NCT04224701) to evaluate safety, immunogenicity and tolerability in uninfected individuals.

3.2.4. Kick and kill strategies

The rationale of kick and kill strategies is to reactivate the latently infected cells with a latency reversing agent (LRA) after having boosted the immune system to eliminate potentially reactivated HIV-1 infected cells. ART is maintained throughout the intervention to avoid spreading of the infection to activated T cells (Figure 9) [107].

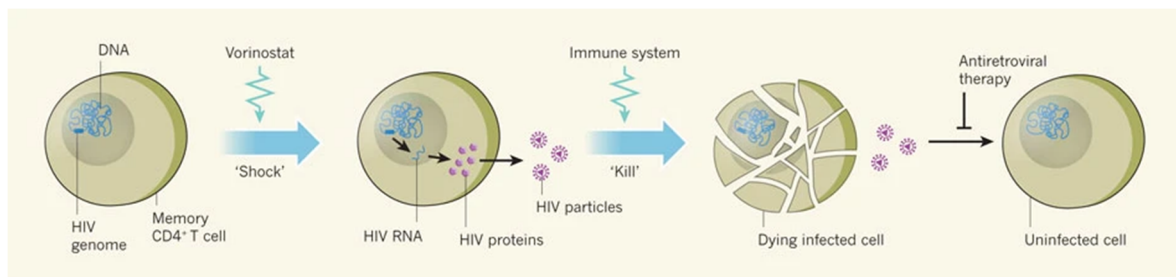


Figure 9. Representation of the kick and kill approach. In this figure we observe Vorinostat as the LRA which induce the expression of HIV-1 particles. Then, reactivated HIV-1 infected cells become visible to the immune system which eliminate the HIV-1 infected cells. Image by permission of Springer Nature Customer Service Centre GmbH: Springer Nature. Nature Reviews Immunology. Deeks SG. Shock and Kill Nature. 2012; 487, 439–440 <https://doi.org/10.1038/487439a> Copyright © Springer Nature Limited 2020.

Due to the complexity of mechanisms that maintain HIV-1 latency, several LRAs with different mechanisms of action have been proposed to achieve reversal of viral latency (Figure 10). As mentioned before, epigenetic mechanisms are important players in the induction and maintenance of the HIV-1 latency, therefore multiple epigenetic modifiers have been proposed as LRAs including histone deacetylase inhibitors (HDACi), inhibitors of DNA methylation or methyl-transferase inhibitors. Other mechanisms include Protein Kinase C agonist, NF-Kb agonists or TLR agonists, ultimately activating NF-Kb to achieve induction of HIV-1 expression [108,109].

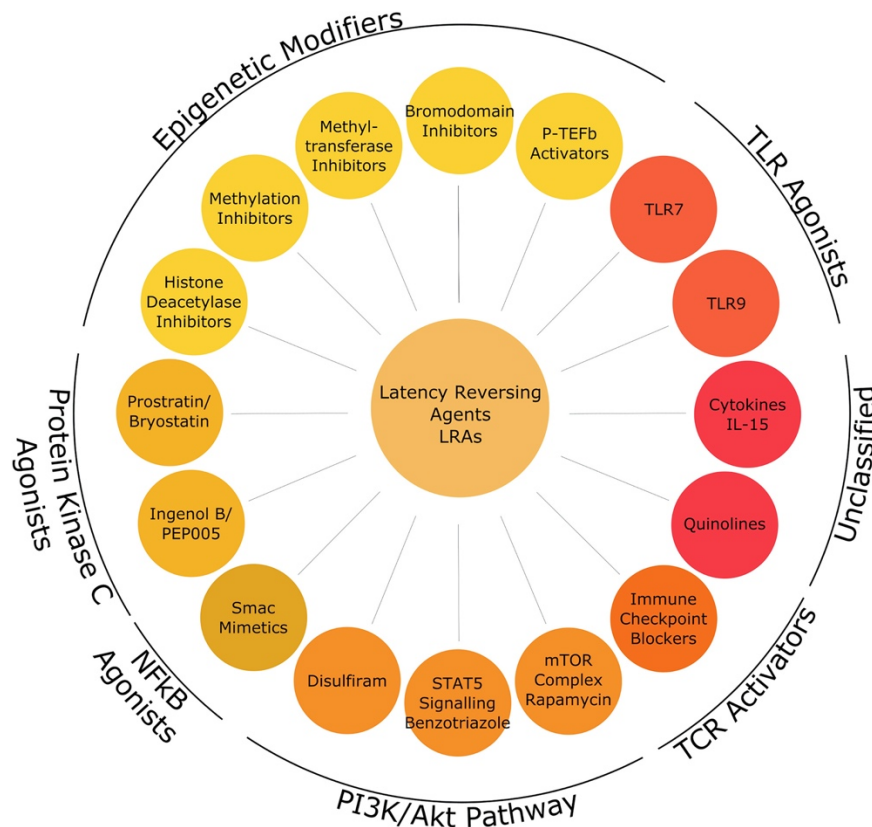


Figure 10. Latency Reversing Agents. Different LRAs are grouped and colored according to mechanisms of action: Epigenetic modifiers, TLR agonists, TCR activators, PI3K/Akt Pathway, NFkB agonists, Protein Kinase C agonists as well as unclassified LRAs like Cytokines and Quinolines. Image by permission of Elsevier. Cell Host & Microbe. Kim, Y., Anderson, J. L., & Lewin, S. R. Getting the "Kill" into "Shock and Kill": Strategies to Eliminate Latent HIV. Cell host & microbe, 2018; 23(1), 14–26. <https://doi.org/10.1016/j.chom.2017.12.004>. Copyright © 2017 Elsevier Inc.

Of all these strategies, HDACi act by increasing global histone acetylation and inducing chromatin relaxation, and they are the LRA clinically best studied in the context of HIV-1 latency reversal. After HDACi treatment, HIV-1 provirus but also other host genes will be transcribed and expressed [110]. *In vivo* studies in chronically ART-suppressed individuals treated with HDACi drugs such as vorinostat, panabinstat or romidepsin (RMD), showed increased levels in HIV-1 transcription, and in a subset of RMD-treated individuals, viral load was as well increased [111–113]. Such observations indicated the feasibility of HDACi administration to disrupt viral latency, although no reductions of the HIV-1 reservoir have been observed. Therefore, these results evidenced the need to combine latency reversal with immunotherapies to more effectively eliminate HIV-1 infected cells.

Introduction

A few clinical trials on HIV-1 infected individuals under cART treatment have attempted to combine HDACi with vaccination. In the REDUC trial (NCT02092116), 17 HIV-1 chronically infected individuals were vaccinated 6 times with Vacc4x (vaccine of synthetic p24 gag peptides) and the adjuvant rhuGM-CSF, which was then followed by the administration of one weekly dose of romidepsin for 3 weeks. A 39.7% reduction in total HIV-DNA was observed from screening to 8 weeks post-romidepsin. Also, a 3.1 fold mean increase on CA-RNA was observed between 30 minutes after the 3rd infusion of romidepsin and the baseline. The study included a monitored antiretroviral pause (MAP) but no delay in viral rebound was observed [114]. Next, the RIVER study (NCT02336074) compared the effect on total HIV DNA proviral copy numbers between a control arm of 30 individuals early treated with ART and a group of 30 individuals early ART-treated and vaccinated with ChAdV63.HIVconsv prime and MVA.HIVconsv boost, and followed by 10 doses of vorinostat treatment taken every 3 days. No differences in total HIV reservoir were found between the two groups in spite of the observed effect of vorinostat in histone acetylation and, the capacity of vaccination to induce strong HIV-1 specific CD8 and CD4 responses [115]. Finally, the BCN02 clinical trial (NCT02616874) enrolled 15 early treated individuals, rolled over from the BCN01 (NCT02616874, prime-boost of ChAdV63.HIVconsv and MVA.HIVconsv) trial. In BCN02, the participants received an MVA.HIVconsv vaccination before and after 3 weekly cycles of romidepsin infusion. Importantly, the study showed a virus control in 23% of the individuals during the 32-week MAP, although only a marginal reduction on the viral reservoir was observed. Importantly, MVA.HIVconsv vaccination re-focused the T-cell responses to the most conserved regions covered in the HIVconsv immunogen [94]. Although this pilot study suggested that T-cell vaccination could induce viral control when the antiretroviral treatment is paused, no durable reduction of the viral reservoir has been achieved, nor was a functional cure that maintain undetectable viral loads. Thus, the available studies point to the need of evaluating new LRAs candidates in combination with even more potent immunotherapies.

3.2.6. Block and lock strategies

Whereas the kick-and-kill strategies aim to disrupt HIV latency, the objective of block-and-lock approaches is to establish a deep latency in order to prevent HIV-1 rebound upon T-cell activation [67,116]. This strategy is based on the observation that in elite controllers, there is a higher proportion of intact provirus in non-genic or pseudogenic genes, regions that are transcriptionally inactive. It has been suggested that in ECs there is an immune-mediated elimination of transcriptionally active cells, leading to an enrichment of CD4 T cells with proviruses integrated into regions of deep latency [71]. Such results have promoted the idea of block-and-lock strategies where latency promoting agents (LPA), such as inhibitors of NF- κ B, NFAT, pTEB or mTOR could be used. To date, the most promising candidate is didehydrocortistatin A (dCA) which blocks the interaction between HIV-1 Tat protein and the TAR-RNA element in the HIV-1 provirus. Such strategies are in its commencement and current and future studies will be needed to elucidate their safety and feasibility [67,116].

3.2.7 Combination of strategies

The highly individual heterogeneity of PLWH at both HIV reservoir and immune level, suggest that multiple strategies may need to be combined to effective cure strategies. As mentioned above, early treatment might be crucial for the efficacy of the different strategies, as this can maintain better immune status and lower viral reservoir [89]. In this regard, the time of treatment with ART before a therapy might well be crucial for therapy efficacy. Thus, to achieve a functional or sterilizing cure, it will likely be necessary to reach low levels of HIV reservoir, low levels of inflammation and exhaustion and, a robust and broad cellular and humoral response [68].

3.4. Analytical treatment interruption (ATI) and Post-treatment controllers (PTCs)

Analytical treatment interruptions (ATI) are necessary to evaluate the efficacy of HIV-1 cure strategies as no surrogates of post-treatment control have been yet identified [114]. The VISCONTI study identified 14 post-treatment controllers (PTCs), defined as HIV RNA levels < 400 copies/mL for 24 months after cART discontinuation, and

highlighted the benefits of early and prolonged antiretroviral treatment. The VISCONTI study also suggested that mechanisms different to the ones identified in natural controllers may drive this PTC phenotype [87]. More recently, a meta-analysis of 14 clinical studies have identified 13% of PTCs in early treated individuals in contrast to 4% in chronic treated ones. In this case, PTCs were defined as ≤ 400 HIV RNA copies/mL for at least two thirds of the time points and who remained off ART for at least 24 weeks. In this study, they also identified a transient increase of viral load ≥ 10.000 HIV RNA copies/ml in many PTCs, suggesting that a certain amount of viral load might be needed to achieve a subsequent immune control of HIV-1 [88]. Therefore, the use of stricter thresholds in clinical interventions of T-cell vaccination, like NCT02919306 (Mosaic HIV-1 vaccine) [97] or NCT02616874 (BCN02) [94], may have missed the identification of more PTCs. In this line, a recommendation guideline for ATIs was published in 2019 to ensure participants safety and render the different clinical trials more comparable. These guidelines suggest a pVL $\geq 10,000$ HIV RNA copies/ml for 4 weeks, a pVL $> 100,000$ HIV RNA copies/ml, or CD4 counts < 350 cells/ul as ART resumption criteria, among others [88]. At the same time, an intense monitoring of viral load and CD4 counts is necessary during treatment interruptions. Importantly, such ATIs should also include the study of biomarkers to predict the viral control when therapy is stopped, ideally before actual treatment interruption, to identify robust predictive biomarkers that can be translated into clinical practice in the long run [88].

4. Systems Biology and omics studies to guide future HIV cure interventions

4.1. Systems biology

The advent of high-throughput molecular technologies over the last years has led to an increase in the number of studies assessing simultaneous measurement of multiple biomolecules, generating data at different biological levels: the genome, the transcriptome, the epigenome, the proteome, the metabolome or the microbiome level among others (Figure 11). Such datasets allow to approach scientific questions from a different perspective: while typical experimental designs have a clear hypothesis, in this

type of analysis the focus is on discovery, i.e. the generation of new hypothesis guided by the knowledge generated in the analyses but which need to be tested afterwards experimentally. Also, many of these analyses aim to identify biomarkers to classify individuals in different groups of interest, or to predict the response to a treatment.

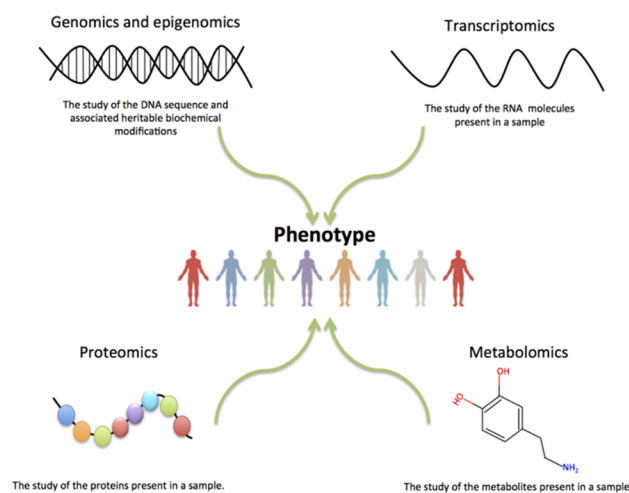


Figure 11. Omics data. Omics data have emerged from the study of the changes in DNA Sequence, gene expression, proteins, metabolites, etc. as a whole, leading to the generation of different omics datasets that aim at better characterizing the heterogeneity of the human population in different settings. Image from Burke M, Huerta L. Functional genomics (I): Introduction and designing experiments. European Bioinformatics Institute (EMBL-EBI); 2016. DOI: 10.6019/tol.fungeni-c.2016.00001.1 under CC BY 4.0 license.

These data are generated using different tools such as microarrays and next generation sequencing (NGS) in the fields of (epi-)genomics and transcriptomics, and Mass Spectrometry (MS) and Nuclear magnetic resonance (NMR) for proteomics and metabolomics studies. Nevertheless, array-based techniques have been widely used in the proteomics field as well [117,118].

4.1.1. Microarrays

Microarrays allow the assessment of multiple entities at the same time and are normally arranged in rows and columns in a solid support that contains different probes, and the nature of such probes determines the type of molecules it will detect. Focusing on gene expression microarrays, these contain oligonucleotides to detect mRNA molecules. Briefly, for use in transcriptomics microarrays, RNA is isolated from the cell/tissue of interest and a sample quality control step is performed to determine the quantity and quality of the RNA sample. Next, RNA is retro transcribed to cDNA and amplified,

followed by an *in-vitro* transcription to produce labelled complementary RNA (cRNA). cRNA is then fragmented and hybridized onto the microarray. After microarray washing and staining, the microarray is scanned, and an image is being generated. The image is then translated into an intensity file which, in turn, is converted to a numeric matrix with genes in rows and samples in columns, each position quantifying gene expression [119–123].

For DNA methylation microarrays, DNA is isolated from samples and treated with bisulfite to convert unmethylated cytosines to uracil, while methylated cytosines remain as cytosines. Then, bisulfite-treated DNA is amplified, fragmented and hybridized to the DNA methylation array like the HumanMethylation450K array from Illumina. Finally, an intensity file is obtained that informs about the intensity of the methylated or the unmethylated signal. In general, in DNA methylation studies, the Beta and the M values are used. While the Beta value makes reference to the methylation ratio ($\text{Intensity methylated signal} / (\text{Intensity Unmethylated signal} + \text{Intensity Methylated signal} + 100)$) and takes values between 0-1, the M value is the logit transformation of the Beta value [124,125].

In the context of proteomic studies, arrays have also been widely used, especially antibody arrays which are based on antigen-antibody binding, and therefore are an extension of the Enzyme-Linked ImmunoSorbent Assay (ELISA). Normally, different antibodies are bound to the solid phase of the array, which will bind the sample proteins to analyze. Then these bound proteins are recognized by a secondary antibody linked to a biotin which is then detected with streptavidin conjugated with a fluorophore that allows for signal amplification [118,126]. An alternative that has appeared more recently is the combination of immunoassays with the proximity extension assay (PEA). In this case, pairs of antibodies are linked to corresponding oligonucleotides. Once the target protein is bound by both antibodies, their oligonucleotides labels hybridize and serve as a template for DNA polymerase, which then is amplified by PCR [127]. The continuous technical evolution in protein microarrays and the increased use in different fields demonstrate the applicability of these technologies [128–131].

4.1.2. Next Generation Sequencing

Next generation sequencing (NGS) has revolutionized the transcriptomics field with the emergence of RNA-Seq. RNA-Seq offers several advantages in contrast to microarrays: experiments have higher resolution, lower background noise, they allow determination of a wider dynamic range of the gene expression levels (so that also low expressed genes can be detected), they are not restricted to genes in the microarray, and they require lower amount of starting RNA material. Additionally, RNA-Seq also allows for additional analyses, including the identification of different SNPs or splicing variants. However, RNA-Seq is still more expensive than microarrays, it requires more computational power and the data analysis is less standardized than that for microarrays [132,133].

In RNA-Seq, similar to microarrays, RNA is extracted and a quality control step is performed. Then, a sample can be enriched by mRNAs by using a capture poly A tail, or alternatively, to study non-coding genes as well, the ribosomal RNA (rRNA) can be depleted. Then, RNA is fragmented (300-500bp approx.) and converted to cDNA fragments, which are tagged with adapters that serve as the primer for PCR amplification. Finally, the different amplified fragments are sequenced. After sequencing, a collection of RNA-Seq reads is obtained, which are aligned to the genome of reference. Finally, for each gene, the number of reads that map to the gene in question is determined and translated into a numeric matrix. In this case, the number of counts that map to each gene can be translated to the gene expression levels after normalization steps [133,134].

4.1.3. Statistical analyses in omics data

The statistical design is the starting point of any -omics analysis, although it is generally constraint by limited sample size, economic resources or both. However, it is important that comparison groups in the design are well-balanced in terms of sex, age and other potential confounders between the two groups. Similarly, if samples need to be processed in different batches, it is important to distribute the individuals in each group equitably in each batch [135], so that later on, this information can be included in statistical analysis to identify and adjust for potential batch effects.

Introduction

A typical pipeline in -omics data analysis includes a quality control step which is followed by data normalization, filtering, and the identification of differentially expressed genes (DEGs) between groups of interest (or differential abundant proteins, or differential methylation, etc.). Finally, the list of DEGs is used in functional analyses to gain insight into the biological pathways or processes differentially regulated between groups [119].

In the quality control step, it is determined whether any sample should be removed from the analysis (e.g. outlier) or whether possible technical sources of variation or other batch effects need to be considered in downstream analyses. This can be done with different exploratory analysis techniques like boxplots and density distributions, hierarchical clustering and principal component analysis (PCA). Next, the data need to be normalized to make the samples comparable by minimizing the differences due to the systematic bias or technical noise, while maintaining the true biological differences. Therefore, for each -omics data type, different normalization methods have been used and developed. The next step is the identification of differential expressed/abundant features between comparison groups. In these steps, a non-specific filtering can be applied *a priori* to eliminate those features that are not expected to be differential between conditions to reduce noise. Then, different statistical tests can be applied to determine differential gene expression, protein abundance, DNA methylation, etc. [119,123,136,137]. In fact, the R/Bioconductor repository includes many different packages with workflows of analysis for the different type of data, such as limma R/Bioconductor which has been widely-used in transcriptomics analysis, and that includes methods for normalization steps, and the linear models to identify differential gene expression in microarrays or RNA-Seq [122,123]. Other packages like edgeR and DESeq2 are also commonly used for the analysis of RNA-Seq data [138,139]. Finally, pathway enrichment analyses are usually performed to gain deeper insights into the biological mechanisms modulated by the list of features [140]. On the one hand, hypergeometric tests are useful to determine whether a list of differentially expressed genes is over- or under-represented among the genes annotated in specific pathways. In parallel, Gene Set Enrichment Analysis (GSEA) requires a list of genes ranked

according to the differential expression, to determine whether the genes in a pathway are preferentially found in the top or in the bottom of the ranked list of genes [140].

The omics data analysis can also be used to identify features to classify individuals in different groups or to predict a continuous value (e.g. viral load). However, in the analysis of large data, there is the challenge of high-dimensional data, meaning there is a larger number of predictors than samples ($p \gg n$) which complicates the model selection and its evaluation. Thereby, methods different from those applied in classical variable selection (Forward and backward stepwise regression) are preferred to construct the model, such as shrinkage methods like lasso penalization, in which the variables with small contribution to the model are reduced to zero. Other methods like random forest models or partial least square discriminant analysis (PLS-DA) have been previously used in omics studies for variable selection and to build classification models as well [141–144]. Importantly, to avoid overfitting problems, building a classifier too dependent on the dataset of study, this process is normally done with k-fold cross validation: the dataset is divided into k parts and each time k-1 parts are used as the training set, which are the parts of the dataset used to build the model, and the kth serves to evaluate the model (Figure 12). Additionally, this process can be done iteratively a number of times to select the best model.

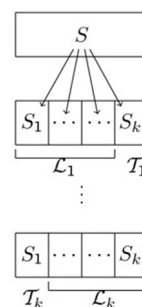


Figure 12. k-fold cross-validation in the construction of a classifier. The dataset is split into k parts (S_1, \dots, S_k), then each time one part is used as the test set (T) and the rest are used as the learning set (L). The L is used to build the model which is then evaluated in T. Such process can be done iteratively to determine which predictors are selected a higher number of times. Image from M Slawski, M Daumer and A-L Boulesteix. CMA – a comprehensive Bioconductor package for supervised classification with high dimensional data. BMC Bioinformatics 2008. <https://doi.org/10.1186/1471-2105-9-439> under CC BY 2.0 license.

Currently, the packages like the CMA R/Bioconductor or caret R/CRAN allow to test different classification models and then to compare among them and select the best

one. Finally, an external dataset would be necessary to evaluate the performance of the classifier [143,145].

There is an increasing interest to combine different -omics layers of information to better capture the drivers of the variety in the immune response to an infection, vaccine or autoimmune disease, and other specific settings of research. Such studies require good study designs to integrate the different types of data with different integration approaches. While some studies are integrated at the conceptual level, that is to analyze omics datasets individually and then integrate them on the basis of current knowledge, others have been based on correlation analyses, although this is not always successful. For instance, although it is expected that gene expression of a protein coding gene is positively correlated with the protein level, this is not always the case due to post-transcriptional regulation mechanisms or simply, for the different timing of regulation mechanisms to take place [146]. To conduct statistical integrative analyses, dimension-reduction techniques are amongst the most used methods, like the extension of partial least squares discriminant analysis (PLS-DA) applied in MixOmics R/Bioconductor [142,147]. Other integration analysis have been performed at the pathway level, especially when a specific pathway appears to be dysregulated in more than one omics datasets [146]. Finally, it is also necessary to integrate omics data with other data types like clinical, immunological or virological variables in order to build predictive biomarkers that can capture the heterogeneity of human systems. Therefore, the development of novel statistical methods to overcome current challenges of integrative analyses, and the standardization of the used models are needed to make studies comparable and improve the subsequent biological interpretation [148].

4.2. Systems immunology

Studies in human blood and plasma have been extensively used as a surrogate of the immune processes. Such coupling of high-throughput technologies like omics data together with blood analysis and clinical parameters have enabled to obtain deeper insights into the immune mechanisms triggered by the different perturbations induced by infection, vaccination or other mechanisms. Additionally, these studies have set off

an iterative process in which systems biology analysis provide information to generate new hypothesis (discovery-based science) that can guide experimental designs to fine-tune current immune therapies and develop novel strategies [141,149]. A recent example of this is a study in tuberculosis (TB) in which, the transcriptomic analysis in lymph node and in a TB granuloma model allowed to identify SphK1 as a therapeutic target, as its inhibition in a model of 3D collagen model showed a suppression of *Mycobacterium tuberculosis* growth but also, a decrease in the inflammatory secretion of monocytes [150]. Similarly, a human systems vaccinology study to the inactivated influenza vaccine (TIV) unveiled a correlation between early expression of TLR5 and the magnitude of the antibody response. A TLR5^{-/-} mice model showed that these animals had lower antibody titers upon vaccination, and suggested this could be due to the inability of these animals to sense microbiota. Effectively, the vaccination in animals treated with antibiotics showed lower antibody response, which could be rescued by the administration of a flagellated *E.Coli* strain. These results showed a role of the gut microbiota on the immune response to vaccination [151], and serve here as example of how systems biology analysis and experimental set up can advance our knowledge.

4.2.1 Transcriptomics and proteomics-based biomarkers of HIV-1 control

As mentioned before in this introduction, many host factors are associated with HIV-1 control, although they are only explicative of this control in a subset of these individuals. To this end, several large-scale studies, mainly based on gene expression or targeted proteomics, have tried to identify specific signatures of HIV-1 control. One of these first analyses (microarray-based) identified 322 upregulated and 136 downregulated genes in T cells of LTNPs in contrast to HIV-1 infected individuals with uncontrolled infection. While upregulated genes were involved in cell cycle, DNA damage and DNA replication, the downregulated ones were enriched in biological processes such as cytokine-cytokine interaction or the control of apoptosis [152]. More recently, a RNA-Seq analysis on PBMCs of EC and LTNPs identified a signature of 20 genes to predict HIV-1 disease progression [153]. Another study from 2018 combined the use of transcriptomics and targeted proteomics in PBMCs and plasma, respectively, in elite controller (ECs) individuals, viremic progressors (VPs) and healthy controls (HCs). In this study, 270 genes

were differentially expressed between ECs and VPs, and were largely involved in pathways like programmed cell death or response to cytokines among others. In the same study, 33 soluble factors clustered samples into two groups: one with mainly ECs and HCs, and a second one with VPs [154]. These are examples of how different studies have identified specific transcriptomics and proteomic signatures that are different according to HIV-1 control levels and which may unveil novel mechanisms that could be therapeutically leveraged to achieve a functional HIV cure.

4.2.2 Systems vaccinology in HIV-1

The first systems vaccinology studies emerged in 2008 in the context of yellow fever vaccine (YF-17D) [155,156]. In one of them, a PBMCs gene signature on innate and antiviral immunity was unveiled the transcription factors STAT1, IRF7 and ETS2 were identified as the master regulators [155]. In parallel, another study identified a gene signature predictive of neutralizing antibodies, and a different one predictive of vaccine-specific CD8 T-cell responses [156]. Since then, many other studies have been performed in the context of different immunizations like Influenza vaccine [157,158], Malaria vaccine [159] as well as in HIV-1 vaccine candidates [160–163] and have identified gene expression signatures associated with protective immune responses and identified new mechanisms of protection.

One of the HIV vaccine studies that have employed integrated omics analyses is the RV144 clinical trial. This prophylactic HIV vaccine trial evaluated the efficacy of a prime-boost HIV-1 vaccine strategy and observed a 31.2% reduction in HIV-1 acquisition in vaccinees compared to placebo recipients. The transcriptomics study of PBMCs from trial participants identified an upregulated transcriptional program associated with the IRF7 activation and the subsequent antiviral response in vaccinated individuals who remained uninfected. On the contrary, individuals either in the vaccination or the placebo group who became infected showed a transcriptional program involving NF- κ B and mTORC1 activation [161]. In another vaccine study (NCT01966900), a different transcriptional program was identified in individuals who elicited high or low levels of vaccine-specific antibodies after vaccination with CN54gp140 adjuvanted with TLR4

[160]. Finally, a systems biology approach applied to samples from the CUTHIVAC-003 clinical trial, showed that healthy volunteers who were vaccinated intramuscularly with the MVA-B vaccine candidate, had a major dysregulation of the gene expression a day after vaccination, and that genes involved in the IL-6 and interferon response were correlated with the strength of the humoral immune response (nAbs) to the vaccine [162]. Interestingly, a recent analysis using an integrated approach combining microbiome and transcriptome data of the participants on the same trial, identified baseline signature explicative of the humoral response, indicating that such analyses have the potential to identify the biological mechanisms associated with the vaccine immunogenicity and efficacy [163]. Together, these observations strongly support the use of systems vaccinology analysis to obtain a better comprehension of the genes associated with the immunogenicity but also, to identify molecular correlates of immune control, which in many cases have not been identified with classical immune-monitoring techniques. In the long run, it is also expected to identify biomarkers of vaccine efficacy and being able to define the differences between vaccine responders and non-responders in order to improve vaccination strategies.

4.3. Epigenetics, DNA methylation biomarkers and HIV-1 infection

The study of epigenetics have allowed to fill a gap in the knowledge between genetics and the environment or the lifestyle of individuals and therefore, have added a new layer of information to disease variability [164,165]. Among the different epigenetic modifications, DNA methylation is particularly accessible for -omics analyses as it offers technical stability and has been demonstrated to be robust and with the potential to identify specific epigenetic biomarkers of disease/health [164,166,167].

Briefly, DNA methylation studies are focused on the study of cytosine methylation, which mainly occurs in CpG islands, which are regions of about 200 base pairs with 50% minimal guanine and cytosine content. These are commonly located at promoters and gene regulatory regions, where high methylation levels are associated with gene silencing because the binding of the transcriptional machinery is impeded. This can also occur in CpG islands shores, which are found 2 kilobases away from CpG islands and are

Introduction

as well associated with gene silencing. In parallel, methylation in gene body regions allow to ensure gene transcription elongation, therefore positive correlations between gene expression and DNA methylation levels can be observed for some of these sites as well (Figure 13). Also, DNA methylation can hinder the binding of specific transcription factors, or on the contrary, can promote the binding of methyl-CpG-binding domain (MBD) proteins which then can trigger other silence epigenetic mechanisms through histones modifications or chromatin remodeling complexes [165,168].

The majority of systems biology studies on PLWH have relied on transcriptomic analysis, but more recently the study of DNA methylation or other epigenetic processes have gained importance in the HIV-1 field. As reported before in this introduction (section 2.3), HIV-1 is integrated into the host genome and infected cells can be maintained in latency through the interplay of different epigenetic factors. Focusing on DNA methylation, DNA Methyltransferases (DNMTs), the enzymes that catalyze the transfer of a methyl group to DNA, are increased upon infection. While DNMT1 is increased by the expression of early HIV-1 viral proteins, DNMT3 is upregulated by the Tat protein [169–171]. Additionally, DNA methylation also plays a key role in the regulation and the plasticity of immune cells during the hematopoietic process and when they are differentiating into different immune cell subsets like Th1 or Th2 cells. Specifically, DNA methylation poises the immune cells to rapidly respond upon an external stimuli and to define the T-cell lineage commitment according to the received stimulus [168]. Therefore, the study of host DNA methylation can unveil novel mechanisms associated with the natural control of HIV-1 infection and provide new biomarkers of such control.

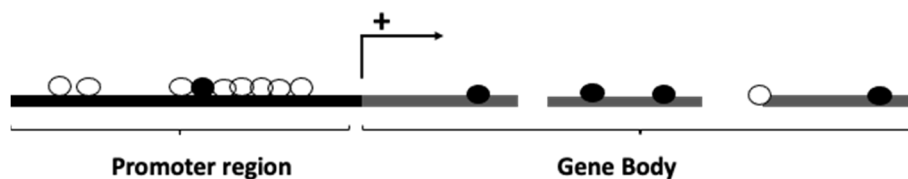


Figure 13. DNA methylation in active transcription. In actively transcribed genes, the CpG islands in promoter regions are generally hypomethylated to allow the binding of transcriptional machinery, while the gene body tend to be generally methylated to ensure gene elongation and to avoid spurious transcription initiation. In the image a blank dot makes reference to unmethylated CpG site, while a filled dot makes reference to a methylated CpG site. This image is made by Bruna Oriol-Tordera based on published information. [165]

A blood DNA methylation study comparing HIV+ and HIV- individuals identified 20 CpG sites with differential methylation levels between the two groups [172]. The same team of researchers, showed more recently, the feasibility to use DNA methylation among PLWH to predict mortality risk [173]. Another study showed that chronic HIV-1 infection increased the biological age by 5 years and that hypomethylation of the HLA system was predictive of a lower CD4/CD8 ratio, which is an indicator of poor immune recovery [174]. Finally, the comparison of PBMC DNA methylation in a pair of monozygotic twins, one HIV-infected and the other uninfected, suggested that HIV-1 infection increases global DNA methylation levels. Additionally, this study also showed an epigenetic regulation of *IGFBP6* and *SATB2*, which were hypermethylated in HIV-infected twin. The physiological relevance of these results were confirmed in cell line models of HIV-1 infection and in independent cohorts of PLWH [175].

Finally, in vaccinology field, the study of DNA methylation has also contributed to gain a better understanding of vaccine responsiveness. In the case of Influenza vaccination, the methylation of a group of CpGs, including CpGs in the gene body of *HLA-B* and *HLA-DQB2* molecules, have been associated with a low or high humoral response [176]. Similarly, a study in BCG vaccination showed that the basal DNA methylation state was predictive of the response to vaccination [177]. Therefore, the use of DNA methylation to better understand the response to immune therapies in the context of HIV-1 infection can be expected to contribute to refine existing therapeutic strategies and to propose new ones, as well as to identify biomarkers of post-treatment control.

Hypothesis and objectives

HIV-1 infection can be effectively treated with combination ART. Such treatment allows to suppress viremia and block progression to AIDS, but cannot eliminate the HIV-1 virus from the body. Additionally, when ART is stopped, viral load rapidly increases in infected individuals due to the capacity of HIV-1 to establish a latent HIV-1 reservoir. Therefore, HIV-1 infected individuals need to be chronically treated with ART and cannot be effectively cured of the infection. To achieve an HIV-1 cure, a better understanding of HIV-1 natural control, HIV-1 pathogenesis and the response to different HIV-1 cure interventions is essential to refine current HIV-1 cure strategies and to develop new ones. To this end, in the present thesis we propose the use of systems biology, based on different complementary -omics technologies, to identify the gaps in the knowledge of HIV-1 control, both, in the context of natural infection and upon a kick-and-kill intervention. In the HIV-1 field, the study of host epigenome through DNA methylation is especially appealing since HIV-1 viral infection can affect the epigenetic landscape, but also the regulation of the immune response is tightly linked to epigenetic mechanisms.

Therefore, the **main hypothesis** of the present thesis is that the omics-based assessment of human samples from HIV-1 infected individuals, and especially the study of the host genome-wide DNA methylation, can yield valuable information to identify host biomarkers of HIV-1 control and to improve future HIV-1 cure strategies.

In line with this hypothesis, the **main objective** is the identification of host factors (epigenetically regulated or not) associated with HIV-1 control either in a setting of HIV-1 natural infection or when a kick-and-kill intervention is applied.

The specific objectives in each of the chapters are:

Chapter I. Methylation regulation of Antiviral host factors, Interferon Stimulated Genes (ISGs) and T-cell responses associated with natural HIV control.

1. Identification of differentially methylated host factors between untreated chronically HIV-1 infected individuals with different levels of HIV-1 control,

- selection of candidate factors with the best classification capacity, and functional analysis of the selected markers.
2. Integration of differentially methylated host factors with viral, clinical and immunological parameters to identify relevant methylation imprints that explain the differential levels of spontaneous HIV-1 control
 3. Validation of specific methylation imprints at gene expression level in the cohort of study and in unrelated cohorts.

Chapter II. TL1A-DR3 Plasma levels are predictive of HIV-1 disease control, and DR3 costimulation boosts HIV-1-specific T-cell responses.

1. Identification of plasma factors discriminative of individuals with different HIV disease phenotype in a cohort of untreated, chronically HIV-1 infected individuals.
2. Selection of lead candidates associated with HIV-1 control, validation in unrelated cohorts and integration with virological and immunological data.
3. *In vitro* validation of lead candidates with the potential to be used in therapeutic strategies.

Chapter III. Host DNA methylation is associated with ATI outcome in the kick-and-kill therapeutic vaccine BCN02 clinical trial

1. Identification of the impact of vaccination and romidepsin administration on the host transcriptional and epigenetic (DNA methylation) programs in PBMCs of participants in the BCN02 clinical trial.
2. Evaluation of the effects of romidepsin administration alone (without vaccination) on the transcriptome of isolated CD4 and PBMCs from the REDUC clinical trial.
3. Identification of the capacity of DNA methylation or gene expression signatures to predict the differential viral rebound kinetics before the monitored antiretroviral pause is started.

Chapter I

Methylation regulation of Antiviral host factors, Interferon Stimulated Genes (ISGs) and T-cell responses associated with natural HIV control.

Oriol-Tordera B¹, Berdasco M^{2,3}, Llano A¹, Mothe B^{1,4,5}, Gálvez C¹, Martínez-Picado J^{1,4,6}, Carrillo J¹, Blanco J^{1,4}, Duran-Castells C¹, Ganoza C^{7,8}, Sanchez J^{7,9,10}, Clotet B^{1,4,5}, Calle ML⁴, Sanchez-Pla A^{11,12}, Esteller M^{3,6,13,14}, Brander C^{1,4,6,15} [¶], Ruiz-Riol M¹ ^{¶*}

1. IrsiCaixa AIDS Research Institute, Hospital Germans Trias i Pujol, Institute for Health Science Research Germans Trias i Pujol (IGTP), Badalona, Spain
2. Cancer Epigenetics and Biology Program (PEBC), Bellvitge Biomedical Research Institute, L'Hospitalet de Llobregat, Barcelona, Spain
3. Josep Carreras Leukaemia Research Institute (IJC), Badalona, Spain
4. University of Vic - Central University of Catalonia, Catalonia, Vic, Spain
5. Fundació Lluita contra la Sida, Infectious Disease Department, Hospital Universitari Germans Trias i Pujol, Badalona, Spain
6. Catalan Institution for Research and Advanced Studies (ICREA), Barcelona, Spain
7. Asociación Civil IMPACTA Salud y Educacion, Lima, Peru
8. Alberto Hurtado School of Medicine, Universidad Peruana Cayetano Heredia, Lima, Peru
9. Department of Global Health, University of Washington, Seattle, USA
10. Centro de Investigaciones Tecnológicas, Biomédicas y Medioambientales, CITBM,
11. Lima, Peru
12. Statistics Department, Biology Faculty, University of Barcelona, Spain;
13. Statistics and Bioinformatics Unit Vall d'Hebron Institut de Recerca [VHIR], Spain
14. Centro de Investigacion Biomedica en Red Cancer (CIBERONC), Madrid, Spain.
15. Physiological Sciences Department, School of Medicine and Health Sciences, University of Barcelona (UB), Barcelona, Catalonia, Spain
16. AELIX Therapeutics, Barcelona, Spain

[¶]These authors contributed equally to this work.

This article has been published in: **PLoS Pathog.** 2020 Aug 6;16(8) DOI: <https://doi.org/10.1371/journal.ppat.1008678>



Institut de Recerca de la Sida

This declaration concerns the following manuscript:

Title: Methylation regulation of Antiviral host factors, Interferon Stimulated Genes (ISGs) and T-cell responses associated with natural HIV control

Authors: Bruna Oriol-Tordera, Maria Berdasco, Anuska Llano, Beatriz Mothe, Cristina Gálvez, Javier Martinez-Picado, Jorge Carrillo, Julià Blanco, Clara Duran-Castells, Carmela Ganoza, Jorge Sanchez, Bonaventura Clotet, M.Luz Calle, Alex Sanchez-Pla, Manel Esteller, Christian Brander, Marta Ruiz-Riol.

Full reference of the article: Oriol-Tordera B, Berdasco M, Llano A, Mothe B, Gálvez C, Martinez-Picado J, Carrillo J, Blanco J, Duran-Castells C, Ganoza C, Sanchez J, Clotet B, Calle ML, Sánchez-Pla A, Esteller M, Brander C, Ruiz-Riol M. Methylation regulation of Antiviral host factors, Interferon Stimulated Genes (ISGs) and T-cell responses associated with natural HIV control. PLoS Pathog. 2020 Aug 6;16(8):e1008678. doi: 10.1371/journal.ppat.1008678. PMID: 32760119; PMCID: PMC7410168.

This Manuscript is: Published Accepted Submitted In preparation

The PhD student has contributed to the elements of this article/manuscript as follows:

- A. No or little contribution
- B. Has contributed (10-30%)
- C. Has contributed considerably (40-60%)
- D. Has done most of the work (70-90%)
- E. Has essentially done all the work

Formulation/identification of the scientific problem	A
Planning the experiments and methodology design and development	C
Involvement in the experimental work / data collection	C
Involvement in data analysis	D
Involvement in results interpretation	D
Writing the first draft of the manuscript	D
Finalization of the manuscript and submission	D

The PhD student has searched the relevant background literature to get involved in the project and to understand the scientific problem and to participate in the selection of the best approach for data analysis. The PhD student has been the responsible for data analysis, results interpretation and writing the first draft of the manuscript with the guidance of their directors and other co-authors.

Dr. Christian Brander (director)

Dra. Marta Ruiz-Riol (director)

Abstract

GWAS, immune analyses and biomarker screenings have identified host factors associated with *in vivo* HIV-1 control. However, there is a gap in the knowledge about the mechanisms that regulate the expression of such host factors. Here, we aimed to assess DNA methylation impact on host genome in natural HIV-1 control. To this end, whole DNA methylome in 70 untreated HIV-1 infected individuals with either high (>50,000 HIV-1-RNA copies/ml, n = 29) or low (<10,000 HIV-1-RNA copies/ml, n = 41) plasma viral load (pVL) levels were compared and identified 2,649 differentially methylated positions (DMPs). Of these, a classification random forest model selected 55 DMPs that correlated with virologic (pVL and proviral levels) and HIV-1 specific adaptive immunity parameters (IFN γ -T-cell responses and neutralizing antibodies capacity). Then, cluster and functional analyses identified two DMP clusters: cluster 1 contained hypomethylated genes involved in antiviral and interferon response (e.g. *PARP9*, *MX1*, and *USP18*) in individuals with high viral loads while in cluster 2, genes related to T follicular helper cell (Tfh) commitment (e.g. *CXCR5* and *TCF7*) were hyper-methylated in the same group of individuals with uncontrolled infection. For selected genes, mRNA levels negatively correlated with DNA methylation, confirming an epigenetic regulation of gene expression. Further, these gene expression signatures were also confirmed in early and chronic stages of infection, including untreated, cART treated and elite controllers HIV-1 infected individuals (n = 37). These data provide the first evidence that host genes critically involved in immune control of the virus are under methylation regulation in HIV-1 infection. These insights may offer new opportunities to identify novel mechanisms of *in vivo* virus control and may prove crucial for the development of future therapeutic interventions aimed at HIV-1 cure.

Author summary

The infection with the human immunodeficiency virus (HIV), as for other viral infections, induce global DNA Methylation changes in the host genome. Herein, we identified for first time the methylation impact on host genome in untreated HIV-1 infection with different degrees of *in vivo* virus control. Specifically, we observed that individuals with a better HIV-1 control showed a hypermethylation of genes associated with antiviral and

interferon pathways and the hypomethylation of genes associated with the differentiation process of T follicular helper cells. Interestingly, these epigenetic imprints in host genome were strongly correlated with virus content and HIV-specific T-cell responses. Therefore, we propose DNA Methylation as the regulation mechanism of host genes involved in immune HIV-1 control that could interfere in the efficacy of cure strategies. We also highlight the importance of DNA Methylation to regulate immune responses not only in HIV-1 but also in chronic infections or other pathologic situations associated with a sustained activation of the immune system.

Introduction

Treatment of HIV-1 infected individuals with antiretroviral drugs (combination antiretroviral therapy, cART) is highly effective in suppressing viral replication to undetectable levels. However, the virus persists in the body in form of a proviral reservoir in latently infected cells and cART needs therefore to be taken for life. Given that the access and adherence to the treatment might be limited, especially in low-income countries and considering the health consequences of long-term cART use, stigma and high costs, there is a need for the development of new strategies to achieve a so-called functional cure and/or interventions that can eliminate the virus from the body [1]. The study of the small-subset of HIV-1 controllers, i.e. HIV-1-infected people that can naturally maintain undetectable or low HIV-1 plasma viral load (pVL) without cART, have been of relevance to understand the mechanisms of spontaneous HIV-1 viral control [2]. Such control has been mainly linked to host factors, especially HLA genetics and antiviral immunity mediated by HIV-1-specific CD8 and CD4 T-cells, as well as to virological factors including viral mutations that reduce viral replicative fitness [3]. Despite this progress, there remain significant gaps in the understanding of spontaneous virus control and how the maintenance of HIV-1 latency can be broken [4,5].

For several viral infections, different epigenetic changes have been described in the genomes of both, the virus and the host [6]. Some of these epigenetic changes, in particular DNA methylation of genes, can be induced upon initial infection. The process is driven mainly by the increase of DNA Methyltransferases (DNMT), the enzymes that

catalyze the transfer of methyl groups to cytosine residues of DNA. At the level of viral DNA, several reports have suggested that the hypermethylation of 5'LTR regions of HIV-1 proviral is of relevance for latency maintenance [7]. In contrast, for methylation changes of host genes, most reports to date have assessed methylation levels of single host genes and only a few studies exist that determined DNA methylation of whole host genomes in HIV-1 infection [8–10]. Among these, the analysis of PBMC DNA methylation patterns in a pair of monozygotic twins sero-discordant for HIV-1 infection, revealed an overall increase in host DNA methylation in the HIV-1 infected compared to the HIV-1 uninfected twin [10]. A subsequent study that assessed differential DNA methylation patterns between HIV-1 infected and uninfected individuals, identified altered epigenetic regulation of host factors such as NLRC5 and LPCAT1 [9]. These studies indicate that HIV-1 infection may leave marked changes in the host DNA methylation patterns that could affect the expression of host factors involved in viral replication as well as in innate and adaptive immune defense. In light of ongoing efforts to restore effective antiviral immunity and achieve sustained functional cure of HIV-1 infection, it will be critical to i) identify such methylation-dependent epigenetic imprints in HIV-1 infection, ii) understand their effects on antiviral immunity and importantly, iii) find ways to not only transiently restore antiviral immune responses but to correct their underlying epigenetic dysregulation to achieve lasting cure [11].

In this report, full host-genome DNA methylation analysis in a cohort of HIV-1 infected individuals with variable ability to spontaneously control viral replication *in vivo*, reveal for the first time, key methylation signatures in peripheral blood predictive of HIV-1 plasma viral loads and proviral levels, as well as HIV-1-specific adaptive immunity, associated with natural HIV-1 control. Therefore, these data strongly support an important role of epigenetics as a regulation mechanism behind HIV-1 control that should be considered in future therapeutic strategies.

Results

Differential DNA methylation patterns in PBMC of untreated HIV-1 chronically infected individuals with variable levels of HIV-1 pVL

With the aim of determining DNA methylation patterns that could be predictive of viral control, PBMC isolated from 70 HIV-1 infected individuals were subjected to a genome-wide DNA methylation analysis. This cohort included a group of subjects with high (HIV-High; pVL >50,000 HIV-1 RNA copies/ml, n = 29) or low HIV-1 viral loads (HIV-Low; pVL <10,000 HIV-1 RNA copies/ml, n = 41).

After a pre-processing step (Fig 1A), 56,513 CpG positions were left to be analyzed for methylation differences between the two groups. A previously described linear model-based approach that adjusts for methylation confounders (including sex, age and estimated cell type proportion [9,12]) was combined with a correction for individuals' CD4 counts due to the significant differences between both groups for this parameter. This analysis identified a total of 3,671 differentially methylated positions (DMPs) considering a p-value < 0.05 as cut-off (Fig 1A). Only the DMPs between both groups of HIV-1 infected individuals that had a gene annotation (n = 2,649) were kept for further analyses. Of them, n = 1,668 (63%) were found in CpG Islands (CGIs) regions: including 29% in the island itself, 27.5% in CpG shores (2Kb from CGI), and 6.5% in CpG shelves (4 Kb from CGI). A total of n = 1,536 (58%) of DMP were localized in promoter regions of the genes (including TSS1500, TSS200, 5'UTR and 1st Exon regions), suggestive of a potential effect on gene expression levels [13]. Fig 1B shows 224 CpG positions hypomethylated (blue) and 910, hypermethylated (red) in HIV-High individuals. Overall, DMPs were widely distributed across the whole genome, with chromosomes 3, 11, 12 and 16 containing the highest number of DMPs relative to the number of analyzed CpG positions per chromosome (Chi-squared test, p < 0.05, Fig 1C). These data highlight that there exist distinct DNA methylation patterns widely distributed across the entire host genome that differentiate chronically HIV-1 infected individuals with spontaneous high or low pVL.

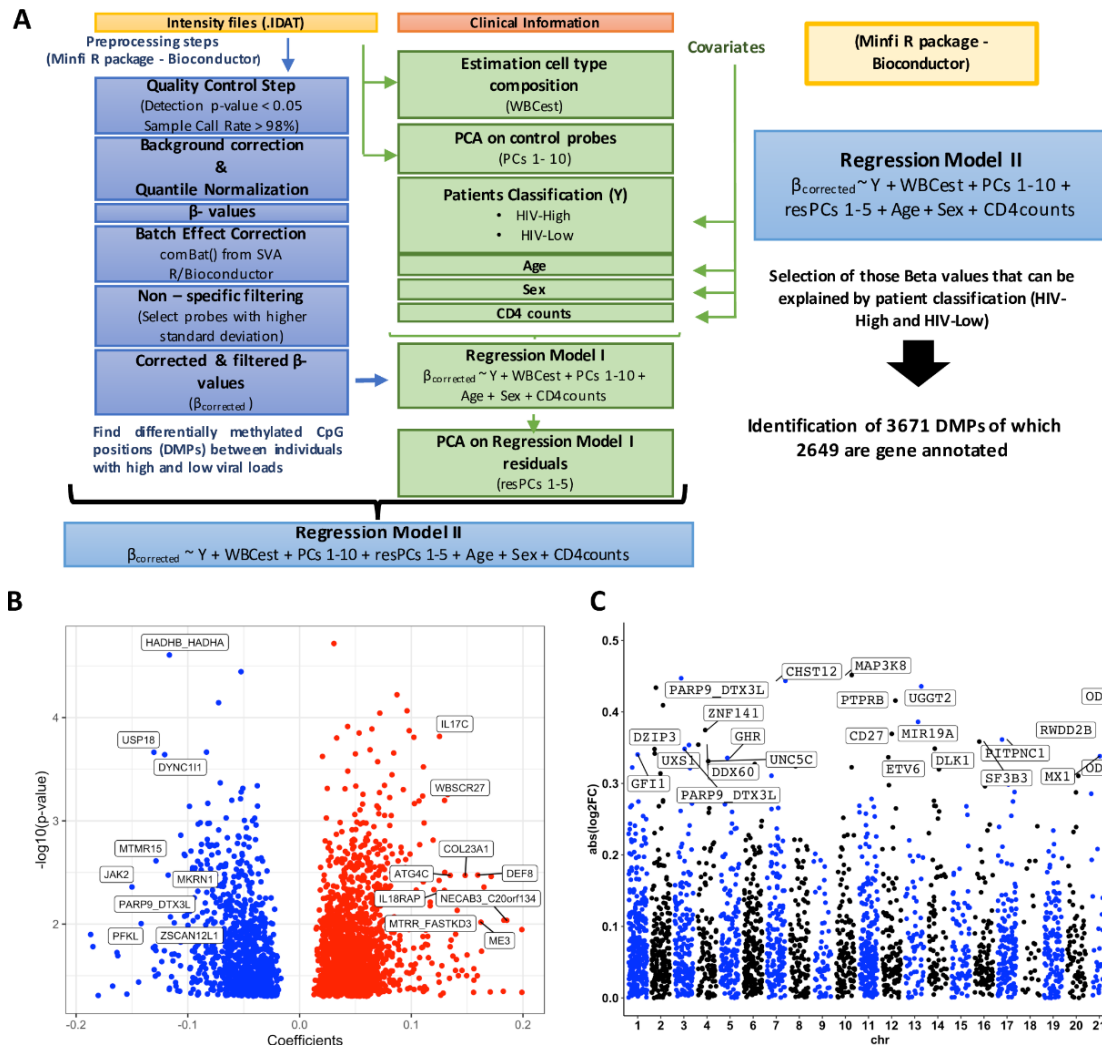


Fig 1. Differentially methylated CpG positions between HIV-1 infected patients with different ranges of plasma viral loads. (A) Analysis strategy for the identification of differentially methylated positions (DMPs). (B) Volcano Plot showing 2,649 gene annotated DMPs (p-value is shown in Y-axis and the regression coefficient from de model on the X-axis). Blue indicates hypomethylation and red, hypermethylation in HIV-High group. Labels indicate top 9 CpG sites with a coefficient higher than $|0.1|$ in HIV-High or HIV-Low. (C) The Manhattan Plot shows the identified DMPs, according the \log_2 Fold-Change (FC) (Y-axis) and their location on different chromosomes (X-axis).

Relative control of in vivo HIV-1 replication is associated with DMPs in gene encoding proteins involved in adaptive and innate immune responses

To select differentially methylated positions (DMPs) that could discriminate between individuals with high or low HIV-1 pVL and to be used in downstream analyses, we applied a random forest model with 1000 iterations and 5-fold cross-validations [14,15] on the 2,649 gene annotated DMPs (AUC = 0.92). This resulted in the identification of 55 DMPs, of which 26 (47%) were located in CpG islands of promoter regions (Table 1).

The most selected DMP, cg22930808, is located in the promoter of PARP9-DTX3L gene on chromosome 3 (hypermethylated in HIV-Low, Table 1).

The selected 55 DMPs clustered in two different groups that differentiate HIV-Low from HIV-High individuals (Table 1 and Fig 2A and 2B): Cluster 1 (Fig 2A) included 31 DMPs hypermethylated in HIV-Low individuals and cluster 2 (Fig 2B), included 24 DMPs hypomethylated in this same group. Gene ontology enrichment analysis (GEA) showed (Fig 2C and 2D, S3 Table) cluster 1 to be enriched for gene ontology (GO) categories involved in antiviral activity such as defense response to virus (GO:0051607, 6 genes), type I interferon signaling pathway (GO:0060337, 3 genes), or regulation of innate immune response (GO:0045088, 5 genes). In contrast, cluster 2 was represented by general immune activation GO categories including leukocyte activation (GO:0045321, 6 genes), T cell activation (GO:0042110, 4 genes), T cell differentiation (GO:0030217, 3 genes) or positive regulation of protein modification process (GO:0031401, 5 genes).

Overall, these data reinforce that the identified epigenetically regulated immune pathways of antiviral activity and innate immune activation are associated with HIV-1 pVL in the peripheral blood. Taken together, different levels of in vivo virus control are associated with markedly different methylation patterns of genes involved in antiviral innate and cellular adaptive host defense mechanisms.

Table 1. Classificatory CpG positions into the groups of HIV-High or HIV-Low

CpG position	Gene	Chr	Relation to Island	Relation to Gene	Mean Beta-value (HIV-Low)	Mean Beta-value (HIV-High)	p-value ^A	Frequency Random Forest ^B	Cluster	Expected Expression ^C
cg22930808	PARP9_DTX3L	chr3	N_Shore	5UTR_TSS1500	0.76	0.56	0.02	821	1	↓
cg20098015	ODF3B	chr22	S_Shore	TSS200	0.64	0.5	0.05	724	1	↓
cg01028142	CMPK2	chr2	N_Shore	Body	0.88	0.8	<0.01	643	1	-
cg23221113	ODF3B	chr22	S_Shore	5UTR_1stExon	0.29	0.22	0.02	613	1	↓
cg20939114	PITPNC1	chr17	OpenSea	Body	0.26	0.33	0.02	607	2	-
cg10152449	CHST12	chr7	S_Shore	5UTR	0.56	0.41	0.05	458	1	↓
cg02217713	PRKAR1B	chr7	N_Shore	Body	0.71	0.62	0.05	452	1	-
cg08122652	PARP9_DTX3L	chr3	N_Shore	5UTR_TSS1500	0.77	0.6	0.02	430	1	↓
cg02538772	SND1	chr7	OpenSea	Body	0.57	0.64	0.04	374	2	↑
cg15413523	TCF7	chr5	S_Shore	5UTR_1stExon	0.47	0.54	0.04	308	2	↑
cg20651018	CARS	chr11	OpenSea	Body	0.52	0.64	0.02	308	2	-
cg14392283	LY6E	chr8	N_Shelf	3UTR	0.84	0.76	0.02	301	1	-
cg13015616	HFE	chr6	OpenSea	TSS1500	0.61	0.71	0.03	264	2	↑
cg26005232	NUDC	chr1	N_Shore	TSS1500	0.48	0.56	0.04	240	2	↑
cg11224765	ODF3B	chr22	S_Shore	TSS200	0.58	0.48	0.01	231	1	↓
cg08863939	TLK1	chr2	OpenSea	5UTR	0.46	0.55	0.04	225	2	↑
cg08926253	IRF7	chr11	Island	Body	0.74	0.66	0.01	225	1	-
cg21535657	ETV6	chr12	S_Shelf	Body	0.32	0.25	0.01	168	1	-
cg04537602	CXCR5	chr11	OpenSea	Body_TSS1500	0.53	0.63	0.05	154	2	↑
cg02679745	C9orf139_FUT7	chr9	S_Shore	Body_TSS1500	0.64	0.56	0.03	148	1	↓
cg11477010	ANKFY1	chr17	OpenSea	Body	0.67	0.73	0.01	141	2	-
cg01190666	PRIC285	chr20	N_Shore	5UTR	0.72	0.66	0.02	126	1	↓
cg22862003	MX1	chr21	N_Shore	TSS1500_5UTR	0.75	0.62	0.05	124	1	↓
cg06981309	PLSCR1	chr3	N_Shore	5UTR	0.75	0.62	0.02	107	1	↓
cg02297838	MIR19A_MIR17HG	chr13	S_Shore	TSS1500_Body	0.52	0.4	0.02	106	1	↓
cg01774027	ARID3A	chr19	Island	Body	0.6	0.52	0.02	95	1	-
cg20631044	C19orf54_SNRPA	chr19	N_Shore	TSS200_TSS1500	0.68	0.61	0.03	95	1	↓
cg18338046	TCF7	chr5	S_Shore	Body	0.58	0.69	<0.01	90	2	-
cg01623438	CTSZ	chr20	S_Shore	TSS1500	0.66	0.6	0.01	89	1	↓
cg14293575	USP18	chr22	S_Shelf	5UTR	0.72	0.6	0.03	78	1	↓
cg06164260	BCL6	chr3	N_Shore	5UTR_TSS200	0.61	0.55	0.01	76	1	↓
cg19400179	DZIP3	chr3	OpenSea	5UTR	0.37	0.47	0.03	70	2	↑
cg02676052	LCP2	chr5	OpenSea	TSS1500	0.62	0.67	0.02	69	2	↑
cg14191134	LOC283050	chr10	S_Shore	Body	0.37	0.3	0.05	68	1	-
cg21549285	MX1	chr21	S_Shore	5UTR	0.77	0.61	0.01	67	1	↓
cg00808969	USP35_KCTD21	chr11	N_Shore	TSS1500_5UTR	0.41	0.48	0.01	66	2	↑
cg13298528	CXCR5	chr11	OpenSea	Body_TSS1500	0.57	0.67	0.04	60	2	↑
cg15065340	TNK2	chr3	N_Shelf	5UTR	0.7	0.62	0.03	58	1	↓
cg05883128	DDX60	chr4	N_Shore	5UTR	0.48	0.37	0.04	45	1	↓
cg19368911	KIF26B	chr1	OpenSea	Body	0.5	0.58	0.05	45	2	-
cg00688810	SHBG_FXR2	chr17	N_Shore	TSS1500_Body	0.72	0.78	0.04	43	2	↑
cg03043696	GNB1	chr1	N_Shore	5UTR	0.61	0.55	0	43	1	↓
cg10435235	ARHGGEF7	chr13	OpenSea	3UTR	0.74	0.69	0.03	42	1	-
cg27519392	CHD7	chr8	OpenSea	Body	0.63	0.71	0.03	40	2	-
cg26567688	COLAA3BP	chr5	OpenSea	Body	0.67	0.74	0.05	29	2	-
cg08179431	HFE	chr6	OpenSea	TSS1500	0.7	0.79	0.03	27	2	↑
cg12042587	GHR	chr5	N_Shore	TSS200	0.22	0.28	0.01	27	2	↑
cg22036538	CD27_LOC678655	chr12	OpenSea	1stExon_5UTR	0.34	0.44	0.02	27	2	↑
cg20321801	CD81	chr11	N_Shelf	Body	0.59	0.53	0.01	27	1	-
cg04858110	SCRN1	chr7	OpenSea	5UTR_Body	0.66	0.72	0.04	24	2	↑
cg12217560	TNFRSF19	chr13	OpenSea	1stExon_5UTR	0.51	0.58	0.04	21	2	↑
cg06872964	IFI44L	chr1	OpenSea	TSS1500	0.7	0.59	0.02	19	1	↓
cg07892167	R3HCC1	chr8	N_Shore	TSS1500	0.52	0.45	0.04	17	1	↓
cg14659511	DOCK9	chr13	OpenSea	Body	0.62	0.69	0.01	14	2	-
cg02385820	RINL	chr19	N_Shore	3UTR	0.71	0.67	<0.01	13	1	-

^A p-value of the regression model applied to determine DMPs.

^B CpG positions ordered according the frequency of selection by random forest model.

^C For CpGs in promoters, it is shown the expected gene expression in case of an epigenetic regulation. Values are relative to HIV-Low group.

Chr = Chromosome.

<https://doi.org/10.1371/journal.ppat.1008678.t001>

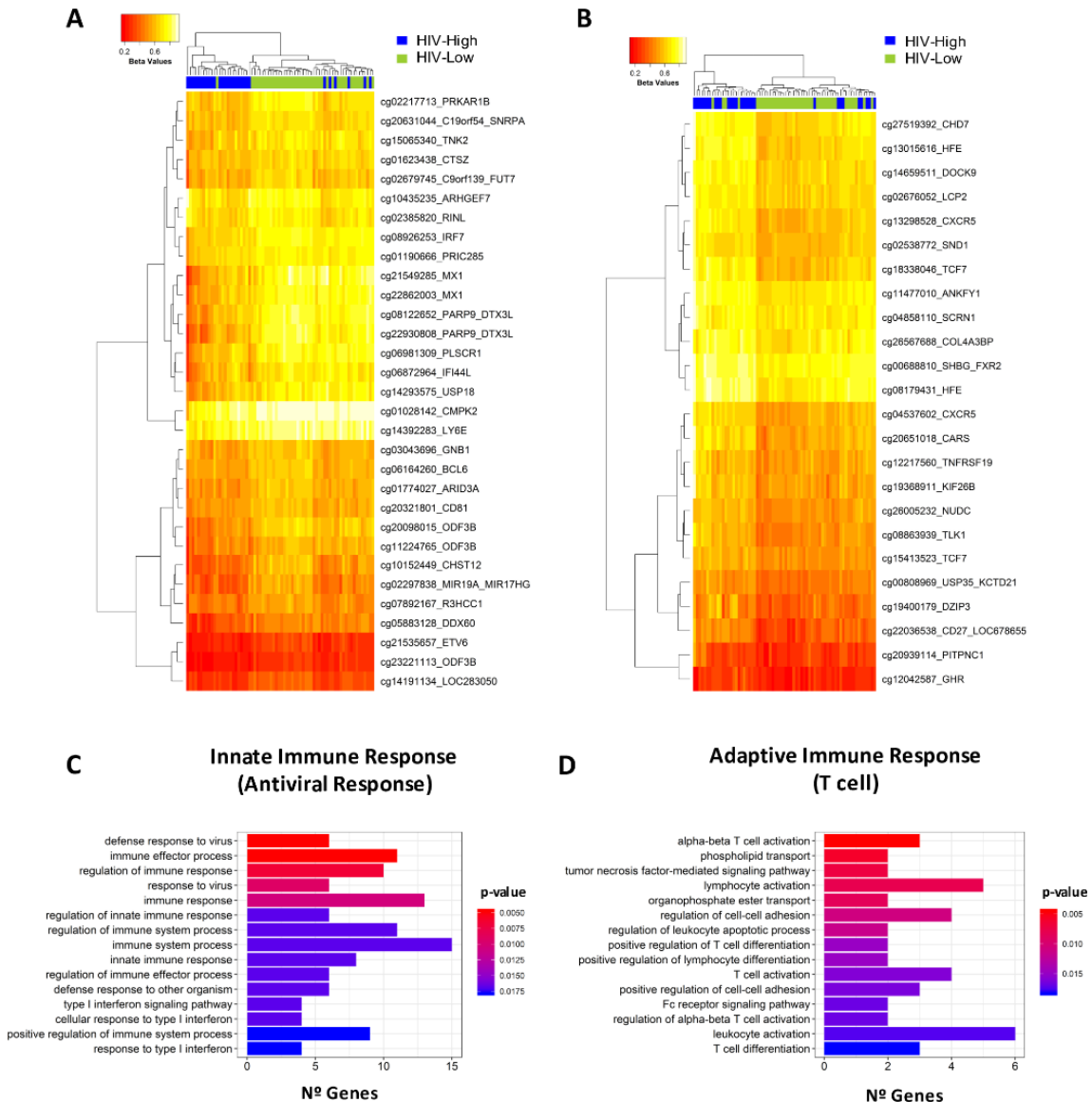


Fig 2. Relevant DMPs for classification in HIV-High and HIV-Low groups. Cluster analyses of the selected CpG positions for the classification of individuals (random forest model). Two clusters are showed in A and B as heatmaps that differentiate HIV-Low from HIV-High subjects. Distances are based on Manhattan and clustering, on complete linkage. Columns represent tested individuals, HIV-High (blue) and HIV-Low (green), and rows depict the Beta-values of the CpGs in each cluster. The colour scale from red to yellow represents from low to high methylation. (C-D) Histogram plots of the Gene Ontology Enrichment Analysis (clusterProfiler R/Bioconductor) for the two identified clusters (A and B) of DMPs. Pathways with the highest significance are shown; the complete output is in S3 Table.

Differential methylation patterns are associated with proviral levels and markers of adaptive host immunity to HIV-1

To determine whether the DMPs associated with additional immune and virological markers beyond pVL, we correlated the methylation levels of the 55 DMPs identified above with proviral (total HIV-1 DNA) in PBMC lysates and extensive immune data, including measurements of cellular and humoral immunity to HIV-1 (S1 Table). T cell

responses were determined by IFN γ ELISpot assay against overlapping peptides of the entire consensus B HIV-1 proteome, and levels of neutralizing Ab (nAb) in plasma were determined against the HIV-1 BaL laboratory adapted strain. Table 2 shows the correlation data (Rho values, $p < 0.05$, Spearman's rank correlation test) between the relevant CpG positions contained in the two clusters and the different virological or immune parameters assessed.

DMPs in cluster 1, related to antiviral defense and innate immunity, showed the highest correlations with HIV-1 pVL and proviral levels. Specifically, the DMPs with the strongest correlations were the ones in the promoter regions of the PARP9-DTXL3 (cg22930808 and cg08122652) and ODF3B genes (cg20098015, cg23221113 and cg11224765) that were also the most frequently selected in the random forest model (Table 2). The PARP9 CpG positions were also correlated with the rest of variables measured, including levels of HIV-1 specific T-cells and nAb activity. Interestingly, in the same antiviral response group, PARP9 (Fig 2B) clustered together with DMPs in MX1 (cg22862003), IRF7 (cg08926253), PLSCR1 (cg06981309), USP18 (cg14293575) and IFI44L (cg06872964), all genes which were also correlated with HIV-1 pVL and proviral (Table 2). Additionally, the methylation levels of the CpG positions in MX1, IRF7 and PLSCR1 were related to the magnitude and breadth of the HIV-1-specific T-cell immune responses (Table 2). With the exception of USP18, all these genes were annotated in the functional category response to virus (GO:0009615) and immune effector processes (GO:0002252) among others (S3 Table). In addition, USP18 was annotated together with MX1, IRF7 and PARP9 in the functional category of genes involved in the regulation of defense response (GO:0031347) and, with MX1 and IRF7, in the category response to type I interferon (GO:0034340).

Table 2: CpG positions correlation with virological and immunological parameters.

CpG	Gene	Cl	Freq. Random Forest	Viral Load (plasma HIV RNA copies/ml)		Proviral DNA		CD4 Counts		CTL Breadth		CTL Magnitude		nAb BaL	
				Rho	p-value	Rho	p-value	Rho	p-value	Rho	p-value	Rho	p-value	Rho	p-value
cg22930808	PARP9 DTX3L	1	821	-0.73	9.39E-13	-0.59	2.20E-06	0.59	7.47E-08	0.36	4.09E-03	0.37	2.62E-03	-0.43	9.34E-04
cg20098015	ODF3B	1	724	-0.69	4.86E-11	-0.51	7.45E-05	0.53	2.36E-06	0.32	1.14E-02	0.34	6.17E-03	-	-
cg01028142	CMPK2	1	643	-0.61	1.53E-08	-0.46	4.79E-04	0.47	4.14E-05	-	-	0.29	2.00E-02	-	-
cg23221113	ODF3B	1	613	-0.74	3.87E-13	-0.56	8.55E-06	0.52	4.87E-06	0.37	2.63E-03	0.39	1.60E-03	-	-
cg10152449	CHST12	1	458	-0.68	7.47E-11	-0.54	2.56E-05	0.58	1.19E-07	0.44	2.92E-04	0.40	1.29E-03	-0.30	2.15E-02
cg02217713	PRKAR1B	1	452	-0.69	4.21E-11	-0.57	6.60E-06	0.60	3.88E-08	0.43	4.27E-04	0.33	8.85E-03	-0.26	4.66E-02
cg08122652	PARP9 DTX3L	1	430	-0.69	4.61E-11	-0.53	3.35E-05	0.55	9.54E-07	0.29	2.30E-02	0.31	1.43E-02	-0.43	7.51E-04
cg14392283	LY6E	1	301	-0.71	4.64E-12	-0.60	1.14E-06	0.48	3.23E-05	0.26	3.71E-02	0.30	1.60E-02	-0.22	-
cg11224765	ODF3B	1	231	-0.66	3.45E-10	-0.56	9.95E-06	0.43	1.95E-04	0.31	1.29E-02	0.36	3.93E-03	-0.07	-
cg08926253	IRF7	1	225	-0.68	1.12E-10	-0.52	5.66E-05	0.51	8.22E-06	0.32	1.04E-02	0.31	1.49E-02	-0.30	2.27E-02
cg21535657	ETV6	1	168	-0.66	4.48E-10	-0.38	4.70E-03	0.45	8.15E-05	0.36	3.30E-03	0.30	1.52E-02	-	-
cg02679745	C9orf139 FUT7	1	148	-0.58	1.46E-07	-0.47	2.64E-04	0.47	4.25E-05	0.37	2.77E-03	0.28	2.90E-02	-	-
cg01190666	PRIC285	1	126	-0.60	5.22E-08	-0.42	1.38E-03	0.48	2.22E-05	0.35	5.29E-03	0.32	1.15E-02	-	-
cg22862003	MX1	1	124	-0.55	8.10E-07	-0.44	6.93E-04	0.51	8.20E-06	0.37	2.58E-03	0.37	3.14E-03	-	-
cg06981309	PLSCR1	1	107	-0.61	2.10E-08	-0.51	5.90E-05	0.43	2.27E-04	0.26	4.10E-02	0.33	8.66E-03	-	-
cg02297838	MIR19A MIR17HG	1	106	-0.64	2.00E-09	-0.52	4.05E-05	0.55	1.01E-06	0.37	2.55E-03	0.36	3.68E-03	-0.36	5.92E-03
cg01774027	ARID3A	1	95	-0.64	1.78E-09	-0.56	9.48E-06	0.61	1.95E-08	0.36	3.43E-03	0.33	7.40E-03	-	-
cg20631044	C19orf54 SNRPA	1	95	-0.58	1.28E-07	-0.53	3.24E-05	0.55	7.25E-07	0.37	2.94E-03	0.27	3.15E-02	-	-
cg01623438	CTSZ	1	89	-0.53	2.01E-06	-0.40	2.58E-03	0.48	3.08E-05	0.36	3.81E-03	0.32	1.12E-02	-	-
cg14293575	USP18	1	78	-0.61	2.46E-08	-0.39	2.92E-03	0.41	3.73E-04	-	-	-	-	-	-
cg06164260	BCL6	1	76	-0.59	9.08E-08	-0.48	1.83E-04	0.51	7.27E-06	0.34	6.43E-03	0.26	4.00E-02	-0.31	1.94E-02
cg14191134	LOC283050	1	68	-0.61	1.81E-08	-0.46	4.82E-04	0.55	6.36E-07	0.36	3.76E-03	0.30	1.80E-02	-	-
cg21549285	MX1	1	67	-0.54	1.43E-06	-0.36	6.96E-03	0.49	2.03E-05	-	-	0.27	3.09E-02	-	-
cg15065340	TNK2	1	58	-0.52	4.35E-06	-0.33	1.39E-02	0.28	1.95E-02	-	-	-	-	-	-
cg05883128	DDX60	1	45	-0.64	2.92E-09	-0.44	7.95E-04	0.41	4.86E-04	0.26	3.68E-02	0.34	6.98E-03	-	-
cg03043696	GNB1	1	43	-0.44	1.21E-04	-0.36	6.44E-03	0.39	7.34E-04	-	-	-	-	-0.27	4.56E-02
cg10435235	ARHGEP7	1	42	-0.46	5.65E-05	-0.38	4.29E-03	0.46	7.08E-05	-	-	-	-	-	-
cg20321801	CD81	1	27	-0.55	8.37E-07	-0.48	1.90E-04	0.55	1.05E-06	0.32	1.03E-02	-	-	-	-
cg06872964	IFI44L	1	19	-0.50	1.31E-05	-0.37	5.13E-03	0.28	2.01E-02	-	-	-	-	-	-
cg07892167	R3HCC1	1	17	-0.53	2.45E-06	-0.31	2.09E-02	0.43	2.28E-04	0.28	2.88E-02	-	-	-	-
cg02385820	RINL	1	13	-0.41	4.10E-04	-0.32	1.79E-02	0.47	4.19E-05	-	-	-	-	-	-
cg20939114	PITPNC1	2	607	0.52	3.62E-06	0.46	4.57E-04	-0.54	1.44E-06	-0.38	2.44E-03	-0.32	9.83E-03	-	-
cg02538772	SND1	2	374	0.59	6.34E-08	0.44	6.99E-04	-0.53	3.07E-06	-0.35	5.15E-03	-0.29	1.98E-02	-	-
cg15413523	TCF7	2	308	0.58	1.55E-07	0.39	3.60E-03	-0.37	1.47E-03	-0.37	3.19E-03	-0.39	1.69E-03	-	-
cg20651018	CARS	2	308	0.63	3.63E-09	0.54	2.05E-05	-0.54	1.38E-06	-0.42	7.09E-04	-0.35	4.75E-03	-	-
cg13015616	HFE	2	264	0.65	1.15E-09	0.52	4.18E-05	-0.55	7.32E-07	-0.43	5.12E-04	-0.34	5.96E-03	-	-
cg26005232	NUDC	2	240	0.60	4.86E-08	0.49	1.23E-04	-0.54	1.59E-06	-0.48	7.14E-05	-0.46	1.45E-04	-	-
cg08863939	TLK1	2	225	0.62	8.27E-09	0.61	9.40E-07	-0.63	4.96E-09	-0.47	8.41E-05	-0.43	5.14E-04	-	-
cg04537602	CXCR5	2	154	0.61	2.30E-08	0.56	7.38E-06	-0.63	5.23E-09	-0.43	4.13E-04	-0.35	4.79E-03	-	-
cg11477010	ANKFY1	2	141	0.63	7.14E-09	0.49	1.47E-04	-0.56	5.66E-07	-0.42	7.15E-04	-0.40	1.28E-03	-	-
cg18338046	TCF7	2	90	0.59	6.20E-08	0.53	2.75E-05	-0.51	5.44E-06	-0.39	1.39E-03	-0.31	1.47E-02	-	-
cg19400179	DZIP3	2	70	0.55	1.03E-06	0.38	4.47E-03	-0.43	1.97E-04	-0.25	4.40E-02	-	-	-	-
cg02676052	LCP2	2	69	0.44	1.44E-04	0.38	3.95E-03	-0.49	1.67E-05	-0.30	1.61E-02	-	-	-	-
cg00808969	USP35 KCTD21	2	66	0.57	3.40E-07	0.40	2.82E-03	-0.57	2.04E-07	-0.32	1.17E-02	-0.28	2.43E-02	-	-
cg13298528	CXCR5	2	60	0.62	7.94E-09	0.50	8.60E-05	-0.57	2.03E-07	-0.42	6.33E-04	-0.31	1.27E-02	-	-
cg19368911	KIF26B	2	45	0.45	9.17E-05	0.32	1.91E-02	-0.48	2.94E-05	-0.37	3.10E-03	-0.34	6.26E-03	-	-
cg00688810	SHBG FXR2	2	43	0.56	4.15E-07	0.41	1.74E-03	-0.51	7.87E-06	-0.38	2.16E-03	-0.29	2.26E-02	-	-
cg27519392	CHD7	2	40	0.60	5.24E-08	0.42	1.43E-03	-0.57	3.09E-07	-0.44	2.91E-04	-0.37	2.57E-03	-	-
cg26567688	COL4A3BP	2	29	0.47	4.92E-05	0.36	6.53E-03	-0.55	7.26E-07	-0.38	2.34E-03	-0.34	5.98E-03	-	-
cg08179431	HFE	2	27	0.60	4.49E-08	0.51	7.53E-05	-0.54	1.65E-06	-0.38	2.32E-03	-0.28	2.46E-02	-	-
cg12042587	GHR	2	27	0.52	3.10E-06	0.48	2.43E-04	-0.38	1.05E-03	-	-	-0.27	3.46E-02	-	-
cg22036538	CD27 LOC678655	2	27	0.53	2.54E-06	0.43	9.09E-04	-0.55	6.26E-07	-0.39	1.49E-03	-0.33	7.35E-03	-	-
cg04858110	SCRN1	2	24	0.49	1.87E-05	0.29	3.46E-02	-0.50	8.87E-06	-0.31	1.40E-02	-0.31	1.49E-02	-	-
cg12217560	TNFRSF19	2	21	0.46	7.12E-05	-	-	-0.56	5.11E-07	-0.33	7.89E-03	-0.26	4.06E-02	-	-
cg14659511	DOCK9	2	14	0.46	5.15E-05	0.41	2.10E-03	-0.52	3.28E-06	-0.34	5.92E-03	-	-	-	-

Rho is indicative of the Spearman's rank correlation test. Only correlations with p-value <0.05 are shown.

Cl: Cluster.

Freq: Frequency

T cell Breadth: Number of reactive peptides measured by IFN γ ELISpot assay.

T cell Magnitude: Median of SFC per 10⁶ PBMC resulted in IFN γ ELISpot assay.

nAb BaL: Neutralizing antibodies to HIV-1-BaL laboratory adapted virus strain (1/IC50 of plasma)

<https://doi.org/10.1371/journal.ppat.1008678.t002>

Similarly, in cluster 2, the DMP in the body of the CARS gene (cg20651018) was correlated with measured viral parameters and levels of HIV-1 specific T cell responses (Table 2). Furthermore, DMPs in promoter region of the HFE gene (cg13015616 and cg08179431) correlated with HIV-1 pVL, proviral levels, and breadth and magnitude of the virus-specific T cell responses. The HFE gene is involved in general T cell activation [16,17] and, interestingly, both DMPs showed the strongest correlation with other DMPs in the circle plot (S1 Fig). In addition, DMPs in the genes CXCR5 (cg04537602 and cg13298528) and TCF7 (cg15413523 cg18338046), both falling into the categories of lymphocyte and T-cell activation (GO:0046649 lymphocyte activation, GO:0046631 alpha-beta T-cell activation, GO:0042110 T-cell activation or GO:0030217 T-cell differentiation), were all correlated with the breadth and magnitude of the virus-specific T-cell response, as well as with pVL and proviral levels (Table 2). Overall, these correlation analyses highlight the potential relevance of epigenetic regulation of PARP9, MX1, IRF7, USP18, PLSCR1 and IFI44L genes from cluster 1 (innate/antiviral response) and HFE, CXCR5 and TCF7 genes from cluster 2 (T-cell activation) in determining levels of virologic parameters, HIV-specific T cell responses and in vivo virus control.

Methylation levels of candidate genes translate inversely into different mRNA levels

To demonstrate a direct relationship between methylation levels and gene expression activity, we determined transcription levels for selected candidates. The top signals emerging from the random forest list (Table 1) included DMPs in promoters of genes PARP9/DTX3L and ODF3B, among others. Of importance, PARP9/DTX3L DMPs (cg22930808 and cg08122652) were strongly correlated with pVL and proviral (Table 2) and were included in the cluster enriched by antiviral gene ontology terms (Fig 2A and 2C). Focusing on that cluster 1, PARP9 was in turn correlated with MX1, PLSCR1, IFI44L and USP18. Gene expression was assessed for PARP9, MX1 and USP18 using available total PBMC samples from the same individuals that were used for the initial methylome screening (n = 16 for HIV-High, n = 31 for HIV-Low, Table 1). HIV-Low individuals showed hypermethylation of PARP9, MX1 and USP18 (Fig 3A–3C); and indeed, all these three genes were less expressed in HIV-Low compared with HIV-High individuals (Fig 3D–3F). Thus, the observed DNA methylation patterns mediated epigenetic control of gene

expression for these lead candidates (Fig 3G–3I). For the validation of the gene expression results and to confirm that the higher expression of these molecules was associated with uncontrolled HIV-1 infection, mRNA levels for PARP9, MX1 and USP18 were validated in independent cohorts of HIV-1 infected individuals. The cohorts included: Untreated early infected individuals (Early, n = 8), Chronic Untreated individuals (Untreated, n = 11), Chronic cART Treated individuals (Treated, n = 5) and Elite Controllers subjects (EC, n = 12) (S2 Table). The group of natural HIV-1 controllers showed consistently significant reductions in the expression levels of these genes compared with the rest of the studied groups (Fig 3J–3L).

When testing for potential correlations between levels of methylation, gene expression and viral parameters for all the individuals in the HIV-High and HIV-Low groups as well as from independent cohorts, the methylation and mRNA levels for all three assessed genes PARP9, MX1 and USP18, strongly correlated with pVL and proviral levels (Fig 4). These data indicate that the differential expression levels of antiviral host factors (PARP9, USP18 and MX1) between individuals with HIV-High and HIV-Low phenotypes are tightly related to epigenetic mechanism and could explain the different gene expression levels observed between HIV-1 elite controllers and the rest of HIV-1 infected subjects.

These conclusions were further supported by the re-analysis of an open access dataset (GSE53840, [18]). Using the same analysis approach as we did in our own data-set, this analysis identified the most relevant DMPs that discriminated patients with $pVL < 10.000 \text{ copies/ml}$ and $pVL > 10.000 \text{ copies/ml}$, and further highlighted the relevance of PARP9 hypermethylation in HIV control (S4 Table).

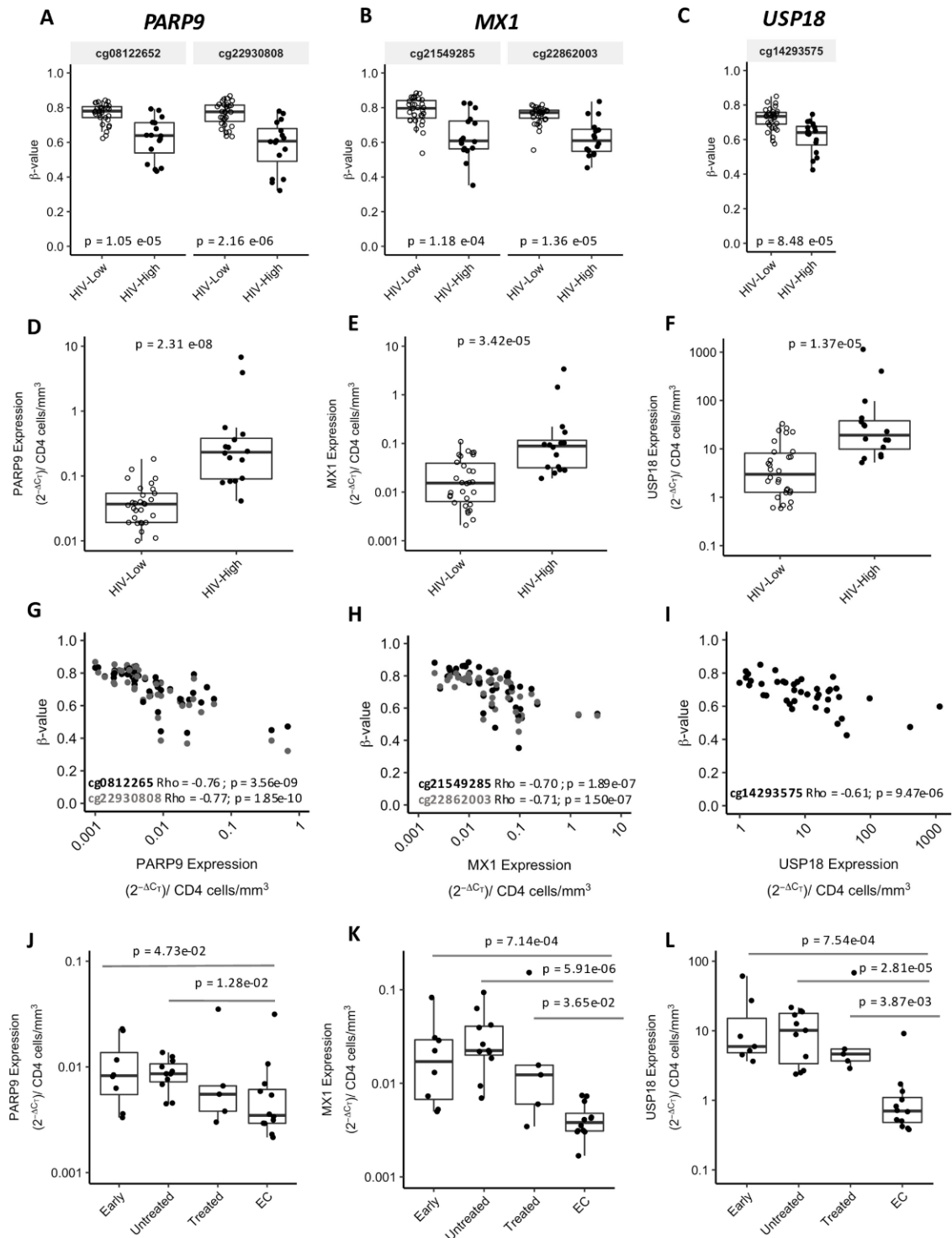


Fig 3. Epigenetic regulation confirmation of selected candidates and gene expression validation in unrelated cohorts. Boxplot for *PARP9* (A), *MX1* (B) and *USP18* (C) with the Beta-values in Y-axis and the HIV-High (n = 15) or HIV-Low (n = 31) groups in X-axis. (D-F) Boxplots of the transcriptional levels of *PARP9* (D), *MX1* (E) and *USP18* (F) analyzed by qRT-PCR, and represented here as the $2^{-\Delta C_T}$ method corrected by the number of CD4 counts in HIV-Low (n = 31) and HIV-High (n = 15). (G-I) Correlation plots, showing the inverse correlation between Beta-values of DMPs and the corresponding gene expression level *PARP9* (G), *MX1* (H) and *USP18* (I). (J-L) Boxplots indicating the gene expression level of *PARP9* (J), *MX1* (K) and *USP18* (L) in the independent cohorts of HIV-1 infection: Early (Early infected untreated individuals, n = 8), Untreated (Chronic infected untreated individuals, n = 11), Treated (Chronic infected cART treated individuals, n = 5) and EC (Elite Controllers, n = 12). Mann Whitney test was applied for groups' comparisons and Spearman's rank correlation test, for correlation analysis. In all the cases, p-values <0.05 were considered significant.

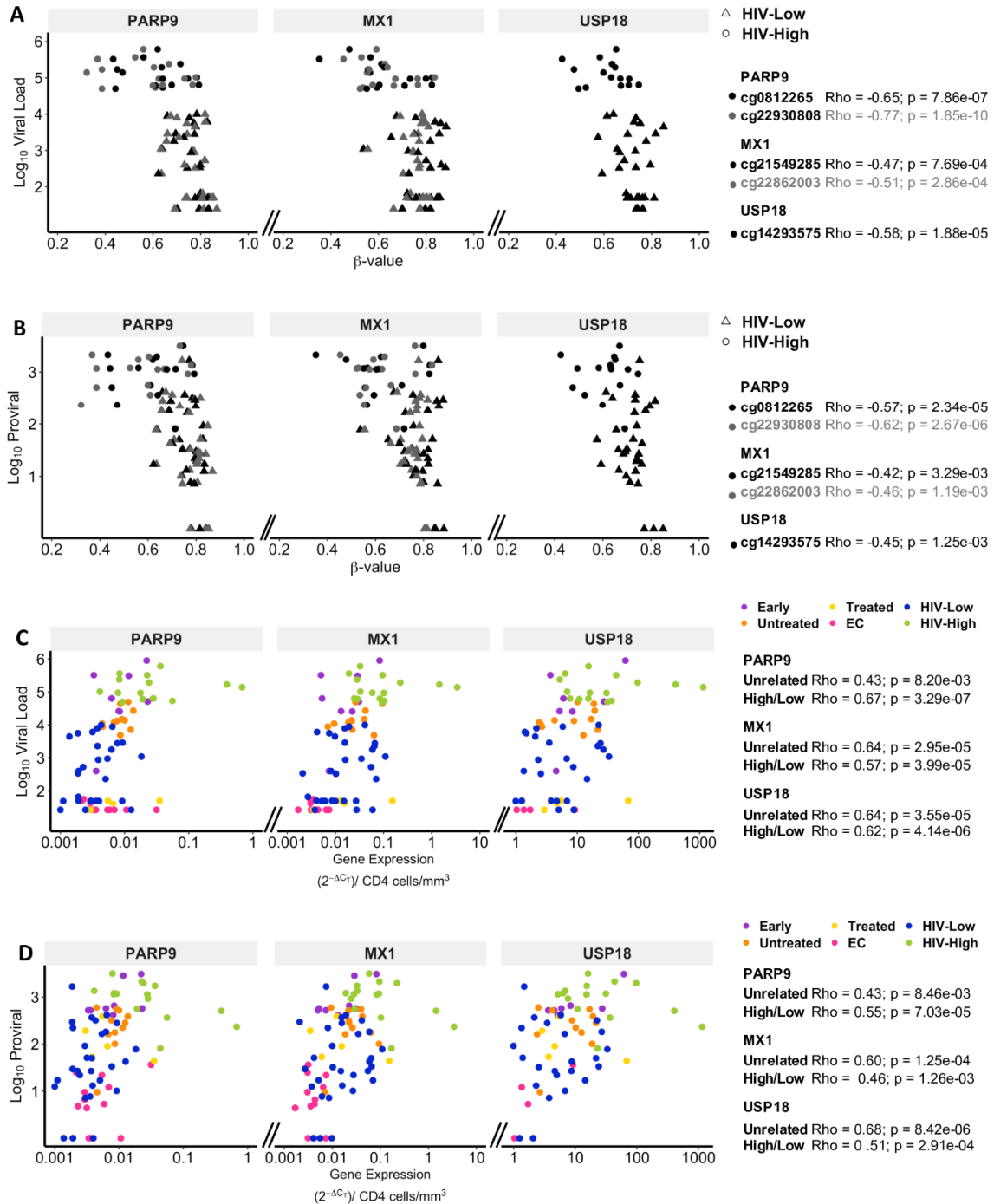


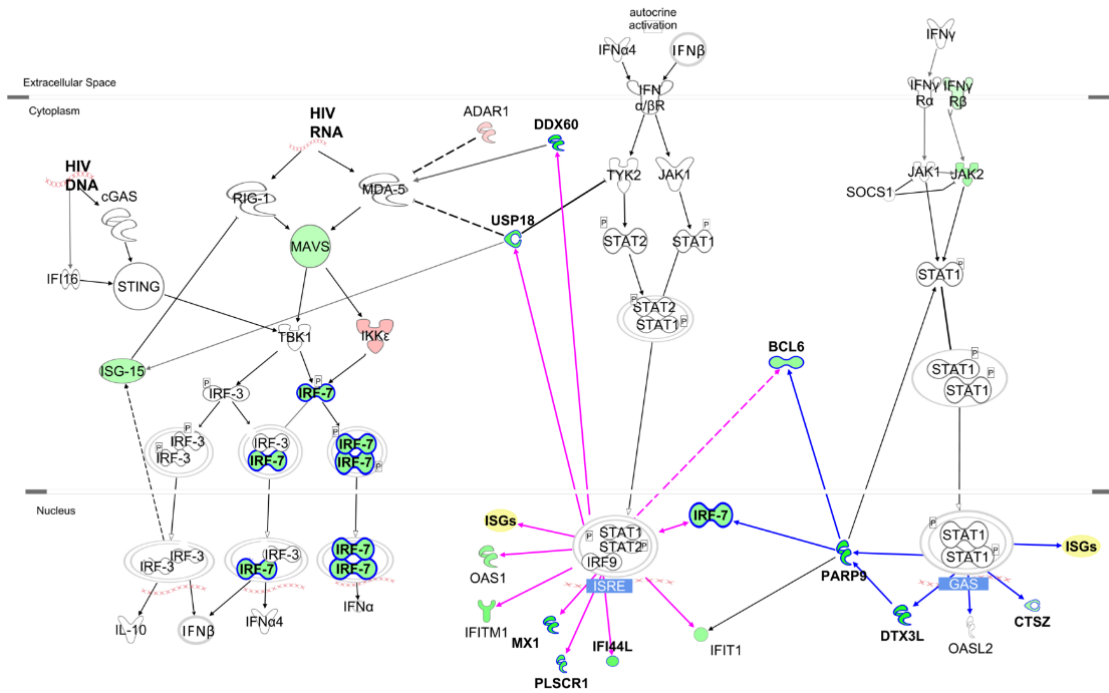
Fig 4. Correlations of gene expression and methylation levels of PARP9, MX1 and USP18 with HIV viral load and proviral. (A and B) PARP9, MX1 and USP18 correlation of methylation levels (X-axis) and HIV plasma viral load (A, Y-axis) or HIV proviral levels at PBMCs (B, Y-axis) in HIV-High and HIV-Low individuals. The different CpG positions are in different color (black and grey) and the two studied groups HIV-High and HIV-Low are indicated with a triangle and a square, respectively. (C and D) Correlation of PARP9, MX1 and USP18 gene expression determined by qRT-PCR and HIV plasma viral load (C, Y-axis) or HIV proviral levels at PBMCs (D, Y-axis). The different colors indicate the different groups of individuals including those in unrelated cohorts (Early in purple, Untreated in orange, Treated in yellow, EC in red) and HIV-High (green) and HIV-Low (blue). Spearman's rank correlation test was applied for correlation analysis. In all cases, p-values <0.05 were considered significant.

Opposite methylation patterns in interferon-related genes and T cell response genes are associated with HIV-1 control

To have a broader overview of the impact of the epigenetic dysregulation in the context of antiviral and T cell differentiation pathways, all the significant DMPs ($p < 0.05$) in the dataset were studied. For the genes up-/downstream of the interferon signaling pathway (Fig 5A), we observed a higher methylation level in HIV-Low individuals, and the same trend was observed in genes of the antiviral pathway RIG-I/MDA-5 (MAVS and IRF7). On the other hand, HIV-Low individuals showed lower methylation levels and thus potentially higher protein levels for molecules involved in T-cell differentiation, including T follicular helper (Tfh) markers such as CXCR5 and TCF7 (Fig 5B).

Furthermore, in HIV-Low individuals we identified a negative correlation between the methylation levels of cg12459932 in RUNX3 and the methylation levels of the CpG positions in CXCR5 (cg04537602 $Rho = -0.56$, $p\text{-value} = 3.67 \times 10^{-07}$ and cg04537602 $Rho = -0.58$, $p\text{-value} = 1.07 \times 10^{-07}$) and TCF7 (cg15413523 $Rho = -0.27$, $p\text{-value} = 0.02$ and cg18338046 $Rho = -0.47$, $p\text{-value} = 3.11 \times 10^{-05}$). RUNX3 (hypermethylation in HIV-Low) is involved in Tfh differentiation and has recently been reported to block CD8 effector T cell differentiation towards Tfh lineage [19]. As a consequence, in HIV-Low individuals RUNX3 may be epigenetically repressed to favor the differentiation of Tfh cells. This epigenetic mechanism could explain the observed higher frequencies of this T-cell population in HIV-1 controllers [20].

A Antiviral and IFN response gene



B T cell differentiation

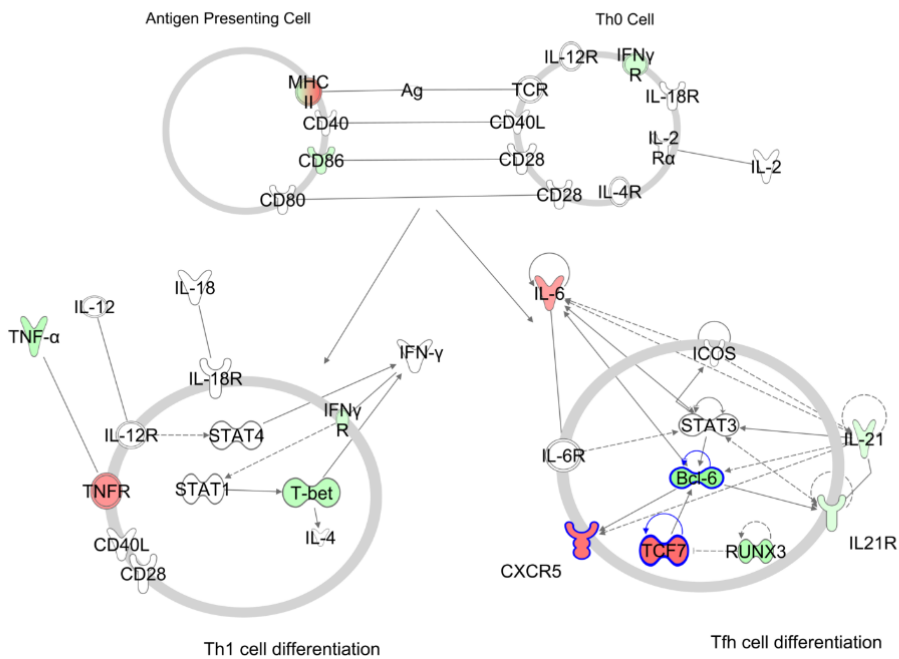


Fig 5. HIV-Low individuals show higher methylation levels in interferon stimulated genes and lower methylation levels in genes related to T follicular helper (Tfh). All differentially methylated CpG positions in the dataset ($p < 0.05$) are shown in the context of two different pathways. A) Pathway representing genes associated with antiviral and interferon response focused on *Role of RIG-I like Receptors in Antiviral Innate Immunity, Antiviral activation of IRF by cytosolic pattern recognition receptors and Interferon Signaling* canonical pathways from IPA. B) Scheme showing *T Helper Cell Differentiation* canonical pathway from IPA combined with reported genes associated with Tfh phenotype. Coloring is based on methylation fold-change HIV-High/HIV-Low. Red refers to lower methylation in HIV-Low, and green higher methylation in HIV-Low. Also, pink and blue in (A) indicate the ISGs that are induced via type I or type II interferon, respectively. Molecules selected in the multivariate are highlighted with a blue border. Solid lines indicate direct interactions and dashed ones, indirect interactions.

Discussion

The main objective of the present study was to investigate the importance of epigenetic regulation of host factors involved in the control of HIV-1 infection by assessing whether chronically untreated HIV-1 infected individuals with high or low plasma viral load levels show marked host genome DNA methylation patterns in the peripheral blood. Our data document significant differences in epigenetic signatures on a wide range of host proteins between these groups of patients and highlight the potential of methylome analyses to identify possible biomarkers associated with spontaneous control of HIV-1 infection. Therefore, the association of HIV-1 infection with differential DNA methylation patterns previously reported in studies comparing HIV+ and HIV- individuals [8,9], would extend the insights to markers and mechanisms underlying the spontaneous capacity to control HIV-1 replication in chronic infection.

In our study, two immune response Gene Ontology (GO) categories were found to be greatly under epigenetic regulation in untreated chronic HIV-1 disease with different virus control. While in HIV-Low individuals the innate immunity GO category (antiviral response and IFN inducible genes) was highly methylated, the GO category of adaptive immune response (T cell activation and differentiation) was poorly methylated compared to HIV-High individuals.

In particular, the most prominent DMPs signals detected in antiviral and interferon response GO categories and correlated with virological parameters included: PARP9/DTX3L, MX1, USP18, IFI44L and PLSCR1. These ISGs have been previously described to be involved in different viral infections, including HIV-1 [21–23]. Furthermore, the epigenetic regulation of the ISGs documented in our study, is in line with recently published data demonstrating a differential transcriptional regulation of ISGs (e.g MX1, PARP genes and USP18 among others) in total PBMC of HIV normal progressors compared with HIV controller phenotypes [24]. Additional confirmation of the findings also stems from the gene expression patterns in the independent cohorts tested in our study, including treated and untreated HIV-1 infected individuals in different stages of HIV-1 infection including elite controller individuals.

The identified three genes play all a role in the interferon-mediated antiviral response: PARP9 is increased in vitro models of HIV-1 infection [25,26] and, together with DTX3L, can target histone H2BJ and increase the expression of interferon stimulated genes (ISGs) [27,28]. Similarly, USP18 has been described as a negative regulator of interferon response [21] and has been associated to HIV-1 replication as well [29]. Contrary to MX2, no role as HIV-1 restriction factor has been described for MX1 [30,31]. However, three different studies associated the lower levels of MX1 expression in the chronic phase of infection with relative virus control [24,32,33]. In line with these findings, our results further indicate that the epigenetic repression of these ISGs may contribute to achieving a spontaneous sustained control of HIV-1.

However, it needs to be stressed that our results identify factors and pathways involved in viral control based on methylome analyses in total PBMC. Thus, the identified factors do not necessarily need to have a direct impact on virus transcription in HIV-infected CD4 T cells. In fact, it may be quite likely that the majority of the identified host immune mechanisms that are associated with high or low viral load, and which are epigenetically controlled, originate from cells not infected by HIV (especially also considering the small number of infected cells in the peripheral blood). Interestingly, Morón-López et al (Morón-López et al. Abstract #228 CROI 2017), have reported full methylome data in isolated CD4 T cells from a small cohort of HIV infected patients with different levels of virus control. These results showed hypermethylation of USP18 in EC when compared to VC, supporting the results in our large cohort where hypermethylation of this gene was associated with better HIV control as well. Evidently, it will be very interesting to further define the methylome profile of this and other markers in latently or productively infected CD4 cells and other target cells of active replication and viral reservoir [34].

The role of activation of IFN pathways in the control of persistent HIV-1 infection is less clear, despite the strong signals observed in our analyses. On one hand, the activation of IFN genes in the acute phase of HIV-1 infection may benefit initial immune responses [35] and it has indeed been associated with protection from HIV-1 acquisition in a recent

systems vaccinology study on the RV144 vaccine clinical trial [36]. On the other hand, the IFN response may become detrimental in the chronic phase of HIV-1 infection and has been related to poor antiviral response, higher virus loads and lower CD4 counts [37]. Supporting this observations, experiments in cART treated, HIV-1 infected humanized mice also showed that the blockade of IFNAR decreased immune activation and the size of the HIV-1 reservoir [38]. Similarly, Non-Human Primate (NHP) models using sooty mangabeys infected with Simian immunodeficiency virus (SIV) demonstrated an upregulation of PARP9 and USP18 among other ISGs that were later decreased in the chronic phase of SIV infection and, may be involved in the reduced disease progression in these animals despite the fact that they present with unusually high viral loads. In contrast, SIVmac239 infected Rhesus Macaques (as a model of continuing disease progression) maintain high levels of ISGs (including MX1) in the chronic phase. This findings derived from NHP models suggests that the downregulation of the IFN response that may help slow disease progression after SIV infection [39]. The same conclusion may be drawn from our dataset, where the higher methylation of ISGs and thus, lower expression levels, might improve the immune control of HIV-1 by downregulating IFN signaling and avoiding the systemic inflammation and consequent associated immune deterioration. Therefore, we suggest that the observed epigenetic brake on IFN signaling pathways may play a critical role in HIV-1 disease progression or HIV-1 control. Further analyses of individuals with known time since infection will be needed to prove this hypothesis. Furthermore, the study of individuals sampled before and after HIV-1 infection would also be insightful to determine when during the HIV-1 infection these differential DNA methylation patterns are established.

Individuals that initiate cART treatment within first days or weeks after HIV-1 show a reduced viral reservoir, but this is not enough to achieve an HIV-1 cure [40]. To date, many eradication and cure strategies aim to reactivate the latent virus with so-called latency reversing agents given in combination with therapeutic vaccines [41]. However, DNA methylation patterns existing in treated individual might well influence the outcome of such therapeutic interventions since our results show an epigenetic regulation of antiviral host factors and point to a possible epigenetic regulation of T cell

differentiation. In regard to the latter, the two CpG positions identified in CXCR5 and TCF7 are of particular interest. While these genes have been associated with T follicular helper (Tfh) phenotypes in the past [42], with our study we now demonstrate that their expression is tightly controlled by epigenetic mechanisms and that this regulation may impact host defense and viral replication as both CpG positions were correlated with the breadth and magnitude of the HIV-1-specific T-cell responses, plasma viral load as well as the proviral levels. Furthermore, multiple DMPs were found in the Tfh pathway (Fig 5B) suggesting the epigenetic regulation of Tfh differentiation as a mechanism that might explain the higher frequencies of circulating Tfh in HIV-1 controllers [20]. As a consequence, the low methylation levels of these genes and elevated gene expression in HIV-Low individuals, may benefit effective anti-viral immune responses by preferentially driving T-cell differentiation towards a follicular-like phenotype, which in turn might avoid T-cell exhaustion of Th1-like cells.

Finally, aside from providing insights into natural control of HIV-1 infection, these findings may be of critical importance for the design and outcome of therapeutic interventions aimed at HIV-1 cure. Since DNA methylation marks are more stable than mechanisms regulating RNA expression [43], these methylation patterns may need to be restored in HIV-1 infected individuals with uncontrolled viral replication to attain sustained virus control. There are rapid advances in the field of gene editing that raise the hope that such modifications could indeed be implemented [43].

Of note, the obtained results were based on DNA methylation patterns on available dry PBMC cell pellets and further analysis of sorted cell type populations would be necessary to identify potential differences in cell-type specific DNA methylation patterns. At the same time, the study of total PBMC methylome allowed the identification of the most prominent DMPs associated with HIV control regardless of the cell subtype. Furthermore, potential bias associated with sample cell-type heterogeneity was partially overcome with a regression model adjusted for cell type proportion estimates [9, 12] and CD4 correction. The latter helped to account for the significant differences in CD4 T cell counts in the two main comparison groups of HIV-Low and HIV-High. Importantly

though, even without applying a CD4 counts correction, a strong selection of anti-viral and T cell response genes and the strong relevance of DMPs in PARP9 as well as USP18 are evident (S5 Table).

Despite these potential limitations, our study conducted in a well characterized HIV-1 infection cohort combined with comprehensive virological and immune functional assessments, provides clear evidence that differential epigenetic imprints on host DNA are tightly related to innate and adaptive immune responses against HIV-1 infection and relative control of in vivo viral replication. It will now be interesting to further our understanding of how DNA methylation itself is regulated in HIV-1 infected individuals and how this may allow to develop new therapeutic strategies to improve virus-specific immunity and HIV-1 cure. Furthermore, while the causal relationship between the epigenetic signals and virus control remains to be unraveled, our data show for first time that many host factors associated with immune control of HIV infection are under global epigenetic regulation, raising potential challenges for future cure strategies [11].

Methods

Ethics statements

The study was approved by the Comitè Ètic d'Investigació Clínica of Hospital Germans Trias i Pujol (CEIC: EO-12-042) and all participants provided written informed consent.

Patients and samples

Chronic HIV-1 seropositive subjects (n = 70) were recruited at the Hospital Germans Trias i Pujol, Badalona, Spain, and the IMPACTA clinics in Lima, Peru. Subjects with plasma viral loads (pVL) <10,000 HIV-1 RNA copies/ml (range 25–9,999; median 2,760) in the absence of antiretroviral treatment were defined as "HIV-Low" (n = 41), while subjects with pVL >50,000 HIV-1 RNA copies/ml (range 50,295–1,200,000; median 237,459) were defined as "HIV-High" (n = 29) individuals (S1 Table). CD4 counts in the HIV-Low group ranged from 404–1,343 cells/mm³ (median 741) and from 11–726 cells/mm³ in the HIV-High group (median 283). Additional unrelated cohorts (S2 Table) were used for

downstream validation of identified signals including: individuals sampled in early phase of HIV-1 infection (Early, median 3 months after seroconversion, n = 8, median viral load = 57,860), untreated individuals in chronic phase of infection (Untreated, n = 11, 1y before cART treatment, median viral load = 13,284), in chronic infected treated individuals (Treated, n = 5, 1y post cART initiation, undetectable viral load) and chronically infected elite controllers (EC, n = 13, undetectable pVL, at least 1y without treatment). For molecular assays, DNA and RNA was extracted using the QiaAmp Kit from available dry pellet PBMCs.

Infinium Human Methylation450 Bead Chip

Bisulfite modification of 600 ng genomic DNA was carried out with the EZ DNA Methylation Kit (Zymo) following the manufacturer's protocol. Next, 4 μ L of bisulfite-converted DNA were used to hybridize on Infinium HumanMethylation450 BeadChip, following Illumina Infinium HD Methylation protocol. Chip analysis was performed using Illumina HiScan SQ fluorescent scanner and the intensities of the images were extracted using GenomeStudio (2010.3) Methylation module (1.8.5) software. Quality control, background correction and quantile normalization across arrays was performed using Minfi R/Bioconductor package [44] available for Bioconductor under the R statistical environment [45]. Methylation level (Beta-value) for each of the 485,577 CpG positions were calculated as the ratio of methylated signal divided by the sum of methylated and unmethylated signals plus 100. After a normalization step, probes related to X and Y chromosomes were removed. Function `dropLociWithSnps()` of Minfi R/Bioconductor package removed all the probes associated with SNPs in the body of the probe, specifically SNPs overlapping the CpG site and 1 or 2 bp extension from it (SBE, single base extension). Finally, the methylation scores were corrected for batch effect by using `comBat()` function from `sva` R/Bioconductor package [46]. Data is available at GEO under the accession number GSE140800.

Definition of CpG methylation differences

A non-specific filtering was used to determine the most variable Beta-values for CpG positions according to standard deviation [47] and finally, we kept 56,513 CpG positions as the most variable CpG by selecting a threshold ($sd > 0.47$) for subsequent analysis. For the definition of CpG methylation differences, we applied an analysis based on an approach (CPACOR, [12]), previously used in DNA methylation studies in HIV-1 [9,48], which consists in a two-step regression model considering different confounders (age, sex, CD4 counts, PBMC composition and technical bias) (Fig 1A). A race confounder was not applied because all patients were of Caucasian origin. To correct for PBMC composition, the proportion of each cell type was estimated (WBCest) from the methylation intensity values of certain probes as described by Houseman et al. [49] and applied in function `estimateCellCounts()` in `Minfi` R/Bioconductor package [44]. For technical bias consideration (Fig 1A), a first model was applied using the 10 principal components (PCs) on 450K array control probes as covariates (PCs 1–10) in addition to the so-called above confounders:

$$\text{Betacorrected} \sim \text{WBCest} + \text{PCs1-10} + \text{Age} + \text{Sex} + \text{CD4counts}$$

Subsequently, a principal component analysis (PCA) was performed on the residuals of the technical bias correction model and 5 PCs (resPCs 1–5) were used in the second regression model:

$$\text{Betacorrected} \sim Y + \text{WBCest} + \text{PCs1-10} + \text{Age} + \text{Sex} + \text{CD4counts} + \text{resPCs1-5}.$$

In this model (Fig 1A), Y refers to the individual class, HIV-High and HIV-Low. We selected those differential Beta-values ($p < 0.05$) between Y classes. The estimate of Y will retrieve the difference of methylation between the 2 groups considering that all the other covariates remain constant.

Functional array analyses

Gene Ontology (GO) Enrichment Analysis was performed using the `ClusterProfiler` package from R/Bioconductor based on a hypergeometric test [50] in which the background were the 2649 gene-mapped DMPs. Heat-Maps (`gplots` R/CRAN package) and Hierarchical Clustering were performed with R software. For cluster analysis on

selected CpG positions for classification of the two comparison groups, distances among DMPs were based on correlation values (Spearman's Rho) and agglomeration, on average linkage method (R/CRAN package Hmisc). The determination of the number of clusters was based on dendrogram height (h) and using the fpc R/CRAN package to determine the robustness of each cluster and determine the best agglomeration method. The analysis of molecule interactions was performed using Ingenuity Pathway Analysis Software IPA (QIAGEN Inc., <https://www.qiagenbioinformatics.com/products/ingenuity-pathway-analysis>) highlighting networks and canonical pathways affected by HIV-High and HIV-Low groups.

Proviral (Total HIV-1-1 DNA) quantification

Proviral (Total HIV-1-1 DNA) was quantified in PBMC lysates by droplet digital polymerase chain reaction (ddPCR) in duplicate, as described previously [51]. Briefly, two different primers/probe sets annealing to the 5'LTR and Gag regions, respectively, were used to circumvent sequence mismatch in the patients' proviruses, and the RPP30 housekeeping gene was quantified in parallel to normalize sample input. Raw ddPCR data were analyzed using the QX100 Droplet Reader and the QuantaSoft v.1.6 software (Bio-Rad).

Measurements of adaptive host immune responses to HIV-1

T cell immunity to HIV-1 was assessed in cryopreserved isolated PBMC by IFN γ ELISpot assay (1x10⁵ PBMC/well), using a set of 410 overlapping peptides (OLPs, (18mers overlapping by 15 aa) covering the consensus B HIV-1 viral proteome as described elsewhere [52]. The breadth (number of reactive OLP) and magnitude (spot forming cells (SFC) per 10⁶ PBMC) were recorded. Neutralization activity of plasma samples was evaluated using a TZM-bl neutralization assay as described elsewhere [53,54]. Briefly, five-fold serial dilutions of plasma samples (inactivated for 1 hour at 56°C) were incubated in 96-well plates in duplicates for 1 hour with 200 TCID₅₀ of the laboratory adapted viral strain HIV-1-BaL, Vesicular stomatitis virus (VSV) envelope pseudotyped

HIV-1 was included as a control for HIV-1 unspecific neutralization. Then, 104 TZM-bl cells were added per well and incubated for 48 hours at 37°C and 5% CO₂. Luciferase activity was determined by luminometry using the BriteLite plus reagent (PerkinElmer) and the Fluoroskan Ascent FL luminometer (Labsystem). The percentage of neutralization was calculated as: % Neutralization = $[1 - (R - R_{cc} / R_{vc})] \times 100$; where R = RLU (relative light units) of the tested plasma, R_{cc} = RLU of cell alone and R_{vc} = RLU of virus alone. The IC₅₀ (dose inducing 50% of total inhibitory capacity) was calculated and results are shown as reciprocal dilution.

Real Time PCR

Dry cell pellets were conserved in RNeasy Protect Cell Reagent (Qiagen) and used for RNA extraction (RNeasy Plus Mini Kit, Qiagen) and retro-transcription (SuperScriptIII First-Strand Synthesis SuperMix). The cDNA was used for RT-PCR using Taqman Gene Expression Assays for detection of: PARP9 (Hs00967084_m1), MX1 (Hs00895608_m1), USP18 (Hs00276441_m1) and Tata binding Box protein (TBP) (Hs99999910_m1) as housekeeping gene with 7500 Fast Dx Real-Time PCR Instrument (Applied Biosystems). The relative expression was calculated as Relative Expression = $2^{-\Delta CT}$ (CT = the median of crossing thresholds from 3 replicates).

Statistics

To identify robust methylation profiles in extreme outcomes of HIV control, we decided for our initial analysis, to classify individuals in our main cohort into two comparison groups (HIV-High and HIV-Low) rather than conducting correlation analysis with viral load as a continuous variable. To this end, we applied a random forest analysis to determine the most relevant features considering the contribution of all the CpGs at the same time. This is also a suitable approach to deal with data collinearity [55]. Accordingly, we applied a random forest classification model based on the previously identified 2649 gene annotated DMPs with five-fold cross validation in an iterative way (1000 iterations) with the CMA R/Bioconductor [15].

The reliability of the model to classify individuals was assessed with the area under the curve (AUC). The output of this analysis provides a ranking of DMPs (frequency) according to the number of times that each CpG position was selected in the random forest analyses (AUC = 0.92). We kept those CpG sites that were selected for a minimum of 10 times. Spearman's rank correlation test was used for correlations among DMPs and clinical, virological and immunological parameters including: CD4 counts, plasma viral load, Proviral levels, T cell responses (T cell breadth and magnitude) and plasma neutralizing antibodies (nAb) activity against the virus strains BaL (see corresponding methods section). The correlation data among DMPs were plotted using Circlize R/CRAN package [56]. Finally, univariate statistical analyses for group comparisons were based on non-parametric Mann-Whitney test and p-value < 0.05 was considered statistically significant.

Acknowledgments

We appreciate the participation of all HIV-1-infected individuals studied in this work. We thank Laura Ordeig and Jhon Jesus Poch for their participation in data analysis and sample processing.

Funding Statement

This project has received funding from the European Union's Horizon 2020 research and innovation programme under grant agreement No. 681137 and was partly funded by National Institute of Allergy and Infectious Diseases of the National Institutes of Health under award number PO1-AI131568, Project SAF2017-89726-R from Spanish Ministry of Science, Innovation and Universities, and the Fondation Dormeur, Vaduz, (Liechtenstein). CG is supported by the PhD fellowship of the Spanish Ministry of Education, Culture and Sport (FPU15/03698). MLC was partially supported by the Spanish Ministry of Economy, Industry and Competitiveness, reference MTM2015-64465-C2-1-R. The funders had no role in study design, data collection and analysis, decision to publish, or preparation of the manuscript.

Data Availability

Data is available at GEO under the accession number GSE140800.

References

1. Davenport MP, Khoury DS, Cromer D, Lewin SR, Kelleher AD, Kent SJ. Functional cure of HIV: the scale of the challenge. *Nat Rev Immunol*. 2019. January 8;19(1):45–54. Available from: <http://www.ncbi.nlm.nih.gov/pubmed/30410126>
2. Deeks SG, Walker BD. Human Immunodeficiency Virus Controllers: Mechanisms of Durable Virus Control in the Absence of Antiretroviral Therapy. *Immunity*. 2007. September;27(3):406–16. Available from: <http://www.ncbi.nlm.nih.gov/pubmed/17892849>
3. Mothe B, Ibarondo J, Llano A, Brander C. Virological, immune and host genetics markers in the control of HIV infection. *Dis Markers*. 2009;27(3):105–20. Available from: <http://www.ncbi.nlm.nih.gov/pubmed/19893207>
4. Pernas M, Tarancón-Diez L, Rodríguez-Gallego E, Gómez J, Prado JG, Casado C, et al. Factors Leading to the Loss of Natural Elite Control of HIV-1 Infection. Silvestri G, editor. *J Virol*. 2017. December 1;92(5). Available from: <http://www.ncbi.nlm.nih.gov/pubmed/29212942>
5. Rosás-Umbert M, Llano A, Bellido R, Olvera A, Ruiz-Riol M, Rocafort M, et al. Mechanisms of Abrupt Loss of Virus Control in a Cohort of Previous HIV Controllers. *J Virol*. 2019. February 15;93(4):e01436–18. Available from: <http://www.ncbi.nlm.nih.gov/pubmed/30487276>
6. Neidhart M. Chapter 6—DNA Methylation and Viral Infections In: Neidhart M, editor. *DNA Methylation and Complex Human Disease*. Elsevier; 2016. p. 81–102. Available from: <https://www.sciencedirect.com/science/article/pii/B9780124201941000063>
7. Kauder SE, Bosque A, Lindqvist A, Planelles V, Verdin E. Epigenetic regulation of HIV-1 latency by cytosine methylation. Ross S, editor. *PLoS Pathog*. 2009. June 26;5(6):e1000495 Available from: <http://www.ncbi.nlm.nih.gov/pubmed/19557157>

8. Gross AM, Jaeger PA, Kreisberg JF, Licon K, Jepsen KL, Khosroheidari M, et al. Methylome-wide Analysis of Chronic HIV Infection Reveals Five-Year Increase in Biological Age and Epigenetic Targeting of HLA. *Mol Cell*. 2016. April 21;62(2):157–68. Available from: <http://www.ncbi.nlm.nih.gov/pubmed/27105112>
9. Zhang X, Justice AC, Hu Y, Wang Z, Zhao H, Wang G, et al. Epigenome-wide differential DNA methylation between HIV-infected and uninfected individuals. *Epigenetics*. 2016. October 2;11(10):750–60.
10. Zhang Y, Li S-K, Yi Yang K, Liu M, Lee N, Tang X, et al. Whole genome methylation array reveals the down-regulation of IGFBP6 and SATB2 by HIV-1. *Sci Rep*. 2015. June 3;5:10806 Available from: <http://www.ncbi.nlm.nih.gov/pubmed/26039376>
11. Ruiz-Riol M, Brander C. Can we just kick-and-kill HIV: possible challenges posed by the epigenetically controlled interplay between HIV and host immunity. *Immunotherapy*. 2019. August;11(11):931–5. Available from: <https://www.futuremedicine.com/doi/10.2217/imt-2019-0092>
12. Lehne B, Drong AW, Loh M, Zhang W, Scott WR, Tan S-T, et al. A coherent approach for analysis of the Illumina HumanMethylation450 BeadChip improves data quality and performance in epigenome-wide association studies. *Genome Biol*. 2015. February 15;16(1):37 Available from: <http://www.ncbi.nlm.nih.gov/pubmed/25853392>
13. Portela A, Esteller M. Epigenetic modifications and human disease. *Nat Biotechnol*. 2010. October 13;28(10):1057–68. Available from: <http://www.ncbi.nlm.nih.gov/pubmed/20944598>
14. Breiman L. Random forests. *Mach Learn*. 2001;45(1):5–32. Available from: <https://link.springer.com/article/10.1023/A:1010933404324>
15. Slawski M, Daumer M, Boulesteix A-L. CMA: a comprehensive Bioconductor package for supervised classification with high dimensional data. *BMC Bioinformatics*. 2008. October 16;9:439 Available from: <http://www.ncbi.nlm.nih.gov/pubmed/18925941>

16. Yewdell JW, Hickman-Miller HD. Back to the fold: T cell recognition of HFE, a MHC class Ib molecule that regulates iron metabolism. *Proc Natl Acad Sci U S A*. 2005. September 6;102(36):12649–50.
17. Reuben A, Phénix M, Santos MM, Lapointe R. The WT hemochromatosis protein HFE inhibits CD8 T-lymphocyte activation. *Eur J Immunol*. 2014. June;44(6):1604–14. Available from: <http://www.ncbi.nlm.nih.gov/pubmed/24643698>
18. Horvath S, Levine AJ. HIV-1 Infection Accelerates Age According to the Epigenetic Clock. *J Infect Dis*. 2015. November 15;212(10):1563–73. Available from: <http://www.ncbi.nlm.nih.gov/pubmed/25969563>
19. Shan Q, Zeng Z, Xing S, Li F, Hartwig SM, Gullicksrud JA, et al. The transcription factor Runx3 guards cytotoxic CD8 effector T cells against deviation towards follicular helper T cell lineage. *Nat Immunol*. 2017. August 12;18(8):931–9. Available from: <http://www.ncbi.nlm.nih.gov/pubmed/28604718>
20. Claireaux M, Galperin M, Benati D, Nouël A, Mukhopadhyay M, Klingler J, et al. A high frequency of HIV-Specific circulating follicular helper T cells is associated with preserved memory B cell responses in HIV Controllers. Simon V, Palese P, editors. *MBio*. 2018. May 8;9(3). Available from: <http://www.ncbi.nlm.nih.gov/pubmed/29739909>
21. Honke N, Shaabani N, Zhang D-E, Hardt C, Lang KS. Multiple functions of USP18. *Cell Death Dis*. 2016. November 3;7(11):e2444 Available from: <http://www.ncbi.nlm.nih.gov/pubmed/27809302>
22. Kusano S, Eizuru Y. Interaction of the phospholipid scramblase 1 with HIV-1 Tat results in the repression of Tat-dependent transcription. *Biochem Biophys Res Commun*. 2013. April 19;433(4):438–44. Available from: <http://www.ncbi.nlm.nih.gov/pubmed/23501106>
23. McLaren PJ, Gawanbacht A, Pyndiah N, Krapp C, Hotter D, Kluge SF, et al. Identification of potential HIV restriction factors by combining evolutionary genomic signatures with functional analyses. *Retrovirology*. 2015. May 16;12(1):41 Available from: <http://www.ncbi.nlm.nih.gov/pubmed/25980612>

24. Díez-Fuertes F, De La Torre-Tarazona HE, Calonge E, Pernas M, Alonso-Socas MDM, Capa L, et al. Transcriptome Sequencing of Peripheral Blood Mononuclear Cells from Elite Controller-Long Term Non Progressors. *Sci Rep*. 2019. October 3;9(1):14265 Available from: <http://www.ncbi.nlm.nih.gov/pubmed/31582776>
25. Johnson TP, Patel K, Johnson KR, Maric D, Calabresi PA, Hasbun R, et al. Induction of IL-17 and nonclassical T-cell activation by HIV-Tat protein. *Proc Natl Acad Sci U S A*. 2013. August 13;110(33):13588–93. Available from: <http://www.ncbi.nlm.nih.gov/pubmed/23898208>
26. König R, Zhou Y, Elleder D, Diamond TL, Bonamy GMC, Irelan JT, et al. Global analysis of host-pathogen interactions that regulate early-stage HIV-1 replication. *Cell*. 2008. October 3;135(1):49–60. Available from: <http://www.ncbi.nlm.nih.gov/pubmed/18854154>
27. Grunewald ME, Chen Y, Kuny C, Maejima T, Lease R, Ferraris D, et al. The coronavirus macrodomain is required to prevent PARP-mediated inhibition of virus replication and enhancement of IFN expression. Weber F, editor. *PLoS Pathog*. 2019. May 16;15(5):e1007756 Available from: <http://www.ncbi.nlm.nih.gov/pubmed/31095648>
28. Zhang Y, Mao D, Roswit WT, Jin X, Patel AC, Patel DA, et al. PARP9-DTX3L ubiquitin ligase targets host histone H2BJ and viral 3C protease to enhance interferon signaling and control viral infection. *Nat Immunol*. 2015. December 19;16(12):1215–27. Available from: <http://www.ncbi.nlm.nih.gov/pubmed/26479788>
29. Osei Kuffour E, Schott K, Jaguva Vasudevan AA, Holler J, Schulz WA, Lang PA, et al. USP18 (UBP43) Abrogates p21-Mediated Inhibition of HIV-1. *J Virol*. 2018;92(20). Available from: <http://www.ncbi.nlm.nih.gov/pubmed/30068654>
30. Bulli L, Apolonia L, Kutzner J, Pollpeter D, Goujon C, Herold N, et al. Complex Interplay between HIV-1 Capsid and MX2-Independent Alpha Interferon-Induced Antiviral Factors. *J Virol*. 2016. August 15;90(16):7469–80. Available from: <http://www.ncbi.nlm.nih.gov/pubmed/27279606>
31. Fricke T, White TE, Schulte B, de Souza Aranha Vieira DA, Dharan A, Campbell EM, et al. MxB binds to the HIV-1 core and prevents the uncoating process of

- HIV-1. *Retrovirology*. 2014. August 14;11(1):68 Available from: <http://www.ncbi.nlm.nih.gov/pubmed/25123063>
32. Furuya AKM, Sharifi HJ, de Noronha CMC. The Curious Case of Type I IFN and MxA: Tipping the Immune Balance in AIDS. *Front Immunol*. 2014. September 2;5:419 Available from: <http://www.ncbi.nlm.nih.gov/pubmed/25228901>
33. Loke P, Favre D, Hunt PW, Leung JM, Kanwar B, Martin JN, et al. Correlating cellular and molecular signatures of mucosal immunity that distinguish HIV controllers from noncontrollers Correlating cellular and molecular signatures of mucosal immunity that distinguish HIV controllers from noncontrollers. *Blood*. 2010;115(15):20–32
34. Andrade VM, Mavian C, Babic D, Cordeiro T, Sharkey M, Barrios L, et al. A minor population of macrophage-tropic HIV-1 variants is identified in recrudescing viremia following analytic treatment interruption. *Proc Natl Acad Sci U S A*. 2020. May 5;117(18):9981–90. Available from: <http://www.ncbi.nlm.nih.gov/pubmed/32300019>
35. Soper A, Kimura I, Nagaoka S, Konno Y, Yamamoto K, Koyanagi Y, et al. Type I Interferon Responses by HIV-1 Infection: Association with Disease Progression and Control. *Front Immunol*. 2017;8:1823 Available from: <http://www.ncbi.nlm.nih.gov/pubmed/29379496>
36. Fourati S, Ribeiro SP, Blasco Tavares Pereira Lopes F, Talla A, Lefebvre F, Cameron M, et al. Integrated systems approach defines the antiviral pathways conferring protection by the RV144 HIV vaccine. *Nat Commun*. 2019. December 20;10(1):863 Available from: <http://www.ncbi.nlm.nih.gov/pubmed/30787294>
37. Sandstrom TS, Ranganath N, Angel JB. Impairment of the type I interferon response by HIV-1: Potential targets for HIV eradication. *Cytokine Growth Factor Rev*. 2017. October;37:1–16. Available from: <http://www.ncbi.nlm.nih.gov/pubmed/28455216>
38. Cheng L, Ma J, Li J, Li D, Li G, Li F, et al. Blocking type I interferon signaling enhances T cell recovery and reduces HIV-1 reservoirs. *J Clin Invest*. 2017;127(1):269–79. Available from: <http://www.ncbi.nlm.nih.gov/pubmed/27941247>

39. Bosinger SE, Li Q, Gordon SN, Klatt NR, Duan L, Xu L, et al. Global genomic analysis reveals rapid control of a robust innate response in SIV-infected sooty mangabeys. *J Clin Invest*. 2009. December 23;119(12):3556–72. Available from: <http://www.ncbi.nlm.nih.gov/pubmed/19959874>
40. Colby DJ, Trautmann L, Pinyakorn S, Leyre L, Pagliuzza A, Kroon E, et al. Rapid HIV RNA rebound after antiretroviral treatment interruption in persons durably suppressed in Fiebig i acute HIV infection brief-communication. *Nat Med*. 2018. July 11;24(7):923–6. Available from: <http://www.ncbi.nlm.nih.gov/pubmed/29892063>
41. Shan L, Siliciano RF. From reactivation of latent HIV-1 to elimination of the latent reservoir: The presence of multiple barriers to viral eradication. *BioEssays*. 2013. June;35(6):544–52. Available from: <http://www.ncbi.nlm.nih.gov/pubmed/23613347>
42. Wu T, Shin HM, Moseman EA, Ji Y, Huang B, Harly C, et al. TCF1 Is Required for the T Follicular Helper Cell Response to Viral Infection. *Cell Rep*. 2015. September 29;12(12):2099–110. Available from: <http://www.ncbi.nlm.nih.gov/pubmed/26365183>
43. Berdasco M, Esteller M. Clinical epigenetics: seizing opportunities for translation. *Nat Rev Genet*. 2019. February 27;20(2):109–27. Available from: <http://www.ncbi.nlm.nih.gov/pubmed/30479381>
44. Aryee MJ, Jaffe AE, Corrada-Bravo H, Ladd-Acosta C, Feinberg AP, Hansen KD, et al. Minfi: A flexible and comprehensive Bioconductor package for the analysis of Infinium DNA methylation microarrays. *Bioinformatics*. 2014;30(10):1363–9. 10.1093/bioinformatics/btu049
45. The R Foundation. The R project for statistical computing . 2016. Available from: <https://www.r-project.org/>
46. Leek JT, Johnson WE, Parker HS, Jaffe AE, Storey JD. The sva package for removing batch effects and other unwanted variation in high-throughput experiments. *Bioinformatics*. 2012. March 15;28(6):882–3. Available from: <http://www.ncbi.nlm.nih.gov/pubmed/22257669>

47. Gonzalo Sanz R, Sánchez-Pla A. Statistical Analysis of Microarray Data In: Bolón-Canedo V, Alonso-Betanzos A, editors. *Microarray Bioinformatics Methods in Molecular Biology*. Humana, New York, NY; 2019. p. 87–121. Available from: http://link.springer.com/10.1007/978-1-4939-9442-7_5
48. Zhang X, Hu Y, Aouizerat BE, Peng G, Marconi VC, Corley MJ, et al. Machine learning selected smoking-associated DNA methylation signatures that predict HIV prognosis and mortality. *Clin Epigenetics*. 2018. December 13;10(1):155 Available from: <http://www.ncbi.nlm.nih.gov/pubmed/30545403>
49. Houseman EA, Accomando WP, Koestler DC, Christensen BC, Marsit CJ, Nelson HH, et al. DNA methylation arrays as surrogate measures of cell mixture distribution. *BMC Bioinformatics*. 2012. May 8;13(1):86 Available from: <http://www.ncbi.nlm.nih.gov/pubmed/22568884>
50. Yu G, Wang L-G, Han Y, He Q-Y. clusterProfiler: an R package for comparing biological themes among gene clusters. *OMICS*. 2012. May;16(5):284–7. Available from: <http://www.ncbi.nlm.nih.gov/pubmed/22455463>
51. Martínez-Bonet M, Puertas MC, Fortuny C, Ouchi D, Mellado MJ, Rojo P, et al. Establishment and Replenishment of the Viral Reservoir in Perinatally HIV-1-infected Children Initiating Very Early Antiretroviral Therapy. *Clin Infect Dis*. 2015. October 1;61(7):1169–78. Available from: <http://www.ncbi.nlm.nih.gov/pubmed/26063721>
52. Frahm N, Korber BT, Adams CM, Szinger JJ, Draenert R, Addo MM, et al. Consistent cytotoxic-T-lymphocyte targeting of immunodominant regions in human immunodeficiency virus across multiple ethnicities. *J Virol*. 2004. March 1;78(5):2187–200. Available from: <http://www.ncbi.nlm.nih.gov/pubmed/14963115>
53. Montefiori DC. Evaluating neutralizing antibodies against HIV, SIV, and SHIV in luciferase reporter gene assays. *Curr Protoc Immunol*. 2005. January;64(1):11 Available from: <http://www.ncbi.nlm.nih.gov/pubmed/18432938>
54. Sánchez-Palomino S, Massanella M, Carrillo J, García A, García F, González N, et al. A cell-to-cell HIV transfer assay identifies humoral responses with broad

- neutralization activity. *Vaccine*. 2011. July 18;29(32):5250–9. Available from: <http://www.ncbi.nlm.nih.gov/pubmed/21609746>
55. James G, Witten D, Hastie T, Tibshirani R. Tree-Based Methods In: *An Introduction to Statistical Learning*. Springer, New York, NY; 2013. p. 303–35. Available from: http://link.springer.com/10.1007/978-1-4614-7138-7_8
56. Gu Z, Gu L, Eils R, Schlesner M, Brors B. Circlize implements and enhances circular visualization in R. *Bioinformatics*. 2014. October;30(19):2811–2. Available from: <http://www.ncbi.nlm.nih.gov/pubmed/24930139>

Supporting information

Figure S1. Random Forest selected CpG sites correlate among them and with antiviral and immunological parameters. Circos plot showing DMPs associated with each of the viral and immunological parameters and their interrelation. The significant correlations (p -value < 0.05) with CpG sites and a maximum of 15 CpG sites is shown per each parameter (based on higher Spearman's Rho values): viral load (orange), HIV-proviral (yellow), breadth (purple) and magnitude (green) of the virus specific T cell response and neutralizing antibody capabilities against NL43 (pink) and BAL (grey). The inter-relation between the different CpG sites methylation levels (only correlations with Spearman's Rho $> |0.6|$ and p -value < 0.05) are also shown (In green there are the positive correlations, and in red, the negative ones).

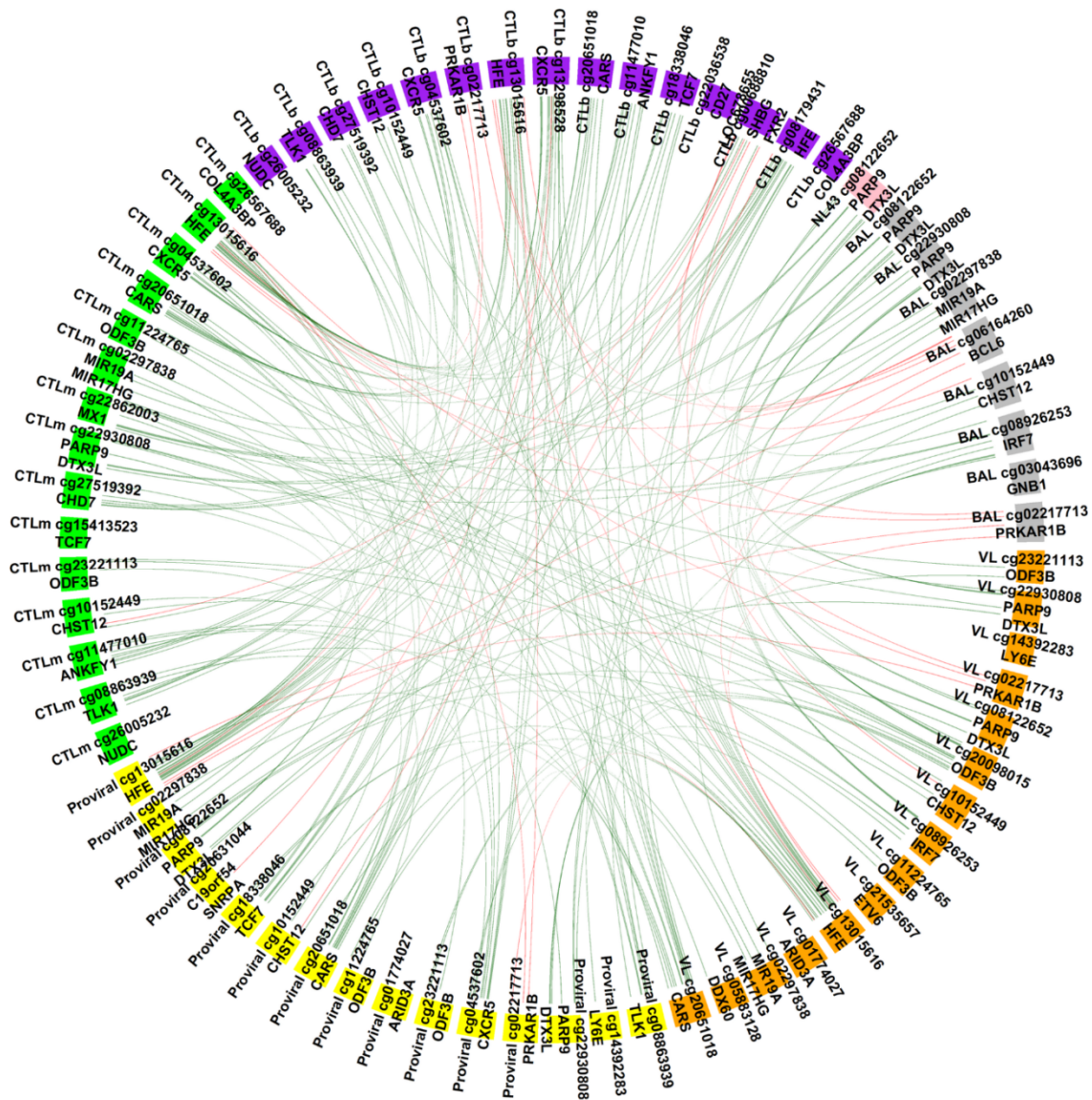


Table S1. Clinical information of HIV-infected individuals

Group	Age (yr)	Gender (M/F)	Viral Load (VL, plasma HIV RNA copies/ml)	Proviral DNA	CD4 count (cells/mm ³)	CTL Breadth	CTL Magnitude	nAb BaL	qRT-PCR
HIV-Low01	34	M	950	163.6	608	14	12280	155.2	Analyzed
HIV-Low02	56	F	49	16.0	873	10	16950	65.6	Analyzed
HIV-Low04	35	M	9999	317.7	438	19	20580	113.5	Analyzed
HIV-Low05	46	M	1100	76.7	485	40	44720	528.4	Analyzed
HIV-Low06	46	F	49	6.7	1083	11	9480	ND	Analyzed
HIV-Low07	40	M	210	ND	786	8	2690	59	ND
HIV-Low08	48	F	8900	412.5	913	38	32100	2500.3	Analyzed
HIV-Low09	28	M	1000	ND	889	16	8380	30.3	ND
HIV-Low10	37	M	810	ND	665	13	25308	399	ND
HIV-Low11	37	F	1800	180.8	511	35	22708	2223.3	Analyzed
HIV-Low12	50	F	49	9.1	487	50	36378	1221.8	Analyzed
HIV-Low13	40	F	340	294.3	832	15	17103	187.1	Analyzed
HIV-Low14	37	F	49	25.7	665	7	5900	0.6	Analyzed
HIV-Low15	38	M	160	ND	512	22	31810	90.8	ND
HIV-Low16	33	M	530	25.8	948	15	21020	662.2	Analyzed
HIV-Low18	29	M	49	0.0	892	8	2830	18.9	Analyzed
HIV-Low19	27	M	7700	ND	733	35	18881.1	15.3	ND
HIV-Low20	45	F	2900	278.5	582	49	35602	587.5	Analyzed
HIV-Low21	30	F	49	ND	1114	14	7190	18.7	ND
HIV-Low22	46	F	2800	32.5	434	22	4810	ND	Analyzed
HIV-Low23	38	M	49	90.4	583	23	10861	1	Analyzed
HIV-Low24	26	M	2300	49.1	642	22	37180	42.7	Analyzed
HIV-Low26	44	M	50	6.2	872	25	12516	241	Analyzed
HIV-Low28	41	F	25	20.9	672	7	1530	114.8	Analyzed
HIV-Low29	50	F	50	0.0	1228	14	15050	17.3	Analyzed
HIV-Low30	46	M	66	28.6	755	ND	ND	182	Analyzed
HIV-Low31	51	M	25	41.5	450	ND	ND	1625.5	Analyzed
HIV-Low32	48	F	230	15.9	516	27	12180	488.7	Analyzed
HIV-Low33	44	M	330	31.3	1237	12	4470	110.2	Analyzed
HIV-Low35	48	M	50	18.4	601	ND	ND	45.3	Analyzed
HIV-Low36	35	F	25	11.5	930	5	660	1	Analyzed
HIV-Low37	36	F	880	12.1	1343	6	1810	123.9	Analyzed
HIV-Low38	40	F	4800	153.5	569	12	5920	1261.8	ND
HIV-Low39	57	F	50	ND	485	8	4840	492	ND
HIV-Low40	46	M	1700	ND	742	ND	ND	54.2	ND
HIV-Low42	31	M	9756	620.7	404	7	1170	95.7	ND
HIV-Low43	29	M	5624	1662.4	823	17	5550	535.8	Analyzed
HIV-Low45	41	M	6127	50.2	531	11	1930	ND	Analyzed
HIV-Low46	34	M	400	220.1	1035	3	650	109.1	Analyzed
HIV-Low47	33	F	7923	366.5	524	2	480	871	Analyzed
HIV-Low50	30	M	4482	0.0	1151	10	2610	ND	Analyzed
HIV-High01	21	F	269431	4.2	212	ND	ND	117.5	ND
HIV-High02	28	F	74922	ND	571	3	220	98.4	ND
HIV-High06	37	F	140000	231.9	11	11	12790	94.8	Analyzed
HIV-High07	40	F	64000	922.6	282	8	3790	5.5	Analyzed
HIV-High09	24	F	610000	1722.4	128	11	3548	ND	Analyzed
HIV-High11	33	F	1200000	80.1	75	12	15230	56.1	Analyzed
HIV-High12	50	F	54000	363.6	67	5	1080	31.2	Analyzed
HIV-High14	45	F	68000	ND	98	9	7190	719.4	ND
HIV-High15	45	F	510000	ND	12	7	1440	2089.3	ND
HIV-High17	22	M	152554	3143.4	293	8	1340	ND	ND
HIV-High19	23	M	70393	223.7	208	8	10730	ND	ND
HIV-High21	23	M	50295	1176.5	505	6	3800	394.5	Analyzed
HIV-High22	23	M	240039	1144.6	388	21	19100	1	Analyzed
HIV-High23	24	M	93928	3246.6	256	1	50	ND	Analyzed
HIV-High24	24	M	365977	1204.6	726	26	13746.8	45.6	Analyzed
HIV-High27	26	M	750000	941.4	239	23	9280	ND	ND
HIV-High29	28	M	216105	3021.1	313	13	6325	ND	ND
HIV-High30	28	M	327087	2127.2	544	8	4530	437.5	Analyzed
HIV-High32	29	M	125701	ND	404	7	5410	134.3	ND
HIV-High34	30	M	61078	558.4	380	19	27260	ND	Analyzed
HIV-High35	31	M	194091	1962.5	271	6	520	96.6	Analyzed
HIV-High39	32	M	170000	507.0	17	56	114630	281.2	Analyzed
HIV-High42	35	M	71739	1562.5	227	5	690	ND	ND
HIV-High43	35	M	95365	3149.2	240	5	660	ND	Analyzed
HIV-High44	35	M	102936	1346.3	283	26	9310	407.4	Analyzed
HIV-High45	35	M	63381	1128.7	384	28	35470	544.5	ND
HIV-High48	37	M	61011	ND	641	2	850	266.7	ND
HIV-High49	37	M	140000	ND	20	26	5980	42.7	ND
HIV-High50	38	M	544275	ND	402	24	18590	266.1	ND

ND: Not determined

T cell Breadth: Number of reactive peptides

T cell Magnitude: Median of SFC per 10⁶ PBMC

nAb BaL: Neutralizing antibodies to HIV-1-BaL(1/IC50 of plasma)

M: Male

F: Female

Table S2. Clinical information of independent cohorts including age, sex, viral load and CD4 counts.

Group	Classification	Age (yr)	Gender (M/F)	Viral Load (VL, plasma HIV RNA copies/ml)	CD4 count (cells/mm ³)	Proviral DNA	qRT-PCR
EC_01	EC	31	F	<25	922	0	Analysed
EC_03	EC	40	F	<40	752	8.5	Analysed
EC_04	EC	46	F	<25	1557	5.6	Analysed
EC_05	EC	43	F	<25	372	4.3	Analysed
EC_06	EC	59	M	<25	411	11.1	Analysed
EC_07	EC	40	F	<25	245	35.4	Analysed
EC_09	EC	40	F	<56	898	3.8	Analysed
EC_10	EC	50	M	<25	450	0	Analysed
EC_12	EC	46	M	<25	940	3.4	Analysed
EC_13	EC	52	M	<25	667	0	Analysed
EC_15	EC	53	M	<25	959	20.8	Analysed
EC_18	EC	55	F	<50	838	23.8	Analysed
Acute_01	Acute	35	M	327023	891	520.2	Analysed
Acute_02	Acute	30	M	312060	332	2839.5	Analysed ^A
Acute_03	Acute	21	M	400	590	520.9	Analysed
Acute_04	Acute	24	M	51638	673	569.7	Analysed
Acute_05	Acute	34	M	25782	463	652.2	Analysed
Acute_06	Acute	33	M	904569	317	3070.2	Analysed
Acute_07	Acute	32	M	26348	646	414.2	Analysed
Acute_08	Acute	27	M	64083	558	569.8	Analysed
Chr-Untreat-5	Untreated	46	M	4900	462	175.5	Analysed
Chr-Untreat-9	Untreated	32	M	7200	328	281.6	Analysed
Chr-Untreat-11	Untreated	30	F	15000	456	549.8	Analysed
Chr-Untreat-12	Untreated	45	M	50000	629	222.2	Analysed
Chr-Untreat-13	Untreated	34	F	8900	572	8.5	Analysed
Chr-Untreat-14	Untreated	29	M	13284	661	317.5	Analysed
Chr_Untreat_16	Untreated	28	M	13893	529	517.9	Analysed
Chr_Untreat_17	Untreated	24	M	11000	914	596.4	Analysed
Chr_Untreat_18	Untreated	40	F	12000	495	160.5	Analysed
Chr_Untreat_19	Untreated	33	M	27342	847	389.5	Analysed
Chr_Untreat_20	Untreated	44	M	44000	437	100.2	Analysed
Chr-treat-5	Treated	47	M	50	532	52.3	Analysed
Chr-treat-6	Treated	41	M	50	426	387.5	Analysed
Chr-treat-11	Treated	30	F	25	786	191.4	Analysed
Chr-treat-12	Treated	45	M	50	558	43	Analysed
Chr-treat-15	Treated	38	M	40	659	89.3	Analysed

A. No sample availability for USP18

M: Male

F: Female

Table S3.1. Gene Enrichment Analysis – Cluster 1 (Top 25)*

* The complete table can be found on: <https://doi.org/10.1371/journal.ppat.1008678.s004>

ID	Description	pvalue	p.adjust	geneID	Count
GO:0051607	defense response to virus	4.09E-06	4.71E-03	<i>DDX60/IFI44L/PLSCR1/PARP9/IRF7/MX1</i>	6
GO:0002252	immune effector process	7.70E-06	4.71E-03	<i>A/PTPRJ/CTS/DDX60/BCL6/IFI44L/PLSCR1/PARP9/IRF7/MX1/SMAD7</i>	11
GO:0050776	regulation of immune response	1.61E-05	6.57E-03	<i>A/PTPRJ/MIR19A/DDX60/BCL6/PLSCR1/PARP9/IRF7/USP18/SMAD7</i>	10
GO:0009615	response to virus	2.99E-05	9.15E-03	<i>DDX60/IFI44L/PLSCR1/PARP9/IRF7/MX1</i>	6
GO:0006955	immune response	4.27E-05	1.05E-02	<i>A/PTPRJ/CTS/MIR19A/DDX60/BCL6/IFI44L/PLSCR1/PARP9/IRF7/USP18/MX1/SMAD7</i>	13
GO:0045088	regulation of innate immune response	9.08E-05	1.68E-02	<i>MIR19A/DDX60/PLSCR1/PARP9/IRF7/USP18</i>	6
GO:0002682	regulation of immune system process	9.66E-05	1.68E-02	<i>A/PTPRJ/MIR19A/DDX60/BCL6/PLSCR1/PARP9/IRF7/USP18/SMAD7/RUNX3</i>	11
GO:0002376	immune system process	1.17E-04	1.68E-02	<i>A/PTPRJ/CTS/MIR19A/DDX60/BCL6/IFI44L/PLSCR1/PARP9/IRF7/USP18/ETV6/MX1/SMAD7/RUNX3</i>	15
GO:0045087	innate immune response	1.39E-04	1.68E-02	<i>A/MIR19A/DDX60/PLSCR1/PARP9/IRF7/USP18/MX1</i>	8
GO:0002697	regulation of immune effector process	1.70E-04	1.68E-02	<i>A/PTPRJ/DDX60/BCL6/PARP9/SMAD7</i>	6
GO:0098542	defense response to other organism	1.70E-04	1.68E-02	<i>DDX60/IFI44L/PLSCR1/PARP9/IRF7/MX1</i>	6
GO:0060337	type I interferon signaling pathway	1.79E-04	1.68E-02	<i>HLA-A/IRF7/USP18/MX1</i>	4
GO:0071357	cellular response to type I interferon	1.79E-04	1.68E-02	<i>HLA-A/IRF7/USP18/MX1</i>	4
GO:0002684	positive regulation of immune system process	2.09E-04	1.78E-02	<i>A/PTPRJ/MIR19A/DDX60/BCL6/PLSCR1/PARP9/IRF7/RUNX3</i>	9
GO:0034340	response to type I interferon	2.18E-04	1.78E-02	<i>HLA-A/IRF7/USP18/MX1</i>	4
GO:0043370	regulation of CD4-positive alpha-beta T cell differentiation	3.57E-04	2.66E-02	<i>BCL6/SMAD7/RUNX3</i>	3
GO:0045089	positive regulation of innate immune response	3.69E-04	2.66E-02	<i>MIR19A/DDX60/PLSCR1/PARP9/IRF7</i>	5
GO:0045581	negative regulation of T cell differentiation	4.86E-04	3.13E-02	<i>BCL6/SMAD7/RUNX3</i>	3
GO:2000514	regulation of CD4-positive alpha-beta T cell activation	4.86E-04	3.13E-02	<i>BCL6/SMAD7/RUNX3</i>	3
GO:0046637	regulation of alpha-beta T cell differentiation	6.41E-04	3.74E-02	<i>BCL6/SMAD7/RUNX3</i>	3
GO:0006952	defense response	6.42E-04	3.74E-02	<i>HLA-A/MIR19A/DDX60/BCL6/IFI44L/PLSCR1/PARP9/IRF7/USP18/MX1</i>	10
GO:0045620	negative regulation of lymphocyte differentiation	8.25E-04	4.56E-02	<i>BCL6/SMAD7/RUNX3</i>	3
GO:0031347	regulation of defense response	8.58E-04	4.56E-02	<i>MIR19A/DDX60/BCL6/PLSCR1/PARP9/IRF7/USP18</i>	7
GO:0002819	regulation of adaptive immune response	1.03E-03	4.93E-02	<i>HLA-A/BCL6/IRF7/SMAD7</i>	4
GO:0050731	positive regulation of peptidyl-tyrosine phosphorylation	1.03E-03	4.93E-02	<i>PTPRJ/MIR19A/PARP9/TNK2</i>	4

Table S3.2. Gene Enrichment Analysis – Cluster 2 (Top 25)*

* The complete table can be found on <https://doi.org/10.1371/journal.ppat.1008678.s004>

ID	Description	pvalue	p.adjust	geneID	Count
GO:0046631	alpha-beta T cell activation	4.48E-03	4.48E-03	<i>ITPKB/HFE/TCF7</i>	3
GO:0015914	phospholipid transport	5.84E-03	5.84E-03	<i>PITPNC1/COL4A3BP</i>	2
GO:0033209	tumor necrosis factor-mediated signaling pathway	7.09E-03	7.09E-03	<i>TNFRSF19/CD27</i>	2
GO:0046649	lymphocyte activation	7.91E-03	7.91E-03	<i>ITPKB/CXCR5/HFE/TCF7/CD27</i>	5
GO:0015748	organophosphate ester transport	8.44E-03	8.44E-03	<i>PITPNC1/COL4A3BP</i>	2
GO:0022407	regulation of cell-cell adhesion	1.08E-02	1.08E-02	<i>ITPKB/HFE/KIF26B/CD27</i>	4
GO:2000106	regulation of leukocyte apoptotic process	1.15E-02	1.15E-02	<i>ITPKB/CD27</i>	2
GO:0045582	positive regulation of T cell differentiation	1.49E-02	1.49E-02	<i>ITPKB/CD27</i>	2
GO:0045621	positive regulation of lymphocyte differentiation	1.49E-02	1.49E-02	<i>ITPKB/CD27</i>	2
GO:0042110	T cell activation	1.60E-02	1.60E-02	<i>ITPKB/HFE/TCF7/CD27</i>	4
GO:0022409	positive regulation of cell-cell adhesion	1.63E-02	1.63E-02	<i>ITPKB/KIF26B/CD27</i>	3
GO:0038093	Fc receptor signaling pathway	1.68E-02	1.68E-02	<i>LCP2/CD247</i>	2
GO:0046634	regulation of alpha-beta T cell activation	1.68E-02	1.68E-02	<i>ITPKB/HFE</i>	2
GO:0045321	leukocyte activation	1.74E-02	1.74E-02	<i>LCP2/ITPKB/CXCR5/HFE/TCF7/C</i>	6
GO:0030217	T cell differentiation	1.83E-02	1.83E-02	<i>D27</i>	3
GO:0071887	leukocyte apoptotic process	1.87E-02	1.87E-02	<i>ITPKB/CD27</i>	2
GO:0050863	regulation of T cell activation	2.50E-02	2.50E-02	<i>ITPKB/HFE/CD27</i>	3
GO:1902107	positive regulation of leukocyte differentiation	2.52E-02	2.52E-02	<i>ITPKB/CD27</i>	2
GO:0002684	positive regulation of immune system process	2.74E-02	2.74E-02	<i>LCP2/ITPKB/HFE/CD247/CD27</i>	5
GO:0045807	positive regulation of endocytosis	2.75E-02	2.75E-02	<i>HFE/ANKFY1</i>	2
GO:1903037	regulation of leukocyte cell-cell adhesion	2.76E-02	2.76E-02	<i>ITPKB/HFE/CD27</i>	3
GO:0006955	immune response	2.94E-02	2.94E-02	<i>LCP2/CXCR5/HFE/TCF7/CD247/C</i>	7
GO:0046632	alpha-beta T cell differentiation	2.99E-02	2.99E-02	<i>D27/COL4A3BP</i>	2
GO:0071356	cellular response to tumor necrosis factor	2.99E-02	2.99E-02	<i>ITPKB/TCF7</i>	2
GO:1903708	positive regulation of hemopoiesis	2.99E-02	2.99E-02	<i>TNFRSF19/CD27</i>	2

Table S4. Classificatory CpG positions into the groups of HIV-High or HIV-Low for validation dataset GSE53840

Dataset	CpG position	Chromosome	Gene	Relation to island	Relation to gene	Mean Beta-value (HIV-Low)	Mean Beta-value (HIV-High)	p-value	FreqMultivariate
GSE53840	cg27414655	chr4	<i>PRDM5</i>	N_Shore	Body	0.15	0.19	0.00	781
GSE53840	cg04605681	chr4	<i>SH3TC1</i>	OpenSea	Body	0.35	0.42	0.00	709
GSE53840	cg04109883	chr10	<i>C10orf72</i>	OpenSea	Body	0.80	0.72	0.00	513
GSE53840	cg02339078	chr5	<i>C100129716_ARFD1</i>	S_Shelf	Body_TSS1500	0.13	0.22	0.00	461
GSE53840	cg06321596	chr16	<i>XYLT1</i>	OpenSea	Body	0.45	0.52	0.01	386
GSE53840	cg02854554	chr1	<i>FAM46C</i>	S_Shore	SUTR	0.09	0.12	0.00	361
GSE53840	cg27549619	chr16	<i>AXIN1</i>	Island	Body	0.12	0.17	0.00	355
GSE53840	cg23792308	chr17	<i>COX10</i>	OpenSea	Body	0.16	0.22	0.01	346
GSE53840	cg22930808	chr3	<i>PARFP9_DTX3L</i>	N_Shore	SUTR_TSS1500	0.57	0.47	0.02	337
GSE53840	cg05326274	chr14	<i>NPAS3</i>	S_Shelf	TSS1500	0.10	0.15	0.00	336
GSE53840	cg10646395	chr11	<i>PRDM11</i>	N_Shore	Body	0.30	0.26	0.03	333
GSE53840	cg081122652	chr3	<i>PARFP9_DTX3L</i>	N_Shore	SUTR_TSS1500	0.78	0.68	0.02	332
GSE53840	cg27517345	chr10	<i>C10orf26</i>	OpenSea	SUTR_Body_1stExon	0.47	0.54	0.00	273
GSE53840	cg00033516	chr4	<i>FLJ13197_KLF3</i>	S_Shore	TSS1500_SUTR	0.10	0.13	0.00	227
GSE53840	cg23522611	chr2	<i>FOSL2</i>	S_Shore	Body	0.15	0.20	0.02	227
GSE53840	cg15658306	chr6	<i>TREML2</i>	OpenSea	TSS200	0.27	0.35	0.00	207
GSE53840	cg11685391	chr10	<i>KCNIP2</i>	S_Shelf	Body	0.19	0.24	0.02	204
GSE53840	cg21115391	chr11	<i>CCDC67</i>	OpenSea	Body	0.70	0.64	0.00	201
GSE53840	cg05568549	chr6	<i>CCND3</i>	N_Shore	Body_5UTR	0.22	0.26	0.02	181
GSE53840	cg07978738	chr10	<i>ABLIM1</i>	OpenSea	Body	0.27	0.23	0.00	153
GSE53840	cg19715094	chr11	<i>TMEM25</i>	S_Shore	Body	0.57	0.62	0.03	128
GSE53840	cg13290370	chr1	<i>FAIM3</i>	Island	Body	0.13	0.20	0.00	119
GSE53840	cg05524529	chr5	<i>C1Q TNF2</i>	Island	1stExon	0.05	0.07	0.02	106
GSE53840	cg09911401	chr10	<i>SVIL</i>	OpenSea	Body	0.86	0.81	0.01	106
GSE53840	cg18297196	chr6	<i>TREML2</i>	OpenSea	TSS200	0.29	0.40	0.00	99
GSE53840	cg14870271	chr17	<i>LGAL S3BP</i>	OpenSea	1stExon_SUTR	0.42	0.34	0.03	98
GSE53840	cg17906105	chr7	<i>NCAPG2</i>	OpenSea	Body	0.19	0.26	0.01	89
GSE53840	cg04410989	chr20	<i>SAMHD1</i>	N_Shore	Body	0.29	0.36	0.01	86
GSE53840	cg26928682	chr6	<i>TREML2</i>	OpenSea	1stExon_SUTR	0.17	0.19	0.00	85
GSE53840	cg02872426	chr6	<i>DDO</i>	OpenSea	TSS200	0.50	0.39	0.00	82
GSE53840	cg09753006	chr1	<i>CFHR2</i>	OpenSea	Body	0.68	0.63	0.01	79
GSE53840	cg00737979	chr5	<i>LOC340074</i>	OpenSea	TSS1500	0.70	0.64	0.00	76
GSE53840	cg23651889	chr3	<i>LPP</i>	OpenSea	SUTR	0.62	0.53	0.05	74
GSE53840	cg23570810	chr11	<i>IFITM1</i>	N_Shore	Body	0.70	0.59	0.03	69
GSE53840	cg25155774	chr3	<i>CCR9</i>	OpenSea	SUTR	0.27	0.30	0.01	68
GSE53840	cg01502396	chr11	<i>MDK</i>	Island	Body	0.12	0.17	0.00	67
GSE53840	cg04912843	chr1	<i>GIPC2</i>	Island	1stExon	0.04	0.05	0.03	64
GSE53840	cg26885488	chr1	<i>MEF2D</i>	OpenSea	SUTR	0.28	0.25	0.04	62
GSE53840	cg05432003	chr11	<i>IFITM1</i>	S_Shore	TSS1500	0.54	0.49	0.01	57
GSE53840	cg05480370	chr5	<i>SPOCK1</i>	OpenSea	Body	0.59	0.50	0.00	56
GSE53840	cg11591520	chr4	<i>IL21</i>	OpenSea	TSS200	0.76	0.69	0.00	55
GSE53840	cg06095752	chr2	<i>MAP4K4</i>	N_Shore	TSS1500	0.36	0.43	0.02	52
GSE53840	cg02534363	chr3	<i>NBEAL2</i>	Island	3UTR	0.31	0.36	0.04	47
GSE53840	cg16592378	chr11	<i>KIRREL3</i>	OpenSea	Body	0.63	0.58	0.02	46
GSE53840	cg10278102	chr11	<i>FRMT3</i>	S_Shore	SUTR_Body	0.46	0.40	0.01	44
GSE53840	cg26846424	chr1	<i>PRDM16</i>	Island	Body	0.15	0.19	0.01	43
GSE53840	cg10755723	chr3	<i>C3orf19</i>	OpenSea	Body	0.66	0.59	0.01	40
GSE53840	cg06098530	chr10	<i>MYST4</i>	OpenSea	Body	0.23	0.31	0.01	39
GSE53840	cg13652336	chr8	<i>PREX2</i>	N_Shore	TSS1500	0.30	0.35	0.00	36
GSE53840	cg06896534	chr4	<i>BMPRI1B</i>	Island	SUTR	0.05	0.07	0.01	35
GSE53840	cg20661965	chr10	<i>ANXA8L2</i>	OpenSea	SUTR_1stExon	0.70	0.64	0.00	31
GSE53840	cg20869844	chr7	<i>RAB19</i>	OpenSea	TSS200	0.10	0.14	0.00	30
GSE53840	cg09361748	chr7	<i>CALN1</i>	OpenSea	Body	0.77	0.72	0.01	29
GSE53840	cg15356966	chr11	<i>LMO2</i>	OpenSea	SUTR	0.33	0.40	0.02	28
GSE53840	cg00804078	chr6	<i>DDO</i>	OpenSea	TSS200	0.30	0.27	0.01	27
GSE53840	cg13779868	chr10	<i>NET1</i>	N_Shore	Body_TSS200	0.25	0.32	0.00	24
GSE53840	cg00353773	chr10	<i>CXCL12</i>	Island	TSS200	0.08	0.13	0.01	22
GSE53840	cg08228703	chr14	<i>TMEM90A</i>	Island	TSS1500	0.04	0.05	0.00	22
GSE53840	cg01714284	chr4	<i>ACSL1</i>	OpenSea	Body	0.11	0.14	0.05	21
GSE53840	cg05423393	chr6	<i>TRAF3IP2</i>	OpenSea	Body_TSS200	0.19	0.24	0.01	20
GSE53840	cg06927323	chr17	<i>TBX21</i>	N_Shore	TSS1500	0.20	0.24	0.01	20
GSE53840	cg26769927	chr16	<i>SPN</i>	N_Shore	SUTR	0.04	0.06	0.00	20
GSE53840	cg07164639	chr6	<i>DDO</i>	OpenSea	TSS1500	0.37	0.32	0.00	19
GSE53840	cg22700686	chr1	<i>S100A2</i>	OpenSea	TSS1500	0.20	0.25	0.00	19
GSE53840	cg14538944	chr2	<i>DIRC3</i>	OpenSea	Body	0.78	0.72	0.01	18
GSE53840	cg17067226	chr3	<i>VEPH1</i>	OpenSea	Body	0.79	0.73	0.01	17
GSE53840	cg23728060	chr2	<i>GALNT5</i>	OpenSea	TSS1500	0.68	0.62	0.00	17
GSE53840	cg14236758	chr9	<i>RXRRA</i>	Island	Body	0.46	0.54	0.00	16
GSE53840	cg10168894	chr12	<i>RAB21</i>	N_Shore	TSS1500	0.22	0.16	0.00	15
GSE53840	cg12436738	chr2	<i>AGAP1</i>	Island	Body	0.05	0.08	0.04	15
GSE53840	cg14716968	chr11	<i>DLG2</i>	OpenSea	TSS1500_Body	0.52	0.45	0.05	15
GSE53840	cg19699140	chr13	<i>LECT1</i>	OpenSea	Body	0.83	0.79	0.00	15
GSE53840	cg06804564	chr1	<i>LRRRC8C</i>	S_Shore	SUTR	0.26	0.29	0.01	14
GSE53840	cg14898127	chr15	<i>IL16</i>	OpenSea	Body_1stExon_SUTR	0.76	0.79	0.05	14
GSE53840	cg26047334	chr2	<i>TNSI</i>	OpenSea	SUTR	0.64	0.55	0.00	14
GSE53840	cg27208925	chr16	<i>IRF8</i>	OpenSea	Body	0.50	0.57	0.00	14
GSE53840	cg12323063	chr17	<i>MAF2K6</i>	OpenSea	Body	0.55	0.65	0.00	13
GSE53840	cg03037761	chr11	<i>FZD4</i>	N_Shelf	Body	0.78	0.72	0.01	12
GSE53840	cg06233503	chr11	<i>KCNQ1</i>	Island	Body	0.21	0.24	0.02	12
GSE53840	cg20364660	chr11	<i>FDX1</i>	S_Shore	Body	0.12	0.15	0.00	12
GSE53840	cg20825022	chr2	<i>CNTNAP5</i>	OpenSea	Body	0.66	0.58	0.00	12
GSE53840	cg27009812	chr16	<i>CLDN9</i>	N_Shore	1stExon_SUTR	0.53	0.60	0.02	12
GSE53840	cg08336300	chr6	<i>SESN1</i>	S_Shore	Body	0.31	0.39	0.00	11
GSE53840	cg15867829	chr4	<i>PABPC4L</i>	OpenSea	3UTR	0.68	0.63	0.00	11

p-value: p-value of the regression model applied to determine DMPs. CpG positions are ordered according the frequency of selection by random forest model. HIV-High = pVL > 10.000copies/ml. HIV-Low = pVL < 10.000copies/ml. Chr = Chromosome.

Table S5. Classificatory CpG positions into the groups of HIV-High or HIV-Low without CD4 counts correction (study dataset: GSE140800).

Dataset	CpG position	Chromosome	Gene	Relation to island	Relation to gene	Mean Beta-value (HIV-Low)	Mean Beta-value (HIV-High)	p-value	FreqMultivariate
GSE140800	cg22930808	chr3	<i>PARP9_DTX3L</i>	N_Shore	5UTR_TSS1500	0.76	0.56	0.03	873
GSE140800	cg20098015	chr22	<i>ODF3B</i>	S_Shore	TSS200	0.64	0.50	0.01	840
GSE140800	cg01028142	chr2	<i>CMPK2</i>	N_Shore	Body	0.88	0.80	0.01	710
GSE140800	cg20939114	chr17	<i>PITPNC1</i>	OpenSea	Body	0.26	0.33	0.02	654
GSE140800	cg06228828	chr13	<i>DLEU2</i>	N_Shelf	Body	0.69	0.60	0.02	622
GSE140800	cg02217713	chr7	<i>PRKAR1B</i>	N_Shore	Body	0.71	0.62	0.04	538
GSE140800	cg10375409	chr1	<i>CD247</i>	N_Shelf	Body	0.71	0.78	0.00	460
GSE140800	cg15413523	chr5	<i>TCF7</i>	S_Shore	5UTR_1stExon_Body	0.47	0.54	0.02	456
GSE140800	cg01027405	chr5	<i>IL7R</i>	OpenSea	Body	0.57	0.68	0.05	452
GSE140800	cg14392283	chr8	<i>LY6E</i>	N_Shelf	3UTR	0.84	0.76	0.02	388
GSE140800	cg11224765	chr22	<i>ODF3B</i>	S_Shore	TSS200	0.58	0.48	0.03	348
GSE140800	cg08863939	chr2	<i>TLK1</i>	OpenSea	5UTR	0.46	0.55	0.02	327
GSE140800	cg04537602	chr11	<i>CXCF5</i>	OpenSea	Body_TSS1500	0.53	0.63	0.02	261
GSE140800	cg11477010	chr17	<i>ANKFY1</i>	OpenSea	Body	0.67	0.73	0.01	249
GSE140800	cg05515866	chr2	<i>FARF2</i>	S_Shore	5UTR	0.71	0.64	0.03	234
GSE140800	cg01553004	chr14	<i>C14orf4</i>	S_Shore	TSS1500	0.57	0.64	0.04	166
GSE140800	cg14293575	chr22	<i>USP18</i>	S_Shelf	5UTR	0.72	0.60	0.02	149
GSE140800	cg01623438	chr20	<i>CTSZ</i>	S_Shore	TSS1500	0.66	0.60	0.02	147
GSE140800	cg13298528	chr11	<i>CXCF5</i>	OpenSea	Body_TSS1500	0.57	0.67	0.01	134
GSE140800	cg00808969	chr11	<i>USP35_KCTD21</i>	N_Shore	TSS1500_5UTR	0.41	0.48	0.05	132
GSE140800	cg18338046	chr5	<i>TCF7</i>	S_Shore	Body	0.58	0.69	0.03	127
GSE140800	cg22763680	chr17	<i>SLFN12L</i>	S_Shore	Body	0.30	0.23	0.00	114
GSE140800	ch.1.839062R	chr1	<i>RUNX3</i>	OpenSea	Body	0.22	0.15	0.04	108
GSE140800	cg21686600	chr1	<i>C1orf201</i>	OpenSea	Body	0.65	0.71	0.01	106
GSE140800	cg03199014	chr1	<i>ITPKB</i>	N_Shore	Body	0.72	0.80	0.04	85
GSE140800	cg05424831	chr7	<i>ATXN7L1</i>	OpenSea	Body	0.76	0.82	0.01	83
GSE140800	cg02676052	chr5	<i>LCP2</i>	OpenSea	TSS1500	0.62	0.67	0.04	73
GSE140800	cg04691264	chr10	<i>LOC387647</i>	N_Shore	TSS1500	0.75	0.81	0.01	70
GSE140800	cg20781967	chr12	<i>NIN12</i>	OpenSea	1stExon_5UTR	0.64	0.73	0.01	69
GSE140800	cg10435235	chr13	<i>ARHGEF7</i>	OpenSea	3UTR	0.74	0.69	0.00	68
GSE140800	cg19400179	chr3	<i>DZIP3</i>	OpenSea	5UTR	0.37	0.47	0.01	67
GSE140800	cg06096336	chr2	<i>PSMD1_HTR2B</i>	OpenSea	Body_1stExon_5UTR	0.68	0.76	0.01	64
GSE140800	cg22036538	chr12	<i>CD27_LOC678655</i>	OpenSea	1stExon_5UTR_Body	0.34	0.44	0.01	59
GSE140800	cg26567688	chr5	<i>COL4A3BP</i>	OpenSea	Body	0.67	0.74	0.01	59
GSE140800	cg17118478	chr2	<i>NAB1</i>	OpenSea	Body	0.69	0.62	0.05	56
GSE140800	cg04858110	chr7	<i>SCRN1</i>	OpenSea	5UTR_Body	0.66	0.72	0.00	46
GSE140800	cg12042587	chr5	<i>GHR</i>	N_Shore	TSS200	0.22	0.28	0.01	39
GSE140800	cg07106927	chr1	<i>LY9</i>	N_Shelf	Body	0.81	0.88	0.00	35
GSE140800	cg08179431	chr6	<i>HFE</i>	OpenSea	TSS1500	0.70	0.79	0.04	35
GSE140800	cg16589461	chr11	<i>GLB1L2</i>	S_Shore	Body	0.65	0.70	0.03	29
GSE140800	cg18349022	chr7	<i>ZNF498</i>	OpenSea	Body	0.55	0.60	0.05	28
GSE140800	cg00950718	chr1	<i>CCDC19</i>	OpenSea	Body	0.46	0.37	0.01	27
GSE140800	cg07405796	chr6	<i>TRIM40</i>	OpenSea	1stExon_5UTR	0.25	0.19	0.03	26
GSE140800	cg12217560	chr13	<i>TNFRSF19</i>	OpenSea	1stExon_5UTR	0.51	0.58	0.04	26
GSE140800	cg00082981	chr6	<i>HLA-A</i>	Island	Body	0.49	0.40	0.00	22
GSE140800	cg00157962	chr1	<i>FAM102B</i>	N_Shore	TSS1500	0.59	0.65	0.02	22
GSE140800	cg14659511	chr13	<i>DOCK9</i>	OpenSea	Body	0.62	0.69	0.01	22
GSE140800	cg25289028	chr19	<i>LRFN3</i>	N_Shore	5UTR	0.67	0.74	0.03	21
GSE140800	cg02385820	chr19	<i>RINL</i>	N_Shore	3UTR	0.71	0.67	0.00	20
GSE140800	cg15718932	chr1	<i>GBP2</i>	OpenSea	TSS1500	0.49	0.56	0.03	19
GSE140800	cg08217526	chr14	<i>C14orf64</i>	OpenSea	TSS1500	0.54	0.60	0.04	12
GSE140800	cg00305585	chr16	<i>IFT140</i>	OpenSea	Body	0.68	0.75	0.00	11
GSE140800	cg15521790	chr11	<i>MAML2</i>	OpenSea	Body	0.57	0.49	0.03	11
GSE140800	cg17994788	chr7	<i>C1GALT1</i>	OpenSea	5UTR	0.74	0.70	0.01	11

p-value: Makes reference to the p-value of the regression model (without CD4 counts correction) applied to determine DMPs. CpG positions are ordered according the frequency of selection by random forest model. HIVHigh = pVL > 50.000copies/ml. HIV-Low = pVL

Chapter II

TL1A-DR3 Plasma Levels Are Predictive of HIV-1 Disease Control, and DR3 Costimulation Boosts HIV-1-Specific T Cell Responses

Bruna Oriol-Tordera^{1,2}, Alex Olvera^{1,3}, Clara Duran-Castells^{1,2}, Anuska Llano¹, Beatriz Mothe^{1,3,4}, Marta Massanella¹, Judith Dalmau¹, Carmela Ganoza^{5,6}, Jorge Sanchez^{5,7,8}, Maria Luz Calle³, Bonaventura Clotet^{1,3,4}, Javier Martinez-Picado^{1,3,9}, Eugènia Negrodo^{3,4}, Julià Blanco J^{1,3}, Dennis Hartigan-O'Connor^{10,11,12}, Christian Brander^{1,3,9,a}, Marta Ruiz-Riol^{1,a}

1. Institut de Recerca de la Sida IrsiCaixa, Hospital Universitari Germans Trias i Pujol, Badalona, 08916, Barcelona, Spain
2. Departament de Biologia Cel·lular, de Fisiologia i d'Immunologia, Universitat Autònoma de Barcelona, Cerdanyola del Vallès, 08193, Barcelona, Spain
3. Universitat de Vic – Universitat Central de Catalunya, Vic, 08500, Barcelona, Spain
4. Fundació Lluita contra la Sida i les Malalties Infeccioses, Servei de Malalties Infeccioses Hospital Universitari Germans Trias i Pujol, Badalona, 08916, Barcelona, Spain
5. Asociación Civil Impacta Salud y Educación, Lima, 15063, Peru
6. Facultad de Medicina Alberto Hurtado de la Universidad Peruana Cayetano Heredia, San Martín de Porres, Lima, 15102, Perú.
7. Department of Global Health, University of Washington, Seattle, WA 98195
8. Centro de Investigaciones Tecnológicas, Biomédicas y Medioambientales, Bellavista, Lima, 07006, Peru
9. Institució Catalana de Recerca i Estudis Avançats, 08010, Barcelona, Spain
10. Department of Medical Microbiology and Immunology, University of California, Davis, Davis, CA 95616
11. California National Primate Research Centre, University of California, Davis, Davis, CA 95616
12. Division of Experimental Medicine, University of California, San Francisco, San Francisco, CA 94110

^a These authors contributed equally to this work.

This article has been published in: **The Journal of Immunology**. 2020 Dec 15;205(12)

DOI: <https://doi.org/10.4049/jimmunol.2000933>

Copyright

This is an unofficial adaptation of the article that appeared in The Journal of Immunology. The American Association of Immunologists, Inc. has not approved this adaptation

Copyright © 2020 by The American Association of Immunologists, Inc. This article is distributed under The American Association of Immunologists, Inc., Reuse Terms and Conditions for Author Choice articles.



Institut de Recerca de la Sida

This declaration concerns the following manuscript:

Title: TL1A-DR3 Plasma Levels Are Predictive of HIV-1 Disease Control, and DR3 Costimulation Boosts HIV-1-Specific T Cell Responses

Authors: Bruna Oriol-Tordera, Alex Olvera, Clara Duran-Castells, Anuska Llano, Beatriz Mothe, Marta Massanella, Judith Dalmau, Carmela Ganoza, Jorge Sanchez, Maria Luz Calle, Bonaventura Clotet, Javier Martinez-Picado, Eugènia Negredo, Julià Blanco J, Dennis Hartigan-O'Connor, Christian Brander, Marta Ruiz-Riol

Full reference of the article: Oriol-Tordera B, Olvera A, Duran-Castells C, Llano A, Mothe B, Massanella M, Dalmau J, Ganoza C, Sanchez J, Calle ML, Clotet B, Martinez-Picado J, Negredo E, Blanco J, Hartigan-O'Connor D, Brander C, Ruiz-Riol M. TL1A-DR3 Plasma Levels Are Predictive of HIV-1 Disease Control, and DR3 Costimulation Boosts HIV-1-Specific T Cell Responses. *J Immunol.* 2020 Dec 15;205(12):3348-3357. doi: 10.4049/jimmunol.2000933. Epub 2020 Nov 11. PMID: 33177161; PMCID: PMC7725879.

This Manuscript is: Published Accepted Submitted In preparation

The PhD student has contributed to the elements of this article/manuscript as follows:

- A. No or little contribution
- B. Has contributed (10-30%)
- C. Has contributed considerably (40-60%)
- D. Has done most of the work (70-90%)
- E. Has essentially done all the work

Formulation/identification of the scientific problem	A
Planning the experiments and methodology design and development	B
Involvement in the experimental work / data collection	C
Involvement in data analysis	D
Involvement in results interpretation	C
Writing the first draft of the manuscript	D
Finalization of the manuscript and submission	D

The PhD student has searched the relevant background literature to get involved in the project and to understand the scientific problem and to participate in the selection of the best approach for data analysis. The PhD student has also performed in vitro validation studies in splenocytes of HTI-vaccinated mice and in PBMCs of HIV-infected individuals. The PhD student has been the responsible for data analysis, results interpretation and writing the first draft of the manuscript.

Dr. Christian Brander (director)

Dra. Marta Ruiz-Riol (director)

Abstract

Relative control of HIV-1 infection has been linked to genetic and immune host factors. In this study, we analyzed 96 plasma proteome arrays from chronic untreated HIV-1–infected individuals using the classificatory random forest approach to discriminate between uncontrolled disease (plasma viral load [pVL] >50,000 RNA copies/ml; CD4 counts 283 cells/mm³, n = 47) and relatively controlled disease (pVL <10,000 RNA copies/ml; CD4 counts 657 cells/mm³, n = 49). Our analysis highlighted the TNF molecule's relevance, in particular, TL1A (TNFSF15) and its cognate DR3 (TNFSRF25), both of which increased in the relative virus control phenotype. DR3 levels (in plasma and PBMCs) were validated in unrelated cohorts (including long-term nonprogressors), thus confirming their independence from CD4 counts and pVL. Further analysis in combined antiretroviral treatment (cART)–treated individuals with a wide range of CD4 counts (137–1835 cells/mm³) indicated that neither TL1A nor DR3 levels reflected recovery of CD4 counts with cART. Interestingly, in cART-treated individuals, plasma TL1A levels correlated with regulatory T cell frequencies, whereas soluble DR3 was strongly associated with the abundance of effector HLA-DR+CD8 T cells. A positive correlation was also observed between plasma DR3 levels and the HIV-1–specific T cell responses. In vitro, costimulation of PBMC with DR3-specific mAb increased the magnitude of HIV-1–specific responses. Finally, in splenocytes of DNA-HTI-vaccinated mice, costimulation of HTI peptides and a DR3 agonist (4C12) intensified the magnitude of T cell responses by 27%. These data describe the role of the TL1A–DR3 axis in the natural control of HIV-1 infection and point to the use of DR3 agonists in HIV-1 vaccine regimens.

Key points

- DR3 levels are associated with spontaneous in vivo control of HIV.
- Upon treatment, TL1A is associated with Tregs and sDR3 with effector CD8 T cells.
- DR3 agonists can be used to boost HIV-specific T cell responses in vitro

Introduction

Combined antiretroviral treatment (cART) administered to HIV-infected subjects suppresses viral replication, leads to recovery of CD4 T cell counts, and reduces T cell activation. Although cART improves the quality of life and life expectancy of people living with HIV (PLWH), it entails substantial lifelong side effects and does not fully restore immune function (1). In addition, access and adherence to treatment are sometimes limited, especially in low-income countries. Therefore, there is an urgent need for strategies to achieve a so-called functional cure and/or intervention that can eliminate the virus from the body (2, 3).

A small group of PLWH, known as long-term nonprogressors (LTNPs), do not experience disease progression, even in the absence of cART over long periods of time. Similarly, CD4 T cell depletion occurs at a slower pace in LTNP than with standard disease progression. This relative control of HIV has been associated with several host factors, including markers of the innate and adaptive immune responses (4). Also, LTNP produce more polyfunctional HIV-specific CTL responses (5, 6), which has served as the rationale for therapeutic CTL vaccines in HIV cure strategies.

Despite the considerable knowledge of the features of LTNPs, we do not fully understand the mechanisms associated with this natural control. In addition, new clinical guidelines recommend early initiation of treatment (7), thus limiting identification of these individuals and, consequently, the definition of new biomarkers to predict natural control.

Multiple mechanisms may contribute to the heterogeneous nature of LTNPs, and many of these processes can be studied in plasma, an accessible biological fluid. Proteomic arrays enable the identification of key processes in plasma. The “communicome” array, a protein array detecting the levels of dozens to hundreds of plasma proteins involved in cell-to-cell communication, has recently been used to identify plasma factors predictive of plasma viral load (pVL) in untreated HIV infection (8). In this study, we extend the analysis of this multiplexed proteomic array in plasma samples from

untreated PLWH using classificatory random forest analysis for discrimination between HIV progressors and individuals with relative virus control. Our analysis identified TNF and TNFR as crucial factors associated with HIV control. Of these, TL1A (TNFSF15) and its cognate death receptor DR3 (TNFRSF25) were of particular interest, given that validation studies in unrelated cohorts including LTNPs confirmed higher levels of DR3 in plasma and PBMCs of individuals with relative virus control. Interestingly, neither pVL nor CD4 counts were associated with DR3 levels. Comprehensive immunological data collected from a cART-treated cohort with a wide range of CD4 T cell recovery (9) indicated that, whereas the TL1A ligand is associated with the frequency of regulatory T cells (Tregs) (CD4 and CD8), soluble DR3 (sDR3) is strongly associated with activated effector CD8 T cells. In addition, plasma DR3 levels are associated with HIV-specific T cell responses, and ex vivo costimulation with DR3-specific Ab boosts these responses in untreated PLWH. An intensification of the HIV response was also detected after ex vivo costimulation of plasmid DNA-vaccinated mice splenocytes with DR3 Ab agonist (4C12). Taken together, these data indicate for the first time that TL1A/DR3 may play an important role in the immune control of HIV and highlight the potential use of DR3 costimulation with specific agonists in T cell–boosting regimens in HIV vaccine interventions.

Materials and Methods

Participants

Antiretroviral-naive HIV-seropositive subjects in the chronic disease stage (n = 96) recruited at Germans Trias i Pujol University Hospital (Badalona, Spain) and the IMPACTA clinics in Lima, Peru were grouped in relation to their ability to control HIV disease, as previously reported (8). In brief, individuals with relative disease control were classed as “HIV-Low” (n = 49) and had pVL <10,000 HIV RNA copies/ml (range 25–9990; median 530 HIV RNA copies/ml). The median CD4 count was 657 cells/mm³ (range 289–1343 cells/mm³). Individuals with uncontrolled disease were classed as “HIV-High” (n = 47) and had pVL >50,000 HIV RNA copies/ml (range 50,295–1,200,000; median 105,520 HIV

RNA copies/ml) and a median CD4 count of 283 cells/mm³ (range 11–726 cells/mm³) (Supplemental Table I).

Additional unrelated cohorts included seronegatives (n = 8), chronic untreated individuals (“untreated,” n = 15), participants with 1 y of cART (“treated,” n = 10), and LTNPs (n = 31, including viremic controllers [n = 13, pVL <2000 copies/ml] and elite controllers [n = 18, undetectable pVL, <50 copies/ml]) (Supplemental Table I and Ref. 8). cART-treated individuals with a wide range of CD4 counts, including immune-concordant (IC, n = 12) and immune-discordant subjects (ID, n = 12), were also included in the study (Table I and Ref. 9). Finally, an additional chronically untreated HIV-infected cohort, “PLWH” (n = 6, pVL range <50–16,041 HIV RNA copies/ml and CD4 counts range 281–1500 cells/mm³), was included for functional in vitro studies (Supplemental Table I). The study was approved by the Clinical Research Ethics Committee of the Germans Trias i Pujol University Hospital (Clinical Research Ethics Committee: EO-12-042), and all participants provided their written informed consent. Blood samples were processed using Lymphoprep (STEMCELL Technologies), and isolated PBMCs, PBMC dry pellets, and plasma samples were frozen until use.

Communicome cytokine determination in plasma samples

Proteomic arrays were run using a custom-designed chip that enabled the detection and quantification of >600 individual proteins, as reported previously (8, 10). Raw data were background subtracted and normalized using cluster analysis and z-scored [$z = (x - \mu)/\sigma$]. Multivariate analyses were then performed with Bioconductor in R software package (<http://www.r-project.org>) (11) using the CMA package R/Bioconductor with five cross-validations (12). This approach combines variable selection and model classification (random forest). The process was repeated 100 times (20 randomly repeated 5-fold cross-validation processes). Finally, the area under the curve was used to evaluate the model. The output of this multivariate analysis provides a ranking of variables according to the number of times that each variable is selected. For further analysis, we included the subset of the top 25 scoring variables with a frequency of ≥ 100 . Gene ontology (GO) enrichment analysis was performed using the GOSTats package R/Bioconductor (13), and

Kyoto Encyclopedia of Genes and Genomes (KEGG) enrichment analysis was conducted with Database for Annotation, Visualization and Integrated Discovery (14, 15). A hypergeometric test was applied in both cases.

Real-time PCR

PBMC dry cell pellet samples were used for RNA extraction (RNeasy Plus Mini Kit; QIAGEN) and retro-transcription (SuperScript III First-Strand Synthesis SuperMix, Invitrogen). The cDNA was used for quantitative real-time PCR based on TaqMan gene expression assays for detection of TL1A (Hs00270802_s1), DR3 (Hs00237054_m1), and TBP (Hs99999910_m1) in a 7500 real-time instrument (Applied Biosystems). Relative expression was calculated as $2^{-\Delta\text{cycle threshold}}$ (mean of three replicates).

Cytokine determination by ELISA

TL1A was determined using an ELISA kit (Human TL1A/TNFSF15 DuoSet ELISA; R&D Systems). DR3 protein in plasma was determined using an ELISA kit from CUSABIO and Booster Immunoleader, following the manufacturer's instructions. Quantification of ligand and receptor (TL1A and DR3) was calculated using a four-parameter logistic nonlinear regression model.

Flow cytometry in treated HIV-infected individuals

Data were generated as described elsewhere (9, 16–19). Spontaneous cell death was evaluated in fresh samples using 40 nM DIOC6 (Invitrogen), as described previously (16), combined with propidium iodide (Sigma-Aldrich, Madrid, Spain). For other staining panels, flow cytometry was performed using a series of different Ab combinations. In brief, T cell maturation and immunosenescence were evaluated using CD3-allophycocyanin-Cy7, CD4-PerCP-Cy5.5, CD8-V500, CD57-FITC, CD27-allophycocyanin, CD28-PE, CCR7-PE-Cy7, and CD45RA-V450 (BD Biosciences). Proliferation and Treg phenotype were assessed using an Ab panel comprising Ki67-FITC, FOXP3-PE, CD25-PE-Cy7, CD127-Alexa Fluor 647, CD3-allophycocyanin-Cy7, CD4-V450, and CD8-V500. The

activation panel included CD95-FITC, CD38-PE, HLA-DR-PerCP, CD3-allophycocyanin-Cy7, CD4-allophycocyanin, and CD8-PE-Cy7. All the stained cells were collected in LSR II flow cytometer (Becton Dickinson) and analyzed with FlowJo Software (version 7.6.5).

Measurement of the adaptive host immune response to HIV

T cell immunity to HIV was assessed in purified PBMCs using the ELISPOT assay (100,000 PBMCs/well), with an overlapping peptide (OLP) set comprising 410 OLPs, as described elsewhere (20). The breadth (number of reactive OLPs) and magnitude (spot forming cells per 10⁶ PBMCs) were recorded.

In vitro TL1A and DR3 costimulation effects on HIV-infected human PBMCs

We cultured thawed cryopreserved PBMCs from untreated PLWH and LTNP (Supplemental Table I) (150,000 PBMCs/well) in duplicate in 96-well ELISPOT plates (MultiScreen HTS MSIPS4W10, Millipore) and stimulated them with a pool of selected reactive OLP peptides (each peptide, 2 µg/ml, Supplemental Table II). We also stimulated cells with a CMV, EBV, and influenza virus (CEF) peptide pool designed to stimulate T cells (CEF-MHC Class I Control Peptide Pool Plus; Cellular Technology, Shaker Heights, OH). Then, we costimulated the cells with 100 ng/ml of soluble TL1A (sTL1A) (Recombinant Human TL1A/TNFSF15; R&D Systems), 500 ng/ml of sDR3 (Recombinant Human DR3/TNFRSF25 Fc Chimera Protein; R&D Systems), and/or 100 ng/ml of mAb anti-DR3 (Purified anti-human DR3 [TRAMP] JD3; BioLegend). Concentrations were based on the manufacturers' recommendations. Cells were incubated overnight at 37°C in 5% CO₂ and processed for the ELISPOT (see above). For evaluation of DR3 expression on T cells, cells were recovered before the ELISPOT development procedure and stained for surface markers (CD3-allophycocyanin-Cy7, CD4-allophycocyanin, CD8-PerCP, and DR3-PE [anti-human DR3 (TRAMP) JD3] from BioLegend) acquired on an LSR Fortessa cytometer (Becton Dickinson) and analyzed using FlowJo 7.6.5 software.

Mouse immunization and splenocyte isolation

Two groups of cohoused C57BL/6 mice (Envigo) were immunized i.m. with 100 µg/animal of DNA.HTI (21) in the Animal Facility of Germans Trias i Pujol University Hospital. The first group (n = 3) received three doses of vaccine and the second group (n = 4) four. All vaccinations were separated by 3 wk, and mice were euthanized 2 wk after the last vaccination. Spleens were removed, and splenocytes isolated by mechanical disruption and passage through a 45-µm cell strainer (Falcon) using a 5-ml rubber syringe plunger. Following RBC lysis with red cell lysis buffer (17 mM Tris and 0.14 M NH₄Cl; Sigma), splenocytes were washed twice with RPMI 1640 supplemented with 10% FCS and penicillin/streptomycin and cryopreserved in N₂ until use in FBS with 10% DMSO. Procedures involving mice followed European Union legislation on animal experimentation and were approved by the Animal Experimentation Ethics Committee of Germans Trias i Pujol Research Institute and the Ministry of Agriculture, Livestock, Fishing, and Food of the Generalitat de Catalunya (order no. 6390 and 9183).

Determination of murine T cell responses to HTI

IFN-γ ELISPOT was used to determine vaccine-specific T cell responses in mice. Briefly, thawed splenocytes (200,000 cells/well in RPMI 1640 and 10% FCS) from the HTI-vaccinated mice were simultaneously stimulated overnight with a set of 15-mer OLPs covering the whole sequence of the HTI immunogen (Supplemental Table II) and increasing doses of the mouse DR3 agonist 4C12 (0.5, 1, and 2 µg/ml). The magnitude of the response (spot forming cells per 10⁶ PBMCs) was recorded.

Statistical analysis

Univariate statistical analyses were performed using Prism Version 6 (GraphPad). For comparisons between patient groups, the Mann–Whitney and Wilcoxon signed rank tests were applied. The Spearman test was applied for the correlation analysis. For all analyses, p values <0.05 were considered statistically significant.

Results

Soluble TNF and TNFR in plasma discriminate between untreated HIV disease phenotypes

The communicate approach has served to identify plasma markers that predict pVL in HIV disease (8) and to define predictive biomarkers of other diseases (10). To explore the soluble factors involved in natural control of HIV infection, a classificatory multivariate approach was applied to discriminate between uncontrolled and relative infection control phenotypes. Multiplexed arrays of HIV-High (n = 47) and HIV-Low individuals (n = 49) (Ref. 8 and Supplemental Table I) were analyzed by applying a random forest model. These analyses revealed a total of 25 soluble molecules among 600 factors that consistently (frequency of >100 of 1000 iterations) distinguished between both groups of individuals (Fig. 1A). The molecules fell most noticeably into the GO categories of chemokines (CCL-8, -18, -22, and CXCL-1) and cytokines (including TGF- β family members), as well as apoptotic factors that belong to the TNF/TNFR family (TNFSF15, TNFRSF10D, and TNFRSF10C) and cell adhesion categories (including SIGLEC9, SELE, and ALCAM) (Fig. 1A, 1B). The important role of the cell death process in the pathology of HIV was further supported by KEGG analysis, which also indicated the relevance of the apoptosis pathway in the control of HIV infection (fold enrichment of 3.5, Fig. 1C). TNF/TNFR fall into this category and discriminate between chronic untreated HIV-infected individuals with controlled or uncontrolled disease.

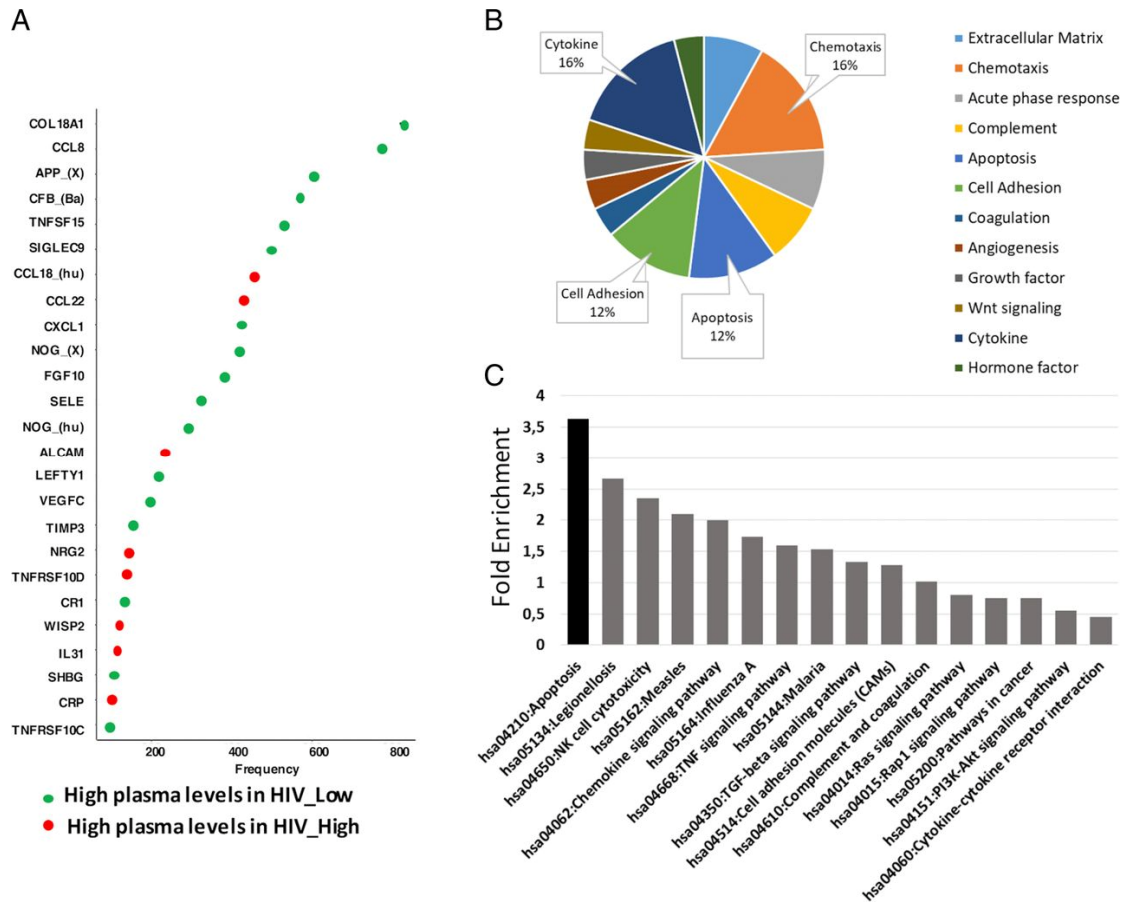


Figure 1. Plasma soluble factors in chronic untreated HIV groups. Communicome arrays performed in 96 HIV-infected individuals with HIV-High (n = 47) and HIV-Low (n = 49) (Ref. 8 and Supplemental Table I) were analyzed by applying a random forest model. (A) Frequency plot indicating the relevance of the top 25 scoring soluble factors with frequency ≥ 100 obtained after cART analysis. (B) Pie chart representing the GO biological processes gene enrichment analysis percentages for each category represented among the top 25 candidates. (C) KEGG enrichment analysis showing the fold enrichment value of each pathway among the top 25 selected factors.

Elevated plasma levels of TL1A and DR3 are associated with relative control of HIV infection

Classificatory analyses of plasma proteomic arrays indicate that TNF/TNFR are relevant for discriminating between the two groups of chronic untreated HIV individuals studied. Among the TNF/TNFR detected, the TNFSF15 (TL1A) molecule stands out as it is the first marker when considering only the apoptosis category (Fig. 1) and the fifth discriminatory factor obtained in the multivariate analyses (frequency of 531). TL1A and its cognate receptor TNFRSF25 (also known as DR3) act as T cell costimulatory signal with pleiotropic and broad functions that have been poorly studied (22, 23). In this study, higher relative plasma levels of TL1A and DR3 were detected in untreated HIV-infected subjects with lower viremia and normal CD4 counts than in those with chronic uncontrolled HIV

infection (Mann–Whitney U test, TL1A $p = 0.0003$ and DR3 $p = 0.0445$, Fig. 2A, 2B). As the HIV-Low group includes individuals with a wide range of pVLs, we compared the relative plasma levels of TL1A and DR3 in HIV-Low individuals, separating those with pVL <50 from those with pVL ranging from 50 to 10,000 copies/ml. No differences were observed between these two groups for either molecule (Supplemental Fig. 1A, 1B). In addition, correlation analyses in chronic untreated HIV individuals with pVL or CD4 counts indicated that sTL1A was associated with these two parameters (pVL: $\rho = -0.2475$, $p = 0.0151$; CD4 counts: $\rho = 0.2355$, $p = 0.0209$; Spearman rank test, data not shown), and no significant correlation was found with sDR3 levels. In addition to DR3, TL1A ligand can also signal through the decoy receptor 3 (DcR3) (24), although the relative plasma levels of DcR3 do not differ between both groups of chronic untreated HIV-infected individuals. This observation holds when pVL differences are considered in the HIV-Low group (Supplemental Fig. 1C, 1D).

Although plasma protein concentration is a reflection of multiple cell sources, not only PBMC, we decided to explore TL1A and DR3 gene expression in PBMCs from chronic untreated HIV-1–infected individuals with different levels of virus control. Although no differences between HIV-High and HIV-Low are observed for TL1A (Fig. 2C), its cognate receptor DR3 is significantly highly expressed in HIV-Low individuals ($p = 0.0289$, Mann–Whitney U test, Fig. 2D), suggesting that in PBMCs, the receptor DR3 plays a more important role in discriminating between the groups than the ligand. Additionally, the expression levels of ligand and receptor in PBMCs were validated in unrelated cohorts of chronic infection including individuals 1 y before cART treatment initiation (untreated, $n = 11$), 1 y after cART initiation (treated, $n = 5$), LTNPs ($n = 23$), and seronegative individuals ($n = 6$). Consistently, these analyses confirmed that TL1A expression was not significantly different between groups (Fig. 2E) and that only the DR3 receptor was significantly highly expressed in LTNPs than in untreated individuals ($p = 0.0107$, Mann–Whitney U test, Fig. 2F). Treated individuals tend to have higher levels of DR3 in PBMCs than untreated individuals (Fig. 2F), although the difference is not statistically significant ($p > 0.05$).

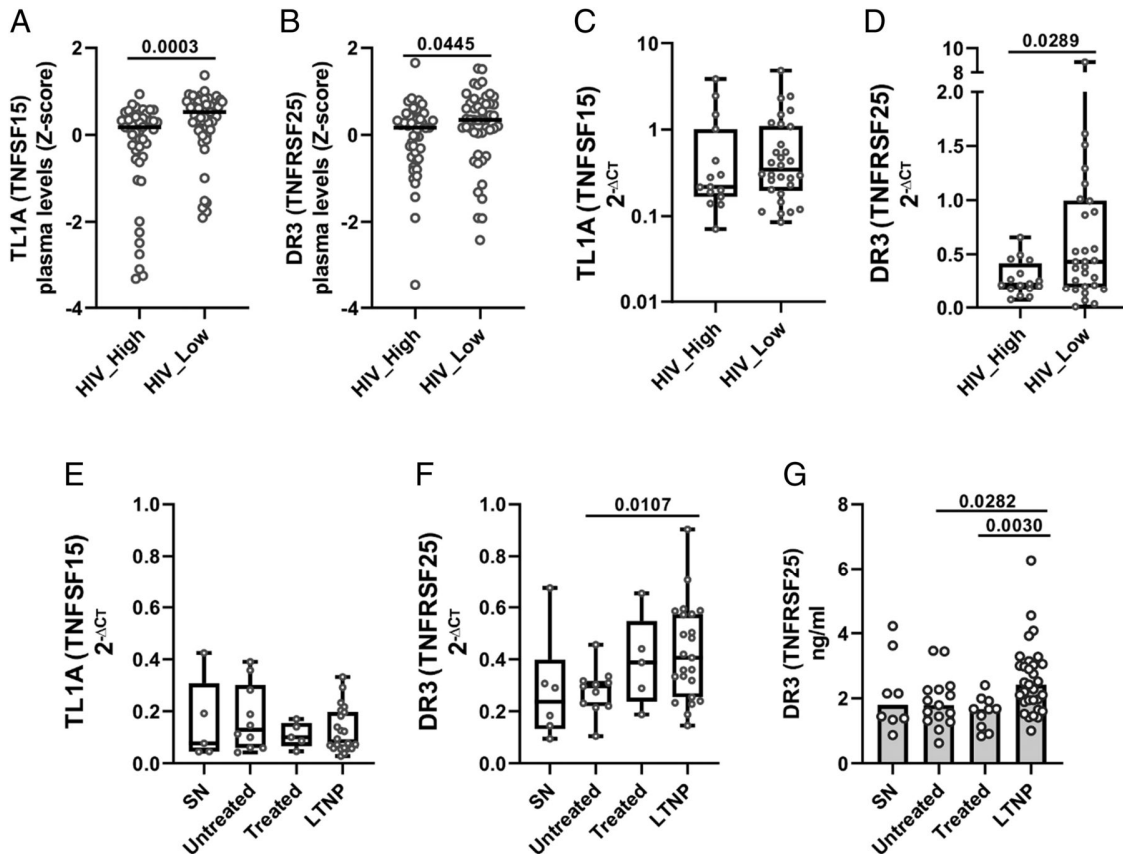


Figure 2. sTL1A and sDR3 plasma levels and PBMC gene expression in chronic HIV-infected individuals. sTL1A (A) and sDR3 (B) relative plasma levels (z-score communicome values) in HIV-High (n = 47) and HIV-Low (n = 49) (Supplemental Table I). (C and D) Gene expression (Supplemental Table I) of TL1A (C) and DR3 (D) in HIV-High (n = 16) and HIV-Low (n = 30). (E and F) Unrelated validation cohorts for gene expression of TL1A (E) and DR3 (F) in dry pellet PBMC samples from seronegatives (SN, n = 6) and HIV-infected individuals 1 y before and after initiation of treatment (untreated [n = 11] and treated [n = 5]) and in LTNP (n = 23) (Supplemental Table I). (G) Absolute DR3 quantifications in plasma (ELISA) in a confirmatory cohort including SN (n = 8) and samples from time points 1 y before and after initiation of treatment (untreated [n = 15] and treated [n = 10]) and controllers (n = 31) (Supplemental Table I). The Mann–Whitney U test was applied for group comparisons, and p values <0.05 were considered significant.

To validate the plasma levels in unrelated cohorts, absolute protein concentration of TL1A and DR3 was quantified. Absolute TL1A levels in plasma did not reach the levels of detection of the assay Human TL1A/TNFSF15 DuoSet ELISA (R&D Systems) in most of the samples measured. In contrast, findings for plasma sDR3 confirmed the higher levels associated with HIV control observed in the plasma proteomic arrays and PBMC gene expression tests (LTNPs versus untreated p = 0.0282; LTNPs versus treated p = 0.0030; Mann–Whitney U test, Fig. 2G). In addition, DR3 levels in the group of HIV-seronegative individuals tended to be lower compared with LTNP and more similar to chronic viremic individuals, suggesting that LTNP had particularly high levels of DR3. Interestingly, ligand and receptor gene expression did not correlate in HIV-infected patients (Supplemental Fig. 1E). Only the plasma levels of TL1A and DR3 correlated positively in untreated HIV

individuals measured in the communicome array ($\rho = 0.2705$, $p = 0.0077$, Spearman rank test, Supplemental Fig. 1F).

These results indicate that higher sDR3 levels in plasma and DR3 expression by PBMCs are associated with control of HIV. Interestingly, plasma and PBMCs DR3 levels did not correlate with pVL or CD4 T cell counts, pointing to mechanisms in HIV controllers that are independent of those directly associated with viral replication or its cytopathic effects.

TL1A is associated with Treg phenotypes and sDR3 with effector HLA-DR+CD8 T cells

in treated HIV-infected individuals

The TL1A/DR3 axis is a key pathway for the development of effective T cell immunity (25). Thus, we investigated whether absolute TL1A and DR3 plasma levels were reflections of differential T cell immunity and were associated with CD4 T cell repopulation upon cART in HIV infection. To do so, we studied cART-treated individuals from a cohort of IC and ID participants. These groups show a wide range of CD4 T cell counts, which differ significantly between the IC (median CD4 T cell counts = 829 cells/mm³) and the ID (median CD4 counts = 214 cells/mm³) (Table I and Ref. 9). No differences in TL1A and DR3 plasma levels were detected between the two groups (TL1A, IC, mean = 45.82 pg/ml versus ID, mean = 50.06 pg/ml, $p = 0.064$; DR3, IC, mean = 0.56 ng/ml versus ID, mean = 0.84 ng/ml, $p = 0.42$; unpaired t test, data not shown), suggesting that CD4 T cell repopulation mechanisms are independent of the TL1A/DR3 signaling axis.

Because the TL1A–DR3 axis is involved in several T cell immune processes (25), the plasma levels of TL1A and DR3 in treated HIV-infected participants were correlated with immune-phenotypic T cell markers measured by flow cytometry (Table I). Whereas sTL1A levels positively correlated with transitional memory phenotype CD4 T cells ($\rho = 0.488$, $p = 0.011$, Spearman rank test, Table I), sDR3 levels were positively correlated with the frequency of effector CD8 T cells ($\rho = 0.6616$, $p = 0.0002$, Spearman rank test,

Fig. 3A, Table I) and inversely correlated with the naive CD8 T cell subpopulation ($\rho = -0.512$, $p = 0.0008$, Spearman rank test, Table I). These data indicated that the TL1A and DR3 plasma levels are associated with different CD4 and CD8 T cell populations and their maturation status, suggesting that the ligand and its receptor may serve variable functions that have been reported for different cell types (23).

Table I. CD4 and CD8 cell markers of maturation, Tregs, and activation evaluated by flow cytometry

PARAMETER		Median Dis	Median Conc	p-value (Mann-Whitney)	Plasma TL1A (pg/ml) correlation Spearman Rho	P (two-tailed)	Plasma DR3 (ng/ml) correlation Spearman Rho	P (two-tailed)	
Clinical Info	Age	49	45	n.s	0.221	ns	0.264	ns	
	Gender (Male : Female)	11 M : 1 F	13 M: 1 F	n.s	0.164	ns	0.040	ns	
	Absolute CD4 (cells/ μ l)	213.5	828.5	<0.0001	-0.226	ns	-0.116	ns	
MATURATION	CD4 T cells	Naïve (CD27+CD45RA+CCR7+)	13.2	41.9	<0.0001	-0.357	ns	-0.369	ns
		Central Memory (CD27+CD45RA-CCR7+)	25.2	26.0	ns	0.390	ns	0.121	ns
		Transitionals (CD27+CD45RA-CCR7-)	32.4	14.2	0.001	0.488	0.011	0.293	ns
		Effector (CD45RA-CCR7-CD27-CD28+)	13.8	6.4	<0.001	0.036	ns	0.167	ns
		TEMRA (CD45RA+CCR7-CD28-CD27-)	8.8	1.2	ns	0.057	ns	0.100	ns
	CD8 T cells	Naïve (CD27+CD45RA+CCR7+)	10.7	28.4	0	-0.290	ns	-0.512	0.008
		Central_Memory (CD27+CD45RA-CCR7+)	6.0	6.8	ns	0.237	ns	0.114	ns
		Transitionals (CD27+CD45RA-CCR7-)	15.2	11.0	ns	0.010	ns	0.279	ns
		Effector (CD27+CD28-)	8.3	5.5	ns	0.036	ns	0.662	<0.001
		TEMRA (CD28-CD27-)	46.2	40.7	ns	0.129	ns	0.113	ns
TREGS	CD4 T cells	CD4 Treg CLASSIC (CD25hiFOXP3+)	8.4	6.4	ns	0.479	0.013	0.094	ns
		Treg classic ki67+	9.7	5.4	0.001	0.134	ns	0.056	ns
	CD8 T cells	CD8 Treg CLASSIC (CD25hiFOXP3+)	0.2	0.3	ns	0.545	0.004	0.192	ns
		Treg CD8 Ki67+	11.9	9.1	ns	-0.120	ns	-0.056	ns
ACTIVATION	CD4 T cells	CD38+ CD45RA- CD4 T cells	39.7	25.5	<0.001	0.302	ns	0.294	ns
		HLADR+ CD95+ CD4 T cells	18.7	6.0	0.002	0.390	ns	0.413	ns
		HLADR+CD38+	11.2	5.5	0.005	0.261	ns	0.121	ns
		CD45RO+CD38+	12.4	8.2	0.020	0.183	ns	0.093	ns
		HLA-DR+CD45RO+	15.1	5.8	<0.001	0.227	ns	0.262	ns
	CD8 T cells	CD38+ CD45RA- CD8 T cells	29.0	24.8	ns	0.088	ns	0.166	ns
		HLADR+ CD95+ CD8 T cells	15.2	10.4	ns	0.280	ns	0.434	0.034
		HLADR+CD38+	15.3	15.6	ns	0.066	ns	0.065	ns
		CD45RO+CD38+	8.9	6.7	ns	0.246	ns	0.152	ns
		HLADR+CD45RO+	9.2	7.4	ns	0.147	ns	0.457	0.019

Table shows the percentage of CD4 and CD8 T cells expressing cell markers of maturation, Tregs, or activation evaluated by flow cytometry. Cells shaded in green indicate a significant Spearman correlation. Bold in the cell subsets indicates there is at least one significant correlation. Conc, immune-concordant; Dis, immune-discordant; Info, information; M, male; ns, not significant; F, female; TEMRA, terminally differentiated effector memory cells.

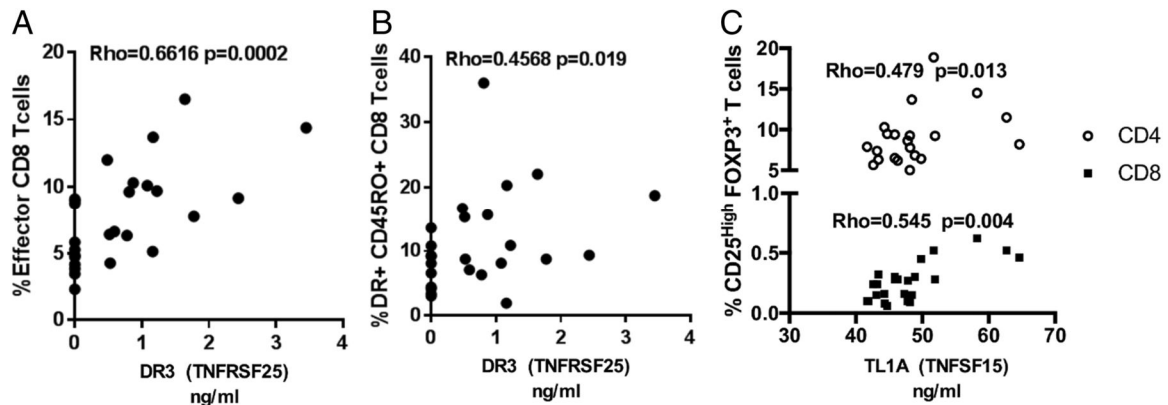


Figure 3. DR3 correlates with effector CD8 T cells and TL1A, with regulatory CD4 and CD8 phenotypes. (A and B) Correlation between plasma DR3 protein levels and the percentage of effector CD8 T cells (A) and HLA-DR+CD45RO+CD8 T cells (B) in a cohort of treated individuals ($n = 26$, Table I). (C) Correlation between ELISA-determined plasma TL1A levels and the percentage of CD25^{high}FOXP3⁺ T cells (circles, CD4 T cells; squares, CD8 T cells) in treated individuals, including IC and ID individuals ($n = 26$, Table I). The Spearman rank test was used for the correlations, and p values <0.05 were considered statistically significant.

Given that DR3 is a multifaceted receptor involved in cell death and proliferation processes (23, 26) and that IC- and ID-treated subjects clearly differ in terms of cell death, proliferation (Ki67⁺), and senescence processes (CD57⁺) (9), we performed an association analysis of these T cell markers and plasma levels of TL1A and DR3. Only TL1A plasma levels correlated with naive CD57⁺CD4 T cells ($\rho = 0.407$, $p = 0.039$, Spearman rank test, data not shown), suggesting a potential relationship between TL1A and the proportion of senescent naive CD4 T cells in peripheral blood.

As this ligand–receptor axis has been shown to play a key role in the activation of T cells and Tregs in several disorders (22, 27, 28), further studies of the association between TL1A and DR3 plasma levels and activation markers and Treg percentages were undertaken. Interestingly, although sDR3 was clearly associated with effector CD8 T cells with an activated cell phenotype (HLA-DR+CD45RO+CD8 T cells, $\rho = 0.457$, $p = 0.019$, Spearman rank test, Fig. 3B, Table I), sTL1A correlated with nonproliferating T cells (CD4 and CD8) with regulatory phenotypes (CD25^{High}Foxp3+CD4 T cells, $\rho = 0.479$, $p = 0.013$; CD25^{High}Foxp3+CD8 T cells, $\rho = 0.545$, $p = 0.004$, Spearman rank test, Fig. 3C, Table I).

As sTL1A is closely associated with CD4 and CD8 Treg subsets and sDR3 is strongly associated with CD8 T cells with an effector and activated phenotype, these data suggest

a dichotomous mode of action for the TL1A ligand and sDR3 in HIV infection, as previously reported for other diseases (22, 28). Accordingly, the disruption of the TL1A/DR3 axis favors tolerance processes, although its stimulation might benefit anti-tumor and antiviral T cell-mediated responses (25, 29), in line with the associations between higher levels of DR3 and TLA1 and improved HIV control (see above).

DR3 as a new marker and costimulator of HIV-specific T cell responses

Given that the TL1A/DR3 axis is a key pathway for the development of effective CD4 and CD8 T cell antiviral responses (25), we evaluated the association between plasma TL1A and DR3 levels in chronic untreated HIV-infected individuals and the magnitude and breadth of HIV-specific T cell responses. Although sTL1A did not correlate with the magnitude or the number of responses, plasma sDR3 levels were associated with broader and stronger HIV-specific T cell responses (breadth: $\rho = 0.2589$, $p = 0.0155$; and magnitude: $\rho = 0.2214$, $p = 0.0393$; Spearman rank test, Fig. 4A, 4B). These results reinforce the aforementioned association between DR3 and activated effector CD8 T cells (Fig. 3A, 3B, Table I). Interestingly, a stronger correlation between sDR3 and T cell breadth was observed in HIV-Low individuals ($\rho = 0.3175$, $p = 0.0380$; Spearman rank test, Fig. 4A), suggesting a potential role for this receptor in the generation of broad HIV T cell responses in the setting of more effective virus control.

Although the TL1A ligand is produced mostly by endothelial and APCs, the DR3 receptor is expressed mainly in Ag-experienced T cells (22). To evaluate the protein levels of DR3 in CD4 and CD8 T cells from HIV-infected subjects with a controller ($n = 3$) or noncontroller phenotype ($n = 3$), we used flow cytometry. Supplemental Fig. 2 shows that upon *in vitro* HIV peptide stimulation, controllers upregulate DR3 expression in CD4 and CD8 T cells, whereas noncontrollers are unable to upregulate this receptor after 24 h of peptide stimulation.

As DR3 is a costimulator of CD8 T cell responses (25, 29) and has been proposed as a potential adjuvant for vaccination regimens (30), *ex vivo* intensification of HIV-specific T cell responses were evaluated in the presence of recombinant sTL1A, sDR3, and anti-

DR3-specific Ab in untreated PLWH (Fig. 4C, Supplemental Table I). After 24 h, the stimulation of HIV-specific peptides combined with DR3-specific Ab significantly enhanced the HIV-specific T cell responses (12%, $p = 0.0210$, Wilcoxon-matched pairs test, Fig. 4C) compared with peptide stimulation alone. Similarly, the CEF-specific T cell response was also boosted upon costimulation with DR3 Ab (20% of increased responses, $p = 0.0781$, Wilcoxon-matched pairs test, Fig. 4D).

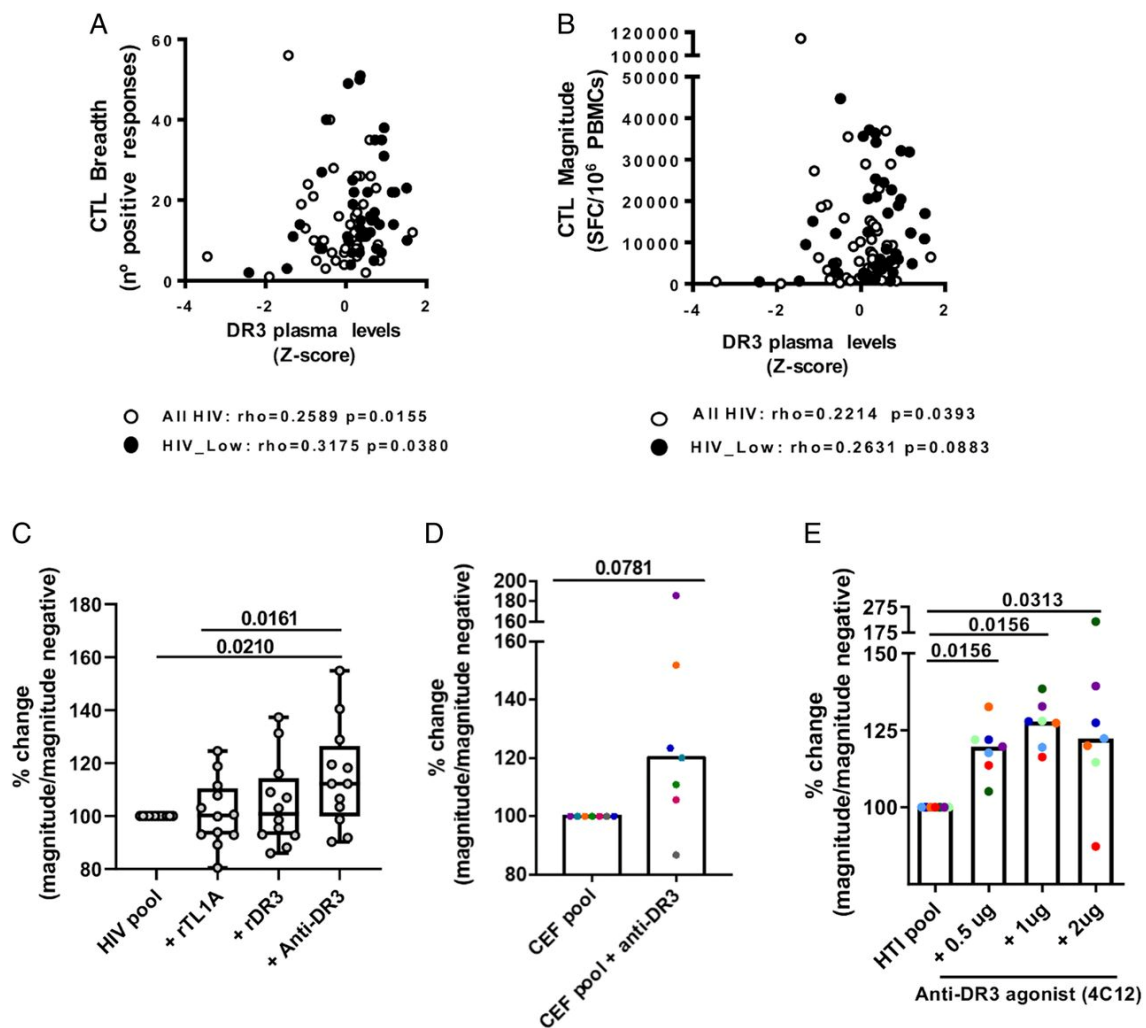


Figure 4. TL1A/DR3 axis role in HIV-specific T cell responses. (A and B) sDR3 relative plasma levels (z-score communicome) correlate with T cell breadth (A) and magnitude (B) in HIV-High ($n = 46$) and HIV-Low ($n = 41$) individuals (Supplemental Table I). (C) IFN- γ ELISPOT (percentage increase in the magnitude of T cell) after HIV-specific peptide pool stimulation in the presence of recombinant TL1A and DR3 and specific anti-DR3 mAb in PBMCs from untreated PLWH (Supplemental Table I). (D) Percentage increase in the magnitude of CEF-specific responses upon costimulation with anti-DR3 mAb. (E) Increase in magnitude of DNA.HTI-specific T cell responses in isolated splenocytes from HTI-vaccinated mice after stimulation with the mouse DR3-specific Ab 4C12 (agonist DR3). The Spearman rank test was used for correlation analysis, and the Wilcoxon signed rank test for group comparisons. The p values < 0.05 were considered statistically significant.

Because no data on agonistic or blocking capacity for human DR3-specific Abs has been reported, we further evaluated the use of DR3 Ab agonist (4C12) in vitro in splenocytes from DNA.HTI-vaccinated mice. In line with the effect of DR3-specific costimulation seen in human cells, when splenocytes from DNA.HTI-vaccinated mice were cultured and stimulated with HTI peptides and 4C12, the HTI-specific responses were boosted by 27% ($p = 0.0156$, Wilcoxon signed rank test, Fig. 4E). These data are in line with the effect of DR3-specific costimulation seen in human cells and further support the important role of the DR3 receptor in driving cellular immunity against HIV (Fig. 5).

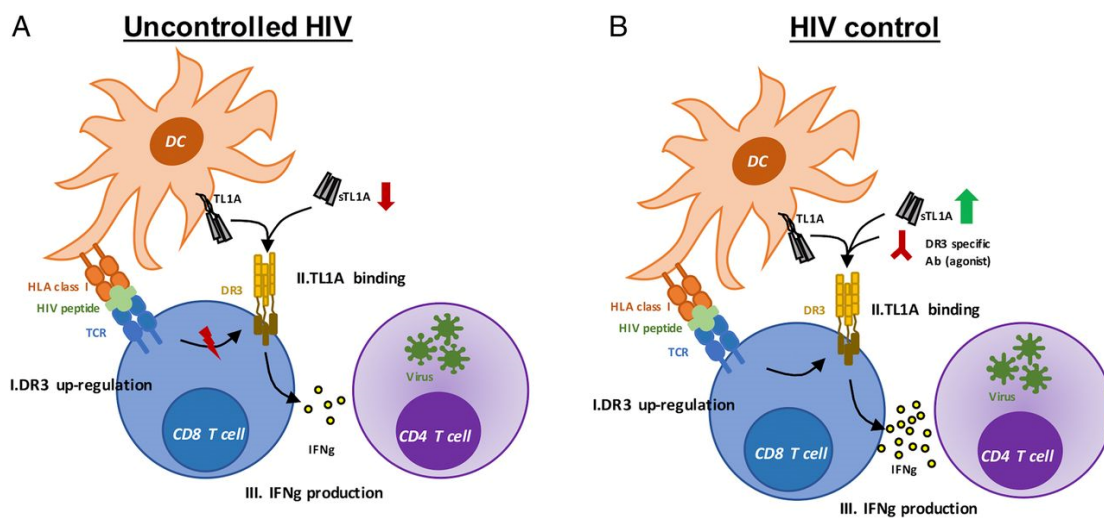


Figure 5. Model of TL1A–DR3 axis in HIV infection. (A) Failure of TL1A–DR3 axis during uncontrolled HIV infection. Upon HIV-specific activation, there is no upregulation of DR3 in the surface membrane of CD8 T cells (AI). The reduced levels of sTL1A do not allow the signaling through DR3 receptor (AII), which would weaken the IFN- γ production (AIII). (B) HIV control. Upon HIV-specific activation, DR3 protein is upregulated on the cell membrane (BI) which, together with higher plasma levels of sTL1A and/or the presence of a DR3 agonist, would ensure the signaling of the TL1A–DR3 axis (BII). This costimulatory effect would enhance the HIV-specific IFN- γ responses (BIII).

Discussion

LTNPs maintain low levels of HIV virus for long periods of time without the need for cART, indicating that some host mechanisms are able to control viral infection without total eradication of the virus. This group of individuals with special features, including highly polyfunctional CTL responses against HIV (5), has been extensively studied with the aim of identifying key mechanisms involved in the relative control of HIV infection and guiding new therapeutic interventions.

In this study, we focused on the search for traits that could discriminate between phenotypes of controlled and uncontrolled HIV infection using a previously reported communime approach (8, 10). The main plasma factors that distinguish between untreated HIV-infected individuals with relative control or absence of control fell into the GO and KEGG categories related to the cell death process. It is known that uncontrolled HIV infection causes direct CD4 cell death as well as indirect immune cell depletion and dysfunction. Thus, although the enrichment of cell death processes in these plasma samples may be expected, the mechanisms involved in CD4 T cell loss remain unclear and could involve cell death and proliferative pathways (31).

Among all the proteins in the cell death category, TL1A (TNFSF15) emerged as the most relevant factor for differentiating between individuals with controlled and uncontrolled HIV infection. In addition, high plasma levels of its cognate receptor DR3 (TNFRSF25) are associated with control of HIV infection. These elevated plasma levels are supported by higher gene expression levels of DR3 in PBMCs in individuals with superior control of HIV. No such association was observed for TL1A plasma protein levels and PBMC gene expression; this observation is consistent with the major source of TL1A being endothelial/epithelial cells and, to a lesser extent, lymphoid and myeloid immune cells, whereas its cognate receptor DR3 is expressed mainly in activated T cells (CD4 and CD8) present in PBMCs (22).

Twenty years ago, the DR3 receptor was classified as a death receptor because of its capacity to activate caspase-dependent and -independent apoptosis processes (32, 33). However, it was subsequently reported that in lymphocytes, DR3 signaling predominantly induces the MAPK and NF- κ B pathways associated with inflammation, survival, and proliferation (22, 24). Although the specific trigger of the different functions of DR3 receptor remains unclear, the increase in DR3 expression in TCR-activated T cells and the enhancement of T cell proliferation as effector functions through the TL1A–DR3 axis are well documented (22, 25). Therefore, levels of DR3 in plasma or PBMCs are not necessarily expected to correlate with CD4 T cell counts or cell death processes in our study. Moreover, the higher plasma levels detected in elite

controllers are not recovered with cART or CD4 T cell repopulation. Therefore, in this report, we point to a key role of the TL1A–DR3 axis in T cell function for the control of HIV infection.

TL1A–DR3 signaling is associated with several T cell–dependent autoimmune diseases as well as with the induction and maintenance of chronic inflammation (23, 24, 28, 34), although its involvement in human infectious disease is unknown. In this study, we found that TL1A was associated with regulatory and exhausted phenotypes in CD4 T cell populations from cART-treated individuals, whereas DR3 was strongly correlated with activated effector CD8 T cells, possibly because of the pleiotropic functions of the TL1A–DR3 axis. In this regard, DR3 is constitutively expressed in Tregs, whereas the TL1A–DR3 axis is involved in Treg expansion. In fact, evidence from murine models has shown that treatment with TL1A–Ig limits graft-versus-host disease (35–37). In contrast, DR3 is only expressed in conventional CD4 and CD8 T cells, and after stimulation of TCRs with foreign cognate Ags, it enhances effector functions. It has been proposed that in infectious disease, TL1A–DR3 signaling in conventional T cells induces killing of infected cells, whereas its signaling in Treg might prevent exacerbated immune responses that damage host tissues (22). Therefore, although blocking of the TL1A–DR3 axis has been suggested when this system is disrupted, such as in autoimmune or chronic inflammatory diseases (24, 34, 38), its stimulation might benefit antitumor and antiviral T cell–mediated responses (25, 29).

Interestingly, we show that in individuals with uncontrolled HIV infection and reduced plasma levels of TL1A, *in vitro* stimulation of their PBMCs with HIV T cell epitopes is not sufficient to upregulate DR3 expression in CD8 T cells (Fig. 5A, Supplemental Fig. 2). In contrast, in a situation of HIV natural control, HIV-1 Ag presentation to CD8 T cells upregulates DR3 on the cell membrane of T cells and, together with high levels of sTL1A, favors TL1A–DR3 axis signaling (Fig. 5B). Actually, in the general untreated HIV population, stimulation of the HIV peptide pool combined with DR3 costimulation by a DR3-specific Ab increased HIV-specific T cell responses by 12%. Therefore, we propose that the agonistic stimulation of the TL1A/DR3 axis would allow a more effective killing

of HIV-infected cells (Fig. 5B). This finding may also hold for other pathogens because the addition of DR3 Ab could increase CEF-induced responses by 20%. In the murine CMV model, the essential role of DR3 for an efficient antiviral T cell response has been documented, and the absence of DR3 been shown to result in dysregulated virus control (25). Although the increases observed upon CEF pool stimulation are modest, stimulation of the TL1A/DR3 axis at the time of induction of de novo responses in vivo may increase their magnitude.

Costimulation with the TL1A and DR3 axis is essential for effective CD4 and CD8 T cell responses against murine CMV infection (25). Accordingly, TL1A protein or DR3 agonistic Abs have been proposed as adjuvants in Ag-specific vaccinations (23, 39). We observed that the use of Ab agonists of DR3 in responder DNA.HTI-vaccinated mice intensified CD8-specific Ag responses by >25% in ex vivo stimulation experiments. These data clearly support the future use of DR3 stimulation in vivo together with vaccine candidates designed for the induction of cellular immunity, as proven in murine cancer models (29) and which could possibly be extended to cure HIV infection.

The TL1A–DR3 axis can be modulated by other host soluble factors such as the DcR3, which binds and neutralizes the signaling function of TL1A, as well as other ligands, such as FasL and light protein. However, although its blockade might be interesting in a cancer setting with increased DcR3 levels (40, 41), we did not detect any differences between HIV-infected controllers and noncontrollers. Inhibition of ADAM17 (a member of the ADAM metallopeptidase family, also known as TNF- α -converting enzyme) has also been proposed as a therapeutic target in inflammatory diseases because it increases levels of sTL1A (42). However, given the pleiotropic effects of this metalloprotease, including supporting HIV virus infection (43–45), it may not offer a therapeutic target in the HIV antiviral response. However, in the communicate array, increased plasma levels of TIMP3, an ADAM17 inhibitor, were detected in HIV controllers, thus further highlighting the potential of targeting the TL1A–DR3 axis in strategies aimed at boosting specific CD8 T cell responses in HIV infection and, by inference, the immune response to other pathogens.

Overall, this study identifies the TL1A–DR3 axis in plasma as a new marker for HIV control and shows that this axis is associated with virus-specific T cell responses. Therefore, these results show that immune intensification involving stimulation of the TL1A–DR3 axis could be considered in future vaccination strategies, not only for HIV, but also for other viruses and emerging pathogens.

Disclosures

B.M. is a consultant for AELIX Therapeutics outside the submitted work. C.B. is founder, chief science officer, and shareholder of AELIX Therapeutics; J.B. is chief executive officer, founder, and shareholder of AlbaJuna Therapeutics. The other authors have no financial conflicts of interest.

Acknowledgments

We thank all the participants involved in the study.

Funding

This work was supported by a grant from the Ministerio de Ciencia e Innovación (SAF2017_89726_R), the European Union Horizon 2020 Framework Programme for Research and Innovation under Grant 681137-EAVI2020, National Institutes of Health, National Institute of Allergy and Infectious Diseases Program Grant P01-AI131568, the Fondation Dormeur, Vaduz, (Liechtenstein), and a research agreement with Aelix Therapeutics. M.L.C. was partially supported by the Spanish Ministry of Economy, Industry and Competitiveness, Reference MTM2015-64465-C2-1-R. This work has been carried out within the framework of the Ph.D. in Advanced Immunology of the Universitat Autònoma de Barcelona for B.O.-T. and C.D.-C. This study has also received funding from “La Caixa” Foundation under Project HR17-00199.

References

1. Ndung'u, T., J. M. McCune, and S. G. Deeks. 2019. Why and where an HIV cure is needed and how it might be achieved. *Nature* 576: 397–405.

2. Bailon, L., B. Mothe, L. Berman, and C. Brander. 2020. Novel approaches towards a functional cure of HIV/AIDS. [Published erratum appears in 2020 *Drugs* 80: 869.] *Drugs* 80: 859–868.
3. Deeks, S. G., B. Autran, B. Berkhout, M. Benkirane, S. Cairns, N. Chomont, T. W. Chun, M. Churchill, M. Di Mascio, C. Katlama, et al; International AIDS Society Scientific Working Group on HIV Cure. 2012. Towards an HIV cure: a global scientific strategy. *Nat. Rev. Immunol.* 12: 607–614.
4. Mothe, B., J. Ibarrodo, A. Llano, and C. Brander. 2009. Virological, immune and host genetics markers in the control of HIV infection. *Dis. Markers* 27: 105–120.
5. Betts, M. R., M. C. Nason, S. M. West, S. C. De Rosa, S. A. Migueles, J. Abraham, M. M. Lederman, J. M. Benito, P. A. Goepfert, M. Connors, et al. 2006. HIV nonprogressors preferentially maintain highly functional HIV-specific CD8 T cells. *Blood* 107: 4781–4789.
6. Ruiz-Riol, M., A. Llano, J. Ibarrodo, J. Zamarreño, K. Yusim, V. Bach, B. Mothe, S. Perez-Alvarez, M. A. Fernandez, G. Requena, et al. 2015. Alternative effector-function profiling identifies broad HIV-specific T-cell responses in highly HIV-exposed individuals who remain uninfected. *J. Infect. Dis.* 211: 936–946.
7. World Health Organization. 2015. Guideline on When To Start Antiretroviral Therapy and on Pre-Exposure Prophylaxis for HIV. World Health Organization, Geneva, Switzerland.
8. Ruiz-Riol, M., D. Berdnik, A. Llano, B. Mothe, C. Gálvez, S. Pérez-Álvarez, B. Oriol-Tordera, A. Olvera, S. Silva-Arrieta, M. Meulbroek, et al. 2017. Identification of interleukin-27 (IL-27)/IL-27 receptor subunit alpha as a critical immune axis for in vivo HIV control. *J. Virol.* 91: e00441-17.
9. Pérez-Santiago, J., D. Ouchi, V. Urrea, J. Carrillo, C. Cabrera, J. Villà-Freixa, J. Puig, R. Paredes, E. Negredo, B. Clotet, et al. 2016. Antiretroviral therapy suppressed participants with low CD4 T-cell counts segregate according to opposite immunological phenotypes. *AIDS* 30: 2275–2287.
10. Ray, S., M. Britschgi, C. Herbert, Y. Takeda-Uchimura, A. Boxer, K. Blennow, L. F. Friedman, D. R. Galasko, M. Jutel, A. Karydas, et al. 2007. Classification and

- prediction of clinical Alzheimer's diagnosis based on plasma signaling proteins. *Nat. Med.* 13: 1359–1362.
11. Gentleman, R. C., V. J. Carey, D. M. Bates, B. Bolstad, M. Dettling, S. Dudoit, B. Ellis, L. Gautier, Y. Ge, J. Gentry, et al. 2004. Bioconductor: open software development for computational biology and bioinformatics. *Genome Biol.* 5: R80.
 12. Slawski, M., M. Daumer, and A.-L. Boulesteix. 2008. CMA: a comprehensive Bioconductor package for supervised classification with high dimensional data. *BMC Bioinformatics* 9: 439.
 13. Falcon, S., and R. Gentleman. 2007. Using GOstats to test gene lists for GO term association. *Bioinformatics* 23: 257–258.
 14. Huang, D. W., B. T. Sherman, and R. A. Lempicki. 2009. Bioinformatics enrichment tools: paths toward the comprehensive functional analysis of large gene lists. *Nucleic Acids Res.* 37: 1–13.
 15. Huang, D. W., B. T. Sherman, and R. A. Lempicki. 2009. Systematic and integrative analysis of large gene lists using DAVID bioinformatics resources. *Nat. Protoc.* 4: 44–57.
 16. Massanella, M., E. Negrodo, N. Pérez-Alvarez, J. Puig, R. Ruiz-Hernández, M. Bofill, B. Clotet, and J. Blanco. 2010. CD4 T-cell hyperactivation and susceptibility to cell death determine poor CD4 T-cell recovery during suppressive HAART. *AIDS* 24: 959–968.
 17. Negrodo, E., M. Massanella, J. Puig, N. Pérez-Alvarez, J. M. Gallego-Escuredo, J. Villarroya, F. Villarroya, J. Moltó, J. R. Santos, B. Clotet, and J. Blanco. 2010. Nadir CD4 T cell count as predictor and high CD4 T cell intrinsic apoptosis as final mechanism of poor CD4 T cell recovery in virologically suppressed HIV-infected patients: clinical implications. *Clin. Infect. Dis.* 50: 1300–1308.
 18. Massanella, M., M. Curriu, J. Carrillo, E. Gómez, J. Puig, J. Navarro, J. Dalmau, J. Martínez-Picado, M. Crespo, C. Cabrera, et al. 2013. Assessing main death pathways in T lymphocytes from HIV infected individuals. *Cytometry A* 83: 648–658.

19. Massanella, M., E. Gómez-Mora, J. Carrillo, M. Curriu, D. Ouchi, J. Puig, E. Negro, C. Cabrera, B. Clotet, and J. Blanco. 2015. Increased ex vivo cell death of central memory CD4 T cells in treated HIV infected individuals with unsatisfactory immune recovery. *J. Transl. Med.* 13: 230.
20. Frahm, N., B. T. Korber, C. M. Adams, J. J. Szinger, R. Draenert, M. M. Addo, M. E. Feeney, K. Yusim, K. Sango, N. V. Brown, et al. 2004. Consistent cytotoxic-T-lymphocyte targeting of immunodominant regions in human immunodeficiency virus across multiple ethnicities. *J. Virol.* 78: 2187–2200.
21. Mothe, B., N. Climent, M. Plana, M. Rosás, J. L. Jiménez, M. A. Muñoz Fernández, M. C. Puertas, J. Carrillo, N. Gonzalez, A. León, et al; RISVAC-03 Study Group. 2015. Safety and immunogenicity of a modified vaccinia Ankarabased HIV-1 vaccine (MVA-B) in HIV-1-infected patients alone or in combination with a drug to reactivate latent HIV-1. *J. Antimicrob. Chemother.* 70: 1833–1842.
22. Schreiber, T. H., and E. R. Podack. 2013. Immunobiology of TNFSF15 and TNFRSF25. *Immunol. Res.* 57: 3–11.
23. Bittner, S., and M. Ehrenschwender. 2017. Multifaceted death receptor 3 signaling-promoting survival and triggering death. *FEBS Lett.* 591: 2543–2555.
24. Siakavellas, S. I., P. P. Sfikakis, and G. Bamias. 2015. The TL1A/DR3/DcR3 pathway in autoimmune rheumatic diseases. *Semin. Arthritis Rheum.* 45: 1–8.
25. Twohig, J. P., M. Marsden, S. M. Cuff, J. R. Ferdinand, A. M. Gallimore, W. V. Perks, A. Al-Shamkhani, I. R. Humphreys, and E. C. Y. Wang. 2012. The death receptor 3/TL1A pathway is essential for efficient development of antiviral CD4 and CD8 T-cell immunity. *FASEB J.* 26: 3575–3586.
26. Bittner, S., G. Knoll, and M. Ehrenschwender. 2017. Death receptor 3 mediates necroptotic cell death. *Cell. Mol. Life Sci.* 74: 543–554.
27. Bittner, S., G. Knoll, and M. Ehrenschwender. 2017. Death receptor 3 signaling enhances proliferation of human regulatory T cells. *FEBS Lett.* 591: 1187–1195.
28. Schreiber, T. H., D. Wolf, and E. R. Podack. 2011. The role of TNFRSF25: TNFSF15 in disease... and health? *Adv. Exp. Med. Biol.* 691: 289–298.

29. Slebioda, T. J., T. F. Rowley, J. R. Ferdinand, J. E. Willoughby, S. L. Buchan, V. Y. Taraban, and A. Al-Shamkhani. 2011. Triggering of TNFRSF25 promotes CD8 T-cell responses and anti-tumor immunity. *Eur. J. Immunol.* 41: 2606–2611.
30. Schreiber, T. H., D. Wolf, M. Boder, L. Gonzalez, and E. R. Podack. 2012. T cell costimulation by TNFR superfamily (TNFRSF)4 and TNFRSF25 in the context of vaccination. *J. Immunol.* 189: 3311–3318.
31. Garg, H., and A. Joshi. 2017. Host and viral factors in HIV-mediated bystander apoptosis. *Viruses* 9: 237.
32. Marsters, S. A., J. P. Sheridan, C. J. Donahue, R. M. Pitti, C. L. Gray, A. D. Goddard, K. D. Bauer, and A. Ashkenazi. 1996. Apo-3, a new member of the tumor necrosis factor receptor family, contains a death domain and activates apoptosis and NF-kappa B. *Curr. Biol.* 6: 1669–1676.
33. Bodmer, J. L., K. Burns, P. Schneider, K. Hofmann, V. Steiner, M. Thome, T. Bornand, M. Hahne, M. Schröter, K. Becker, et al. 1997. TRAMP, a novel apoptosis-mediating receptor with sequence homology to tumor necrosis factor receptor 1 and Fas(Apo-1/CD95). *Immunity* 6: 79–88.
34. Xu, W. D., D. J. Chen, R. Li, C. X. Ren, and D. Q. Ye. 2015. Elevated plasma levels of TL1A in newly diagnosed systemic lupus erythematosus patients. *Rheumatol. Int.* 35: 1435–1437.
35. Mavers, M., F. Simonetta, H. Nishikii, J. V. Ribado, K. Maas-Bauer, M. Alvarez, T. Hirai, M. Turkoz, J. Baker, and R. S. Negrin. 2019. Activation of the DR3- TL1A axis in donor mice leads to regulatory T cell expansion and activation with reduction in graft-versus-host disease. *Front. Immunol.* 10: 1624.
36. Khan, S. Q., M. S. Tsai, T. H. Schreiber, D. Wolf, V. V. Deyev, and E. R. Podack. 2013. Cloning, expression, and functional characterization of TL1A-Ig. *J. Immunol.* 190: 1540–1550.
37. Wolf, D., H. Barreras, C. S. Bader, S. Copsel, C. O. Lightbourn, B. J. Pfeiffer, N. H. Altman, E. R. Podack, K. V. Komanduri, and R. B. Levy. 2017. Marked in vivo donor regulatory T cell expansion via interleukin-2 and TL1A-ig stimulation ameliorates graft-versus-host disease but preserves graft-versus-leukemia in recipients after

- hematopoietic stem cell transplantation. *Biol. Blood Marrow Transplant.* 23: 757–766.
38. Jia, L.-G., G. Bamias, K. O. Arseneau, L. C. Burkly, E. C. Y. Wang, D. Gruszka, T. T. Pizarro, and F. Cominelli. 2016. A novel role for TL1A/DR3 in protection against intestinal injury and infection. *J. Immunol.* 197: 377–386.
39. Kayamuro, H., Y. Yoshioka, Y. Abe, K. Katayama, T. Yoshida, K. Yamashita, T. Yoshikawa, T. Hiroi, N. Itoh, Y. Kawai, et al. 2009. TNF superfamily member, TL1A, is a potential mucosal vaccine adjuvant. *Biochem. Biophys. Res. Commun.* 384: 296–300.
40. Wu, Q., Y. Zheng, D. Chen, X. Li, C. Lu, and Z. Zhang. 2014. Aberrant expression of decoy receptor 3 in human breast cancer: relevance to lymphangiogenesis. *J. Surg. Res.* 188: 459–465.
41. Hsieh, S.-L., and W.-W. Lin. 2017. Decoy receptor 3: an endogenous immunomodulator in cancer growth and inflammatory reactions. *J. Biomed. Sci.* 24: 39.
42. Weizman, T., I. Levin, M. Zaretsky, I. Sagi, and A. Aharoni. 2017. Increased potency of a bi-specific TL1A-ADAM17 (TACE) inhibitor by cell surface targeting. *Front. Mol. Biosci.* 4: 61.
43. Arenaccio, C., C. Chiozzini, S. Columba-Cabezas, F. Manfredi, E. Affabris, A. Baur, and M. Federico. 2014. Exosomes from human immunodeficiency virus type 1 (HIV-1)-infected cells license quiescent CD4 T lymphocytes to replicate HIV-1 through a Nef- and ADAM17-dependent mechanism. *J. Virol.* 88: 11529–11539.
44. Lee, J. H., S. Schierer, K. Blume, J. Dindorf, S. Wittki, W. Xiang, C. Ostalecki, N. Koliha, S. Wild, G. Schuler, et al. 2016. HIV-Nef and ADAM17-containing plasma extracellular vesicles induce and correlate with immune pathogenesis in chronic HIV infection. *EBioMedicine* 6: 103–113.
45. Düsterhöft, S., J. Lokau, and C. Garbers. 2019. The metalloprotease ADAM17 in inflammation and cancer. *Pathol. Res. Pract.* 215: 152410.

Supplementary Information

Table S1. HIV infected patients in Communicome and unrelated cohorts for validation

Group (n)	Age Median (Min-Max)	Gender (M : F)	Viral Load Median (Mlx-Max)	CD4 count Median (Mlx-Max)	Communicome	ELISA	RT-PCR	IFN γ -Elispot	Functional IFN γ -Elispot	Functional Cytometry
HIV-Low (n=49)	40 (26-57)	28 M : 21 F	530 (-50-9,990)	657 (289-1,343)	100% (n=49)	ND	63% (n=31)	84% (n=41)	n=3	n=3
HIV-High (n=47)	31 (21-50)	34 M : 13 F	105,520 (50,295-1,200,000)	283 (11-726)	100% (n=47)	ND	34% (n=16)	98% (n=46)	n=3	n=3
Untreated (n=15)	39 (24-62)	12 M : 3 F	13,284 (1,067-50,000)	495 (255-914)	ND	100% (n=15)	73% (n=11)	ND	ND	ND
Treated (n=10)	40 (30-63)	8 M : 2 F	50	383 (426-1,055)	ND	100% (n=10)	50% (n=5)	ND	ND	ND
LTNP (n=31)	47 (31-59)	19 M : 12 F	50 (-50-1,978)	584 (245-1,840)	ND	100% (n=31)	74% (n=23)	ND	ND	ND
PLWH (n=6)	46 (35-53)	4 M : 2 F	7000 (-50 -16,000)	469 (281 - 1,500)	ND	ND	ND	ND	n=6	ND
SN (n=8)	31 (21-35)	8 M	ND	ND	ND	100% (n=8)	75% (n=6)	ND	ND	ND

LTNP: Long-term non-progressors
 PLWH: People living with HIV
 SN: Seronegatives
 Age = years
 M: Male
 F: Female
 Viral Load = HIV-RNA copies/ml
 CD4 counts (CD4 counts/mm³)
 ND: Not determined

Table S2. Peptides used in IFN γ ELISpots and flow cytometry analysis

Human/Mice Cohort (For human Experiment)	HUMAN COHORTS				MICE STUDY	
	PLWH Cohort IFN γ ELISpot		HIV-High and HIV-Low cohort IFN γ ELISpot and Flow Cytometry		H1I vaccinated mice IFN γ ELISpot	
	Peptide	Sequence	Peptide	Sequence	Peptide (Protein)	Sequence
	01-Gag-B25	GATPODLNMLNTVGGH	01-Gag-B5	KHIVWASRELERFAV	HTI-OLP15mer-#23 (GAG)	KSLYNTVATLYCVH
	01-Gag-B29	AAEWDRLEHPVHAGPIA	01-Gag-B22	WVKVVEEKAFSPEVIPMF	HTI-OLP15mer-#51 (GAG)	MYSPTSIAAAYVDRF
	01-Gag-B41	YVDRFYKTLRAEQASQEV	01-Gag-B23	AFSPEVIPMFSALSEGA	FA11 (GAG)	FYKTLRAEQAA
	01-Gag-B42	LRAEQASQEVKNWMTETL	01-Gag-B25	GATPODLNMLNTVGGH	V111 (PRT/RT)	VLVGPTPVNII
	01-Gag-B45	NANPDCKTILKALGPAA	01-Gag-B27	GGHQAAAMQMLKETINEEA	CV9 (PRT/RT)	CTLNFAALV
	01-Nef-B10	EVGFPVVPQVPLRPMTYK	01-Gag-B28	LKETINEEAAEWDRLEHPV	KL9 (PRT/RT)	KWTVQPIVL
	01-Nef-B16	LWVYHTQGYFPDWQNY	01-Gag-B36	PVGEIYKRWILGLNKIV	WY10 (INT/VIF)	WAAAKIRDY
	01-Nef-B18	NYTPGPGIRYPLTFGWCF	01-Gag-B54	CFNCGKEGHIKNCRAPR	HA11 (INT/VIF)	HHYESTHPRAA
	01-Pro-B16	FIKVRQYDQILLIICGHK	01-Nef-B18	NYTPGPGIRYPLTFGWCF		
	01-RT-B16	KKKSVTVLDVGDAYFSV	01-RT-B20	PSINNETPGIRYQYNVL		
	01-RT-B23	QGWKGSPIAFQSSMTKIL	01-RT-B26	RKQNPDIIVYQYMDLLYV		
	01-RT-B26	RKQNPDIIVYQYMDLLYV	01-RT-B39	IYAGIKVKQLCKLLRGTK		
	01-RT-B34	YELHPDKWTVQPIVLEPK	01-RT-B44	LKEPVHGVYVYDPSKDLIA		
	01-RT-B36	EKDSWTVNDIQKLVGKL	01-RT-B45	YYDPSKDLIAEQKGGQGGQ		
	01-RT-B40	QLCKLLRGTKALTEVPL	01-Int-B4	MASDFNLPPVVAKEIVA		
	01-RT-B53	VIWGTKPKFKLPIQKETW	01-Int-B9	GIWQLDCTHLEGKILVA		
	01-RT-B64	VSLDTTNTQKTELQAIHL	01-Int-B12	GYIEAEVPAETGQETAY		
	01-RT-B72	QLIKKEKVVLAWVPAHK	01-Vpr-B4	ELKNEAVRHFPRIWLHSL		
	01-Int-B27	SAGERIVDIIATDIQTK	01-Vpr-B8	AGVEAIRILQQLLFIHF		
	01-gp120-B26	YRLSICNTSVITQACPKV	01-gp120-B6	TVYYGVPVWKEATTLF		
	01-gp120-B61	TRDGGNNNTTEIFR				
	01-gp41-B5	AASMTLTVQARQLLSGIV				
	01-Vif-B23	TKLTEDRWKPKQKTRGHR				

Figure S1. Relative plasma levels for TL1A, DR3, and DcR3 and gene expression in PBMCs of TL1A and DR3. Relative plasma levels (Z-score) for TL1A (A) and DR3 (B) in HIV-Low individuals with pVL<50 or pVL of 50-10,000 HIV RNAcopies/ml. C-D show the relative plasma levels (Z-score) for DcR3 in HIV-High and HIV-Low individuals (C) and stratifying HIV-Low individuals as those with pVL < 50 or pVL of 50-10,000 HIV RNA copies/ml. E shows the correlation between TL1A and DR3 gene expression in PBMCs, and F the plasma level (Z-score) correlation between TL1A and DR3.

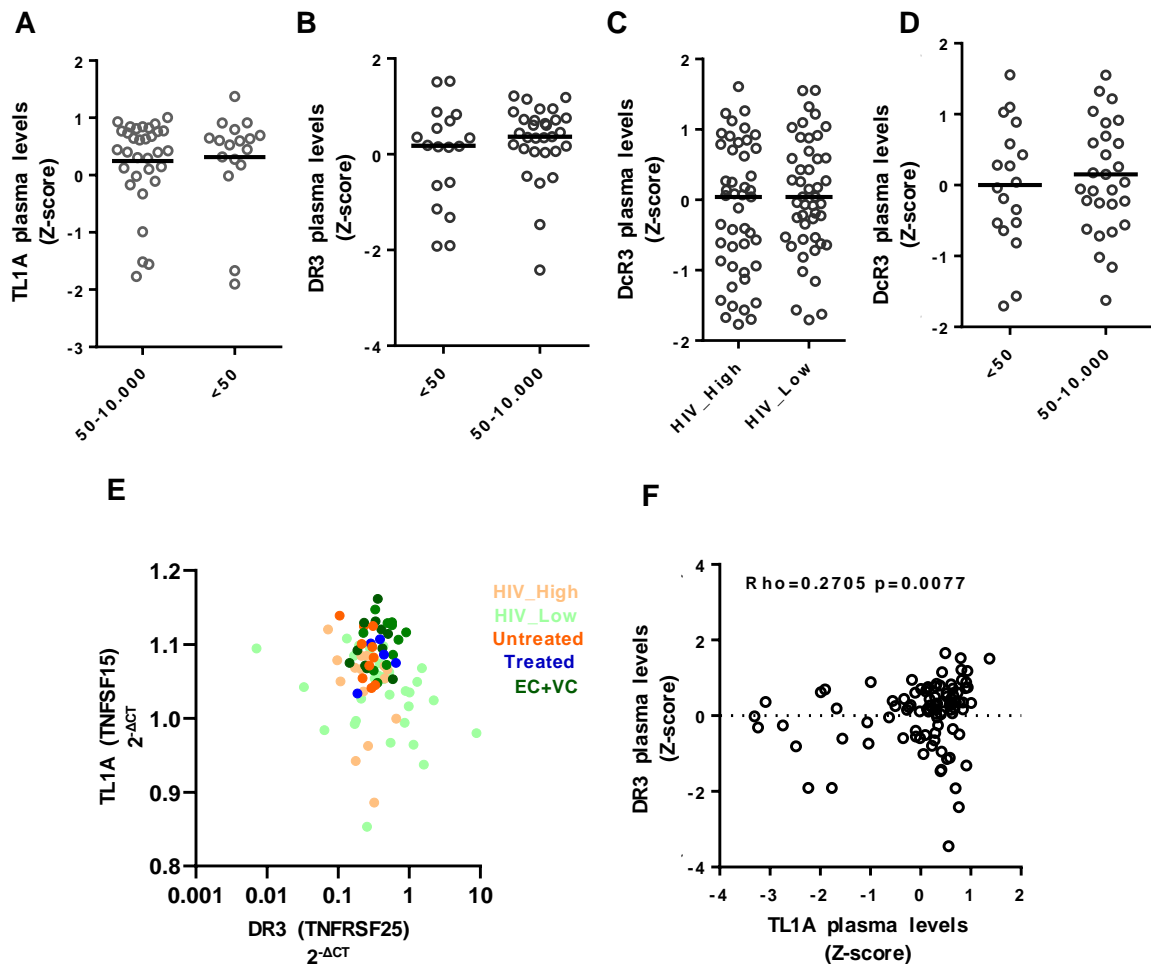
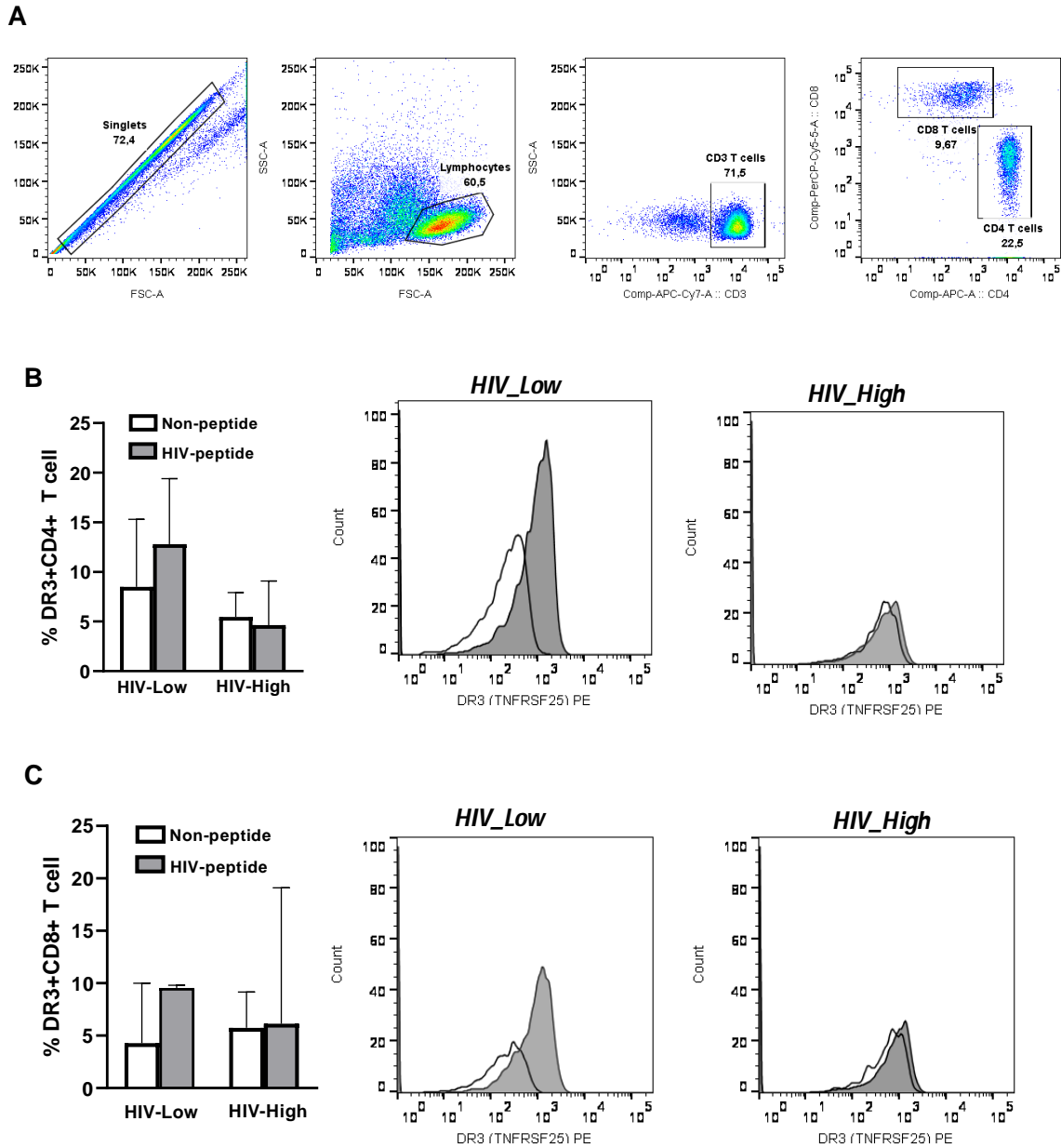


Figure S2. Expression of DR3 receptor on the membrane of CD4 and CD8 T cells in HIV-High and HIV-Low individuals. A) Gating strategy followed for detection of DR3 at surface of CD4 and CD8 T cells. Percentages and MFI levels are shown for CD4 (B) and CD8 (C) T cells expressing DR3 receptor on the membrane with or without HIV pool peptide stimulation. All results are for HIV-Low and HIV-High individuals. White color indicated absence of peptide stimulation and grey, stimulation with HIV peptide pool. Bars represent median values and error bars indicate median \pm IQR (interquartile range).



Chapter III

Host DNA methylation is associated with ATI outcome in the kick-and-kill therapeutic vaccine BCN02 clinical trial

Bruna Oriol-Tordera (1, 2), Anna Esteve-Codina (3, 4), María Berdasco (5, 6), Míriam Rosás-Umbert (1,7), Elena Gonçalves (8), Clara Duran-Castells (1,2), Francesc Català-Moll (1), Anuska Llano (1), Samandhy Cedeño (1), Maria C. Puertas (1), Martin Tolstrup (7), Ole S. Søggaard (7), Bonaventura Clotet (1, 9, 10), Javier Martínez-Picado (1, 10, 11), Tomáš Hanke (12, 13), Behazine Combadiere (8), Roger Paredes (1, 9, 10), Dennis Hartigan-O'Connor (14, 15), Manel Esteller (11, 16, 17, 18), Michael Meulbroek (19), María Luz Calle (20), Alex Sanchez-Pla (21, 22), José Moltó (9), Beatriz Mothe (1, 9, 10), Christian Brander (1, 9, 11), Marta Ruiz-Riol (1)

1. IrsiCaixa, AIDS Research Institute, Hospital Germans Trias i Pujol, Institute for Health Science Research Germans Trias i Pujol (IGTP), Badalona, 08916, Barcelona, Spain
2. Departament de Biologia Cel·lular, de Fisiologia i d'Immunologia, Universitat Autònoma de Barcelona, Cerdanyola del Vallès, 08193 Barcelona, Spain
3. Centro Nacional de Análisis Genómico (CNAG), Parc Científic de Barcelona, Barcelona, 08028, Barcelona, Spain
4. Universitat Pompeu Fabra (UPF), Barcelona, Spain.
5. Cancer Epigenetics and Biology Program (PEBC), Bellvitge Biomedical Research Institute, L'Hospitalet de Llobregat, 08907, Barcelona, Spain
6. Epigenetic Therapies Group, Experimental and Clinical Hematology Program (PHEC), Josep Carreras Leukaemia Research Institute, Badalona, Barcelona, Catalonia, Spain
7. Department of Clinical Medicine - Department of Infectious Disease, Aarhus University Hospital, Aarhus, 8200, East Jutland, Denmark
8. Sorbonne Université, Centre d'Immunologie et des Maladies Infectieuses – Paris (Cimi-Paris), INSERM U1135, Paris, 75013, Île de France, France
9. Fundació Lluita contra la Sida, Infectious Diseases Department, Hospital Universitari Germans Trias i Pujol, Badalona, Spain
10. Centre for Health and Social Care Research (CESS), Faculty of Medicine, University of Vic - Central University of Catalonia (UVic - UCC), Vic, 08500, Barcelona, Spain.
11. Institució Catalana de Recerca i Estudis Avançats (ICREA), Barcelona, 08019, Barcelona, Spain
12. The Jenner Institute, University of Oxford, Oxford, OX3 2DQ, Oxfordshire UK;
13. Joint Research Center for Human Retrovirus Infection, Kumamoto University, Kumamoto, 860-0811, Kumamoto, Japan;
14. Department of Medical Microbiology and Immunology, University of California, Davis, 95616, California, US
15. Division of Experimental Medicine, University of California, Davis, 95616, California, US
16. Cancer and Leukemia Epigenetics and Biology Program (PEBCL), Josep Carreras Leukaemia Research Institute, Badalona, Barcelona, Catalonia, Spain

Chapter III

17. Centro de Investigacion Biomedica en Red Cancer (CIBERONC), Madrid, Spain
18. Department of Physiological Sciences II, School of Medicine, University of Barcelona, L'Hospitalet de Llobregat, 08907, Barcelona, Spain
19. Projecte dels NOMS-Hispanosida, BCN Checkpoint, Barcelona, 08015, Barcelona, Spain.
20. Biosciences Department, Faculty of Sciences and Technology, University of Vic-Central University of Catalonia, 08500 Vic, Barcelona, Spain.
21. Statistics Department, Biology Faculty, University of Barcelona, Barcelona, 08028, Barcelona, Spain
22. Statistics and Bioinformatics Unit Vall d'Hebron Institut de Recerca (VHIR), Barcelona, 08035, Barcelona, Spain

This manuscript has been submitted for publication and is currently under review.



Institut de Recerca de la Sida

This declaration concerns the following manuscript:

Title: Host DNA methylation is associated with ATI outcome in the kick-and-kill therapeutic vaccine BCN02 clinical trial

Authors: Bruna Oriol-Tordera, Anna Esteve-Codina, María Berdasco, Miriam Rosas-Umbert, Elena Gonçalves, Clara Duran-Castells, Francesc Català-Moll, Anuska Llano, Samandhy Cedeño¹, Maria C. Puertas, Martin Tolstrup, Ole S. Søgaard, Bonaventura Clotet, Javier Martínez-Picado, Tomas Hanke, Behazine Combadiere, Roger Paredes, Dennis Hartigan-O'Connor, Manel Esteller, Michael Meulbroek, María Luz Calle, Alex Sanchez-Pla, José Moltó, Beatriz Mothe, Christian Brander, Marta Ruiz-Riol

This Manuscript is: Published Accepted Submitted In preparation

The PhD student has contributed to the elements of this article/manuscript as follows:

- A. No or little contribution
- B. Has contributed (10-30%)
- C. Has contributed considerably (40-60%)
- D. Has done most of the work (70-90%)
- E. Has essentially done all the work

Formulation/identification of the scientific problem	C
Planning the experiments and methodology design and development	D
Involvement in the experimental work / data collection	D
Involvement in data analysis	D
Involvement in results interpretation	D
Writing the first draft of the manuscript	E
Finalization of the manuscript and submission	D

The PhD student has searched the relevant background literature to get involved in the project and to understand the scientific problem and to participate in the selection of the best approach for data analysis. The PhD student has been the responsible for nucleic acid extraction, data analysis, results interpretation and writing the first draft of the manuscript with the guidance of their directors and other co-authors.

Dr. Christian Brander (director)

Dra. Marta Ruiz-Riol (director)

Abstract

BCN02 was an exploratory, single arm study designed to evaluate a kick-and-kill therapeutic vaccine strategy in early-treated HIV-1-infected individuals. The participants in the study received an MVA.HIVconsv vaccination before and after three cycles of infusion of romidepsin (RMD), an inhibitor of histone deacetylases that acts as a viral latency reversing agent. The inclusion of a monitored antiretroviral pause (MAP) identified 8 individuals with an early viral rebound (pVL > 2,000 HIV RNA copies/mL, within 4 weeks of MAP initiation) and 4, with a late viral rebound (reaching 2,000 HIV RNA copies/mL, > 4 weeks after MAP initiation). A systems biology analysis was conducted to identify the pathways modulated at transcriptomic and epigenetic levels during the clinical intervention, involving vaccination and RMD, and to identify biomarkers associated with HIV viral rebound during MAP. To this end, we studied gene expression and whole-genome DNA methylation in longitudinal PBMC samples prior to and after the intervention. The main impact on host transcriptional and epigenetic signatures was observed after vaccination and RMD infusion (Vacc+RMD) with multiple pathways related to HIV infection and immune response showing changes at gene expression and DNA methylation level. Analysis of an independent cohort of individuals ART-suppressed with RMD alone showed that these changes were mainly driven by CD4 T cells. DNA methylation patterns in full PBMC obtained after the complete Vacc+RMD intervention allowed to discriminate individuals with an Early versus Late viral rebound. These individuals also showed a differential enrichment on chromatin accessibility and transcription factor binding sites. Intriguingly, 30 of the differentially methylated positions (DMPs) between Early and Late rebounders at Vacc+RMD were present at baseline and were more accentuated after RMD infusion. Overall, this study provides a deeper understanding of the mechanisms modulated during the BCN02 study and highlights the importance of DNA methylation profiles in HIV cure.

Introduction

Human immunodeficiency virus-1 (HIV-1) infection forms a viral reservoir during early stages of infection which makes lifelong antiretroviral treatment (ART) indispensable and presents the main barrier to an HIV-1 cure. Additionally, despite the effectiveness of ART, it is not available worldwide, it is costly and is associated with viral resistance and treatment-related side effects. The establishment of HIV-1 reservoir along with sub-optimal and dysfunctional antiviral immune responses lays the basis of uncontrolled viral replication and HIV disease progression in the absence of ART. To this end, different kick-and-kill strategies are being designed to disrupt viral latency and enhance the host's immune system to eliminate HIV-1-infected cells (1–3).

A wide variety of latency reversing agents (LRAs) have been proposed to reactivate the viral reservoir, including epigenetic modifiers and agonists of NF- κ B, Toll-Like-Receptor (TLR) and protein kinase C, among others (4). Histone deacetylase inhibitors (HDACi) like vorinostat, panabinstat or romidepsin (RMD), originally developed for other medical indications (cancer), were first to be translated to the HIV cure field (4, 5). HDACi administration is associated with a global increase of histone acetylation that leads to chromatin relaxation and an increase in gene expression, including HIV transcripts, thus rendering virally infected cells visible to the immune system. However, LRA administration has generally failed to eliminate HIV-infected cells efficiently and no clinically relevant reductions in provirus loads have been measured (4, 6, 7). Given that HDACi were developed as anticancer drugs, they may hinder the effective clearance of reactivated virus-infected cells by a transient immune-suppression of CD8 T-cell activity, whose effects would be cumulative with a generally dysfunctional CTL immune response due to viral infection (8–10). To overcome these limitations, clinical trials combining LRAs with therapeutic T-cell vaccination aim to control rebounding HIV virus by intensifying the anti-HIV specific CTL responses (11–13). However, the effects of LRAs administration on non-viral, host genes involved in antiviral immunity are poorly understood, although they may play an important role in shaping effective vaccine-induced immunity.

BCN02 (NCT02616874) was a pilot study that combined the MVA.HIVconsv (14) vaccination before and after the administration of three cycles of RMD in early treated individuals

rolled-over from the BCN01 (NCT01712425) clinical trial (13, 15). In BCN02, RMD led to a transient increase of HIV transcription and histone 3 acetylation levels (H3Ac) that were short-lived and returned to basal levels one week after the last RMD cycle, while MVA.HIVconsv vaccination boosted the HIV-specific CTL response effectively (13). Additionally, the BCN02 study included a 32-week monitored antiretroviral pause (MAP) to evaluate virus control post-intervention. Of the 13 individuals eligible for MAP, 4 maintained viral loads < 2000 HIV RNA copies/mL for more than 4 weeks and of these, 3 completed the entire 32w of MAP without the need to restart ART (13). To gain insight of the molecular and immunological processes modulated during the clinical study as well as to identify predictors of ATI outcome before ART interruption, a systems biological analysis was conducted combining whole-genome gene expression and DNA methylation assessments in PBMCs samples from 14 individuals enrolled in the BCN02 clinical trial at three different time points (Figure S1A).

Recent findings of specific DNA methylation patterns associated with the natural ability to control HIV replication in vivo (16, 17), raised the questions of whether stable methylation profiles prior to ART interruption could determine the treatment outcome, and whether kick-and-kill strategies would have the power to restore potentially epigenetically dysregulated host gene pathways important for virus control. Therefore, DNA methylation was evaluated together with gene expression in the context of the BCN02 trial. These results revealed the main pathways that were modulated by the cumulative effect of the vaccination and RMD, as well as their impact on chromatin states and histone marks. Despite the small number of participants, specific DNA methylation imprints in pre-MAP samples were identified that discriminate Early (n=8) or Late (n=4) rebounding individuals. Such marks were identified in genes of relevant pathways for HIV-1 infection and specific immune signatures, and were mapped in regions with differential chromatin relaxation states and transcription factor binding sites (TFBS). Future analyses in larger clinical trials, ideally double-blinded, and placebo-controlled, will be needed to confirm these results and to warrant the use of DNA methylation signatures to predict viral rebound before treatment interruptions are initiated.

Results

1. Gene expression and DNA methylation changes one week after MVA.HIVconsv vaccination in the BCN02 study

To evaluate the impact of the first MVA.HIVconsv vaccination (Vacc) on the host transcriptional and epigenetic signatures, whole genome gene expression and DNA methylation screenings were conducted. Principal component analysis (PCA) and volcano plot of data from samples drawn one week after the HIV.cons v vaccination, revealed a strong impact on the host gene transcriptional program (Figure S1B and 1A). Specifically, compared to basal time point, 673 upregulated and 524 downregulated genes were identified (p-value < 0.05, Table S3). After adjusting for multiple comparisons with false discovery rate (FDR), there were 95 DEGs (adjusted p-value < 0.1), of which 88 were upregulated and 7 downregulated. The majority of differentially expressed genes (DEGs, p-value < 0.05) were protein coding genes (67%) and 7%, immunoglobulin coding genes (Table S4). In parallel, 5447 differentially methylated positions (DMPs, p-value < 0.05, Table S5) were identified, that were symmetrically distributed in hypermethylated (n=2864) and hypomethylated DMPs (n=2583) one week after MVA.HIVcons v vaccination, as shown in the volcano plot (Figure 1B and S1C). After FDR adjustment only 2 hypermethylated DMPs remain significant (adjusted p-value < 0.1). Of the identified DMPs (p-value < 0.05), 57% mapped to regulatory regions (TSS200, TSS1500, 1stExon and 5'UTR regions), 38% to Body regions, and 5% to 3'UTR regions (Figure S1D, and Table S6). Overall, 40% of DMPs were located in CpG islands, while 22% were from islands shores and 7%, from island shelves. The remaining 32% of DMPs, were found to open sea regions (Figure S1E, and Table S6).

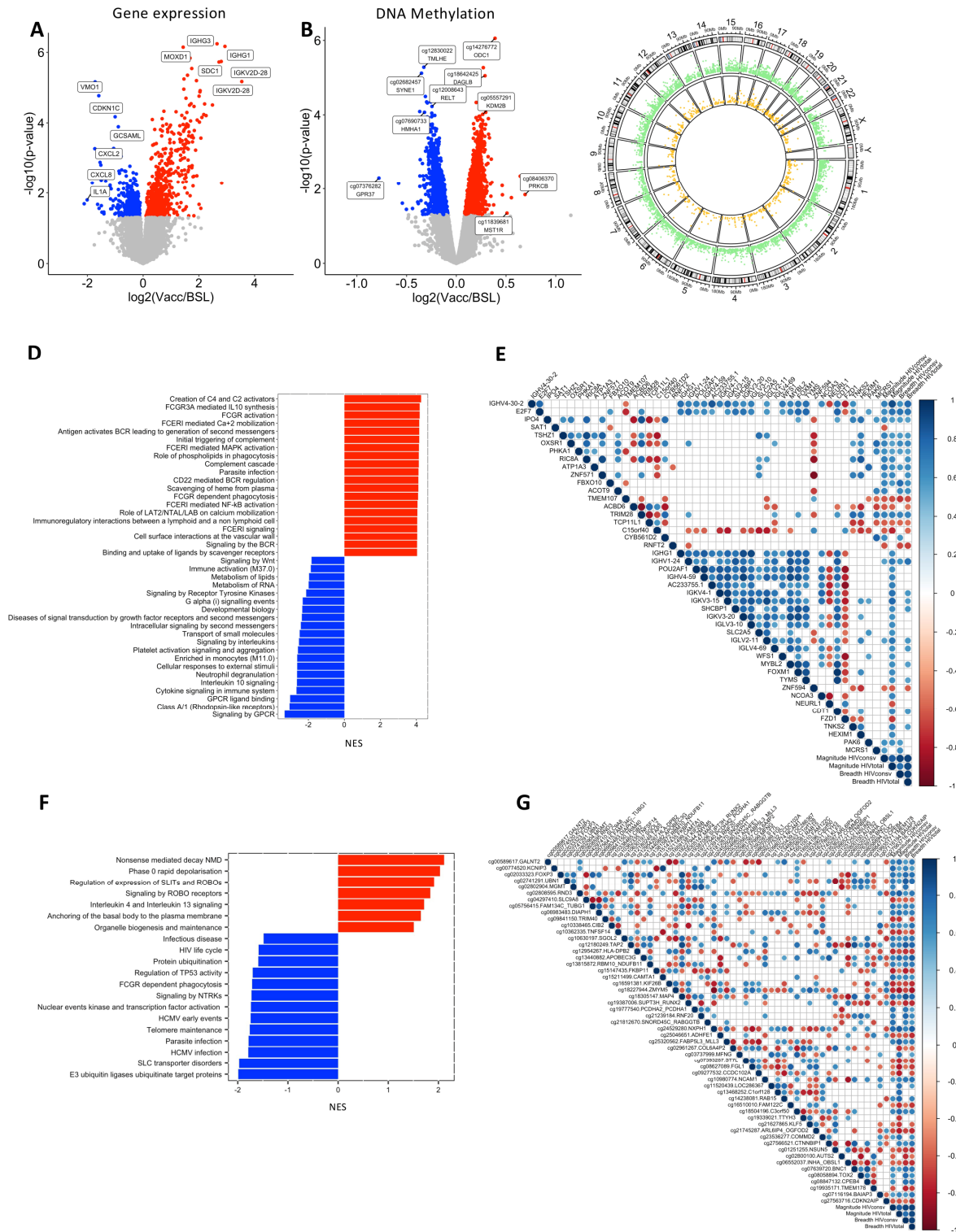


Figure 1. Impact of vaccination on gene expression and DNA methylation in the BCN02 trial. A) and B) show the Volcano Plots for the 1287 DEGs and the 5447 DMPs between post-vaccination and baseline, respectively (p-value < 0.05). X-axis show the log₂ Fold-Change, and Y-axis the -log₁₀ p-value. Color grey indicates p-value > 0.05; red, p-value < 0.05 and FC > 0 and blue, p-value < 0.05 and FC < 0. C) CIRCOS plot that includes an outer track with the chromosomes, genes and CpG sites positions in the genome. The two inner tracks are the Manhattan plots for DMPs (green) and DEGs (orange) between post-vaccination and baseline time points. D) and F) show the pathway enrichment (GSEA) for DEGs and DMPs, respectively. Red color reflects NES>0 and blue, NES < 0. E) Correlation plots of DEGs with breadth and magnitude of the virus and vaccine-specific T-cell response (p-value < 0.05 & Rho > |0.6|). For both DEGs and magnitude and bread the log₂ change between Vacc and baseline was used. G) Correlation plot for DMPs with T-cell responses (p-value < 0.01 & Rho > |0.6|) against HIVconsV immunogen or total HIV-1. For both DMPs and magnitude and bread the log₂ change between Vacc and baseline was used. Blue indicates positive and red negative Rho values (Spearman's correlation). Blanks make reference to non-significant correlations.

While DEGs and DMPs between Vacc and BSL time points were widely distributed among the different chromosomes (Figure 1C). The highest proportion of DEGs and DMPs were found in chromosome 1 (chr1), which is the largest chromosome, and overall DEGs and DMPs in each chromosome were proportional to its length (Figure S1F-G, Table S4-S6). In DNA methylation, chr8 and chrX showed a significant reduction in the proportion of DMPs in comparison to CpG positions that are included in the array (Figure S1G and Table S6)

At pathway and blood transcription modules (BTMs) level, based on DEGs, the majority of genes upregulated after vaccination (Normalized Enrichment Score, NES > 0) were related to Fc receptors, complement activation, phagocytosis and B cell receptor (BCR) activation. In parallel, the majority of downregulated genes (NES < 0) were linked to pathways of GPCR (G protein-coupled receptors) as well as interleukin and cytokine signaling (Figure 1D). Correlation analysis of DEGs belonging to these categories were associated with the magnitude of the T-cell responses against total HIV-1 (including the sum of HIVregions in plus out of HIVconsv), while fewer were correlated with T cells against HIVconsv (Figure 1E). Of these, MCRC5 is a gene involved in chromatin organization, and the genes SAT1, RNFT2 and ACOT9 are all involved in metabolic processes (18, 19).

DNA methylation pathway analyses showed an overall negative enrichment, with the majority of the gene-annotated DMPs being hypomethylated after vaccination. These DMPs are mainly involved in infection-related pathways (e.g. HIV life cycle, HCMV early events) (Figure 1F). In parallel, pathways like interleukin 4 and 3 signaling and SLITs and ROBOs signaling contain mainly hypermethylated DMPs (NES > 0). Interestingly, Slits2 protein has been described as an inhibitor of HIV-1 replication in T cells (20). When assessing correlations between DMPs and IFN γ T-cell response against total HIV or HIVconsv, the methylation levels of 32 CpG positions showed a positive correlation with these parameters, while 22 were negatively correlated. Of relevance, the methylation levels of APOBEC3G, involved in HIV-1 antiviral function, and TAP2, a gene involved in antigen presentation were both positively correlated with HIV total and HIVconsv breadth and magnitude. Of the DMPs positively correlated with HIVconsv but not HIV total, the majority of associated genes are involved in chromatin regulation and gene transcription

(e.g. MGMT, RNF20, RABGGTB, TOX2 and CPEB (18, 19). Finally, the methylation levels of AUTS2 gene, associated with the chromatin remodeling complex PRC1, were negatively correlated with HIVconsv magnitude (18, 19).

These data demonstrate a strong impact of vaccination on the gene transcriptional program, particularly for immune response pathways including immunoglobulins genes, Fc receptors, interleukins and cytokines and complement pathways. The same intervention impacted DNA methylation levels of genes involved in responses to infection. Interestingly, DNA methylation imprints correlated with measures of the HIVconsv vaccine-specific T-cell immunity, suggesting a direct role of epigenetic modulation on vaccine responsiveness or an impact of vaccination on epigenetic cascades.

2. Cumulative transcriptional and methylation changes after vaccination and RMD intervention

RMD administration impacts the global chromatin condensation state of host genome, thus affecting not only HIV-1 transcription but also other host genes. To evaluate the cumulative effects of the intervention (Vacc+RMD) on the host transcriptome and epigenome, DEGs and DMPs between Vacc+RMD and baseline were identified (Table S7-8). Overall, 1404 genes were upregulated and 1561 downregulated (Figure 2A, p -value < 0.05), and after adjusting by false discovery rate 240 genes were upregulated and 103, downregulated considering an adjusted p -value < 0.05 . Of all DEG (p -value < 0.05), 79% were found in protein coding genes (Table S9). For DNA methylation, there were 7025 hypermethylated and 9114 hypomethylated CpG positions between Vacc+RMD and baseline considering a p -value < 0.05 (Figure 2B). After adjusting for multiple comparisons, 1301 DMPs were hypermethylated and 2707 hypomethylated (FDR adjusted p -value < 0.05). Of the identified DMPs (p -value < 0.05), the 54% were located in regulatory regions (5'UTR, 1stExon, TSS1500 and TSS200), the 42%, in body and, the 4%, in 3'UTR (Figure S2A, Table S10). The number of DMPs in the regulatory regions 1stExon, TSS1500 and TSS200 were underrepresented compared to their coverage in the array, while the proportion of DMPs in 5'UTR and the body was slightly overrepresented (Table S10). Overall, 30.9% of the DMPs

were found in islands, 24.4%, in shores, 7.6%, in shelves, and 37.1% in open sea regions, respectively (Figure S2B, Table S10). The different DEGs and DMPs were distributed in the different chromosomes, and generally, the size of the chromosome was associated with the number of DEGs and DMPs (Figure 2C-D, Table S9 -10). Only in chr3, a higher number of DMPs ($p=0.01$) was found when compared to their representation in the methylation array (Figure S2C-D, Table S9-10).

Since RMD can trigger epigenetic cascades also outside regulatory regions, to define potential epigenetic landscape changes from baseline to the Vacc+RMD time points, enrichment analyses were applied on DMPs or DEGs using the ChromHMM and Histone marks in PBMCs from the Roadmap database (E062) (https://egg2.wustl.edu/roadmap/web_portal/chr_state_learning.html) (Figure 2D-G). These ChromHMM enrichment analyses showed that hypermethylated DMPs at Vacc+RMD time point were enriched in regions of active TSS (Transcription start site) and genic enhancers (EnhG2), while hypomethylated DMPs dominated predominantly in regions of weak transcription (Figure 2D). Similarly, downregulated genes were found in regions of active TSS, and upregulated ones in less active regions or on regions associated with poised expression (Figure 2F). In addition, histone acetylation marks enrichment followed the same trend, with hypermethylated DMPs and downregulated DEGs being enriched in regions of active transcription (e.g.H3K27ac) (Figure 2E and 2G). These results show that, although RMD is infused to increase histone acetylation, and consequently gene expression, one week after RMD infusion, the majority of upregulated genes were found in regions of transcriptional repression or poised promoters and enhancers rather than regions of active transcription.

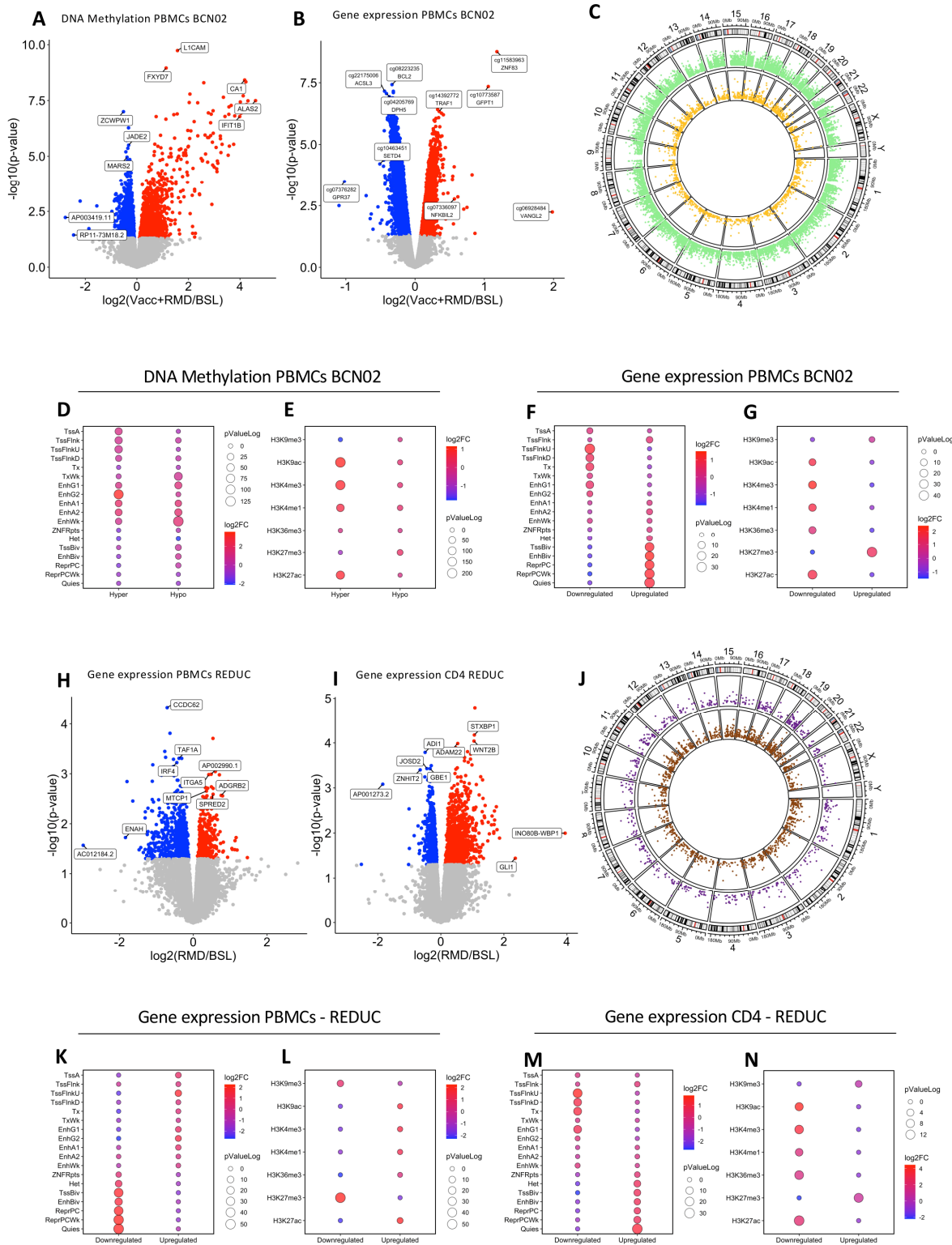


Figure 2. Effect of combined intervention on gene expression and DNA methylation. A) Volcano plot of the 3106 DEGs between time points Vacc+RMD and BSL. B) Volcano plot of the 15139 DMPs between time points Vacc+RMD and BSL. C) Manhattan plot in CIRCOS. The outer circle shows the chromosomes and positions of DEGs and DMPs. The inner tracks show the Manhattan plot for DMPs (green) and DEGs (orange) between Vacc+RMD and BSL time points. D) shows the 18-state ChromHMM enrichment and E) the histone mark enrichment for DMPs. The same was done for DEGs in Figures 2F and 2G and 2H. I) Volcano plots of for DEGs in PBMCs and isolated CD4 T cell from the REDUC clinical trial, respectively. Color key is the same as in A and B. J) Manhattan plot for REDUC DEGs in PBMC (purple) and CD4 (brown). K) ChromHMM 18-state enrichment based on DEGs in PBMCs and L) CD4 T cells. M) Histone marks enrichment for DEGs in PBMC and N) for CD4 T cells. For Volcano plots (A, B, H, I) X-axis show the \log_2 Fold-Change, and Y-axis the $-\log_{10}$ p-value. Grey color indicates $p\text{-value} > 0.05$; red, $p\text{-value} > 0.05$ and $FC > 0$ and blue, $p\text{-value} > 0.05$ and $FC < 0$. For ChromHMM and Histone marks enrichments, the color of the dots is associated with the \log_2 Fold-change enrichment, and the dots size, with the \log_{10} p-value.

Since the Vacc+RMD intervention reflected the cumulative changes derived from MVA.HIVconsV and RMD infusion (Figure S1H-I), in order to identify RMD-specific effects, a transcriptomics assessment was conducted on samples from participants in the part A REDUC study (NCT02092116) (6), in which ART-suppressed participants received 3 cycles RMD without prior vaccination. As in BCN02, it was compared the gene expression profiles one week after the 3-cycle RMD infusion (post-RMD) with the baseline. Due to sample availability, no methylation analyses were conducted in these samples. The transcriptomic analysis in PBMCs showed 224 upregulated and 567 downregulated genes, respectively (Figure 2H, Table S11). When analyzing purified CD4 only, a higher number of DEGs was found, 883 upregulated and 613 downregulated (Figure 2I, Table S12). In both sample sets, DEGs were spread among all chromosomes (Figure 2J). Interestingly, the ChromHMM and histone marks enrichment from CD4 DEGs in the REDUC clinical trials (Figure 2K-N) was similar to the results observed in BCN02 (Figure 2F-G).

Restoration of dysregulated gene expression profiles and their underlying epigenetic mechanisms may be critical to induce effective antiviral activity in kick-and-kill interventions (6). Therefore, gene set enrichment analyses (GSEA) were conducted to identify the dysregulated pathways upon Vacc+RMD (BCN02) or RMD only treatment (REDUC) (Figure 3, Table S13). For the combined regimen of therapeutic vaccine and RMD, the data show a strong impact on the HIV pathways in infectious disease and HIV module (HIV infection and HIV life cycle) as well as on the pathways in immune signature module (e.g. T-cell activation and antigen presentation). Particularly, Host interactions of HIV factors, HIV infection, HIV life cycle, Infectious Disease and Cellular responses to external stimuli, were enriched in DEGs of REDUC CD4 cells and BCN02 PBMC (Figure 3). Interestingly, there are many other pathways that were shared between the two datasets, including pathways in the metabolism module like Metabolism of RNA or TCA cycle and respiratory electron transport), the pathway Translation from the protein module, the pathway Signaling by ROBO receptors in the module neuronal-related processes, and the pathways DNA double strand break and cell cycle mitotic in modules DNA repair and cell cycle, respectively. In parallel, the pathways in modules transport and cell signaling are mainly impacted at transcriptome level in isolated CD4 cells of REDUC clinical trial. Finally,

only few pathways showed an overlap between the two datasets in the module of immune signature, possibly due to the fact that the two studies differ by the inclusion of a therapeutic vaccine in BCN02. Still, among the immune signature module, pathways like signaling by interleukins, FCER1 mediated NF- κ B activation and antigen processing cross presentation were mainly found dysregulated in isolated CD4 from REDUC trial. Interestingly, regarding B cells, there was an enrichment in DEGs from REDUC CD4 cells as well (Signaling by BCR) and PBMC (B cell surface) and DMPs from BCN02 (Enriched in B cells and Antigen activates BCR leading to generation of second messengers). In the case of T cells, the majority of the pathways were associated with DEGs in BCN02, although TCR signaling is also present in isolated CD4 from REDUC (Figure 3). Of note, aside from a large number of pathways in the gene expression module that were modulated by the therapy, there was a marked regulation of pathways like HATs acetylated histones and Chromatin modifying enzymes, indicating the complexity of the epigenetic mechanisms dysregulated at Vacc+RMD and reflecting the RMD activity.

Focusing on the BCN02 dataset only (Figure S3), there were many pathways suggesting an epigenetic regulation, as they showed opposite NES. Many of these pathways located to the immune signature module, like Enriched in Monocytes, show a majority of upregulated and hypomethylated genes. Also, T cells and T-cell activation, mainly contained hypermethylated DMPs and downregulated expression of genes. The same trend was observed for HIV life cycle pathway and in other pathways of the modules cell cycle, metabolism, gene expression or protein translation.

Overall these results suggest that after a Vacc+RMD regimen, a homeostatic mechanism might be activated since the global epigenetic state of the cells attempts to counteract the acetylation effects induced by RMD, whose main effects (4 hours post infusion) are waned 1 week after its administration.

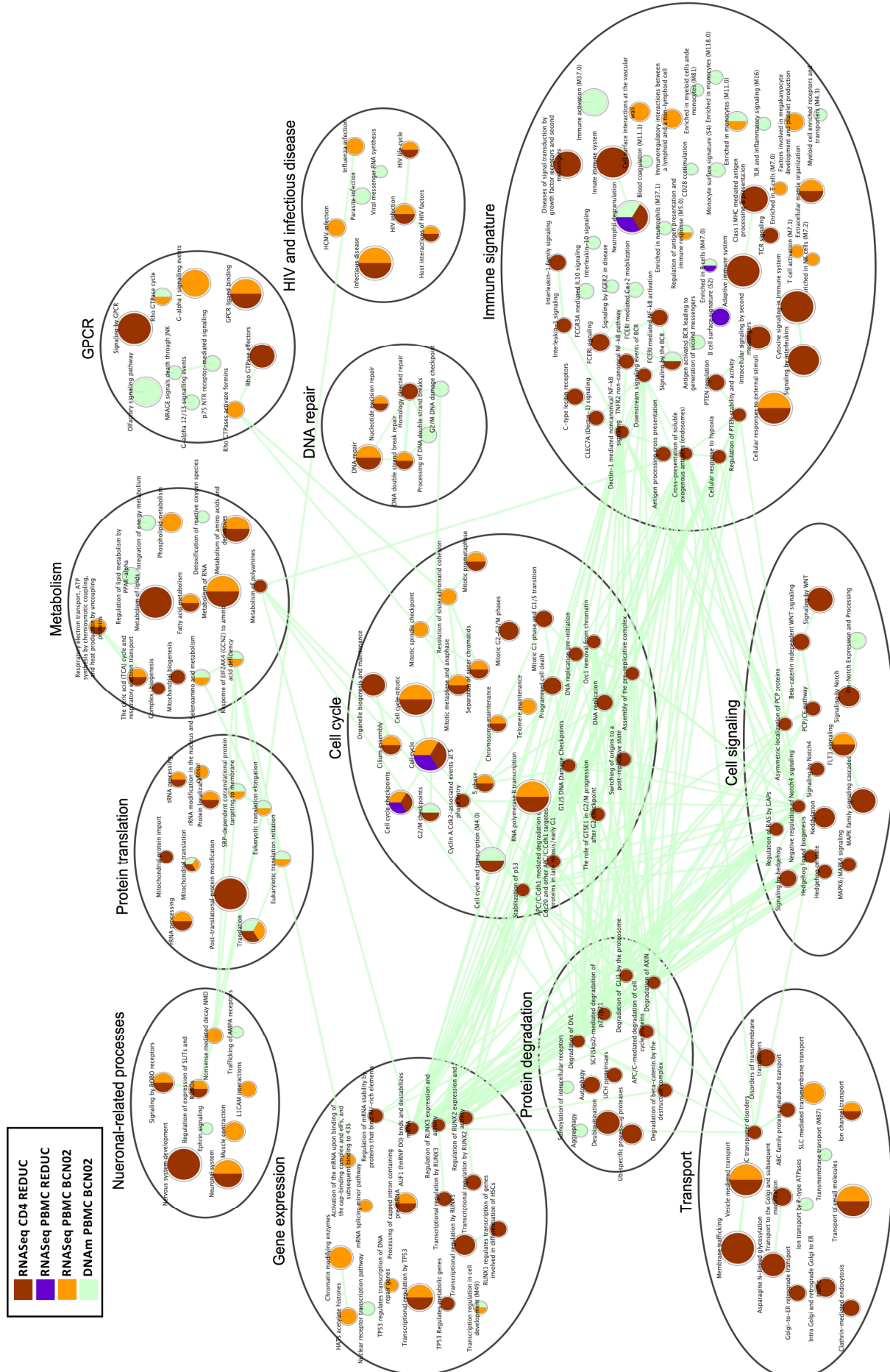


Figure 3. Effect of RMD on gene expression and DNA methylation in the BCN02 and REDUC trial (see figure on page before). EnrichmentMap of enriched pathways and BTMs (GSEA adjusted p-value < 0.2) in DEGs before and after RMD infusion in PBMCs of BCN02 (Orange) and in REDUC PBMC (Purple) or isolated REDUC CD4 T cells (Brown). DMPs before and after RMD infusion in BCN02 are shown (Green). The color of the nodes indicates the different datasets. Edges represent the similarity of the nodes (cutoff = 0.7).

3. DNA methylation imprints after intervention can predict viral rebound before ATI

Next, it was tested the hypothesis that changes on gene expression and/or methylation induced by vaccination and RMD treatment, observed before MAP, might explain the different viral rebound kinetics. An unsupervised PCA of DNA methylation data in samples from the Vacc+RMD time point showed individuals with early or late rebound (VL reaching 2,000 HIV RNA copies/mL before ["Early rebounders"] or after ["Late rebounders"] 4 weeks of MAP) to cluster closely together (Figure 4A). The same clustering was not observed when performing PCA with gene expression data (Figure S4A). A logistic regression model using the PC1 and PC2 as covariates, confirmed the potential of DNA methylation to discriminate between individuals with an Early versus Late rebound (DNA methylation AUC=0.812 and gene expression AUC=0.594 at the Vacc+RMD time point, Figure 4A and S4A). The heatmaps on Figure 4B and Figure S4B confirm these results. At earlier time points, the discriminative capacity of DNA methylation was lower (AUC BSL = 0.563, AUC Vacc = 0.687), which was also true for gene expression (AUC BSL = 0.563, AUC Vacc = 0.594).

Given the potential of DNA methylation to discriminate between Early and Late rebounders at the Vacc+RMD time point, the DMPs (p-value < 0.05) between Early and Late rebounders were further analyzed at this time point. Specifically, of the identified DMPs, 3835 DMPs were hypermethylated and 3761, hypomethylated in Early rebounders; of which 5 and 1 DMPs, respectively, were maintained significantly differentially methylated with a FDR adjusted p-value < 0.05 (Figure 4B, Table S14). The hypermethylated DMPs (p-value < 0.05) in Early rebounders were found in bivalent and inactive regions of the genome, which were enriched in the histone mark H3K27me3 (Figure 4C). In parallel, the hypomethylated DMPs in Early rebounders were found in active regions of the genome. Interestingly, when assessing DMPs at transcription factor binding sites (TFBS), hypermethylated DMPs in Early rebounders were strongly enriched for factors of the ETS family, while the hypomethylated

DMPs were enriched in transcription factors of the Zf, bZIP and IRF families (Figure 4D-E). These data suggest that the epigenetic landscape after vaccination and RMD infusion may aid in controlling viral replication either directly, by the modulation of chromatin accessibility in regions of active/inactive transcription, or through the binding of specific TFs.

When analyzing the main pathways enriched by DMPs between Early and Late rebounders at the Vacc+RMD time point, differential methylation levels were observed in genes involved in pathways and modules related to HIV host factors, immune parameters (Antigen presentation, TCR signaling and signaling by interleukins), metabolism of lipids and RNA, membrane trafficking and ER-Golgi transport, MAPK and TGF- β signaling, and cell cycle processes (Figure S5). To further characterize these pathways, heatmaps of pathway-associated DMPs (p -value < 0.01 and $\log_2FC > |0.5|$) were created and the correlation with viral and immune parameters was studied (Figure 4F and Table S15). These analyses showed that hypomethylated CpGs in Late rebounders and thereby, hypermethylated in Early rebounders, positively correlated with three measures of viral reservoir and replicative activity under ART (proviral size, single copy assay and cell-associated RNA levels (CA-RNA)) as well as with the magnitude of the T-cell response against HIV_{consv} and HIV_{total} (HIV regions not covered by the immunogen). On the other hand, hypermethylated DMPs in Early individuals were negatively correlated with the time off antiretroviral treatment and the time with undetectable viral load during MAP. In addition, these DMPs showed an association with the time from HIV infection until cART initiation as well as the time on cART at BCN02 entry, suggesting that some epigenetic marks are defined even before ART initiation which could explain the differential viral rebound during MAP.

Focusing on specific DMPs in the HIV infection module, the methylation levels of PRKCO gene were negatively correlated with cell-associated (CA)-RNA and proviral levels. In the immune signature module, a differential methylation was found for genes in the HLA locus. In particular, DNA methylation at the HLA-B locus was positively correlated with time off ART treatment, while DNA methylation in positions of the HLA-DPA1 and HLA-DRB1 locus

were negatively correlated with this parameter. In the case of MAP2K3, a gene annotated in the modules HIV and immune signature, and hypermethylated in Late rebounders, its methylation levels are negatively correlated with SCA while a positive correlation is observed with the time off cART, the time with undetectable viremia in MAP and the time from HIV infection to cART treatment initiation. On the other hand, in these two categories, the IL6 and JAK1 genes were hypomethylated in Late rebounders, with methylation levels positively correlated with CA-RNA. Also, methylation levels in IL6 positively correlated to the time with undetectable viral load in MAP while methylation levels in JAK1 were significantly related to the magnitude of the IFN γ response against HIV. Finally, for the metabolism module there are 9 DMPs associated with RUFY1 gene, which was positively correlated with the time on cART at BCN02 entry. Interestingly, the levels of gene associated DMPs classed in metabolism, cell cycle and cell transport with reported interaction with HIV virus (HADHA (21, 22), KIF2A (23), CHMP2B (23)) correlated with viral and immune parameters.

Of special importance, of the 150 DMPs that differed between Early and Late rebounders at the Vacc+RMD time point and represented in the GSEA analysis (Figure S5), 66 were also differentially methylated between the two groups at the baseline time point and maintained a differential methylation signature after vaccination. Of these 66 DMPs, RMD administration further increased the difference of the median methylation levels between the two groups for 30 of them. At the MAP time point, 52 of these 66 DMPs were common in all the different time points. Such results indicate that certain DMPs between Early and Late rebounders are maintained during MAP and in the presence of viral replication (Table S14).

Together, these results provide evidence that specific host-gene methylation profiles are associated with clinical, virological and immunological parameters and allow for the discrimination between Early and Late rebounders. Additionally, the data also show that RMD impacts the epigenetic landscape broadly and further accentuates the differences in DNA methylation between individuals with an Early or Late virus rebound, which partly could have already been detected at the baseline time points.

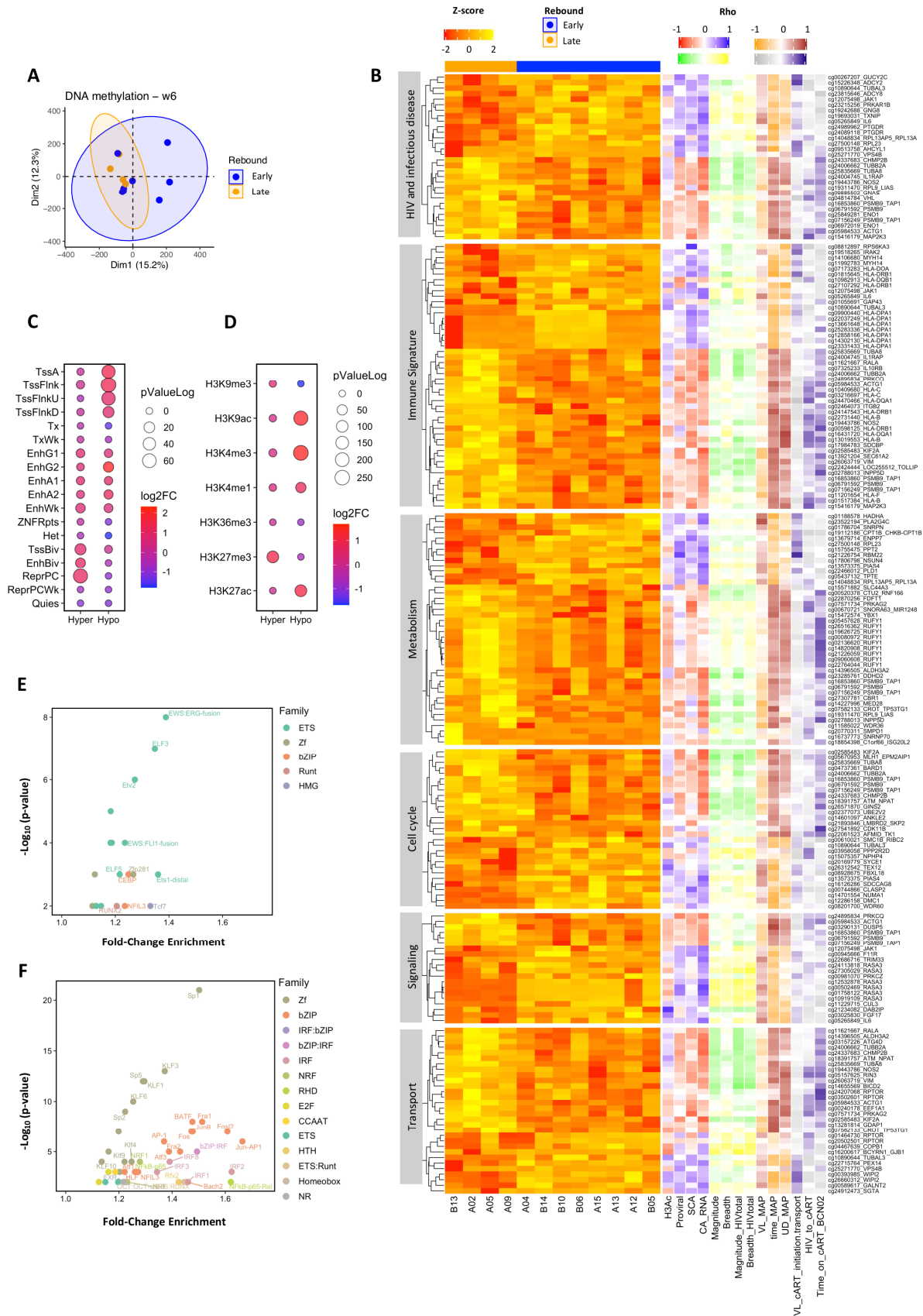


Figure 4. Differential DNA methylation between individuals with an Early or Late rebound. A) PCA for DNA methylation at time point Vacc+RMD. Blue and orange colors indicate Early and Late rebounders, respectively. B) 18-state ChromHMM enrichment and C) the histone marks enrichment for DMPs between and Early and Late rebounders. In the x axis, Hyper and Hypo make reference to DMPs hypermethylated or hypomethylated in Early rebounding individuals. The Log2 Fold-Change is shown by the dot color, while the $-\log_{10}$

p-value, with the dot size. D) Transcription factor (TF) enrichment based on DMPs hypermethylated in Early individuals, and E) based on DMPs hypomethylated in Early individuals. Colors indicate the TF family, and the name of the TF is shown when Log₂ Fold-Change > 0.3. F) Heatmap of Z-score methylation levels of DMPs (p-value < 0.01) between Early and Late rebound at Vacc+RMD in different pathways (Y-axis). The part of the heatmap shows the correlation (Spearman's Rho) between DMPs methylation levels and different parameters. For correlations with histone 3 acetylation (H3Ac), proviral levels, ultrasensitive viral load (SCA) and cell-associated RNA (CA-RNA), red shows a negative correlation and blue a positive one. For correlations with the magnitude and breadth of the HIVconsv- or HIVtotal-specific T-cell response, green shows a negative correlation and yellow a positive one. For correlations with viral load at day of cART resumption (VL MAP), time on MAP and time in MAP with undetectable viral load (UD MAP), orange shows a negative correlation and brown a positive one. For correlations with VL at cART initiation, time from HIV infection until cART initiation (HIV to cART) and time on cART at BCN02 entry, grey shows a negative correlation and purple a positive one.

Discussion

This study assessed the impact of a kick-and-kill strategy combining therapeutic T-cell vaccination and RMD on host transcriptional and epigenomic patterns. It also tested the hypothesis that that epigenetic imprints could serve as biomarkers of HIV control during the monitored antiretroviral pause (MAP). BCN02 was a phase I, open-label clinical trial that combined the latency reversing agent (LRA) romidepsin (RMD), an inhibitor of histone deacetylases (HDACi), with HIVconsv vaccination in order to reactivate the HIV provirus at the time of a boosted killer T-cell response against vulnerable parts of the virus. During the MAP, 4 out of 13 individuals maintained a VL < 2,000 HIV RNA copies/mL for more than 4 weeks (13). Systems biology analyses identified molecular pathways, including those involved in infectious diseases and immune activation that were modulated during the combined intervention at transcriptional and epigenetic levels. Finally, differentially DNA methylated positions after the intervention (Vacc+RMD) discriminated individuals with an Early or Late virus rebound during MAP, with some signatures having been present even before the therapeutic intervention.

The present analysis showed that MVA.HIVconsv vaccination had an effect on the expression levels of genes involved in the humoral immune response (e.g. IGHG1, IGHV1-24 and C1QA), as well as on genes involved in interleukin signaling. After vaccination, there was also an impact on DNA methylation levels of genes involved in infectious disease pathways (e.g. APOBEC3G, TUBB3, and FURIN) and, importantly, on genes potentially involved in further downstream epigenetic processes, including PRC1, MGMT and RNF20. Interestingly, the methylation levels of genes associated with epigenetic processes were directly correlated with the magnitude of the vaccine-elicited T-cell response specific for the conserved HIV regions (14, 24–27). This observation is in line with a previous report on

influenza vaccination demonstrating that gene-associated DMPs correlated with the vaccine-induced humoral response (27, 28). Similarly, BCG vaccination has been reported to induce an innate immune like-memory in monocytes that was driven by epigenetic processes, and some reports suggest this antigen-unspecific effect may also be induced by other vaccine vectors and adjuvants (27, 29, 30). However, in all these analyses, choosing the adequate time point to document possible associations between vaccine take, transcriptomic changes or epigenetic profiles may be critical. This dependence on timepoint also applies to the present study, were the selection of other time points than the one studied (1 week after the first BCN02 MVA.HIVconsv vaccination) might have helped to capture more profound effects on the vaccine-induced T-cell response and allowed to better document the transient changes in transcriptomic activity (31). In addition, the observed transcriptomics patterns reflect a recall immune response, as the individuals in BCN02 were previously vaccinated in BCN01 with a heterologous vector prime-boost of ChAd63.HIVconsv and MVA.HIVconsv (15). Thus, the selected time points could blur the observation of a major effect on immune transcriptional effects. At the same time, epigenetic signatures, which are more stable over time (32, 33) may be less sensitive to precise timing.

The availability of samples from the REDUC trial, where participants received RMD without a therapeutic T-cell vaccine, allowed to assess the contribution of RMD to the combined intervention in BCN02. Indeed, RMD administration had a marked effect on both gene expression and DNA methylation, although at gene-level major negative correlations were not captured between gene expression and DNA methylation. This outcome is partially due to the low sample size and the different time to respond to stimuli. However, different DMPs and DEGs converged in the same pathways, suggesting an epigenetic regulation of these pathways at different levels. Among the pathways modulated by Vacc+RMD, pathways related to HIV life cycle and infectious diseases were identified as the most severely impacted. The fact that these observations were made using samples taken after the most prominent effect of RMD on histone acetylation had already waned, suggests that a dysregulation of HIV transcription is further maintained. In the REDUC clinical trial, it has been shown that while RMD was able to induce the initiation and elongation of the virus

transcription, the drug failed to increase late events in HIV-1 transcription (34). This finding is in line with several other reports that suggest that more potent LRA, and potentially combinations of them would be needed to efficiently purge the viral reservoir. This could indeed support broader reactivation of latent virus through combining LRAs with different effects on HIV transcription, affecting differentially distinct integration sites in the host genome and in different cell types (35, 36).

In addition to a strong latency reversing activity that is able to induce HIV antigen expression, the stimulation of an effective immune response to eliminate cells with reactivated virus will also be critical to achieve and HIV-1 remission in the absence of ART (8, 37). In the BCN02 study, the virus-specific T-cell immunity was clearly enhanced during the therapy (13, 38) and in the present study, related pathways (including T-cell activation, TLR signaling and/or antigen presentation) appeared to be modulated at both the epigenetic and transcriptional levels. These pathways were also observed in the transcriptional program of CD4 cells from the individuals in the REDUC clinical trial, in which only RMD was administered. These findings suggest that the vaccination of individuals in BCN01 and BCN02 prior to RMD infusion may have poised the immune system to respond and exert its antiviral activity against HIV. Indeed, *in vitro* studies showed that inducing an efficient HIV-specific CD8 response before the administration of a LRA resulted in a more effective removal of infected cells (8).

Genes in pathways of HIV infection or in immune signature and metabolism, among others, showed a differential DNA methylation between individuals with an Early and Late viral rebound. Interestingly, some of these methylation imprints were already observed at baseline and after vaccination and could thus be host-specific or modulated by HIV infection, antiretroviral treatment or previous prime-boost vaccination in BCN01. To the best of our knowledge, this study hints at the possibility that epigenetic signatures, including those assessed before kick-and-kill interventions, could predict eventual virus control in treatment interruption. This is in line with a previous report from our group showing that differential capacity to control HIV infection in the absence of ART was associated with a differential methylation profile of genes involved in antiviral response

and T-cell immunity (16, 39). Furthermore, different DNA methylation in CD4 T cells is associated with distinct viral progression and can be impacted by cART treatment initiation (17).

Previous report in Cutaneous T Cell Lymphoma showed that RMD increased the chromatin accessibility mainly of regions with open or relaxed chromatin (40), while the present data showed that RMD administration further potentiated the epigenetic differences between individuals with an early or late viral rebound. Such observations were not present at transcriptional level (Figure S4B-C). Actually, at Vacc+RMD time point, while Early rebounders showed hypomethylation mainly in regions of active transcription, Late rebounders were hypomethylated in regions of repressed chromatin. This differential epigenetic landscape could be also affecting viral rebound, since late rebounding individuals may have HIV-1 integrated in regions of the host genome that are transcriptionally less active, as has been suggested in the setting of natural HIV control (41).

Limitations of this work include small study size, limited sampling time points and lack of a placebo control arm. This prevented us from determining, for example, to what extent the basal levels of DNA methylation (BCN01 enrollment) could have predicted viral rebound kinetics in the treatment interruption phase. Actually, in well powered studied selection of a combination of DNA methylation candidates and viral and clinical data may yield with predictive models of viral rebound. Another potential limitation was the study of total PBMCs rather than sorted lymphocyte subsets, as it is not possible to determine the precise cellular origin of some of the observed signals. To overcome this limitation, samples from the REDUC trial were evaluated and showed different signals from PBMC or from isolated CD4 T cells. Interestingly, the transcriptional patterns of the isolated CD4 T cells in the REDUC clinical trial were similar to those observed in PBMCs from the BCN02 study. With this results it is tempting to hypothesis that previous vaccination may increase the signals from CD4 T cells in BCN02 clinical trial, although this should be tested in isolated fractions from BCN02 which unfortunately are not available. Even though, from a biomarker point of view, the use of total PBMCs is potentially more appealing.

All in all, this is a unique exploratory study of a clinical trial testing a kick-and-kill strategy that showed a partial clinical signal in terms of virus control during treatment interruption. The data clarified the different molecular pathways that were modulated in response to this specific intervention, and highlighted that DNA methylation profiling could be further explored to interrogate its use as a biomarker to predict viral control before treatment interruption. These results warrant further confirmation in larger, placebo-controlled clinical trials and may inform future refined strategies to achieve a functional HIV cure.

Material and methods

Study design

BCN02 (NCT02616874) was a pilot kick-and-kill study that included 15 early-treated individuals who were rolled-over from the prior clinical trial BCN01 (NCT01712425) (Table S1) (15). In BCN01, individuals were immunized with a heterologous prime/boost regimen delivering the HIVconsv immunogen. In BCN02, the participants were vaccinated again with MVA.HIVconsv before and after the administration of RMD (RMD) (Figure S1A), an inhibitor of histone deacetylases (HDACi) which acts as a latency reversing agent (LRA). The BCN02 included a monitored antiretroviral pause (MAP) to evaluate the viral rebound kinetics whereby participants were monitored for viral load rebounds on a weekly basis for up to 32 weeks. Two participants were excluded from MAP evaluations, one who did not meet the criteria for treatment interruption, and one who showed a protocol deviation during this phase. Specifically, the present sub-omics study was restricted to the 14 male individuals enrolled in the BCN02, of which 12 were eligible for MAP. These 12 individuals were classed in Early rebound (n=8) or Late rebound group (n=4) according if they reached the threshold of 2,000 HIV RNA copies/mL before or after the 4 weeks of treatment interruption.

In order to evaluate the contribution of RMD on gene expression profiles in isolated CD4 T cells and whole PBMCs, samples from the part A of the clinical trial REDUC (NCT02092116) (6) were used. REDUC was designed to evaluate the in vivo effect of RMD administration in ART-treated individuals and showed that RMD could disrupt latency and showed a 2.4-to-

5-fold increased HIV-1 transcription (cell-associated un-spliced HIV-1 RNA). Here, we included 5 participants from this clinical trial, sampled before and after RMD administration (Table S2).

PBMCs and CD4 T cell isolation and acid nucleic extraction

Blood samples from BCN02 participants were processed using Lymphoprep (STEMCELL technologies) and 2x10⁶ dry pelleted PBMCs were frozen until use. DNA and RNA were isolated simultaneously from the same sample (AllPrep DNA/RNA Mini Kit, Qiagen) and were frozen until use. PBMC's were isolated from blood samples from REDUC trial participants using Ficoll separation followed by CD4 T-cells isolation using a CD4 T-cell isolation kit and magnetic-activated cell sorting (MACS) columns (Miltenyi Biotec, purity >95%). Isolated CD4 cells were lysed AllPrep lysis buffer and lysates were stored at -80°C until RNA was extracted (AllPrep isolation kit, Qiagen).

RNAseq library preparation and sequencing and data pre-processing

The total RNA was quantified by Qubit® RNA BR Assay kit (Thermo Fisher Scientific) and the RNA integrity was estimated by using RNA 6000 Nano Bioanalyzer 2100 Assay (Agilent). The RNASeq libraries from total PBMC RNA samples were prepared using a TruSeq™ Stranded Total RNA kit protocol (Illumina) and the rRNA was depleted from 20-500 ng of total RNA using the RiboZero Magnetic Gold Kit. The libraries were sequenced on HiSeq2000 (Illumina) in paired-end mode with a read length of 2x76 bp using TruSeq SBS Kit v4 in a fraction of a sequencing v4 flow cell lane, following the manufacturer's protocol. Image analysis, base calling and quality scoring of the run were processed using the manufacturer's software Real Time Analysis (RTA 1.18.66.3) and followed by generation of FASTQ sequence files by CASAVA. RNA-seq paired-end reads were mapped against the human (GRCh38) genome using STAR version 2.5.3a (42) with ENCODE parameters. Annotated genes (genecode version 28) were quantified using RSEM version 1.3.0 with default parameters (43). The quality control of the mapping and quantification steps was performed with GEMtools (<https://gemtools.github.io/>) and custom python scripts. Following RSEM expected counts were normalized with TMM method from edgeR

R/Bioconductor and genes with less than 5 counts were filtered out (44). Finally, counts were transformed with the `voom` function in `limma` R/Bioconductor and used in downstream analyses (45).

DNA methylation array

Genomic DNA was bisulfite converted using EZ DNA methylation Kit (Zymo) following manufacturer's protocol. Next, 4 μ L of bisulfite-converted DNA were hybridized to Infinium HumanMethylation450 BeadChip following Illumina Infinium HD Methylation protocol. Chip analysis was performed using Illumina HiScan SQ fluorescent scanner and the intensities of the images were extracted using GenomeStudio (2010.3) Methylation module (1.8.5) software. Quality control, background correction and quantile normalization across arrays was performed using ChAMP R/Bioconductor package with functions extracted from Minfi R/Bioconductor package (46–48).

Differential gene expression and DNA methylation analysis

In exploratory data analysis of both -omics data sets, principal component analysis (PCA) was used to identify batch effects and the major source of variation. This led to the removal of the only female participant in the study as its samples appeared as an outlier in the PCA analyses of both gene expression and DNA methylation datasets. The clinical trial site in which samples were processed was also identified as a source of variation in gene expression data. Therefore, `ComBat` function from `SVA` R/Bioconductor was used to correct for this effect in unsupervised analysis (49). Differential gene expression and methylation analyses between time points and Early and Late rebounders were performed with `limma` (45). For longitudinal comparisons, '`duplicateCorr`' function was used to consider the participants variable as a random effect. To identify the changes in gene expression over time, the model `~Hospital+Week` was fitted, to adjust for the confounding variable `Hospital`. For DNA methylation (M-values), the model `~Week` was used. Next, to identify the individuals with an Early (n=8) or Late (n=4) rebound in the different time points, the fitted model was `~Week_Rebound`.

Gene expression and DNA methylation profiles

Soft clustering (MFuzz R/Bioconductor) allowed discerning different longitudinal clusters of gene expression or DNA methylation (50). Briefly, genes or CpG positions that showed a p-value < 0.05 in any of the pairwise comparison between time points were included. Next, for each gene in each of the time points, the median expression/methylation standardized value was used for clustering. The function MFuzz:mestimate() was used to estimate the fuzzier parameters, and the number of clusters was determined with the MFuzz::Dmin() function. Finally, a minimal membership of 0.1 was used for gene expression, and of 0.2, for DNA methylation.

Integrated functional pathways analysis of genes and CpG positions modulated during the kick-and-kill therapy

For integration of the differentially expressed genes (DEGs, p-value < 0.05) and differentially methylated positions (DMP p-value < 0.05) data sets corresponding to one week after RMD administration (Vacc+RMD) and the baseline (BSL) (Figure S1), a published protocol was followed (51). For functional analyses, a pre-ranked GSEA was run in GSEA JAVA desktop program (MacOSX Version 4.03). Genes were ranked according to the $-\log_{10}$ p-value multiplied by the sign of \log_2 Fold-Change (51). As database, a combination of the REACTOME subset of Canonical pathways from Molecular Signature database (MSigDB, v7.4), and the blood transcriptional modules (BTMs) previously described elsewhere (27) was used. The majority of parameters were set to default (1000 permutations, weighted enrichment statistic and only gene sets between 15-500 genes were considered). Combined GSEA results for gene expression and DNA methylation were plotted using EnrichmentMap (52) in Cytoscape (MacOSX version 3.7.3). The different nodes represent the pathways, and the edges showed the mutual overlap. The largest pathway was maintained when there were one or more pathways with similar names, one embedded inside the other. BTMs annotations in the miscellaneous groups TBC were as well removed (53). Finally, groups of pathways were done using AutoAnnotate (54) and modified according authors criteria based on REACTOME data base and PubMed bibliographic research and considering the context of the study and the sample type (PBMCs).

Chromatin state and histone marks enrichment

To identify in which chromatin regions and histone marks were enriched the DEGs or DMPs identified between time points or between early or late rebound, a genomic regions enrichment was run with LOLA R/Bioconductor (55) based on the publicly available Roadmap datasets of 18-chromatin states (ChromHMM) and histone marks of PBMCs (E062, https://egg2.wustl.edu/roadmap/web_portal/chr_state_learning.html) were used. As background non-differentially expressed genes or the non-differentially methylated CpGs positions were used.

Transcription factor (TF) enrichment

To determine the enrichment of the TF binding site motifs in DMPs between Early and Late rebound (at the Vacc+RMD time point), HOMER motif discovery software was used (56), considering a 250-bp window upstream and downstream of the DMPs. The other CpGs in the 450K array were used as background.

Evaluation of DNA methylation and gene expression capacity to discriminate between

Early and Late rebound

To test the capacity of DNA methylation and gene expression to differentiate Early or Late rebound at the different time points analyzed, a PCA in each of the datasets for each time point was used, and a logistic regression was fitted with PC1 and PC2 as predictors. AUC values showed how well the PC1 and PC2 classified the Early or Late rebounder groups. Based on the DMPs between Early and Late Rebound at Vacc+RMD time point, a GSEA analysis was applied using canonical pathways and BTMs as described before. Based on GSEA results, 6 modules of DMPs were identified, and the Z-score methylation levels (M-values) of DMPs on genes in these pathways were represented in a heatmap (ComplexHeatmap R/Bioconductor) (57). Additionally, the Rho values (Spearman Correlation) of DMPs with specific viral and immune parameters were plotted.

Data and code availability:

Transcriptomics and DNA Methylation is uploaded at Gene Expression Omnibus (GEO): GSE184653, contains the transcriptomics data for BCN02 study; GSE185391, the DNA Methylation data for BCN02 study; and GSE185027, the transcriptomics data for REDUC study. The R code used in the analysis can be found in the github <https://github.com/hostimmuneOMICS> under the repository BCN02_OmicsAnalysis.

Statistics

The moderated t-test in limma was used to identify the differentially methylated positions or the differentially expressed genes between different time points or between an Early and Late rebound as explained before. Although false discovery rate (FDR) adjusted p-value was calculated for each gene transcript or CpG position, due to the small sample size and the exploratory character of the present study, an uncorrected p-value < 0.05 was used to define the subset of differentially expressed genes (DEGs) and differentially methylated positions (DMPs) used in downstream analysis. Chi-square tests were applied to evaluate the different abundance of DMPs or DEGs in certain chromosomes in contrast to the evaluated CpG positions or transcripts. The same test was applied for DMPs in relation to island (island, open sea, shore or self) or in relation to gene (5'UTR, TSS200, TSS1500, 1stExon, Body, 3'UTR) and for DEGs in relation to biotypes. For chi-square test a p-value < 0.05 was considered significant. Finally, Spearman's rank correlation test was used in correlation analysis and a p-value < 0.05 was considered significant.

Study approval:

The study of all samples used in the present study was approved by the Clinical Research Ethics Committee of the Germans Trias i Pujol University Hospital (Reference number PI-18-183).

References

1. Ward AR, Mota TM, Jones RB. Immunological approaches to HIV cure.. *Semin. Immunol.* 2021;51:101412.
2. Ndung'u T, McCune JM, Deeks SG. Why and where an HIV cure is needed and how it might be achieved.. *Nature* 2019;576(7787):397–405.
3. Bailon L, Mothe B, Berman L, Brander C. Novel Approaches Towards a Functional Cure of HIV/AIDS. *Drugs* 2020;80(9):859–868.
4. Kim Y, Anderson JL, Lewin SR. Getting the “Kill” into “Shock and Kill”: Strategies to Eliminate Latent HIV. *Cell Host Microbe* 2018;23(1):14–26.
5. Delagrèverie HM, Delaugerre C, Lewin SR, Deeks SG, Li JZ. Ongoing Clinical Trials of Human Immunodeficiency Virus Latency-Reversing and Immunomodulatory Agents. *Open Forum Infect. Dis.* 2016;3(4). doi:10.1093/ofid/ofw189
6. Søgaard OS et al. The Depsipeptide Romidepsin Reverses HIV-1 Latency In Vivo. *PLOS Pathog.* 2015;11(9):e1005142.
7. Elliott JH et al. Activation of HIV Transcription with Short-Course Vorinostat in HIV-Infected Patients on Suppressive Antiretroviral Therapy. *PLoS Pathog.* 2014;10(11):e1004473.
8. Shan L et al. Stimulation of HIV-1-Specific Cytolytic T Lymphocytes Facilitates Elimination of Latent Viral Reservoir after Virus Reactivation. *Immunity* 2012;36(3):491–501.
9. Ruiz A et al. Antigen Production After Latency Reversal and Expression of Inhibitory Receptors in CD8 T Cells Limit the Killing of HIV-1 Reactivated Cells. *Front. Immunol.* 2019;9(JAN):3162.
10. Sereti I et al. Persistent, Albeit reduced, chronic inflammation in persons starting antiretroviral therapy in acute HIV infection. *Clin. Infect. Dis.* 2017;64(2):124–131.
11. Sáez-Cirión A et al. Post-Treatment HIV-1 Controllers with a Long-Term Virological Remission after the Interruption of Early Initiated Antiretroviral Therapy ANRS VISCONTI Study. *PLoS Pathog.* 2013;9(3). doi:10.1371/journal.ppat.1003211
12. Fidler S et al. Antiretroviral therapy alone versus antiretroviral therapy with a kick and kill approach, on measures of the HIV reservoir in participants with recent HIV

- infection (the RIVER trial): a phase 2, randomised trial. *Lancet* 2020;395(10227):888–898.
13. Mothe B et al. HIVconsV Vaccines and Romidepsin in Early-Treated HIV-1-Infected Individuals: Safety, Immunogenicity and Effect on the Viral Reservoir (Study BCN02). *Front. Immunol.* 2020;11(10):823.
 14. Létourneau S et al. Design and pre-clinical evaluation of a universal HIV-1 vaccine.. *PLoS One* 2007;2(10):e984.
 15. Mothe B et al. Therapeutic Vaccination Refocuses T-cell Responses Towards Conserved Regions of HIV-1 in Early Treated Individuals (BCN 01 study). *EClinicalMedicine* 2019;11:65–80.
 16. Oriol-Tordera B et al. Methylation regulation of Antiviral host factors, Interferon Stimulated Genes (ISGs) and T-cell responses associated with natural HIV control. *PLOS Pathog.* 2020;16(8):e1008678.
 17. Moron-Lopez S et al. The Genome-wide Methylation Profile of CD4 T Cells From Individuals With Human Immunodeficiency Virus (HIV) Identifies Distinct Patterns Associated With Disease Progression. *Clin. Infect. Dis.* [published online ahead of print: July 26, 2020]; doi:10.1093/cid/ciaa1047
 18. Stelzer G et al. The GeneCards suite: From gene data mining to disease genome sequence analyses. *Curr. Protoc. Bioinforma.* 2016;2016(1):1.30.1-1.30.33.
 19. GeneCards – the human gene database. www.genecards.org 2017;https://www.genecards.org/. cited May 17, 2021
 20. Anand AR, Tirumuru Nagaraja, Ganju RK. A novel role for Slit2/Robo1 axis in modulating HIV-1 replication in T cells. *AIDS* 2011;25(17):2105–2111.
 21. Jäger S et al. Global landscape of HIV-human protein complexes.. *Nature* 2011;481(7381):365–70.
 22. Luo Y et al. HIV-host interactome revealed directly from infected cells.. *Nat. Microbiol.* 2016;1(7):16068. J
 23. Jarboui MA et al. Nucleolar protein trafficking in response to HIV-1 Tat: rewiring the nucleolus.. *PLoS One* 2012;7(11):e48702.

24. Cirovic B et al. BCG Vaccination in Humans Elicits Trained Immunity via the Hematopoietic Progenitor Compartment. *Cell Host Microbe* 2020;28(2):322-334.e5.
25. Lai AY et al. Dna methylation profiling in human b cells reveals immune regulatory elements and epigenetic plasticity at alu elements during b-cell activation. *Genome Res.* 2013;23(12):2030–2041.
26. Dogra P, Ghoneim HE, Abdelsamed HA, Youngblood B. Generating long-lived CD8 T-cell memory: Insights from epigenetic programs. *Eur. J. Immunol.* 2016;46(7):1548–1562.
27. Bannister S, Messina NL, Novakovic B, Curtis N. The emerging role of epigenetics in the immune response to vaccination and infection: a systematic review. *Epigenetics* 2020;15(6–7):555–593.
28. Zimmermann MT et al. System-wide associations between DNA-methylation, gene expression, and humoral immune response to influenza vaccination. *PLoS One* 2016;11(3):e0152034.
29. Sui Y, Berzofsky JA. Myeloid Cell-Mediated Trained Innate Immunity in Mucosal AIDS Vaccine Development. *Front. Immunol.* 2020;11:315.
30. Palgen JL et al. Optimize Prime/Boost Vaccine Strategies: Trained Immunity as a New Player in the Game. *Front. Immunol.* 2021;12:612747.
31. Sanchez J et al. Immune Profiles Identification by Vaccinomics After MVA Immunization in Randomized Clinical Study.. *Front. Immunol.* 2020;11:586124.
32. Gallego-Paüls M et al. Variability of multi-omics profiles in a population-based child cohort. *BMC Med.* 2021 191 2021;19(1):1–16.
33. Hofmeister BT, Lee K, Rohr NA, Hall DW, Schmitz RJ. Stable inheritance of DNA methylation allows creation of epigenotype maps and the study of epiallele inheritance patterns in the absence of genetic variation.. *Genome Biol.* 2017;18(1):155.
34. Moron-Lopez S et al. Characterization of the HIV-1 transcription profile after romidepsin administration in ART-suppressed individuals. *AIDS* 2019;33(3):425–431.

35. Chen HC, Martinez JP, Zorita E, Meyerhans A, Filion GJ. Position effects influence HIV latency reversal. *Nat. Struct. Mol. Biol.* 2017;24(1):47–54.
36. Grau-Expósito J et al. Latency reversal agents affect differently the latent reservoir present in distinct CD4 T subpopulations. *PLoS Pathog.* 2019;15(8):e1007991.
37. Ruiz A et al. Antigen production after latency reversal and expression of inhibitory receptors in CD8 T cells limit the killing of HIV-1 reactivated cells. *Front. Immunol.* 2019;10(JAN):3162.
38. Rosás-Umbert M et al. In vivo Effects of Romidepsin on T-Cell Activation, Apoptosis and Function in the BCN02 HIV-1 Kick&Kill Clinical Trial. *Front. Immunol.* 2020;11:418.
39. Ruiz-Riol M, Brander C. Can we just kick-and-kill HIV: possible challenges posed by the epigenetically controlled interplay between HIV and host immunity. *Immunotherapy* 2019;11(11):931–935.
40. Qu K et al. Chromatin Accessibility Landscape of Cutaneous T Cell Lymphoma and Dynamic Response to HDAC Inhibitors. *Cancer Cell* 2017;32(1):27-41.e4.
41. Jiang C et al. Distinct viral reservoirs in individuals with spontaneous control of HIV-1. *Nature* 2020;585(7824):261–267.
42. Dobin A et al. STAR: Ultrafast universal RNA-seq aligner. *Bioinformatics* 2013;29(1):15–21.
43. Li B, Dewey CN. RSEM: Accurate transcript quantification from RNA-Seq data with or without a reference genome. *BMC Bioinformatics* 2011;12(1):1–16.
44. Robinson MD, McCarthy DJ, Smyth GK. edgeR: A Bioconductor package for differential expression analysis of digital gene expression data. *Bioinformatics* 2009;26(1):139–140.
45. Ritchie ME et al. limma powers differential expression analyses for RNA-sequencing and microarray studies. *Nucleic Acids Res.* 2015;43(7):e47.
46. Aryee MJ et al. Minfi: a flexible and comprehensive Bioconductor package for the analysis of Infinium DNA methylation microarrays. *Bioinformatics* 2014;30(10):1363–1369.

47. Fortin JP, Triche TJ, Hansen KD. Preprocessing, normalization and integration of the Illumina HumanMethylationEPIC array with minfi. *Bioinformatics* 2017;33(4):558–560.
48. Morris TJ et al. ChAMP: 450k Chip Analysis Methylation Pipeline. *Bioinformatics* 2014;30(3):428–430.
49. T. Leek, Jeffrey Johnson, W. Evan Parker, Hilary S. Fertig, Elana J. E. Jaffe, Andrew Storey, John D. Zhang, Yuqing Collado Torres L. sva: Surrogate Variable Analysis 2019; <https://bioconductor.org/packages/release/bioc/html/sva.html>. cited May 17, 2021
50. Kumar L, Futschik ME. Mfuzz: A software package for soft clustering of microarray data. *Bioinformatics* 2007;2(1). doi:10.6026/97320630002005
51. Reimand J et al. Pathway enrichment analysis and visualization of omics data using g:Profiler, GSEA, Cytoscape and EnrichmentMap. *Nat. Protoc.* 2019;14(2):482–517.
52. Merico D, Isserlin R, Stueker O, Emili A, Bader GD. Enrichment map: A network-based method for gene-set enrichment visualization and interpretation. *PLoS One* 2010;5(11). doi:10.1371/journal.pone.0013984
53. Li S et al. Molecular signatures of antibody responses derived from a systems biology study of five human vaccines. *Nat. Immunol.* 2014;15(2):195–204.
54. Kucera M, Isserlin R, Arkhangorodsky A, Bader GD. AutoAnnotate: A Cytoscape app for summarizing networks with semantic annotations [version 1; referees: 2 approved]. *F1000Research* 2016;5. doi:10.12688/F1000RESEARCH.9090.1
55. Sheffield NC, Bock C. LOLA: Enrichment analysis for genomic region sets and regulatory elements in R and Bioconductor. *Bioinformatics* 2016;32(4):587–589.
56. S H et al. Simple combinations of lineage-determining transcription factors prime cis-regulatory elements required for macrophage and B cell identities. *Mol. Cell* 2010;38(4):576–589.
57. Gu Z, Eils R, Schlesner M. Complex heatmaps reveal patterns and correlations in multidimensional genomic data. *Bioinformatics* 2016;32(18):2847–2849.

Supplementary Methods

The IFN γ ELISpot Assay

Thawed cryopreserved PBMC from individuals samples at different time points were cultured in duplicated in 96-well ELISpot plates (MultiScreen HTS MSIPS4W10, Millipore) and stimulated them with pools of 15-mer peptides overlapping peptides covering the HIVconsv immunogen or the regions outside the immunogen as described elsewhere (13). The negative and positive controls, as well as the calculation of the breadth and the magnitude are described elsewhere (13).

Viral parameters assessments

Peripheral blood proviral reservoir (CA-HIV-1 DNA) was measured by ddPCR in isolated CD4 T cells. The RPP30 housekeeping gene was used for normalization. Cell-associated HIV-1 RNA (CA-HIV-1 RNA) was assessed using two different sets of primers/probe annealing to 5'LTR and Gag. Gene expression of TBP housekeeping gene before RMD administration was used for normalization. Single Copy Assay (SCA) was used to determine the HIV-1 RNA plasma levels < 20 copies/ml. For SCA, plasma samples from participants obtain at indicated time points were ultra-centrifugated (170,000xg, 4°C, 30 minutes) prior to RNA viral extraction (m2000sp Abbot device). Abbott Real-Time HIV-1 assay was used to determine HIV-1 RNA copies.

Histone H3 Acetylation (H3Ac)

Cryopreserved PBMCs were used to evaluate the H3Ac in lymphocytes by flow cytometry as described elsewhere (13). Briefly, after a 20-minutes blocking with PBS 10% FBS, cells were stained for 30 minutes with anti-acetyl histone H3 polyclonal rabbit (MerckMillipore 06–599) or with the control stain normal rabbit serum (LifeTechnologies 10510). After washing, a 30 minutes incubation with the secondary antibody in the dark was performed (donkey anti-rabbit IgG, LifeTechnologies A21206). The median fluorescence intensity (MFI) for acetyl histone H3 stain was determined and the background was subtracted using the MFI of the isotype control staining.

Supplementary Figures

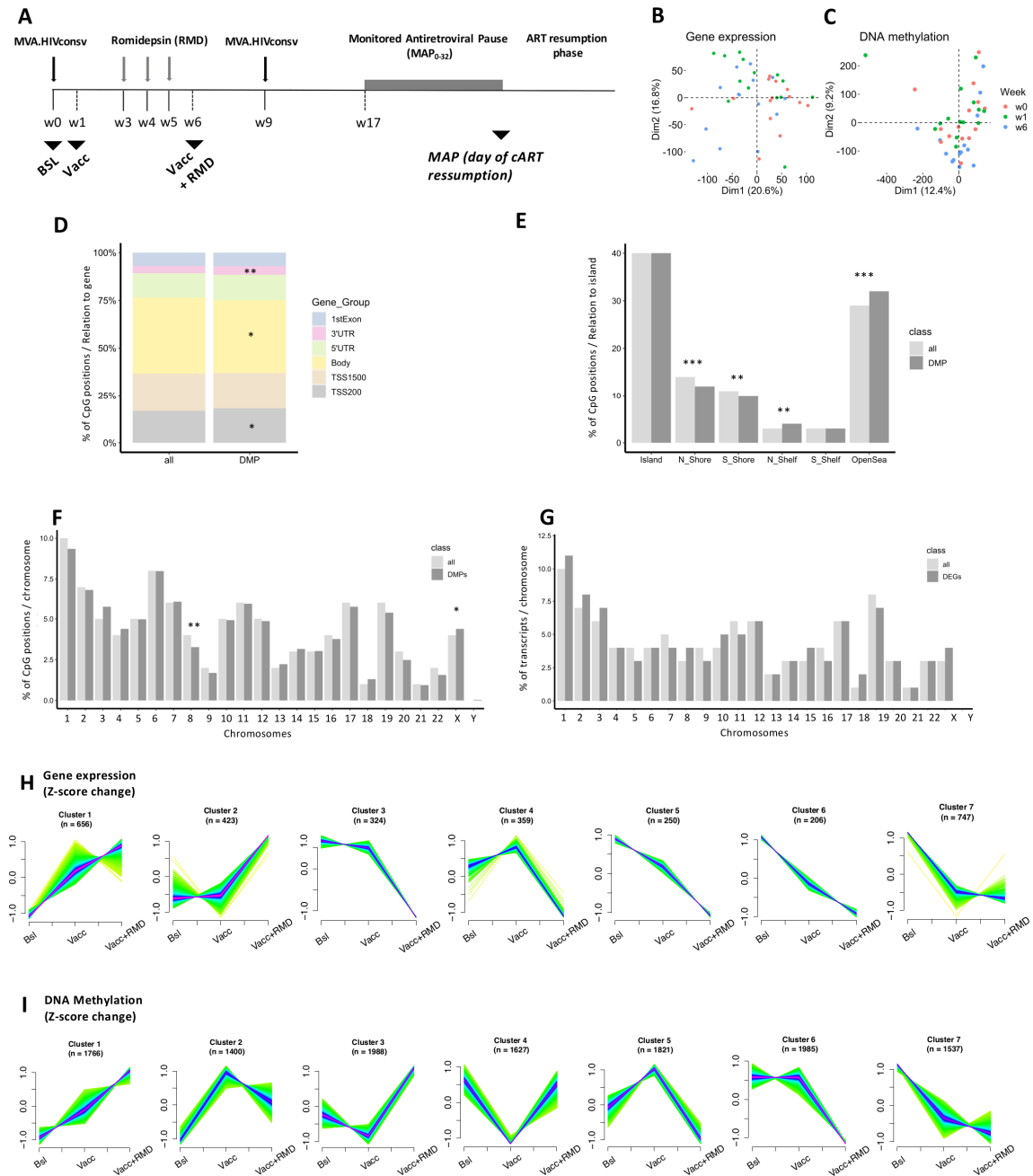


Figure S1. Longitudinal gene expression and DNA methylation and impact of vaccination A) Scheme of the BCN02 clinical trial. B) and C) show the PCA according normalized gene expression and DNA methylation (colors according to time point). D) Percentage of CpGs according to relation to Gene in DMPs (Vacc-BSL) and in 450K array (All). E) Percentage of CpGs according to relation to Island in DMPs (Vacc-BSL) and in 450K array (All). F) show the proportion of genes in each chromosome in DMPs (Vacc-BSL) and in 450K array. G) Percentage of genes in each chromosome in DEGs (Vacc-BSL) and all the genes that passed the QC. * indicates p-value < 0.05, ** p-value < 0.01 and *** p-value < 0.001. H) and I) show the longitudinal gene expression and DNA methylation cluster profiles during the clinical trial based on standardized data. The scale goes from green to dark blue and to pink according to the membership of each gene, depending on how well a gene fits the profile.

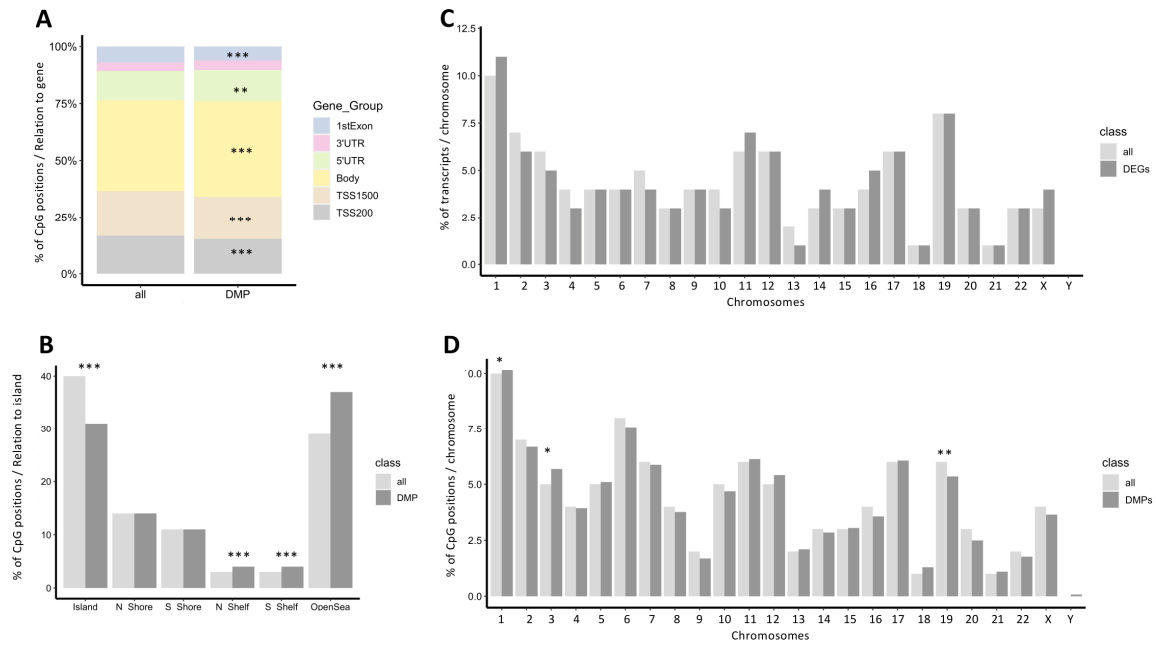


Figure S2. DMPs and DEGs between the Vacc+RMD and the baseline time point. A) Proportion of CpGs according to relation to Gene in DMPs and in 450K array (All). B) Percentage of CpGs according to relation to Island in DMPs and in 450K array (All). C) and D) proportions of genes in each chromosome in DMPs and 450K array (All) and DEGs and all the genes that passed the QC (All), respectively. * indicates p-value < 0.05, ** p-value < 0.01 and *** p-value < 0.001.

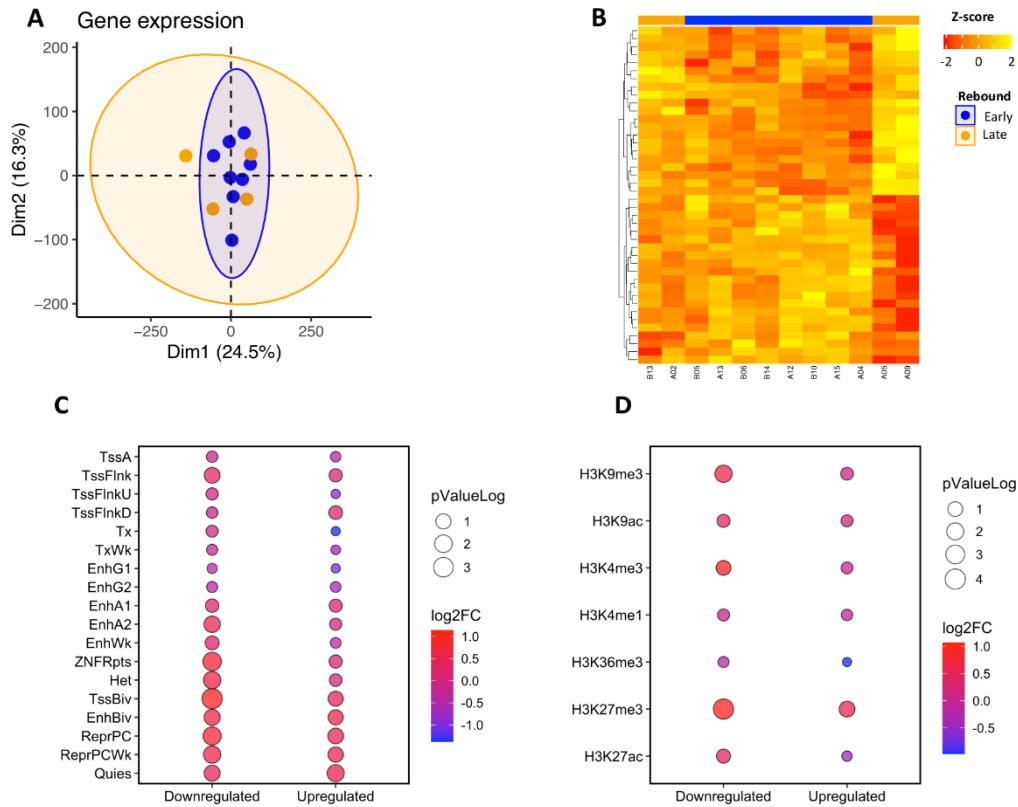


Figure S4. DEGs between Early and Late individuals at the Vacc+RMD time point. A) PCAs for gene expression at time point Vacc+RMD colored according Early (Blue) or Late rebound (Orange). B) Heatmap of DEGs (p -value < 0.01 , $n = 42$) between Early (Blue) and Late (Orange) rebounders at Vacc+RMD timepoint. Gene expression is represented as Z-score. C) ChromHMM enrichment based on DEGs and D), histone mark enrichment. Downregulated and Upregulated are respective to Early rebounders in comparison to Late rebounders. Dot color indicates \log_2 Fold-change and the dots size, the $-\log_{10}$ p -value.

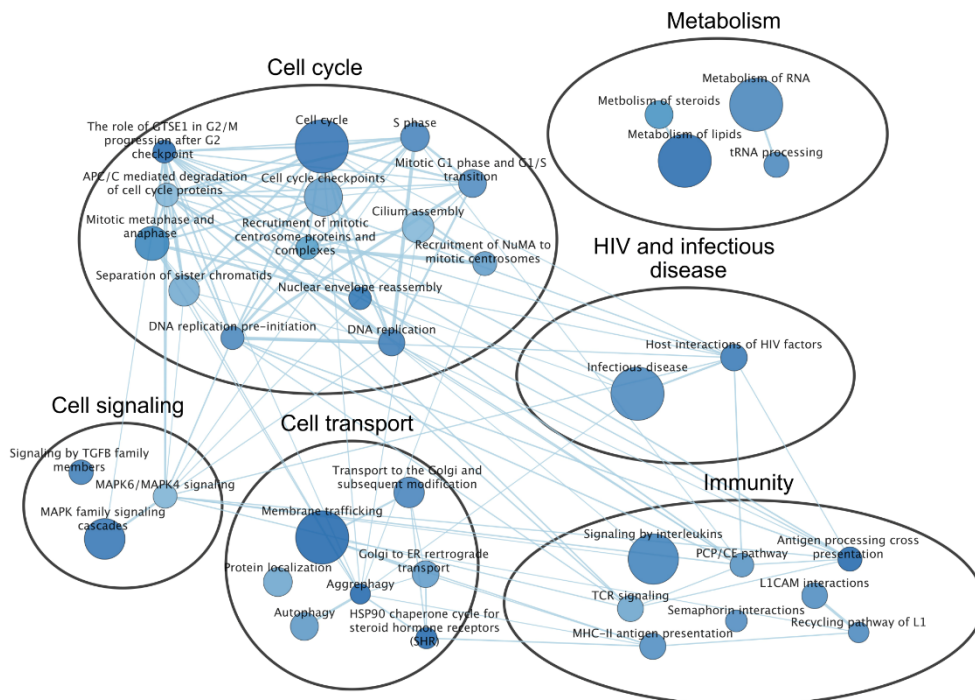


Figure S5. GSEA DMPs between Early and Late rebound. Pathways and BTMs enriched according to DMPs between and Early and Late rebound at time points Vacc+RMD. All the pathways have a negative NES and an adjusted p -value < 0.2 , indicating that the majority of the genes in the pathways were hypermethylated in individuals with a Late rebound. The pathways are clustered in different groups based on function. Node color is not associated with any feature.

Supplementary Tables

Table S1: Clinical information participants BCN02

Table S1: Clinical and viral information of participants in BCN02 clinical trial
 1. B07 and B03 are only included in longitudinal analysis (BSL, Vacc and Vacc+RMD)
 2. Results are from 3 weeks post RMD infusion

ID	Sex	Age	Rebound	Inclusion in sub-omics analysis 1	cART initiation		BCN02 Entry			MAP			Weeks since last Vax to MAP
					Days since HIV to cART initiation	pVL at cART initiation (copies/ml) Log10	Time on cART BCN02 Entry	CD4 counts BCN02 Entry	CD4 counts MAP	CD4/CD8 MAP	Total time on cART MAP	Time on UD pVL MAP	
A02	Male	40	Late	Y	106	2.03	3.77	645.00	533	1.64	4.25	4.16	9.71
A04	Male	39	Early	Y	65	1.81	3.35	728.00	735	1.75	3.90	3.15	17.29
A05	Male	30	Late	Y	164	2.21	3.53	657.00	496	0.76	3.90	3.85	8.57
A09	Male	40	Late	Y	28	1.45	3.47	971.00	854	1.52	3.98	3.54	15.57
A12	Male	42	Early	Y	67	1.83	3.16	1383.00	1075	1.30	3.67	3.46	13.29
A13	Male	45	Early	Y	100	2.00	3.07	476.00	480	1.11	3.76	3.68	24.86
A14	Female	33	NA	N	118	2.07	3.03	1331.00	1269	1.52	3.71	3.64	23.43
A15	Male	37	Early	Y	82	1.91	3.13	1408.00	1230	0.87	3.49	3.22	8.14
B03	Male	41	NA	Y*	52	1.72	3.19	885.00	741	1.56	3.60	3.36	8.14
B05	Male	46	Early	Y	107	2.03	3.24	728.00	484	1.29	3.86	3.61	19.29
B06	Male	48	Early	Y	32	1.51	3.24	416.00	468	1.38	3.64	3.41	8.14
B07	Male	36	NA	Y*	92	1.96	3.24	1182.00	840	1.75	NA	NA	NA
B10	Male	44	Early	Y	73	1.86	3.42	950.00	882	1.48	3.86	3.41	8.14
B13	Male	32	Late	Y	112	2.05	3.08	648.00	950	1.61	3.58	3.50	11.86
B14	Male	38	Early	Y	116	2.06	3.42	533.00	560	1.25	3.85	3.80	10.71

ID	Magnitude HIVconsV			Breadth HIVconsV			Magnitude HIVtotal			Breadth HIVtotal		
	BSL	Vacc	post-Vacc+RMD 2	BSL	Vacc	post-Vacc+RMD 2	BSL	Vacc	post-Vacc+RMD 2	BSL	Vacc	post-Vacc+RMD 2
A02	1650	1680	880	5	6	5	2175	1890	880	3	3	2
A04	2260	2970	1475	3	3	3	4655	8355	2825	1	1	1
A05	0	665	685	0	4	4	0	1195	1175	0	0	0
A09	55	1165	330	1	6	5	285	2030	875	0	2	0
A12	0	170	205	0	2	1	240	525	550	1	1	2
A13	280	1060	6901	3	4	6	280	1120	7152	0	0	1
A14	1979	870	1120	4	5	3	4037	1865	1810	0	4	1
A15	405	1200	3210	2	5	3	545	1415	3515	0	0	1
B03	330	400	260	1	2	2	550	525	330	2	2	1
B05	100	310	1797	1	2	4	680	940	2502	1	2	2
B06	0	455	450	0	3	4	0	455	580	0	2	1
B07	55	575	375	1	5	0	55	575	375	1	1	0
B10	0	215	670	0	3	2	425	1025	1900	0	1	1
B13	445	1525	1110	1	3	5	445	1525	1110	1	1	1
B14	510	470	930	4	3	5	710	640	1080	0	0	0

ID	Proviral			SCA			CA-RNA			H3Ac
	BSL	Vacc	Vacc+RMD	BSL	Vacc	Vacc+RMD	BSL	Vacc	Vacc+RMD	Vacc+RMD
A02	169.06	278.82	128.37	1.11	1.11	0.91	2.36	2.36	1.43	14206
A04	107.10	157.10	131.43	22.56	1.16	5.97	0.91	NA	2.63	9131
A05	64.63	46.01	42.52	1.11	1.25	1.00	UD	UD	UD	111
A09	167.54	154.46	327.57	1.11	1.16	12.36	1.63	2.36	0.35	598
A12	139.91	110.16	104.80	20.75	4.44	4.18	0.32	0.37	0.38	17899
A13	751.59	795.92	655.74	1.19	1.67	1.00	9.38	8.08	10.77	4856
A14	465.86	892.31	464.42	1.19	1.04	0.91	4.62	5.53	7.50	17442
A15	17.56	38.52	60.12	NA	NA	10.00	0.49	0.22	0.58	7857
B03	110.53	97.25	152.38	1.19	13.33	15.09	1.42	1.01	1.50	16750
B05	361.11	494.02	535.56	4.22	1.11	0.94	5.99	3.49	12.91	1211
B06	66.10	25.97	96.20	5.75	4.29	6.04	0.07	0.05	0.04	13478
B07	17.39	84.34	24.84	1.11	1.11	5.82	0.08	0.17	0.16	12143
B10	190.48	127.36	105.40	2.20	1.14	17.40	1.52	0.84	2.27	11427
B13	60.15	23.17	30.48	NA	NA	1.19	UD	UD	UD	12434
B14	434.34	313.04	395.79	1.25	1.00	1.82	2.08	2.67	3.69	5543

Table S2: Clinical information of participants in REDUC clinical trial

Table S2: Clinical information of participants in REDUC clinical trial

ID	Sex	Age	CD4 counts
1101	Male		49 760
1102	Male		53 760
1105	Male		60 510
1106	Male		59 530
1107	Male		69 510

Table S3. Top100 DEGs Vacc - Baseline

	Mean_w0	Mean_w1	diffMean	Median_w0	Median_w1	diffMedian	logFC	AveExpr	t	P.Value	adjP.Val	B
ENSG00000211897.9.IGHG3.IG_C_gene	3.802	6.453	2.651	3.793	6.278	2.486	2.651	4.527	5.594	5.71E-07	3.96E-03	5.741
ENSG00000211896.7.IGHG1.IG_C_gene	6.002	8.937	2.935	6.115	9.039	2.924	2.935	6.811	5.550	6.76E-07	3.96E-03	5.592
ENSG00000209931.14.MOXD1.protein_coding	-1.483	-0.047	1.436	-1.446	-0.030	1.416	1.436	-1.111	5.536	7.12E-07	3.96E-03	5.547
ENSG00000088340.15.FER1L4.transcribed_unitary_pseudogene	-2.148	-0.465	1.682	-2.192	-0.671	1.522	1.682	-1.169	5.346	1.45E-06	5.22E-03	4.920
ENSG00000211950.2.IGHV1-24.IG_V_gene	-0.810	1.992	2.802	-0.920	1.717	2.637	2.802	0.013	5.287	1.81E-06	5.22E-03	4.728
ENSG00000115884.10.SDC1.protein_coding	-2.363	0.360	2.722	-2.258	0.594	2.852	2.722	-1.636	5.278	1.88E-06	5.22E-03	4.696
ENSG00000211956.2.IGHV4-34.IG_V_gene	2.011	3.755	1.744	2.044	3.869	1.825	1.744	2.232	5.164	2.87E-06	6.84E-03	4.324
ENSG00000254709.7.IGLL5.protein_coding	2.921	4.513	1.592	2.781	4.596	1.815	1.592	3.296	5.045	4.45E-06	9.28E-03	3.939
ENSG00000239264.8.TXNDC5.protein_coding	6.308	7.772	1.465	6.331	7.816	1.485	1.465	6.655	4.978	5.69E-06	9.55E-03	3.722
ENSG00000259772.6.RP11-16E12.2.lincRNA	-2.725	-0.811	1.913	-2.624	-1.088	1.536	1.913	-2.029	4.948	6.33E-06	9.55E-03	3.628
ENSG00000242534.2.IKIV2D-28.IG_V_gene	-3.042	0.496	3.539	-2.679	0.403	3.082	3.539	-1.863	4.932	6.72E-06	9.55E-03	3.576
ENSG000002050274.1.CTB-114C7.4.lincRNA	-0.652	2.375	1.723	-0.740	1.978	1.238	-1.723	-1.249	4.926	6.86E-06	9.55E-03	3.557
ENSG00000170476.15.MZB1.protein_coding	3.287	4.746	1.459	3.247	4.796	1.550	1.459	3.668	4.794	1.11E-05	1.42E-02	3.138
ENSG00000105974.11.CAV1.protein_coding	-1.938	0.107	2.046	-2.042	0.206	2.248	2.046	-1.413	4.768	1.22E-05	1.45E-02	3.055
ENSG00000244116.3.IKIV2-28.IG_V_gene	2.566	4.603	2.037	2.547	4.752	2.205	2.037	2.939	4.745	1.32E-05	1.47E-02	2.983
ENSG00000182853.11.VMO1.protein_coding	-0.391	-1.982	1.591	-0.483	-1.986	1.503	-1.591	-0.693	4.676	1.69E-05	1.71E-02	2.765
ENSG00000211967.3.IGHV3-53.IG_V_gene	0.425	2.432	2.007	0.355	2.557	2.202	2.007	0.895	4.668	1.74E-05	1.71E-02	2.739
ENSG00000211938.2.IGHV3-7.IG_V_gene	2.831	4.369	1.538	2.872	4.355	1.483	1.538	3.136	4.630	2.00E-05	1.85E-02	2.620
ENSG00000211675.2.IGLT1.IG_C_gene	4.060	5.781	1.721	4.121	5.867	1.745	1.721	4.392	4.529	2.86E-05	2.39E-02	2.306
ENSG00000211976.2.IGHV3-73.IG_V_gene	-0.436	1.770	2.206	-0.669	1.934	2.603	2.206	-0.012	4.525	2.90E-05	2.39E-02	2.293
ENSG00000211639.2.IGLV4-60.IG_V_gene	-2.712	-0.225	2.487	-2.494	-0.151	2.343	2.487	-1.851	4.505	3.10E-05	2.39E-02	2.233
ENSG00000243466.1.IKIV1-5.IG_V_gene	3.548	5.213	1.665	3.656	5.333	1.676	1.665	3.845	4.501	3.15E-05	2.39E-02	2.221
ENSG00000211933.2.IGHV6-1.IG_V_gene	0.115	1.941	1.826	-0.081	2.019	2.101	1.826	0.570	4.478	3.42E-05	2.48E-02	2.149
ENSG00000170456.15.DENND5B.protein_coding	3.171	3.916	0.745	3.192	4.054	0.864	0.745	3.381	4.388	4.67E-05	3.23E-02	1.874
ENSG00000136010.13.ALDH12.protein_coding	-1.129	-0.053	1.182	-1.038	-0.076	0.962	1.182	-0.693	4.379	4.83E-05	3.23E-02	1.845
ENSG00000211955.2.IGHV3-33.IG_V_gene	2.505	4.074	1.569	2.472	4.093	1.621	1.569	2.925	4.365	5.06E-05	3.25E-02	1.805
ENSG00000178445.9.GLDC.protein_coding	-0.303	1.872	2.175	-0.279	2.028	2.306	2.175	0.359	4.326	5.79E-05	3.57E-02	1.687
ENSG00000211949.3.IGHV3-23.IG_V_gene	3.882	5.270	1.388	4.028	5.314	1.286	1.388	4.232	4.311	6.11E-05	3.57E-02	1.640
ENSG00000248571.1.RP11-768B22.2.antisense	-2.992	-0.733	2.260	-2.680	-0.488	2.192	2.260	-3.227	4.307	6.20E-05	3.57E-02	1.627
ENSG00000129757.13.CDKN1C.protein_coding	3.376	2.371	1.005	3.116	2.181	0.935	-1.005	3.355	-4.284	6.70E-05	3.73E-02	1.558
ENSG00000180535.3.BHHA15.protein_coding	-2.539	-0.432	2.107	-2.726	-0.272	2.455	2.107	-1.944	4.271	7.00E-05	3.77E-02	1.520
ENSG00000244575.3.IKIV1-27.IG_V_gene	0.841	2.333	1.491	0.672	2.290	1.618	1.491	1.228	4.259	7.31E-05	3.81E-02	1.483
ENSG00000142675.17.CNRSR1.protein_coding	0.207	0.888	0.681	0.189	0.950	0.762	0.681	0.454	4.247	7.61E-05	3.85E-02	1.448
ENSG00000128891.15.C1orf57.protein_coding	4.265	4.595	0.330	4.244	4.458	0.214	0.330	4.470	4.231	8.04E-05	3.95E-02	1.400
ENSG00000243290.3.IKIV1-12.IG_V_gene	1.378	3.318	1.940	1.543	3.310	1.767	1.940	1.885	4.222	8.30E-05	3.96E-02	1.371
ENSG00000211653.2.IGLV1-40.IG_V_gene	1.964	3.666	1.702	1.754	3.763	2.009	1.702	2.282	4.205	8.80E-05	4.08E-02	1.321
ENSG00000253755.1.IGHG16.C_pseudogene	-1.648	0.372	2.020	-1.080	0.514	1.593	2.020	-1.123	4.182	9.50E-05	4.29E-02	1.254
ENSG00000243288.1.IKIV2-30.IG_V_gene	1.550	3.117	1.567	1.684	3.225	1.541	1.567	2.002	4.146	1.07E-04	4.57E-02	1.146
ENSG00000110777.11.POU2AF1.protein_coding	3.266	4.104	0.838	3.208	4.083	0.875	0.838	3.568	4.143	1.09E-04	4.57E-02	1.136
ENSG00000211947.2.IGHV3-21.IG_V_gene	2.228	3.659	1.435	2.208	3.621	1.412	1.435	2.504	4.138	1.10E-04	4.57E-02	1.122
ENSG00000090889.11.KIF4A.protein_coding	-0.038	0.945	0.983	-0.108	0.999	1.107	0.983	0.379	4.124	1.16E-04	4.57E-02	1.081
ENSG00000211970.3.IGHV4-61.IG_V_gene	1.563	3.181	1.618	1.491	3.285	1.794	1.618	1.954	4.123	1.16E-04	4.57E-02	1.077
ENSG00000211644.3.IGLV1-51.IG_V_gene	2.340	3.656	1.317	2.641	3.670	1.029	1.317	2.561	4.113	1.20E-04	4.57E-02	1.047
ENSG00000051341.13.POLO.protein_coding	1.366	2.071	0.705	1.431	1.998	0.567	0.705	1.731	4.112	1.21E-04	4.57E-02	1.045
ENSG00000211652.2.IGLV7-43.IG_V_gene	0.155	1.697	1.542	0.175	1.718	1.443	1.542	0.408	4.104	1.24E-04	4.57E-02	1.022
ENSG00000211962.2.IGHV1-46.IG_V_gene	0.283	1.895	1.612	0.324	2.043	1.718	1.612	0.830	4.097	1.27E-04	4.57E-02	1.001
ENSG00000169224.12.GCSAML.protein_coding	2.848	1.458	0.890	2.333	1.338	0.995	-0.890	1.688	-4.093	1.29E-04	4.57E-02	0.988
ENSG00000197705.9.KLHL14.protein_coding	1.824	2.770	0.946	1.965	2.853	0.888	0.946	2.067	4.086	1.31E-04	4.57E-02	0.970
ENSG00000221437.3.IGHV4-59.IG_V_gene	2.340	3.866	1.525	2.586	3.795	1.209	1.525	2.703	4.075	1.36E-04	4.65E-02	0.937
ENSG00000244479.7.RNA-798C1.7.antisense	0.332	1.210	0.878	0.407	1.103	0.696	0.878	0.914	4.043	1.52E-04	4.91E-02	0.844
ENSG00000123525.17.SPATS2.protein_coding	1.559	3.174	0.416	1.704	3.159	0.454	0.416	2.926	4.040	1.54E-04	4.91E-02	0.834
ENSG00000144395.17.GCCD150.protein_coding	-0.803	-0.180	0.623	-0.667	-0.196	0.471	0.623	-0.433	4.036	1.56E-04	4.91E-02	0.823
ENSG00000211677.2.IGLC2.IG_C_gene	5.765	7.237	1.471	5.859	7.417	1.558	1.471	6.042	4.035	1.56E-04	4.91E-02	0.820
ENSG00000048462.10.TNFRSF17.protein_coding	0.671	2.507	1.836	0.580	2.513	1.933	1.836	1.024	4.020	1.64E-04	5.08E-02	0.775
ENSG00000100162.14.CENPM.protein_coding	0.360	1.047	0.688	0.205	1.065	0.860	0.688	0.619	4.010	1.70E-04	5.16E-02	0.745
ENSG00000211592.8.IKIV1-6.IG_V_gene	7.527	8.977	1.450	7.636	8.963	1.327	1.450	5.717	4.003	1.74E-04	5.17E-02	0.727
ENSG00000239855.1.IKIV1-6.IG_V_gene	-0.201	1.445	1.647	-0.344	1.223	1.567	1.647	0.307	3.991	1.81E-04	5.18E-02	0.690
ENSG00000240505.8.TNFRSF13B.protein_coding	0.504	1.388	0.884	0.385	1.452	1.067	0.884	0.859	3.990	1.81E-04	5.18E-02	0.689
ENSG00000163053.10.SLC16A14.protein_coding	-1.754	-0.727	1.027	-1.777	-0.791	0.985	1.027	-1.302	3.988	1.83E-04	5.18E-02	0.681
ENSG00000129173.12.EZFB.protein_coding	-1.129	0.148	1.277	-0.997	0.242	1.239	1.277	-0.606	3.968	1.95E-04	5.43E-02	0.625
ENSG00000123485.11.HURP.protein_coding	-0.198	0.901	1.099	-0.313	0.797	1.110	1.099	0.318	3.953	2.05E-04	5.61E-02	0.582
ENSG00000221437.3.IGHV4-59.IG_V_gene	1.992	3.329	1.338	1.955	3.204	1.249	1.338	2.301	3.945	2.11E-04	5.68E-02	0.558
ENSG00000211937.3.IGHV2-5.IG_V_gene	1.278	3.037	1.759	1.298	3.110	1.712	1.759	1.651	3.921	2.26E-04	6.03E-02	0.490
ENSG00000211941.3.IGHV3-11.IG_V_gene	1.095	2.729	1.635	1.332	2.907	1.575	1.635	1.506	3.915	2.33E-04	6.03E-02	0.470
ENSG00000135916.15.ITM2C.protein_coding	4.754	5.419	0.665	4.769	5.444	0.676	0.665	4.903	3.912	3.35E-04	6.03E-02	0.464
ENSG00000106341.10.PPP1R17.protein_coding	-0.523	-1.583	1.060	-0.494	-1.743	1.249	-1.060	-0.986	-3.898	2.46E-04	6.23E-02	0.422
ENSG00000251546.1.IKIV10-39.IG_V_gene	3.570	5.300	1.731	3.499	5.361	1.862	1.731	3.979	3.892	2.51E-04	6.25E-02	0.407
ENSG00000211934.3.IGHV1-2.IG_V_gene	1.552	3.352	1.800	1.595	3.617	2.023	1.800	2.011	3.875	2.66E-04	6.52E-02	0.357
ENSG00000275063.1.AC233755.1.protein_coding	-1.493	0.579	2.072	-1.127	0.557	1.684	2.072	-0.192	3.870	2.70E-04	6.54E-02	0.341
ENSG00000211666.2.IGLV2-14.IG_V_gene	3.852	5.170	1.319	3.692	5.186	1.495	1.319	4.142	3.848	2.90E-04	6.91E-02	0.280
ENSG00000254122.2.PCDHGB7.protein_coding	-1.326	-0.366	0.960	-1.076	-0.301	0.803	0.960	-0.800	3.843	2.75E-04	6.93E-02	0.265
ENSG00000211650.2.IGLV5-45.IG_V_gene	-0.449	1.081	1.531	-0.511	0.819	1.329	1.531	-0.208	3.839	2.99E-04	6.93E-02	0.254
ENSG00000211964.3.IGHV3-48.IG_V_gene	1.882	3.283	1.401	1.951	3.276	1.315	1.401	2.233	3.818	3.20E-04	7.32E-02	0.194
ENSG00000211662.2.IGLV3-21.IG_V_gene	2.336	3.912	1.576	1.968	4.104	2.136	1.576	2.682	3.805	3.34E-04	7.54E-02	0.157
ENSG00000280411.1.IGHV1-69.IG_V_gene	0.981	2.751	1.771	0.898	2.941	2.043	1.771	1.548	3.795	3.45E-04	7.62E-02	0.128
ENSG00000211598.2.IKIV4-1.IG_V_gene	3.751	5.088	1.337</									

Table S5. Top 100 DMPs Vacc-Baseline

Table S5: Top100 (p-value) differentially methylated positions between Vacc and BSL

	Mean_w0	Mean_w1	DiffMean	Median_w0	Median_w1	DiffMedian	logFC	AveExpr	t	P.Value	adj.P.Val	B	chr	Relation_to_Island	UCSC_RefGene_Group	Gene
cg14276772	0.127	0.160	0.033	0.124	0.160	0.035	0.389	-2.664	5.492	8.79E-07	9.52E-02	3.55	chr2	Island	TSS200	ODC1
cg02721336	0.053	0.066	0.013	0.053	0.062	0.009	0.343	-4.021	5.337	1.57E-06	9.52E-02	3.17	chr13	Island	5'UTR_TSS200_1stExon	UBAC2
cg12830022	0.711	0.662	-0.049	0.706	0.673	-0.034	-0.327	1.279	-5.009	5.25E-06	1.64E-01	2.36	chrX	S_Shore	TSS1500	TM6HE
cg02200642	0.777	0.808	0.030	0.769	0.806	0.038	0.272	1.945	5.001	5.39E-06	1.64E-01	2.34	chr11	OpenSea	Body	ORSE1P
cg02682457	0.086	0.070	-0.017	0.086	0.068	-0.018	-0.350	-3.557	-4.906	7.62E-06	1.80E-01	2.11	chr6	Island	Body	SYNE1
cg18642425	0.780	0.813	0.033	0.774	0.816	0.043	0.288	1.956	4.863	8.91E-06	1.80E-01	2.00	chr7	OpenSea	Body	DAGLB
cg23456409	0.240	0.198	-0.042	0.246	0.202	-0.045	-0.358	-1.791	-4.752	1.33E-05	2.30E-01	1.73	chr2	N_Shore	TSS1500	TMEM177
cg07927617	0.740	0.777	0.037	0.739	0.777	0.038	0.297	1.664	4.525	2.97E-05	3.63E-01	1.19	chr4	N_Shore	TSS1500	DCAF4L1
cg26166446	0.865	0.838	-0.027	0.861	0.841	-0.021	-0.311	2.541	-4.503	3.21E-05	3.63E-01	1.14	chr4	N_Shelf	Body	NOP14
cg06452544	0.826	0.795	-0.031	0.828	0.801	-0.028	-0.298	2.130	-4.406	4.50E-05	3.63E-01	0.91	chr6	OpenSea	Body	REP51
cg15023057	0.099	0.084	-0.015	0.099	0.083	-0.016	-0.258	-3.285	-4.405	4.50E-05	3.63E-01	0.91	chr6	S_Shore	Body	C6orf136
cg01352294	0.542	0.575	0.034	0.540	0.566	0.026	0.200	0.349	4.397	4.64E-05	3.63E-01	0.89	chr6	S_Shelf	TSS1500	CCDC162
cg20677814	0.803	0.768	-0.035	0.803	0.780	-0.022	-0.291	1.932	-3.488	4.78E-05	3.63E-01	0.87	chr7	OpenSea	Body	ANKMY2
cg12008643	0.880	0.861	-0.019	0.881	0.863	-0.018	-0.245	2.753	-4.325	5.94E-05	4.18E-01	0.72	chr11	OpenSea	Body	RELT
cg23747525	0.051	0.040	-0.011	0.054	0.039	-0.015	-0.368	-4.444	-4.233	8.15E-05	4.18E-01	0.50	chr20	Island	TSS200_TSS1500	LOC388796_SNOR
cg18202167	0.118	0.143	0.025	0.121	0.138	0.017	0.296	-2.826	4.219	8.54E-05	4.18E-01	0.47	chr12	Island	TSS200	OS9
cg07690733	0.046	0.037	-0.009	0.047	0.035	-0.012	-0.320	-4.513	-4.219	8.55E-05	4.18E-01	0.47	chr19	Island	TSS200	HMH41
cg25124605	0.060	0.051	-0.009	0.061	0.050	-0.011	-0.247	-4.070	-4.203	9.01E-05	4.18E-01	0.44	chrX	Island	TSS200	BCORL1
cg05557291	0.810	0.837	0.027	0.818	0.836	0.017	0.266	2.216	4.183	9.66E-05	4.18E-01	0.39	chr12	OpenSea	Body	KDM2B
cg19841859	0.084	0.074	-0.011	0.087	0.072	-0.015	-0.216	-3.580	-4.162	1.04E-04	4.18E-01	0.34	chr14	S_Shore	TSS1500	PRMT5
cg25350065	0.761	0.729	-0.033	0.764	0.736	-0.028	-0.242	1.580	-4.152	1.07E-04	4.18E-01	0.32	chr8	N_Shelf	Body	ZNF251
cg20412250	0.082	0.095	0.013	0.083	0.094	0.011	0.236	-3.411	4.148	1.09E-04	4.18E-01	0.31	chr8	1stExon	SNIP1	
cg21161891	0.276	0.309	0.033	0.276	0.313	0.037	0.229	-1.221	-1.148	1.09E-04	4.18E-01	0.30	chr4	Island	TSS200	KDR
cg13017854	0.800	0.770	-0.030	0.808	0.785	-0.022	-0.248	1.954	-4.138	1.12E-04	4.18E-01	0.29	chr14	N_Shore	Body_TSS1500	SLC25A21_LOC100
cg13304035	0.049	0.040	-0.009	0.047	0.039	-0.007	-0.292	-4.453	-4.133	1.14E-04	4.18E-01	0.27	chrX	Island	TSS200	MAP1D3
cg25647989	0.795	0.748	-0.037	0.787	0.752	-0.034	-0.285	1.683	-4.124	1.18E-04	4.18E-01	0.25	chrX	N_Shelf	Body	BRWD3
cg07477602	0.643	0.674	0.031	0.651	0.667	0.015	0.198	0.923	4.122	1.19E-04	4.18E-01	0.25	chr1	OpenSea	3'UTR	PPAP2B
cg08897844	0.762	0.722	-0.040	0.762	0.734	-0.028	-0.293	1.604	-4.118	1.20E-04	4.18E-01	0.24	chr5	OpenSea	TSS1500	SLC1A3
cg11631265	0.074	0.091	0.017	0.072	0.084	0.012	0.323	-3.518	4.103	1.26E-04	4.25E-01	0.21	chr8	OpenSea	Body	ZC3H3
cg15980802	0.058	0.069	0.011	0.058	0.067	0.009	0.245	-3.918	4.096	1.30E-04	4.25E-01	0.19	chr16	Island	1stExon	TK2
ch.15.1197129R	0.044	0.052	0.007	0.044	0.049	0.006	0.214	-4.311	4.074	1.39E-04	4.42E-01	0.14	chr15	OpenSea	Body	ARID3B
cg15798530	0.842	0.864	0.022	0.841	0.861	0.020	0.265	2.522	4.069	1.42E-04	4.42E-01	0.13	chr4	S_Shore	Body_TSS1500	TRPC3
cg13468174	0.072	0.056	-0.016	0.071	0.057	-0.014	-0.358	-3.977	-4.026	1.64E-04	4.50E-01	0.03	chr19	Island	TSS200	ZNF584
cg10524576	0.352	0.380	0.028	0.355	0.377	0.022	0.174	-0.816	4.010	1.73E-04	4.50E-01	-0.01	chr12	OpenSea	Body	PPM1H
cg22550330	0.082	0.098	0.016	0.079	0.100	0.021	0.268	-3.402	4.004	1.76E-04	4.50E-01	-0.02	chr3	Island	5'UTR_Body	HYAL3_NAT6
cg10054262	0.202	0.176	-0.026	0.205	0.174	-0.032	-0.242	-2.056	-4.001	1.78E-04	4.50E-01	-0.03	chr7	Island	1stExon_5'UTR	UNC84A
ch.12.1870160F	0.067	0.079	0.012	0.065	0.078	0.012	0.250	-3.697	4.001	1.78E-04	4.50E-01	-0.03	chr12	N_Shelf	5'UTR	NR2C1
cg15537082	0.142	0.170	0.029	0.138	0.161	0.023	0.295	-2.483	3.994	1.82E-04	4.50E-01	-0.04	chr8	N_Shore	TSS1500	MIR124-1_LOC157
cg11806945	0.145	0.125	-0.020	0.150	0.128	-0.022	-0.259	-2.729	-3.992	1.83E-04	4.50E-01	-0.05	chr19	Island	TSS200	LSR
cg16824069	0.103	0.088	-0.015	0.103	0.089	-0.014	-0.258	-3.264	-3.988	1.86E-04	4.50E-01	-0.06	chrX	Island	TSS200	KDM5C
cg13274938	0.677	0.713	0.036	0.669	0.706	0.037	0.243	1.103	3.967	1.99E-04	4.50E-01	-0.10	chr17	N_Shelf	Body	RARA
cg20107201	0.802	0.773	-0.029	0.803	0.780	-0.023	-0.243	1.965	-3.964	2.01E-04	4.50E-01	-0.11	chr22	N_Shelf	Body	TEF
cg24901637	0.109	0.128	0.018	0.108	0.127	0.019	0.254	-2.940	3.959	2.04E-04	4.50E-01	-0.12	chr4	OpenSea	TSS200	MNRN1
cg20213866	0.795	0.753	-0.042	0.802	0.750	-0.052	-0.341	1.874	-3.957	2.06E-04	4.50E-01	-0.13	chr6	S_Shelf	Body	MSH5
cg07023852	0.638	0.676	0.038	0.655	0.677	0.022	0.248	0.984	3.948	2.12E-04	4.50E-01	-0.15	chr15	N_Shore	TSS1500	IVS
ch.17.958355F	0.073	0.087	0.014	0.074	0.082	0.008	0.256	-3.576	3.938	2.20E-04	4.50E-01	-0.17	chr17	OpenSea	Body	DKD52
cg12513249	0.177	0.204	0.027	0.173	0.194	0.022	0.256	-2.119	3.934	2.22E-04	4.50E-01	-0.18	chr11	N_Shore	TSS1500	CCDC85B_FIBP
cg26896255	0.791	0.762	-0.029	0.797	0.770	-0.027	-0.239	1.849	-3.929	2.25E-04	4.50E-01	-0.19	chr1	OpenSea	Body	DNM3
cg15957807	0.665	0.632	-0.034	0.660	0.637	-0.023	-0.215	0.933	-3.923	2.30E-04	4.50E-01	-0.20	chr4	OpenSea	3'UTR	PDGFRC
cg02176858	0.687	0.712	0.025	0.688	0.717	0.029	0.178	1.204	3.918	2.34E-04	4.50E-01	-0.22	chr2	N_Shore	Body	CLASP1
cg05493509	0.787	0.762	-0.025	0.791	0.780	-0.011	-0.199	1.805	-3.912	2.39E-04	4.50E-01	-0.23	chr10	Island	Body	SNT32C
cg06919693	0.729	0.767	0.038	0.740	0.767	0.027	0.286	1.607	3.911	2.40E-04	4.50E-01	-0.23	chr2	OpenSea	Body	MEI51
cg20048245	0.842	0.813	-0.029	0.839	0.828	-0.011	-0.274	2.278	-3.905	2.45E-04	4.50E-01	-0.24	chr13	N_Shelf	Body	LAMP1
cg13422850	0.072	0.061	-0.011	0.071	0.060	-0.011	-0.264	-3.883	-3.895	2.52E-04	4.50E-01	-0.27	chr9	Island	Body	NTNG2
cg18082788	0.138	0.118	-0.020	0.144	0.124	-0.020	-0.287	-2.719	-3.877	2.68E-04	4.50E-01	-0.31	chr6	OpenSea	TSS200	ZC3H12D
cg13184777	0.114	0.096	-0.018	0.112	0.093	-0.019	-0.263	-3.123	-3.872	2.72E-04	4.50E-01	-0.32	chr1	Island	Body	SERINC2
cg25012577	0.102	0.100	-0.012	0.102	0.087	-0.016	-0.205	-3.172	-3.872	2.72E-04	4.50E-01	-0.32	chr1	S_Shore	TSS1500	ADAR
cg23501605	0.707	0.741	0.035	0.699	0.745	0.046	0.248	1.460	3.871	2.73E-04	4.50E-01	-0.32	chrX	Island	TSS1500_Body	ASB11
cg21302017	0.041	0.049	0.008	0.041	0.049	0.008	0.255	-4.416	3.870	2.74E-04	4.50E-01	-0.32	chrX	OpenSea	TSS1500	GEMIN8
cg14153118	0.857	0.833	-0.024	0.860	0.841	-0.019	-0.254	2.479	-3.862	2.82E-04	4.50E-01	-0.34	chr4	S_Shelf	Body	ZFYVE28
cg10653713	0.236	0.263	0.027	0.243	0.258	0.015	0.209	-1.617	3.860	2.83E-04	4.50E-01	-0.34	chr17	N_Shore	TSS1500	ARL4D
cg18901378	0.589	0.546	-0.043	0.598	0.561	-0.037	-0.254	0.418	-3.854	2.88E-04	4.50E-01	-0.36	chr17	S_Shelf	Body	XYL2
cg22547485	0.076	0.091	0.014	0.072	0.084	0.013	0.247	-3.505	3.851	2.92E-04	4.50E-01	-0.37	chr4	Island	Body	ELF2
cg00347616	0.075	0.063	-0.012	0.075	0.062	-0.013	-0.282	-3.822	-3.850	2.93E-04	4.50E-01	-0.37	chr2	N_Shore	TSS200	ACTR3
cg10417386	0.453	0.485	0.032	0.456	0.482	0.026	0.187	-0.180	3.823	3.19E-04	4.71E-01	-0.43	chr17	OpenSea	TSS1500	PIK3R6
cg08832195	0.793	0.821	0.028	0.794	0.822	0.028	0.261	2.139	3.821	3.21E-04	4.71E-01	-0.43	chr7	OpenSea	Body	CDK13
cg00083188	0.262	0.290	0.028	0.261	0.286	0.025	0.200	-1.458	3.817	3.25E-04	4.71E-01	-0.44	chr10	OpenSea	Body	KCNMA1
cg26404669	0.074	0.092	0.018	0.072	0.089	0.017	0.324	-3.463	3.812	3.31E-04	4.71E-01	-0.45	chr12	OpenSea	TSS200	CCDC65
cg03173502	0.814	0.836	0.022	0.813	0.839	0.025	0.219	2.197	3.807							

Table S6. Information DMPs Vacc – Baseline

DMPs - Gene relation				Chi-square DMPs - Gene relation			
Gene relation	Counts	class	Proportion	Gene relation	pval	qual	Percentage
1stExon	384	DMP	0.07	3'UTR	7.56E-03	3.70E-02	7
3'UTR	249	DMP	0.05	TSS200	1.23E-02	3.70E-02	5
5'UTR	719	DMP	0.13	Body	2.48E-02	4.97E-02	13
Body	2082	DMP	0.38	TSS1500	6.71E-02	1.01E-01	38
TSS1500	1030	DMP	0.19	5'UTR	3.77E-01	4.53E-01	19
TSS200	983	DMP	0.18	1stExon	7.88E-01	7.88E-01	18
1stExon	6251	all	0.07				7
3'UTR	3458	all	0.04				4
5'UTR	11502	all	0.13				13
Body	35792	all	0.40				40
TSS1500	17947	all	0.20				20
TSS200	15060	all	0.17				17

DMPs - Relation to Island				Chi-square DMPs - Gene relation			
Relation to Island	Counts	class	Proportion	Gene relation	pval	qual	Percentage
Island	2158	DMP	0.40	N_Shore	6.33E-04	2.43E-03	40
N_Shelf	210	DMP	0.04	OpenSea	8.11E-04	2.43E-03	4
N_Shore	664	DMP	0.12	S_Shore	2.33E-03	4.63E-03	12
OpenSea	1723	DMP	0.32	N_Shelf	9.03E-03	1.35E-02	32
S_Shelf	171	DMP	0.03	S_Shelf	2.45E-01	2.94E-01	3
S_Shore	521	DMP	0.10	Island	8.98E-01	8.98E-01	10
Island	35748	all	0.40				40
N_Shelf	2881	all	0.03				3
N_Shore	12459	all	0.14				14
OpenSea	28543	all	0.29				29
S_Shelf	2573	all	0.03				3
S_Shore	9806	all	0.11				11

Relation to Island				Chromosome distribution of DMPs w/1-w0			
chr	counts	class	Proportion	chr	counts	class	Proportion
chr1	509	DMPs	0.09	chr1	509	DMPs	0.09
chr10	268	DMPs	0.05	chr10	268	DMPs	0.05
chr11	323	DMPs	0.06	chr11	323	DMPs	0.06
chr12	265	DMPs	0.05	chr12	265	DMPs	0.05
chr13	121	DMPs	0.02	chr13	121	DMPs	0.02
chr14	172	DMPs	0.03	chr14	172	DMPs	0.03
chr15	165	DMPs	0.03	chr15	165	DMPs	0.03
chr16	205	DMPs	0.04	chr16	205	DMPs	0.04
chr17	313	DMPs	0.06	chr17	313	DMPs	0.06
chr18	71	DMPs	0.01	chr18	71	DMPs	0.01
chr19	293	DMPs	0.05	chr19	293	DMPs	0.05
chr2	372	DMPs	0.07	chr2	372	DMPs	0.07
chr20	135	DMPs	0.02	chr20	135	DMPs	0.02
chr21	51	DMPs	0.01	chr21	51	DMPs	0.01
chr22	85	DMPs	0.02	chr22	85	DMPs	0.02
chr3	313	DMPs	0.06	chr3	313	DMPs	0.06
chr4	239	DMPs	0.04	chr4	239	DMPs	0.04
chr5	271	DMPs	0.05	chr5	271	DMPs	0.05
chr6	435	DMPs	0.08	chr6	435	DMPs	0.08
chr7	330	DMPs	0.06	chr7	330	DMPs	0.06
chr8	106	DMPs	0.02	chr8	106	DMPs	0.02
chr9	192	DMPs	0.03	chr9	192	DMPs	0.03
chrX	239	DMPs	0.04	chrX	239	DMPs	0.04
chrY	2	DMPs	0.00	chrY	2	DMPs	0.00
chr1	8600	all	0.10	chr1	8600	all	0.10
chr10	4470	all	0.05	chr10	4470	all	0.05
chr11	5277	all	0.06	chr11	5277	all	0.06
chr12	4544	all	0.05	chr12	4544	all	0.05
chr13	2051	all	0.02	chr13	2051	all	0.02
chr14	2526	all	0.03	chr14	2526	all	0.03
chr15	2723	all	0.03	chr15	2723	all	0.03
chr16	3376	all	0.04	chr16	3376	all	0.04
chr17	5125	all	0.06	chr17	5125	all	0.06
chr18	1270	all	0.01	chr18	1270	all	0.01
chr19	5307	all	0.06	chr19	5307	all	0.06
chr2	5953	all	0.07	chr2	5953	all	0.07
chr20	2310	all	0.03	chr20	2310	all	0.03
chr21	935	all	0.01	chr21	935	all	0.01
chr22	1676	all	0.02	chr22	1676	all	0.02
chr3	4709	all	0.05	chr3	4709	all	0.05
chr4	3719	all	0.04	chr4	3719	all	0.04
chr5	4628	all	0.05	chr5	4628	all	0.05
chr6	6904	all	0.08	chr6	6904	all	0.08
chr7	5261	all	0.06	chr7	5261	all	0.06
chr8	3623	all	0.04	chr8	3623	all	0.04
chr9	1553	all	0.02	chr9	1553	all	0.02
chrX	3353	all	0.04	chrX	3353	all	0.04
chrY	117	all	0.00	chrY	117	all	0.00

Chromosome distribution of DMPs w/1-w0				Chi-square chromosome distribution w/1-w0			
chr	counts	class	Proportion	chromosome	pval	qual	Percentage
chr1	509	DMPs	0.09	chr8	6.15E-03	1.48E-01	9
chr10	268	DMPs	0.05	chrX	1.39E-02	1.67E-01	5
chr11	323	DMPs	0.06	chrY	8.98E-02	4.79E-01	6
chr12	265	DMPs	0.05	chr3	1.05E-01	4.79E-01	5
chr13	121	DMPs	0.02	chr22	1.22E-01	4.79E-01	2
chr14	172	DMPs	0.03	chr19	1.22E-01	4.79E-01	3
chr15	165	DMPs	0.03	chr14	1.40E-01	4.79E-01	3
chr16	205	DMPs	0.04	chr4	3.74E-01	9.38E-01	4
chr17	313	DMPs	0.06	chr6	4.10E-01	9.38E-01	6
chr18	71	DMPs	0.01	chr21	5.11E-01	9.38E-01	1
chr19	293	DMPs	0.05	chr7	5.34E-01	9.38E-01	5
chr2	372	DMPs	0.07	chr18	5.52E-01	9.38E-01	7
chr20	135	DMPs	0.02	chr2	5.53E-01	9.38E-01	2
chr21	51	DMPs	0.01	chr12	5.79E-01	9.38E-01	1
chr22	85	DMPs	0.02	chr5	6.11E-01	9.38E-01	2
chr3	313	DMPs	0.06	chr1	6.25E-01	9.38E-01	6
chr4	239	DMPs	0.04	chr20	7.23E-01	9.38E-01	4
chr5	271	DMPs	0.05	chr13	8.19E-01	9.38E-01	5
chr6	435	DMPs	0.08	chr11	8.61E-01	9.38E-01	8
chr7	330	DMPs	0.06	chr9	8.63E-01	9.38E-01	6
chr8	106	DMPs	0.02	chr10	8.98E-01	9.38E-01	2
chr9	192	DMPs	0.03	chr16	9.01E-01	9.38E-01	4
chrX	239	DMPs	0.04	chr16	9.01E-01	9.38E-01	4
chrY	2	DMPs	0.00	chr15	1.00E-00	1.00E-00	0
chr1	8600	all	0.10	chr15	1.00E-00	1.00E-00	10
chr10	4470	all	0.05				5
chr11	5277	all	0.06				6
chr12	4544	all	0.05				5
chr13	2051	all	0.02				2
chr14	2526	all	0.03				3
chr15	2723	all	0.03				3
chr16	3376	all	0.04				4
chr17	5125	all	0.06				6
chr18	1270	all	0.01				1
chr19	5307	all	0.06				6
chr2	5953	all	0.07				7
chr20	2310	all	0.03				3
chr21	935	all	0.01				1
chr22	1676	all	0.02				2
chr3	4709	all	0.05				5
chr4	3719	all	0.04				4
chr5	4628	all	0.05				5
chr6	6904	all	0.08				8
chr7	5261	all	0.06				6
chr8	3623	all	0.04				4
chr9	1553	all	0.02				2
chrX	3353	all	0.04				4
chrY	117	all	0.00				0

Table S7. Top 100 DEGs Vacc+RMD - Baseline

Table S7. Top100 (p-value) differentially expressed genes between Vacc+RMD and BSL	Mean_w0	Mean_w6	diffMean	Median_w0	Median_w6	diffMedian	logFC	AveExpr	t	P.Value	adj.P.Val	B
ENSG00000198910.13.L1CAM.protein_coding	-0.565	0.987	1.552	-0.294	1.200	1.494	1.574	0.194	7.657	1.83E-10	3.05E-06	13.404
ENSG00000221946.7.FXYD7.protein_coding	0.554	1.676	1.122	0.621	1.678	1.057	1.133	0.828	7.201	1.11E-09	9.23E-06	11.746
ENSG00000133742.13.CA1.protein_coding	0.677	4.733	4.056	0.513	4.830	4.317	4.180	2.204	6.887	3.81E-09	1.69E-05	10.605
ENSG0000004939.14.SLCA4A1.protein_coding	3.301	7.382	4.080	3.338	7.518	4.180	4.227	4.710	6.838	4.62E-09	1.69E-05	10.428
ENSG00000079308.17.TNSI.protein_coding	3.618	6.148	2.530	3.532	6.228	2.696	2.594	4.464	6.815	5.05E-09	1.69E-05	10.344
ENSG00000088340.15.FER1L4.transcribed_unitary_pseudogene	-2.148	-0.075	2.073	-2.192	-0.012	2.180	2.057	-1.169	6.517	1.63E-08	4.53E-05	9.263
ENSG00000166947.12.EPB42.protein_coding	-0.043	3.902	3.945	0.303	4.073	3.769	4.123	1.297	6.471	1.95E-08	4.64E-05	9.097
ENSG00000173868.11.PHOSPHO1.protein_coding	-0.255	2.984	3.239	-0.253	2.690	2.943	3.356	1.206	6.433	2.26E-08	4.71E-05	8.960
ENSG00000158578.19.ALAS2.protein_coding	3.545	7.956	4.411	3.891	8.215	4.324	4.602	5.135	6.344	3.19E-08	5.12E-05	8.639
ENSG00000169877.9.AHSP.protein_coding	-0.541	3.600	4.140	-0.265	4.008	4.274	4.308	0.882	6.338	3.26E-08	5.12E-05	8.620
ENSG00000143416.20.SELBNP1.protein_coding	1.119	4.964	3.845	1.323	5.220	3.897	4.012	2.363	6.309	3.65E-08	5.12E-05	8.515
ENSG00000187017.16.ESPN.protein_coding	-1.654	0.363	2.017	-1.388	0.042	1.430	2.030	-0.209	6.293	3.89E-08	5.12E-05	8.457
ENSG00000147454.13.SL2C5A37.protein_coding	6.165	8.470	2.304	6.078	8.124	2.046	2.358	7.006	6.287	3.99E-08	5.12E-05	8.434
ENSG00000284931.1.CTD-26437.4.protein_coding	0.649	4.708	4.059	0.854	4.784	3.930	4.253	2.039	6.239	4.81E-08	5.12E-05	8.261
ENSG00000206177.6.HBM.protein_coding	-1.471	2.047	3.518	-1.336	2.233	3.569	3.657	-0.228	6.216	5.25E-08	5.84E-05	8.180
ENSG00000206172.8.HBA1.protein_coding	7.895	11.310	3.415	7.934	11.364	3.430	3.571	9.153	6.177	6.09E-08	6.36E-05	8.041
ENSG00000184792.15.OSBP2.protein_coding	1.355	4.228	2.873	1.304	4.146	2.843	2.955	2.364	6.074	9.08E-08	8.92E-05	7.672
ENSG00000078487.17.ZCWPV1.protein_coding	2.166	1.629	-0.537	2.173	1.551	0.622	-0.520	2.013	-6.050	9.98E-08	9.26E-05	7.585
ENSG00000162722.8.TRIM5B.protein_coding	3.132	5.837	2.705	3.088	5.520	2.432	2.772	4.051	6.017	1.13E-07	9.44E-05	7.467
ENSG00000170180.21.GWPA.protein_coding	-3.381	0.529	3.910	-2.973	0.471	3.444	4.044	-0.207	6.009	1.17E-07	9.44E-05	7.438
ENSG000002059726.1.RP11-671M22.5.unprocessed_pseudogene	-0.322	1.226	1.549	-0.323	1.335	1.658	1.563	-0.281	5.990	1.26E-07	9.44E-05	7.369
ENSG00000130821.15.SLCA6A.protein_coding	0.903	3.723	2.821	0.785	3.418	2.633	2.882	1.867	5.983	1.29E-07	9.44E-05	7.346
ENSG00000244734.4.HBB.protein_coding	10.398	13.801	3.402	10.821	13.943	3.122	3.565	11.580	5.979	1.31E-07	9.44E-05	7.333
ENSG00000196739.14.COL27A1.protein_coding	-1.158	0.272	1.431	-1.209	0.419	1.628	1.432	-0.721	5.970	1.36E-07	9.44E-05	7.300
ENSG00000223609.8.HBD.protein_coding	0.671	4.305	3.634	0.904	4.612	3.707	3.794	1.790	5.937	1.54E-07	9.89E-05	7.180
ENSG00000188536.13.HBA2.protein_coding	8.985	12.256	3.271	9.233	12.134	2.901	3.416	10.170	5.922	1.63E-07	9.89E-05	7.128
ENSG00000204010.3.FIT1B.protein_coding	-0.436	3.404	3.840	-0.308	3.893	4.201	3.989	0.909	5.920	1.65E-07	9.89E-05	7.121
ENSG00000171914.16.TLX2.protein_coding	0.494	1.234	0.740	0.452	1.319	0.867	0.747	0.765	5.918	1.66E-07	9.89E-05	7.114
ENSG0000011028.13.MRC2.protein_coding	1.226	2.368	1.142	1.319	2.295	0.976	1.125	1.617	5.848	2.17E-07	1.25E-04	6.867
ENSG00000136929.12.HEMGN.protein_coding	2.181	4.344	2.163	2.182	4.809	2.627	2.221	2.841	5.783	2.78E-07	1.55E-04	6.636
ENSG00000163554.13.SPTA1.protein_coding	-0.869	1.920	2.790	-1.087	1.917	3.004	2.860	0.175	5.753	3.12E-07	1.68E-04	6.528
ENSG00000224177.6.ACO99344.4.lincRNA	-4.302	-1.011	3.292	-4.162	-1.138	3.023	3.366	-3.330	5.727	3.44E-07	1.80E-04	6.439
ENSG0000004975.11.DVL2.protein_coding	4.747	4.417	0.330	4.762	4.428	0.334	-0.324	4.615	-5.614	5.29E-07	2.68E-04	6.041
ENSG00000197256.10.KANK2.protein_coding	0.358	2.299	1.940	0.265	2.022	1.757	1.974	0.988	5.543	6.94E-07	3.41E-04	5.790
ENSG00000151474.21.FRMD4A.protein_coding	-0.699	1.352	2.051	-0.764	0.789	1.553	2.093	-0.084	5.531	7.24E-07	3.45E-04	5.750
ENSG00000238243.3.ORZ3W3.protein_coding	-0.930	1.956	2.886	-1.001	2.074	3.075	2.962	0.078	5.467	9.24E-07	4.28E-04	5.525
ENSG00000145335.15.SNCA.protein_coding	3.669	6.221	2.552	3.662	6.231	2.569	2.644	4.473	5.417	1.12E-06	5.00E-04	5.351
ENSG00000208280.18.ASAP3.protein_coding	0.053	0.965	0.911	0.188	1.078	0.890	0.917	0.376	5.410	1.14E-06	5.00E-04	5.299
ENSG00000070182.20.SPTB.protein_coding	2.164	4.937	2.773	1.709	4.737	3.028	2.859	3.080	5.402	1.18E-06	5.00E-04	5.298
ENSG00000137198.9.GMPR.protein_coding	1.675	3.981	2.305	1.558	3.800	2.242	2.361	2.444	5.396	1.21E-06	5.00E-04	5.278
ENSG00000260592.1.CTA-363E6.6.antisense	-3.492	-0.350	3.142	-2.946	-0.990	1.957	3.237	-2.305	5.391	1.23E-06	5.00E-04	5.263
ENSG00000105610.5.KLF1.protein_coding	-1.556	1.164	2.720	-1.695	0.750	2.445	2.788	-0.721	5.350	1.43E-06	5.58E-04	5.119
ENSG00000196517.11.SLCA6A9.protein_coding	-2.546	0.123	2.670	-2.673	-0.534	2.139	2.744	-1.520	5.349	1.44E-06	5.58E-04	5.117
ENSG00000088441.16.NFIX.protein_coding	2.494	3.935	1.441	2.440	3.588	1.148	1.463	2.978	5.333	1.53E-06	5.79E-04	5.061
ENSG00000197721.16.CR1L.protein_coding	-2.269	-0.312	1.957	-2.076	-0.062	2.014	2.048	-1.610	5.323	1.58E-06	5.87E-04	5.027
ENSG00000110693.17.SOX6.protein_coding	-1.480	1.624	3.104	-0.974	1.772	2.746	3.241	-0.446	5.316	1.63E-06	5.91E-04	5.001
ENSG00000163346.16.PBP1P1.protein_coding	8.112	7.706	0.405	8.111	7.688	0.422	-0.402	7.957	5.271	1.92E-06	6.83E-04	4.848
ENSG00000167994.11.RAB31L1.protein_coding	-3.486	-0.637	2.848	-3.161	-0.717	2.445	2.929	-2.757	5.219	2.33E-06	8.11E-04	4.669
ENSG00000129472.13.RAB2B.protein_coding	4.311	4.995	0.684	4.291	4.863	0.572	0.695	4.478	5.165	2.85E-06	9.47E-04	4.483
ENSG00000180537.12.RNF182.protein_coding	-3.031	0.227	3.258	-3.270	0.282	-1.998	5.162	2.89E-06	5.162	2.89E-06	9.47E-04	4.471
ENSG00000140892.16.KLC3.protein_coding	-4.219	-0.571	3.647	-4.546	-0.359	4.187	3.753	-2.727	5.161	2.89E-06	9.47E-04	4.469
ENSG0000043143.20.JADE2.protein_coding	7.451	7.125	0.326	7.432	7.060	0.372	-0.321	7.304	-5.136	3.18E-06	1.02E-03	4.483
ENSG00000198336.9.MYL4.protein_coding	-2.108	1.322	3.430	-1.608	1.429	3.038	3.586	-0.826	5.110	3.50E-06	1.08E-03	4.295
ENSG00000125841.12.NR5A2.protein_coding	-0.899	-0.899	0.811	-0.976	-0.082	0.895	0.815	-0.619	5.106	3.55E-06	1.08E-03	4.282
ENSG0000029534.20.ANK1.protein_coding	3.362	5.312	1.950	3.358	5.001	1.643	1.998	4.009	5.105	3.56E-06	1.08E-03	4.278
ENSG00000158856.18.DAT1M.protein_coding	3.815	5.745	1.929	3.750	5.310	1.550	1.984	4.492	5.088	3.79E-06	1.13E-03	4.220
ENSG00000204613.10.TROM10.protein_coding	-1.803	1.124	2.927	-1.399	1.256	2.655	3.072	-0.681	5.074	3.99E-06	1.17E-03	4.172
ENSG00000270120.1.RP11-327F22.6.antisense_intronic	0.469	1.416	0.947	0.427	1.302	0.875	0.932	0.840	5.064	4.14E-06	1.19E-03	4.139
ENSG00000169239.12.CASB.protein_coding	5.285	4.921	0.364	5.335	4.947	-0.352	5.122	-0.505	4.386	0.46E-06	1.23E-03	4.090
ENSG00000180667.10.YOD1.protein_coding	5.275	6.576	1.301	5.246	6.312	1.066	1.309	5.785	5.042	4.48E-06	1.25E-03	4.063
ENSG00000101210.11.EEF1A2.protein_coding	-1.737	-0.043	1.694	-1.953	-0.016	-1.374	5.032	4.65E-06	4.65E-06	1.27E-03	4.041	
ENSG00000171552.12.BCL2L1.protein_coding	5.532	7.125	1.593	5.537	6.977	1.440	1.645	6.080	5.007	5.10E-06	1.37E-03	3.946
ENSG00000133069.15.TMCC2.protein_coding	1.786	3.647	1.861	1.768	3.532	1.764	1.890	2.422	5.000	5.24E-06	1.39E-03	3.922
ENSG00000167535.7.CACNB3.protein_coding	1.704	2.379	0.675	1.561	2.539	0.978	0.680	1.878	4.956	6.15E-06	1.60E-03	3.773
ENSG00000163001.11.CFAP36.protein_coding	3.650	3.210	0.440	3.601	3.182	0.419	-0.408	3.517	-4.950	6.28E-06	1.61E-03	3.754
ENSG00000196565.14.HBG2.protein_coding	0.740	3.799	3.059	1.014	3.976	2.961	3.259	1.567	4.929	6.79E-06	1.72E-03	3.683
ENSG00000143479.15.DWRK3.protein_coding	-1.454	0.321	1.776	-1.243	0.055	1.298	1.816	-0.967	4.918	7.07E-06	1.76E-03	3.645
ENSG00000198876.12.DCAF12.protein_coding	5.658	7.473	1.815	5.639	7.491	1.852	1.890	6.281	4.915	7.15E-06	1.76E-03	3.635
ENSG00000185222.9.TCEAL9.protein_coding	-0.980	0.329	1.309	-0.864	0.268	1.132	1.315	-0.845	4.905	7.42E-06	1.77E-03	3.601
ENSG00000275832.4.ARHGAP23.protein_coding	-0.874	0.129	1.003	-0.895	0.183	1.078	0.985	-0.271	4.904	7.43E-06	1.77E-03	3.600
ENSG00000275527.1.CTD-3154N5.2.lincRNA	-3.726	-1.114	2.611	-3.223	-0.592	2.631	2.663	-2.691	4.888	7.88E-06	1.85E-03	3.544
ENSG00000076864.19.RAP1GAP.protein_coding	-2.000	1.454	3.454	-2.235	1.950	4.185	3.540	-0.719	4.853	8.96E-06	2.03E-03	3.426
ENSG00000082146.12.STRADB8.protein_coding	4.208	5.960	1.752	4.250	5.814	1.564	1.811	4.741	4.851	9.03E-06	2.03E-03	3.420
ENSG00000163359.15.COL6A3.protein_coding	2.291	2.930	0.639	2.212	2.862	0.650	0.666	2.449	4.850	9.06E-06	2.03E-03	3.416
ENSG0000047597.6.IKAP1.protein_coding	1.620	3.493	1.873	1.580	3.136	1.555	1.907	2.158	4.849	9.10E-06	2.03E-03	3.412
ENSG0000006926.10.FECH.protein_coding	4.405	5.988	1.584	4.341	6.197	1.856	1.625	4				

Chapter III

Table S8. Top 100 DMPs Vacc+RMD – Baseline

Table S8. Top100 (p-value) differentially methylated positions between Vacc+RMD and BSU

	Mean_w0	Mean_w6	DiffMean	Median_w0	Median_w6	DiffMedian	logFC	AveExpr	t	P.Value	adj.P.Val	B	chr	Relation_to_Island	UCSC_RefGene_Group	Gene
cg11553963	0.069	0.158	0.089	0.068	0.134	0.067	1.182	-3.331	7.109	1.75E-09		2,12E-04	11,218 chr19	Island	TSS200	ZNF83
cg18223235	0.513	0.456	-0.057	0.501	0.460	-0.042	-0.333	-0.042	-6.319	3.76E-08		1,26E-03	8,421 chr18	OpenSea	Body	BC12
cg10773587	0.066	0.140	0.075	0.063	0.145	0.083	1.057	-3.252	6.273	4.49E-08		1,26E-03	8,259 chr2	Island	Body	GP11
cg22175006	0.706	0.639	-0.066	0.722	0.633	-0.089	-0.441	1.093	-6.160	6.93E-08		1,26E-03	7,862 chr2	OpenSea	5'UTR	AC3L3
cg26761016	0.620	0.548	-0.072	0.617	0.566	-0.051	-0.313	0.599	-4.158	4.99E-08		1,26E-03	7,854 chr11	OpenSea	1stExon_5'UTR	MS4A3
cg06529969	0.652	0.644	-0.008	0.655	0.644	-0.011	-0.313	1.077	-4.125	7.93E-08		1,26E-03	7,740 chr1	OpenSea	Body	PCD
cg04205769	0.704	0.641	-0.063	0.709	0.638	-0.071	-0.413	1.120	-6.103	8.64E-08		1,26E-03	7,661 chr1	N_Shelf	Body	DHHS
cg25153741	0.645	0.585	-0.060	0.633	0.594	-0.039	-0.370	0.745	-6.026	1.16E-07		1,26E-03	7,390 chr5	OpenSea	Body	COL23A1
cg10208075	0.671	0.619	-0.051	0.673	0.618	-0.055	-0.323	0.922	-5.996	1.30E-07		1,26E-03	7,286 chr8	N_Shelf	Body	EP3A1
cg09694044	0.127	0.158	0.031	0.126	0.152	0.026	0.357	-2.661	5.941	1.60E-07		1,26E-03	7,095 chr20	S_Shore	Body	REM38
cg19739596	0.637	0.583	-0.054	0.632	0.581	-0.051	-0.328	0.706	-5.941	1.61E-07		1,26E-03	7,094 chr11	OpenSea	1stExon_5'UTR	MS4A3
cg27207183	0.625	0.570	-0.055	0.629	0.571	-0.058	-0.335	0.623	-5.939	1.62E-07		1,26E-03	7,089 chr6	OpenSea	5'UTR_Body_TSS200	CDTL
cg10028625	0.781	0.732	-0.049	0.788	0.723	-0.065	-0.387	1.722	-5.939	1.62E-07		1,26E-03	7,086 chr3	OpenSea	Body	ECT2
cg13180038	0.103	0.123	0.019	0.104	0.122	0.018	0.275	-3.029	5.901	1.87E-07		1,26E-03	6,954 chr2	S_Shore	5'UTR_TSS200	GF2D
cg05714778	0.593	0.651	0.058	0.591	0.646	0.055	0.357	0.736	5.900	1.88E-07		1,26E-03	6,953 chr12	N_Shore	TSS1500	TM6PR312
cg20780705	0.660	0.610	-0.050	0.662	0.606	-0.057	-0.313	0.849	-5.881	2.02E-07		1,29E-03	6,886 chr5	N_Shelf	Body	CSorf43
cg25420665	0.656	0.605	-0.051	0.655	0.611	-0.043	-0.320	0.866	-5.852	2.25E-07		1,30E-03	6,785 chr2	OpenSea	Body	C2orf59
cg15936066	0.527	0.480	-0.048	0.534	0.468	-0.067	-0.276	0.061	-5.830	2.45E-07		1,35E-03	6,708 chr8	OpenSea	5'UTR	SLC20A2
cg18084554	0.571	0.516	-0.055	0.569	0.511	-0.058	-0.320	0.301	-5.768	3.10E-07		1,51E-03	6,492 chr19	N_Shore	5'UTR	AUID3A
cg04159302	0.671	0.619	-0.052	0.553	0.595	-0.048	-0.300	0.242	-5.726	3.63E-07		1,60E-03	6,349 chr5	S_Shelf	Body	CSorf62
cg01380609	0.651	0.700	0.049	0.654	0.710	0.056	0.326	1.074	5.713	3.83E-07		1,60E-03	6,302 chr6	N_Shore	5'UTR	RPS6A2
cg05533539	0.585	0.529	-0.056	0.587	0.517	-0.069	-0.327	0.370	-5.680	4.32E-07		1,69E-03	6,190 chr17	OpenSea	MAPT	SLC20A2
cg00479314	0.234	0.194	-0.040	0.229	0.196	-0.033	-0.348	-1.880	-5.667	4.55E-07		1,69E-03	6,143 chr4	Island	TSS200	CXCL1
cg14322772	0.143	0.175	0.032	0.144	0.181	0.036	0.349	-2.491	5.665	4.59E-07		1,69E-03	6,136 chr9	OpenSea	5'UTR	TBRF1
cg08764162	0.677	0.621	-0.056	0.669	0.618	-0.050	-0.359	0.979	-5.638	5.07E-07		1,77E-03	6,045 chr10	OpenSea	Body_5'UTR	ZNF438
cg12894711	0.614	0.565	-0.049	0.607	0.560	-0.047	-0.295	0.570	-5.634	5.15E-07		1,77E-03	6,020 chr7	OpenSea	Body	BLVR4
cg17714703	0.202	0.247	0.045	0.193	0.248	0.055	0.381	-1.868	5.623	5.37E-07		1,77E-03	5,992 chr19	S_Shore	Body	UHRF1
cg18949409	0.240	0.240	0.000	0.242	0.244	0.002	0.409	-1.798	-5.583	6.25E-07		1,88E-03	5,853 chr2	OpenSea	Body	SETD3B
cg05298510	0.707	0.649	-0.057	0.705	0.654	-0.051	-0.379	1.181	-5.581	6.29E-07		1,88E-03	5,847 chr16	OpenSea	Body	USP10
cg10884794	0.721	0.676	-0.045	0.721	0.668	-0.053	-0.307	1.283	-5.579	6.35E-07		1,88E-03	5,839 chr5	OpenSea	Body	AKS8
cg08282835	0.680	0.626	-0.054	0.685	0.623	-0.061	-0.345	0.998	-5.573	6.49E-07		1,88E-03	5,818 chr6	OpenSea	Body	E2F3
cg13348811	0.539	0.480	-0.059	0.533	0.485	-0.048	-0.347	0.097	-5.530	7.62E-07		1,91E-03	5,812 chr19	S_Shelf	5'UTR	TME491
cg00026290	0.352	0.310	-0.042	0.351	0.307	-0.044	-0.274	-0.977	-5.519	7.97E-07		1,91E-03	5,635 chr4	OpenSea	TSS200	CLNK
cg01544877	0.385	0.442	0.057	0.381	0.443	0.062	0.400	-0.522	5.512	8.16E-07		1,91E-03	5,609 chr6	N_Shore	5'UTR	BCLAF1
cg25126296	0.617	0.570	-0.047	0.621	0.577	-0.044	-0.285	0.527	-5.511	8.18E-07		1,91E-03	5,607 chr1	OpenSea	Body	PRKAT
cg12339228	0.700	0.639	-0.061	0.620	0.690	-0.070	-0.390	1.089	-5.500	8.24E-07		1,91E-03	5,600 chr20	OpenSea	Body	SETD3B
cg17936145	0.803	0.771	-0.033	0.803	0.769	-0.035	-0.280	1.938	-5.505	8.38E-07		1,91E-03	5,585 chr10	N_Shore	5'UTR	IFI2
cg10515048	0.156	0.130	-0.026	0.152	0.128	-0.024	-0.303	-2.626	-5.502	8.47E-07		1,91E-03	5,575 chr14	N_Shore	Body	SOS2
cg18175523	0.785	0.719	-0.066	0.791	0.718	-0.073	-0.495	0.716	-5.495	8.71E-07		1,91E-03	5,550 chr4	Island	TSS200	KIF3B
cg16416987	0.556	0.511	-0.045	0.546	0.499	-0.047	-0.261	0.245	-4.487	8.95E-07		1,91E-03	5,525 chr1	N_Shore	Body_TSS1500	THBS3_MTX1
cg22655038	0.092	0.073	-0.018	0.094	0.072	-0.022	-0.352	-3.470	-5.485	9.04E-07		1,91E-03	5,516 chr22	Island	TSS200	SMTN
cg04573500	0.479	0.427	-0.052	0.481	0.423	-0.058	-0.307	-0.268	-5.477	9.31E-07		1,91E-03	5,489 chr17	OpenSea	Body	MS2
cg18433866	0.620	0.581	-0.040	0.627	0.572	-0.056	-0.283	0.679	-5.469	9.54E-07		1,91E-03	5,464 chr7	OpenSea	5'UTR_1stExon	CLEC5A
cg02041484	0.594	0.536	-0.058	0.591	0.538	-0.053	-0.344	0.479	-4.468	9.66E-07		1,91E-03	5,461 chr7	OpenSea	Body	NRF1
cg26298914	0.730	0.673	-0.058	0.722	0.662	-0.061	-0.400	1.330	-4.465	9.73E-07		1,91E-03	5,448 chr14	OpenSea	Body	RADS11B
cg17404534	0.706	0.665	-0.041	0.711	0.662	-0.049	-0.274	1.167	-4.463	9.79E-07		1,91E-03	5,443 chr7	OpenSea	Body	DGKB
cg167630078	0.223	0.273	0.050	0.219	0.276	0.057	0.457	-1.571	4.449	9.94E-07		1,91E-03	5,394 chr16	OpenSea	Body	IFAF213
cg10426076	0.679	0.620	-0.059	0.669	0.623	-0.046	-0.377	0.994	-4.441	1.06E-06		1,99E-03	5,367 chr11	OpenSea	TSS200	PRG2
cg11645658	0.079	0.095	0.016	0.078	0.093	0.015	0.286	-3.363	5.423	1.14E-06		2,01E-03	5,304 chr22	Island	TSS200	HDAC10
cg12764201	0.703	0.657	-0.046	0.699	0.656	-0.043	-0.304	1.175	-5.419	1.16E-06		2,01E-03	5,291 chr1	OpenSea	1stExon_Body_5'UTR	COR1AIP1
cg11865768	0.536	0.536	0.000	0.536	0.536	0.000	0.000	1.391	5.413	1.16E-06		2,01E-03	5,287 chr13	OpenSea	Body	SRC
cg05111779	0.592	0.537	-0.055	0.597	0.528	-0.069	-0.325	0.427	-5.415	1.17E-06		2,01E-03	5,278 chr14	OpenSea	Body	RC3H1
cg00435173	0.643	0.592	-0.051	0.644	0.584	-0.060	-0.312	0.759	-5.411	1.19E-06		2,01E-03	5,265 chr17	OpenSea	5'UTR	RAB5C
cg0496389	0.600	0.550	-0.050	0.599	0.545	-0.054	-0.296	0.586	-5.390	1.20E-06		2,01E-03	5,193 chr2	OpenSea	5'UTR	MARCKS
cg00471180	0.681	0.625	-0.056	0.682	0.627	-0.055	-0.359	0.968	-5.388	1.20E-06		2,01E-03	5,187 chr4	OpenSea	Body	KLHL5
cg00295213	0.584	0.532	-0.052	0.590	0.518	-0.072	-0.306	0.390	-5.380	1.33E-06		2,01E-03	5,160 chr1	S_Shore	TSS1500	ZNF124
cg05542101	0.648	0.600	-0.049	0.646	0.595	-0.050	-0.300	0.822	-5.380	1.33E-06		2,01E-03	5,160 chr7	OpenSea	Body	MAOCC1
cg00686823	0.601	0.547	-0.054	0.599	0.540	-0.059	-0.326	0.488	-5.379	1.34E-06		2,01E-03	5,155 chr19	S_Shore	TSS1500	TBR1
cg05962781	0.570	0.521	-0.049	0.563	0.514	-0.048	-0.285	0.307	-5.377	1.35E-06		2,01E-03	5,148 chr1	OpenSea	Body	TSPAN2
cg24618413	0.593	0.546	-0.047	0.590	0.540	-0.051	-0.278	0.444	-5.371	1.38E-06		2,01E-03	5,127 chrX	S_Shore	5'UTR	BCOR
cg02160884	0.728	0.683	-0.045	0.737	0.684	-0.053	-0.312	1.322	-5.366	1.41E-06		2,01E-03	5,111 chr8	S_Shelf	Body	TBR1
cg0111721	0.611	0.562	-0.049	0.619	0.568	-0.051	-0.294	0.579	-5.353	1.48E-06		2,08E-03	5,068 chr20	N_Shore	5'UTR	SRC
cg05697976	0.589	0.534	-0.055	0.587	0.543	-0.044	-0.326	0.440	-5.348	1.50E-06		2,10E-03	5,050 chr12	OpenSea	TSS200	FAR2
cg07283015	0.706	0.655	-0.051	0.699	0.652	-0.047	-0.341	1.172	-5.334	1.59E-06		2,19E-03	5,002 chr18	OpenSea	TSS1500	HRH4
cg00453717	0.676	0.621	-0.055	0.686	0.617	-0.068	-0.353	0.958	-5.329	1.62E-06		2,19E-03	4,995 chr11	OpenSea	Body	PCOLCE
cg18390643	0.738	0.698	-0.040	0.746	0.695	-0.051	-0.296	1.413	-5.323	1.65E-06		2,19E-03	4,986 chr3	OpenSea	Body	ERV1
cg10283505	0.676	0.629	-0.047	0.682	0.632	-0.050	-0.299	0.973	-5.317	1.69E-06		2,19E-03	4,946 chr11	Island	1stExon_3'UTR	FUT4
cg12555086	0.647	0.593	-0.054	0.649	0.582	-0.067	-0.330	0.771	-5.315	1.70E-06		2,19E-03	4,937 chr10	OpenSea	Body	LPA
cg02528681	0.737	0.689	-0.048	0.742	0.683	-0.059	-0.342	1.392	-5.313	1.72E-06		2,19E-03	4,930 chr10	OpenSea	TSS200	ANKRD22

Table S9. Information DEGs Vacc-RMD – Baseline

Biotype distribution gene expression w6-w0				Chr distribution gene expression w6-w0				Chi Square Biotypes						
Biotype	counts	Proportion	Percentage	chromosome	counts	Proportion	Percentage	chromosome	counts	Proportion	Percentage	Biotypes	pval	qval
3prime_overlapping_ncRNA	3	0.00	0	chr1	239	0.11	11	chr16	88	0.04	4	TR_V_gene	9.65E-06	3.28E-04
antisense	90	0.03	3	chr2	138	0.06	6	chr2	138	0.06	6	IG_V_gene	8.83E-04	8.83E-04
bidirectional_promoter_lncRNA	3	0.00	0	chr3	109	0.05	5	chr3	109	0.05	5	sense_intronic	7.79E-05	8.83E-04
lincRNA	104	0.04	4	chr4	75	0.03	3	chr4	75	0.03	3	antisense	8.81E-03	6.31E-02
misc_RNA	11	0.00	0	chr5	88	0.04	4	chr5	88	0.04	4	processed_pseudogene	1.08E-02	6.31E-02
non_coding	1	0.00	0	chr6	84	0.04	4	chr6	84	0.04	4	snoRNA	1.23E-02	6.31E-02
processed_pseudogene	113	0.04	4	chr7	98	0.04	4	chr7	98	0.04	4	unprocessed_pseudogene	7.35E-02	2.96E-01
processed_transcript	34	0.01	1	chr8	71	0.03	3	chr8	71	0.03	3	transcribed_unprocessed_pseudogene	1.00E-00	1.00E-00
protein_coding	2366	0.80	80	chr9	100	0.04	4	chr9	100	0.04	4	TR_C_gene	7.83E-02	2.96E-01
ribozyme	1	0.00	0	chr10	74	0.03	3	chr10	74	0.03	3	sRNA	1.23E-01	4.17E-01
scarRNA	1	0.00	0	chr11	152	0.07	7	chr11	152	0.07	7	IG_C_gene	2.57E-01	7.96E-01
sense_intronic	71	0.02	2	chr12	138	0.06	6	chr12	138	0.06	6	lincRNA	3.09E-01	8.76E-01
sense_overlapping	10	0.00	0	chr13	30	0.01	1	chr13	30	0.01	1	TEC	3.61E-01	9.25E-01
snoRNA	2	0.00	0	chr14	86	0.04	4	chr14	86	0.04	4	3prime_overlapping_ncRNA	3.81E-01	9.25E-01
sRNA	1	0.00	0	chr15	66	0.03	3	chr15	66	0.03	3	protein_coding	4.82E-01	1.00E+00
TEC	48	0.02	2	chr16	122	0.05	5	chr16	122	0.05	5	rRNA	4.85E-01	1.00E+00
TR_C_gene	4	0.00	0	chr17	143	0.06	6	chr17	143	0.06	6	misc_RNA	6.41E-01	1.00E+00
TR_V_gene	35	0.01	1	chr18	22	0.01	1	chr18	22	0.01	1	transcribed_unitary_pseudogene	6.65E-01	1.00E+00
transcribed_processed_pseudogene	18	0.01	1	chr19	176	0.08	8	chr19	176	0.08	8	polymorphic_pseudogene	7.51E-01	1.00E+00
transcribed_unitary_pseudogene	4	0.00	0	chr20	65	0.03	3	chr20	65	0.03	3	processed_transcript	9.06E-01	1.00E+00
transcribed_unprocessed_pseudogene	36	0.01	1	chr21	18	0.01	1	chr21	18	0.01	1	ribozyme	9.39E-01	1.00E+00
unitary_pseudogene	1	0.00	0	chr22	59	0.03	3	chr22	59	0.03	3	sense_overlapping	9.45E-01	1.00E+00
unprocessed_pseudogene	8	0.00	0	chrX	83	0.04	4	chrX	83	0.04	4	scarRNA	9.94E-01	1.00E+00
3prime_overlapping_ncRNA	7	0.00	0	chrY	2	0.00	0	chrY	2	0.00	0	bidirectional_promoter_lncRNA	1.00E-00	1.00E+00
antisense	679	0.04	4	all	1299	0.10	10	all	1299	0.10	10	transcribed_processed_pseudogene	1.00E+00	1.00E+00
bidirectional_promoter_lncRNA	18	0.00	0	chr1	828	0.07	7	chr1	828	0.07	7	ML_RNA	1.00E+00	1.00E+00
IG_C_gene	13	0.00	0	chr2	728	0.06	6	chr2	728	0.06	6	TR_V_pseudogene	1.00E+00	1.00E+00
IG_C_pseudogene	2	0.00	0	chr3	446	0.04	4	chr3	446	0.04	4	IG_V_pseudogene	1.00E+00	1.00E+00
IG_V_gene	98	0.01	1	chr4	547	0.04	4	chr4	547	0.04	4	IG_C_pseudogene	1.00E+00	1.00E+00
IG_V_pseudogene	2	0.00	0	chr5	530	0.04	4	chr5	530	0.04	4	unitary_pseudogene	1.00E+00	1.00E+00
lincRNA	654	0.04	4	chr6	583	0.05	5	chr6	583	0.05	5	non_coding	1.00E+00	1.00E+00
macro_lincRNA	1	0.00	0	chr7	410	0.03	3	chr7	410	0.03	3	translated_processed_pseudogene	1.00E+00	1.00E+00
misc_RNA	50	0.00	0	chr8	499	0.04	4	chr8	499	0.04	4	macro_lincRNA	1.00E+00	1.00E+00
non_coding	3	0.00	0	chr9	468	0.04	4	chr9	468	0.04	4	pseudogene	1.00E+00	1.00E+00
non_coding	3	0.00	0	chr10	726	0.06	6	chr10	726	0.06	6			
processed_pseudogene	5	0.00	0	chr11	701	0.06	6	chr11	701	0.06	6			
processed_transcript	487	0.03	3	chr12	211	0.02	2	chr12	211	0.02	2			
protein_coding	199	0.01	1	chr13	425	0.03	3	chr13	425	0.03	3			
pseudogene	13219	0.79	79	chr14	560	0.04	4	chr14	560	0.04	4			
ribozyme	2	0.00	0	chr15	776	0.06	6	chr15	776	0.06	6			
rRNA	8	0.00	0	chr16	169	0.01	1	chr16	169	0.01	1			
scarRNA	9	0.00	0	chr17	983	0.08	8	chr17	983	0.08	8			
sense_intronic	234	0.01	1	chr18	335	0.03	3	chr18	335	0.03	3			
sense_overlapping	61	0.00	0	chr19	117	0.01	1	chr19	117	0.01	1			
snoRNA	62	0.00	0	chr20	321	0.03	3	chr20	321	0.03	3			
sRNA	29	0.00	0	chr21	422	0.03	3	chr21	422	0.03	3			
snoRNA	231	0.01	1	chr22	14	0.00	0	chr22	14	0.00	0			
TEC	6	0.00	0	chrX				chrX						
TR_C_gene	6	0.00	0	chrY				chrY						
TR_V_gene	81	0.00	0	all				all						
TR_V_pseudogene	2	0.00	0	all				all						
transcribed_processed_pseudogene	99	0.01	1	all				all						
transcribed_unitary_pseudogene	32	0.00	0	all				all						
transcribed_unprocessed_pseudogene	281	0.02	2	all				all						
translated_processed_pseudogene	1	0.00	0	all				all						
unitary_pseudogene	3	0.00	0	all				all						
unprocessed_pseudogene	113	0.01	1	all				all						

Table S9. Information related to differentially expressed genes between Vacc-RMD and BSL

Table S10. Information DMPs Vacc-RMD – Baseline

Table S10. Information related to differentially methylated positions between Vacc-RMD and BSL										Table S10. Information related to differentially methylated positions between Vacc-RMD and BSL												
DMPs vs w0 - Gene relation					Chi-square Gene relation					Relation to Island					Chi-square Relation to Island							
Gene relation	counts	class	Proportion	Percentage	promoter	Gene relation	pval	qual	chromosome	counts	class	Proportion	Percentage	Sum percentage	Island Relation	pval	qual	chromosome	counts	class	Proportion	Percentage
3'UTR	987	DMP	0.06	0.06	6	Body	6.83E-08	4.10E-07	chr19	1639	DMPs	0.10	10	8	Island	9.38E-99	5.63E-98	chr1	1639	DMPs	0.10	10
5'UTR	669	DMP	0.04	0.04	4	TSS200	4.60E-06	1.38E-05	chr1	1078	DMPs	0.07	7	24	OpenSea	4.40E-83	1.24E-82	chr2	1078	DMPs	0.07	7
Body	6783	DMP	0.42	0.42	14	1stExon	1.28E-04	2.95E-04	chr3	917	DMPs	0.06	6	4	S_Shelf	8.83E-99	1.77E-08	chr3	917	DMPs	0.06	6
TSS200	2023	DMP	0.15	0.15	42	TSS1500	7.92E-04	1.79E-03	chr4	625	DMPs	0.04	4	14	N_Shelf	1.75E-05	2.83E-05	chr4	625	DMPs	0.04	4
TSS200	2023	DMP	0.15	0.15	42	3'UTR	2.64E-03	3.14E-03	chr5	653	DMPs	0.04	4	4	S_Shore	1.00E-01	4.88E-01	chr5	653	DMPs	0.04	4
TSS200	2023	DMP	0.15	0.15	42	3'UTR	6.74E-02	6.74E-02	chr5	1223	DMPs	0.08	8	4	N_Shore	7.08E-01	7.08E-01	chr5	1223	DMPs	0.08	8
3'UTR	3458	all	0.07	0.07	7	Body	0.00	0.00	chr6	948	DMPs	0.06	6	4	all	0.00	0.00	chr6	948	DMPs	0.06	6
3'UTR	3458	all	0.04	0.04	4	N_Shelf	0.00	0.00	chr8	607	DMPs	0.04	4	3	all	0.00	0.00	chr8	607	DMPs	0.04	4
5'UTR	11502	all	0.13	0.13	13	OpenSea	0.00	0.00	chr9	272	DMPs	0.02	2	14	all	0.00	0.00	chr9	272	DMPs	0.02	2
Body	35792	all	0.40	0.40	40	OpenSea	2.65E-43	2.65E-43	chr10	756	DMPs	0.05	5	29	all	0.00	0.00	chr10	756	DMPs	0.05	5
TSS1500	17947	all	0.20	0.20	20	S_Shelf	2.57E-3	2.57E-3	chr11	988	DMPs	0.06	6	3	all	0.00	0.00	chr11	988	DMPs	0.06	6
TSS200	15060	all	0.17	0.17	17	S_Shore	9.80E-6	9.80E-6	chr12	873	DMPs	0.05	5	11	all	0.00	0.00	chr12	873	DMPs	0.05	5

Table S10. Information related to differentially methylated positions between Vacc-RMD and BSL									
Relation to Island					Chi-square Relation to Island				
chromosome	counts	class	Proportion	Percentage	Island Relation	pval	qual	chromosome	counts
chr1	1639	DMPs	0.10	10	Island	9.38E-99	5.63E-98	chr1	1639
chr2	1078	DMPs	0.07	7	OpenSea	4.40E-83	1.24E-82	chr2	1078
chr3	917	DMPs	0.06	6	S_Shelf	8.83E-99	1.77E-08	chr3	917
chr4	625	DMPs	0.04	4	N_Shelf	1.75E-05	2.83E-05	chr4	625
chr5	1223	DMPs	0.08	8	S_Shore	1.00E-01	4.88E-01	chr5	1223
chr6	948	DMPs	0.06	6	N_Shore	7.08E-01	7.08E-01	chr6	948
chr7	521	DMPs	0.03	3	all	0.00	0.00	chr7	521
chr8	607	DMPs	0.04	4	all	0.00	0.00	chr8	607
chr9	272	DMPs	0.02	2	all	0.00	0.00	chr9	272
chr10	756	DMPs	0.05	5	all	0.00	0.00	chr10	756
chr11	988	DMPs	0.06	6	all	0.00	0.00	chr11	988
chr12	873	DMPs	0.05	5	all	0.00	0.00	chr12	873
chr13	338	DMPs	0.02	2	all	0.00	0.00	chr13	338
chr14	459	DMPs	0.03	3	all	0.00	0.00	chr14	459
chr15	463	DMPs	0.03	3	all	0.00	0.00	chr15	463
chr16	575	DMPs	0.04	4	all	0.00	0.00	chr16	575
chr17	978	DMPs	0.06	6	all	0.00	0.00	chr17	978
chr18	209	DMPs	0.01	1	all	0.00	0.00	chr18	209
chr19	864	DMPs	0.05	5	all	0.00	0.00	chr19	864
chr20	402	DMPs	0.02	2	all	0.00	0.00	chr20	402
chr21	177	DMPs	0.01	1	all	0.00	0.00	chr21	177
chr22	285	DMPs	0.02	2	all	0.00	0.00	chr22	285
chrX	588	DMPs	0.04	4	all	0.00	0.00	chrX	588
chrY	17	DMPs	0.00	0	all	0.00	0.00	chrY	17
chr1	8600	all	0.10	10	all	0.00	0.00	chr1	8600
chr2	5963	all	0.07	7	all	0.00	0.00	chr2	5963
chr3	4709	all	0.05	5	all	0.00	0.00	chr3	4709
chr4	3719	all	0.04	4	all	0.00	0.00	chr4	3719
chr5	4628	all	0.05	5	all	0.00	0.00	chr5	4628
chr6	6904	all	0.08	8	all	0.00	0.00	chr6	6904
chr7	5261	all	0.06	6	all	0.00	0.00	chr7	5261
chr8	3623	all	0.04	4	all	0.00	0.00	chr8	3623
chr9	1922	all	0.02	2	all	0.00	0.00	chr9	1922
chr10	4420	all	0.05	5	all	0.00	0.00	chr10	4420
chr11	5277	all	0.06	6	all	0.00	0.00	chr11	5277
chr12	4544	all	0.05	5	all	0.00	0.00	chr12	4544
chr13	2051	all	0.02	2	all	0.00	0.00	chr13	2051
chr14	2526	all	0.03	3	all	0.00	0.00	chr14	2526
chr15	2723	all	0.03	3	all	0.00	0.00	chr15	2723
chr16	3376	all	0.04	4	all	0.00	0.00	chr16	3376
chr17	5125	all	0.06	6	all	0.00	0.00	chr17	5125
chr18	1070	all	0.01	1	all	0.00	0.00	chr18	1070
chr19	1520	all	0.02	2	all	0.00	0.00	chr19	1520
chr20	2310	all	0.03	3	all	0.00	0.00	chr20	2310
chr21	935	all	0.01	1	all	0.00	0.00	chr21	935
chr22	1676	all	0.02	2	all	0.00	0.00	chr22	1676
chrX	3353	all	0.04	4	all	0.00	0.00	chrX	3353
chrY	117	all	0.00	0	all	0.00	0.00	chrY	117

Table S11. Top100 DEGs post-pre RMD in PBMcs

Table S11. Top100 (p-value) differentially expressed genes between post-RMD and pre-RMD in PBMcs of REDUC clinical trial	Mean_v1	Mean_v9	DiffMean	Median_v1	Median_v9	DiffMedian	logFC	AveExpr	t	P.Value	adj.P.Val	B
ENSG00000130783.14.CC2C62.protein_coding	0.426	-0.282	-0.708	0.302	-0.262	-0.564	-0.708	0.072	-6.850	4.58E-05	6.64E-01	-1.509
ENSG00000242615.1.ACO22415.1.transcribed_processed_pseudogene	0.614	-0.017	-0.632	0.559	-0.166	-0.724	-0.632	0.298	-5.898	1.55E-04	7.56E-01	-1.785
ENSG00000286532.1.PARTICL.lncRNA	0.493	1.027	0.534	0.535	0.947	0.412	0.534	0.760	5.723	1.96E-04	7.56E-01	-1.845
ENSG00000174944.9.P2RY14.protein_coding	3.208	2.436	-0.773	3.305	2.418	-0.887	-0.773	2.822	-5.294	3.57E-04	7.56E-01	-2.005
ENSG00000283149.1.AC068631.2.protein_coding	0.616	-0.134	-0.750	0.554	-0.131	-0.685	-0.750	0.241	-5.105	4.69E-04	7.56E-01	-2.083
ENSG00000143498.18.TAF1A.protein_coding	2.864	2.477	-0.387	2.772	2.400	-0.372	-0.387	2.671	-5.073	4.91E-04	7.56E-01	-2.096
ENSG00000186446.12.ZNF501.protein_coding	2.289	1.976	-0.313	2.235	2.021	-0.214	-0.313	2.133	-5.071	4.93E-04	7.56E-01	-2.097
ENSG00000246273.8.SBF2-AS1.lncRNA	2.237	1.701	-0.537	2.273	1.646	-0.627	-0.537	1.969	-5.043	5.13E-04	7.56E-01	-2.109
ENSG00000137265.15.IRF4.protein_coding	5.832	5.386	-0.446	5.953	5.489	-0.464	-0.446	5.609	-4.940	5.97E-04	7.56E-01	-2.154
ENSG00000211973.2.IGHV1_69.IG_V_gene	1.225	0.127	-1.098	1.122	0.497	-0.625	-1.098	0.676	-4.870	6.62E-04	7.56E-01	-2.185
ENSG00000137936.18.BCAR3.protein_coding	0.502	-0.037	-0.538	0.379	-0.003	-0.381	-0.538	0.233	-4.815	7.19E-04	7.56E-01	-2.210
ENSG00000198342.10.ZNF442.protein_coding	1.339	0.795	-0.545	1.441	0.761	-0.680	-0.545	1.067	-4.789	7.47E-04	7.56E-01	-2.222
ENSG00000272146.6.ARF4-AS1.lncRNA	0.058	0.669	0.611	0.160	0.857	0.697	0.611	0.364	4.744	7.99E-04	7.56E-01	-2.243
ENSG00000211942.3.IGHV3_13.IG_V_gene	0.518	-0.234	-0.752	0.198	-0.421	-0.619	-0.752	0.142	-4.694	8.61E-04	7.56E-01	-2.266
ENSG00000279520.1.AC093525.8.TEC	1.434	2.031	0.597	1.467	2.066	0.599	0.597	1.732	4.663	9.04E-04	7.56E-01	-2.281
ENSG00000164236.12.ANKRD338.protein_coding	1.342	0.001	-0.523	3.599	2.897	-0.702	-0.523	3.252	-4.612	9.76E-04	7.56E-01	-2.306
ENSG00000255508.7.APO02990.1.protein_coding	0.507	0.993	0.486	0.490	0.873	0.383	0.486	0.750	4.581	1.02E-03	7.56E-01	-2.321
ENSG00000161638.11.ITGA5.protein_coding	7.019	7.440	0.421	7.092	7.400	0.307	0.421	7.229	4.571	1.04E-03	7.56E-01	-2.326
ENSG00000270177.1.AC104109.2.lncRNA	0.109	0.817	0.708	0.188	1.195	1.007	0.708	0.463	4.565	1.05E-03	7.56E-01	-2.329
ENSG00000168502.17.MTC11.protein_coding	0.712	-0.147	-0.860	1.097	0.045	-1.052	-0.860	0.282	-4.552	1.07E-03	7.56E-01	-2.335
ENSG00000163376.11.KBTBD8.protein_coding	4.420	3.897	-0.523	4.452	3.858	-0.594	-0.523	4.158	-4.537	1.09E-03	7.56E-01	-2.342
ENSG00000151748.15.SAV1.protein_coding	4.246	3.811	-0.435	4.291	3.826	-0.465	-0.435	4.029	-4.404	1.34E-03	7.56E-01	-2.410
ENSG00000156172.6.C8orf37.protein_coding	1.572	1.155	-0.416	1.550	1.137	-0.413	-0.416	1.363	-4.402	1.35E-03	7.56E-01	-2.411
ENSG00000231475.3.IGHV4_31.IG_V_gene	1.780	0.669	-1.111	1.764	0.645	-1.119	-1.111	1.225	-4.372	1.41E-03	7.56E-01	-2.427
ENSG00000128641.19.MYB19.protein_coding	2.401	0.603	-1.797	2.305	0.709	-1.597	-1.797	1.502	-3.364	1.43E-03	7.56E-01	-2.431
ENSG00000232220.3.LINC00167.lncRNA	-0.311	0.625	0.946	-0.170	0.888	1.058	0.946	0.162	3.860	1.44E-03	7.56E-01	-2.433
ENSG00000235609.7.AF127577.4.lncRNA	0.981	0.630	-0.352	1.041	0.636	-0.405	-0.352	0.806	-4.236	1.75E-03	7.56E-01	-2.498
ENSG00000088451.11.TCDS.protein_coding	3.710	3.394	-0.316	3.716	3.414	-0.302	-0.316	3.552	-4.219	1.80E-03	7.56E-01	-2.508
ENSG00000286177.1.AC011462.5.lncRNA	1.860	2.351	0.491	1.835	2.442	0.606	0.491	2.105	4.208	1.83E-03	7.56E-01	-2.514
ENSG0000044574.8.HSPA5.protein_coding	6.846	7.191	0.345	6.871	7.139	0.268	0.345	7.018	4.185	1.89E-03	7.56E-01	-2.526
ENSG00000240137.6.ERIC6-AS1.lncRNA	1.399	1.729	0.331	1.265	1.775	0.510	0.331	1.564	4.183	1.90E-03	7.56E-01	-2.527
ENSG00000158156.9.KKR8.protein_coding	3.879	4.271	0.392	3.947	4.146	0.199	0.392	4.075	4.168	1.95E-03	7.56E-01	-2.535
ENSG00000260339.1.HEXA-AS1.lncRNA	-0.154	0.385	0.539	-0.036	0.448	0.483	0.539	0.116	4.163	1.96E-03	7.56E-01	-2.538
ENSG00000157654.19.PALM2AKAP2.protein_coding	6.213	5.789	-0.423	6.171	5.749	-0.422	-0.423	6.001	-4.110	2.14E-03	7.56E-01	-2.568
ENSG00000214827.11.MTC11.protein_coding	0.299	0.656	0.356	0.366	0.636	0.270	0.356	0.477	4.086	2.22E-03	7.56E-01	-2.581
ENSG00000154359.13.LONRF1.protein_coding	3.642	3.191	-0.452	3.750	3.399	-0.351	-0.452	3.417	-4.083	2.23E-03	7.56E-01	-2.583
ENSG00000133119.13.RFC3.protein_coding	2.798	2.492	-0.306	2.728	2.488	-0.241	-0.306	2.645	-4.056	2.33E-03	7.56E-01	-2.598
ENSG00000269834.6.ZNF528-AS1.lncRNA	0.615	0.115	-0.500	0.606	0.188	-0.417	-0.500	0.365	-4.037	2.40E-03	7.56E-01	-2.609
ENSG00000136197.12.C7orf25.protein_coding	0.754	0.403	-0.351	0.879	0.393	-0.486	-0.351	0.579	-4.030	2.43E-03	7.56E-01	-2.613
ENSG00000198369.10.SPRED2.protein_coding	0.544	1.082	0.538	0.691	1.235	0.544	0.538	0.813	3.994	2.57E-03	7.56E-01	-2.633
ENSG00000121753.12.ADGRB2.protein_coding	0.399	1.155	0.757	0.510	1.085	0.575	0.757	0.777	3.961	2.71E-03	7.56E-01	-2.653
ENSG00000227398.4.KIF9-AS1.lncRNA	1.127	1.498	0.371	1.122	1.430	0.308	0.371	1.313	3.950	2.76E-03	7.56E-01	-2.659
ENSG00000164050.13.PLXNB1.protein_coding	0.892	1.686	0.794	0.820	1.749	0.929	0.794	1.289	3.948	2.77E-03	7.56E-01	-2.660
ENSG00000188542.10.DUSP28.protein_coding	3.294	3.554	0.260	3.359	3.586	0.227	0.260	3.424	3.927	2.87E-03	7.56E-01	-2.673
ENSG00000286931.1.ALT36419.3.lncRNA	0.057	0.413	0.357	0.028	0.396	0.369	0.357	0.235	3.926	2.87E-03	7.56E-01	-2.673
ENSG00000244115.1.DNAJC25-GNG10.p.protein_coding	1.587	1.918	0.331	1.719	1.999	0.280	0.331	1.753	3.907	2.96E-03	7.56E-01	-2.684
ENSG00000283064.1.ALS3759.1.lncRNA	0.394	0.895	0.501	0.636	1.070	0.433	0.501	0.645	3.898	3.00E-03	7.56E-01	-2.689
ENSG00000186265.10.BTLA.protein_coding	5.797	5.171	-0.626	5.695	5.326	-0.370	-0.626	5.484	-3.856	3.21E-03	7.56E-01	-2.714
ENSG00000144468.17.RHBDD1.protein_coding	5.352	5.120	-0.232	5.410	5.172	-0.238	-0.232	5.236	-3.854	3.22E-03	7.56E-01	-2.716
ENSG00000176058.13.TPRN.protein_coding	2.548	2.860	0.312	2.619	2.809	0.190	0.312	2.704	3.854	3.22E-03	7.56E-01	-2.716
ENSG00000130270.16.ATP8B3.protein_coding	1.311	1.657	0.347	1.277	1.503	0.226	0.347	1.484	3.850	3.25E-03	7.56E-01	-2.718
ENSG00000196263.8.ZNF471.protein_coding	0.402	-0.711	-1.113	0.575	-0.386	-0.962	-1.113	-0.154	-3.844	3.27E-03	7.56E-01	-2.721
ENSG00000189057.11.FAM111B.protein_coding	2.356	1.417	-0.940	2.353	1.362	-0.991	-0.940	1.887	-3.837	3.32E-03	7.56E-01	-2.726
ENSG00000184786.6.TCE3.protein_coding	1.475	1.920	0.445	1.544	2.007	0.464	0.445	1.698	3.811	3.46E-03	7.56E-01	-2.741
ENSG00000145569.6.TULUL1.protein_coding	5.656	5.958	0.302	5.738	5.986	0.249	0.302	5.807	3.808	3.48E-03	7.56E-01	-2.743
ENSG00000109272.4.PF4V1.protein_coding	1.684	0.044	-1.641	1.262	0.127	-1.135	-1.641	0.864	-3.801	3.51E-03	7.56E-01	-2.747
ENSG00000119333.11.WDR34.protein_coding	2.319	1.847	-0.472	2.235	1.806	-0.429	-0.472	2.083	-3.788	3.59E-03	7.56E-01	-2.755
ENSG00000149218.5.ENDOD1.protein_coding	5.763	5.508	-0.255	5.675	5.466	-0.209	-0.255	5.635	-3.782	3.63E-03	7.56E-01	-2.759
ENSG00000176160.11.HSF5.protein_coding	1.676	1.092	-0.584	1.835	1.085	-0.750	-0.584	1.384	-3.776	3.66E-03	7.56E-01	-2.763
ENSG00000117322.18.CR2.protein_coding	4.455	3.376	-1.078	4.518	3.371	-1.147	-1.078	3.915	-3.774	3.67E-03	7.56E-01	-2.764
ENSG00000106829.20.TLE4.protein_coding	6.037	6.278	0.241	6.077	6.193	0.115	0.241	6.157	3.758	3.77E-03	7.56E-01	-2.774
ENSG00000175544.13.CABP4.protein_coding	1.081	0.500	-0.581	1.041	0.422	-0.619	-0.581	0.790	-3.754	3.79E-03	7.56E-01	-2.776
ENSG00000196724.13.ZNF418.protein_coding	2.647	2.120	-0.528	2.693	2.226	-0.467	-0.528	2.383	-3.740	3.88E-03	7.56E-01	-2.784
ENSG00000130382.9.MLLT1.protein_coding	4.914	5.152	0.238	4.860	5.199	0.339	0.238	5.033	3.738	3.90E-03	7.56E-01	-2.786
ENSG00000102755.12.FLT1.protein_coding	1.476	0.786	-0.690	1.440	0.769	-0.677	-0.690	1.131	-3.735	3.92E-03	7.56E-01	-2.788
ENSG00000122591.12.FAM126A.protein_coding	5.945	5.725	-0.221	5.907	5.718	-0.190	-0.221	5.835	-3.724	3.99E-03	7.56E-01	-2.794
ENSG000000008516.17.MMP25.protein_coding	1.593	2.282	0.689	1.414	2.506	1.092	0.689	1.937	3.722	4.00E-03	7.56E-01	-2.796
ENSG00000197299.12.BLM.protein_coding	3.951	3.673	-0.278	3.926	3.621	-0.305	-0.278	3.812	-3.713	4.06E-03	7.56E-01	-2.801
ENSG00000079819.19.EPB41L2.protein_coding	4.069	3.606	-0.463	4.126	3.460	-0.666	-0.463	3.838	-3.710	4.08E-03	7.56E-01	-2.803
ENSG00000101849.17.TBL1X.protein_coding	5.237	5.504	0.267	5.214	5.626	0.412	0.267	5.371	3.702	4.13E-03	7.56E-01	-2.808
ENSG00000223797.6.ENTPD3-AS1.lncRNA	1.342	0.999	-0.342	1.350	1.137	-0.213	-0.342	1.171	-3.675	4.32E-03	7.56E-01	-2.825
ENSG00000105497.8.ZNF175.protein_coding	4.152	3.974	-0.179	4.149	3.978	-0.171	-0.179	4.063	-3.633	4.63E-03	7.56E-01	-2.851
ENSG00000130348.11.QRS11.protein_coding	5.058	4.688	-0.370	5.099	4.654	-0.444	-0.370	4.873	-3.621	4.72E-03	7.56E-01	-2.859
ENSG00000173715.18.C11orf80.protein_coding	2.917	2.397	-0.520	2.758	2.264	-0.494	-0.520	2.657	-3.620	4.73E-03	7.56E-01	-2.859
ENSG00000277369.1.AC010654.1.lncRNA	0.172	0.797	0.625	0.394	0.840	0.447	0.625	0.484	3.613	4.78E-03	7.56E-01	-2.864
ENSG00000166086.13.JAM3.protein_coding	4.101	3.429	-0.672	3.940								

Table S12. Top100 DEGs post-pre RMD in isolated CD4 T-cells

Table S12. Top100 (p-value) differentially expressed genes between post-RMD and pre-RMD in CD4 of REDUC clinical trial

	Mean_v1	Mean_v9	DiffMean	Median_v1	Median_v9	DiffMedian	logFC	AveExpr	t	P.Value	adj.P.Val	B
ENSG0000025395.6.FCGBP.protein_coding	4.762	5.843	1.081	4.709	5.916	1.207	1.081	5.303	7.793	1.61E-05	2.28E-01	2.418
ENSG00000136854.23.STXB1.protein_coding	-0.013	1.051	1.063	0.177	0.878	0.701	1.063	0.519	6.576	6.71E-05	2.75E-01	1.482
ENSG00000134245.18.WNT2B.protein_coding	-0.395	0.658	1.052	-0.286	0.740	1.026	1.052	0.131	6.329	9.16E-05	2.75E-01	1.265
ENSG00000008277.14.ADM22.protein_coding	1.652	2.188	0.536	1.601	2.232	0.631	0.536	1.920	6.233	1.04E-04	2.75E-01	1.177
ENSG00000151612.18.ZNF827.protein_coding	3.613	4.085	0.472	3.618	4.097	0.479	0.472	3.849	6.070	1.28E-04	2.75E-01	1.026
ENSG00000124466.9.LYPD3.protein_coding	0.542	1.389	0.847	0.462	1.258	0.796	0.847	0.966	5.913	1.58E-04	2.75E-01	0.875
ENSG00000182551.14.ADI1.protein_coding	5.255	4.755	-0.500	5.329	4.796	-0.533	-0.500	5.005	-5.886	1.63E-04	2.75E-01	0.849
ENSG00000236753.7.MKLN1-AS1.lncRNA	0.004	0.948	0.944	-0.051	1.055	1.106	0.944	0.476	5.819	1.78E-04	2.75E-01	0.784
ENSG00000225151.10.GOLGA2P7.transcribed_unprocessed	3.009	3.763	0.754	2.962	3.948	0.985	0.754	3.386	5.693	2.12E-04	2.75E-01	0.658
ENSG00000164989.17.CCDC171.protein_coding	0.782	1.722	0.940	0.716	1.691	0.975	0.940	1.252	5.632	2.00E-04	2.75E-01	0.596
ENSG00000164440.15.TXNBP1.protein_coding	1.779	2.528	0.749	1.689	2.620	0.931	0.749	2.154	5.568	2.51E-04	2.75E-01	0.530
ENSG00000271964.1.ACO90948.1.lncRNA	1.160	2.028	0.868	1.388	2.146	0.757	0.868	1.594	5.517	2.70E-04	2.75E-01	0.477
ENSG00000151320.11.AKAP6.protein_coding	1.719	2.706	0.987	1.720	2.772	1.051	0.987	2.213	5.417	3.10E-04	2.75E-01	0.372
ENSG00000131100.13.ATP6V1E1.protein_coding	6.351	6.047	-0.304	6.336	6.051	-0.285	-0.304	6.199	-5.392	3.21E-04	2.75E-01	0.345
ENSG00000213190.4.MLLT11.protein_coding	1.602	2.124	0.523	1.608	2.110	0.502	0.523	1.863	5.312	3.59E-04	2.75E-01	0.259
ENSG00000161677.12.JOSD2.protein_coding	2.511	2.068	-0.443	2.554	2.022	-0.532	-0.443	2.290	-5.284	3.73E-04	2.75E-01	0.230
ENSG00000114480.13.GBE1.protein_coding	3.906	3.565	-0.342	3.907	3.570	-0.337	-0.342	3.735	-5.282	3.74E-04	2.75E-01	0.228
ENSG00000171044.11.XKR6.protein_coding	0.985	1.462	0.477	1.039	1.464	0.425	0.477	1.223	5.263	3.85E-04	2.75E-01	0.206
ENSG00000174276.7.ZNF127.protein_coding	2.703	2.047	-0.656	2.779	2.012	-0.767	-0.656	2.375	-5.238	3.99E-04	2.75E-01	0.180
ENSG00000204650.14.LINC02210.transcribed_unitary_pse	4.094	4.544	0.450	4.106	4.616	0.510	0.450	4.319	5.110	4.79E-04	2.75E-01	0.038
ENSG00000183662.5.1.TAFA11.protein_coding	1.586	2.374	0.788	1.634	2.511	0.877	0.788	1.980	5.036	5.33E-04	2.75E-01	-0.045
ENSG00000113732.9.ATP6V0E1.protein_coding	6.982	6.649	-0.333	6.979	6.624	-0.355	-0.333	6.816	-5.019	5.46E-04	2.75E-01	-0.064
ENSG00000261000.1.AC24034.2.lncRNA	-0.778	0.487	1.265	-0.801	0.651	1.453	1.265	-0.146	4.996	5.65E-04	2.75E-01	-0.090
ENSG00000226200.7.SGMS1-AS1.lncRNA	2.538	3.173	0.635	2.673	3.204	0.531	0.635	2.856	4.996	5.65E-04	2.75E-01	-0.090
ENSG00000119328.12.ABITRAM.protein_coding	3.231	2.722	-0.508	3.226	2.604	-0.621	-0.508	2.976	-4.990	5.70E-04	2.75E-01	-0.098
ENSG00000186814.14.ZSCAN30.protein_coding	3.652	4.184	0.532	3.561	4.143	0.583	0.532	3.918	4.985	5.74E-04	2.75E-01	-0.103
ENSG00000249825.6.CTD-201118.1.lncRNA	0.910	1.547	0.637	0.942	1.652	0.742	0.637	1.228	4.979	5.79E-04	2.75E-01	-0.110
ENSG00000120697.9.ALG5.protein_coding	4.171	3.787	-0.385	4.209	3.731	-0.478	-0.385	3.979	-4.943	6.11E-04	2.75E-01	-0.151
ENSG00000128040.11.SPINK2.protein_coding	-0.226	1.098	1.324	-0.076	1.424	1.501	1.324	0.436	4.887	6.64E-04	2.75E-01	-0.216
ENSG00000129255.16.MPDJ1.protein_coding	4.793	4.377	-0.416	4.801	4.323	-0.478	-0.416	4.585	-4.883	6.67E-04	2.75E-01	-0.220
ENSG00000272502.1.AC104958.2.lncRNA	0.150	0.794	0.644	0.017	0.736	0.719	0.644	0.472	4.837	7.14E-04	2.75E-01	-0.273
ENSG00000204220.12.PFDN6.protein_coding	4.078	3.741	-0.337	4.127	3.787	-0.340	-0.337	3.910	-4.831	7.20E-04	2.75E-01	-0.280
ENSG00000224903.2.RNF32-AS1.lncRNA	0.036	0.781	0.745	-0.063	0.775	0.838	0.745	0.408	4.796	7.59E-04	2.75E-01	-0.322
ENSG0000017732.8.SOX12.protein_coding	2.428	3.330	0.902	2.386	3.582	1.195	0.902	2.879	4.761	8.00E-04	2.75E-01	-0.363
ENSG00000161835.11.TAMALIN.protein_coding	3.043	3.576	0.533	3.022	3.630	0.608	0.533	3.309	4.744	8.20E-04	2.75E-01	-0.383
ENSG00000284055.1.APO01273.2.protein_coding	1.680	-0.164	-1.843	1.882	-0.220	-2.101	-1.843	0.758	-4.738	8.28E-04	2.75E-01	-0.390
ENSG00000110092.4.CCND1.protein_coding	0.082	1.208	1.126	0.215	1.245	1.030	1.126	0.645	4.726	8.42E-04	2.75E-01	-0.404
ENSG00000162971.11.TYW5.protein_coding	3.369	3.971	0.421	3.443	3.765	0.323	0.421	3.580	4.687	8.93E-04	2.75E-01	-0.450
ENSG00000154723.12.ATP5PF.protein_coding	4.506	4.141	-0.365	4.574	4.071	-0.503	-0.365	4.324	-4.663	9.26E-04	2.75E-01	-0.479
ENSG00000088899.15.LZTS3.protein_coding	1.414	2.156	0.742	1.501	2.136	0.635	0.742	1.785	4.661	9.29E-04	2.75E-01	-0.482
ENSG00000131779.11.PEX1B.protein_coding	4.695	4.413	-0.281	4.654	4.421	-0.233	-0.281	4.554	-4.623	9.84E-04	2.75E-01	-0.528
ENSG00000065361.16.ERBB3.protein_coding	-0.226	0.578	0.804	-0.157	0.495	0.652	0.804	0.176	4.622	9.85E-04	2.75E-01	-0.529
ENSG00000245552.7.AP000787.1.lncRNA	2.353	2.702	0.350	2.385	2.706	0.321	0.350	2.528	4.606	1.01E-03	2.75E-01	-0.549
ENSG00000225035.5.AL162586.1.lncRNA	1.574	2.434	0.860	1.700	2.476	0.776	0.860	2.004	4.590	1.03E-03	2.75E-01	-0.568
ENSG00000131019.11.ULBP3.protein_coding	0.812	1.330	0.518	0.759	1.248	0.490	0.518	1.071	4.554	1.09E-03	2.75E-01	-0.611
ENSG00000136379.12.ABHD17A.protein_coding	0.887	1.662	0.775	1.131	1.704	0.573	0.775	1.274	4.534	1.13E-03	2.75E-01	-0.636
ENSG00000141543.12.EIF4A3.protein_coding	5.826	5.557	-0.268	5.871	5.563	-0.308	-0.268	5.692	4.521	1.15E-03	2.75E-01	-0.652
ENSG00000162337.12.LRP5.protein_coding	1.021	1.830	0.809	1.003	1.960	0.957	0.809	1.425	4.515	1.16E-03	2.75E-01	-0.659
ENSG00000163013.11.FBXO41.protein_coding	3.745	4.237	0.492	3.694	4.164	0.470	0.492	3.991	4.507	1.17E-03	2.75E-01	-0.669
ENSG00000141873.11.SLC39A3.protein_coding	4.069	3.702	-0.367	4.100	3.730	-0.371	-0.367	3.886	-4.501	1.18E-03	2.75E-01	-0.677
ENSG00000228486.10.C2orf92.protein_coding	0.157	1.101	0.943	-0.003	1.097	1.100	0.943	0.629	4.500	1.19E-03	2.75E-01	-0.678
ENSG00000184076.13.UQCRO17.protein_coding	5.425	5.167	-0.257	5.441	5.165	-0.277	-0.257	5.296	-4.476	1.23E-03	2.75E-01	-0.707
ENSG00000231999.7.LRRBC-DT.lncRNA	2.392	2.922	0.531	2.468	2.953	0.485	0.531	2.657	4.470	1.24E-03	2.75E-01	-0.714
ENSG00000188079.9.C11orf95.protein_coding	2.198	3.127	0.929	2.198	3.173	0.975	0.929	2.663	4.445	1.29E-03	2.75E-01	-0.745
ENSG00000188706.13.ZDHHC9.protein_coding	1.569	2.377	0.808	1.456	2.585	1.128	0.808	1.973	4.426	1.33E-03	2.75E-01	-0.769
ENSG00000178449.9.COX14.protein_coding	4.558	4.242	-0.316	4.571	4.225	-0.347	-0.316	4.400	-4.419	1.34E-03	2.75E-01	-0.777
ENSG00000245573.9.BDNF-AS.lncRNA	-0.054	0.621	0.675	-0.125	0.666	0.791	0.675	0.284	4.413	1.35E-03	2.75E-01	-0.785
ENSG00000117862.13.TXNDC12.protein_coding	5.538	5.278	-0.260	5.508	5.265	-0.244	-0.260	5.408	-4.411	1.36E-03	2.75E-01	-0.788
ENSG00000165060.15.FNXC.protein_coding	3.494	3.864	0.370	3.565	3.866	0.302	0.370	3.679	4.409	1.37E-03	2.75E-01	-0.791
ENSG00000213923.13.CSNK1E.protein_coding	5.093	5.404	0.311	5.100	5.405	0.305	0.311	5.248	4.400	1.38E-03	2.75E-01	-0.801
ENSG00000072506.13.HSD17B10.protein_coding	4.933	4.581	-0.353	4.960	4.685	-0.275	-0.353	4.757	-4.399	1.39E-03	2.75E-01	-0.803
ENSG00000140545.15.MFGE8.protein_coding	3.519	3.982	0.464	3.402	4.075	0.673	0.464	3.750	4.389	1.41E-03	2.75E-01	-0.815
ENSG00000125148.7.MT2A.protein_coding	3.633	4.147	0.515	3.616	4.266	0.650	0.515	3.890	4.387	1.41E-03	2.75E-01	-0.818
ENSG00000213949.10.ITGA1.protein_coding	2.383	3.598	1.215	2.232	3.808	1.577	1.215	2.990	4.378	1.43E-03	2.75E-01	-0.829
ENSG00000133639.6.BTG1.protein_coding	9.125	9.520	0.395	9.134	9.557	0.422	0.395	9.323	4.375	1.44E-03	2.75E-01	-0.833
ENSG0000021995.5.TIAF1.protein_coding	1.629	2.022	0.393	1.641	2.024	0.383	0.393	1.826	4.371	1.45E-03	2.75E-01	-0.838
ENSG00000166762.19.CATSPEK2.protein_coding	0.204	1.064	0.860	0.359	1.123	0.764	0.860	0.634	4.368	1.45E-03	2.75E-01	-0.842
ENSG00000156411.10.ATP5MPL.protein_coding	5.702	5.368	-0.335	5.769	5.381	-0.388	-0.335	5.535	-4.367	1.46E-03	2.75E-01	-0.843
ENSG00000223960.7.CHROMR.lncRNA	2.714	3.308	0.594	2.677	3.236	0.649	0.594	3.011	4.365	1.46E-03	2.75E-01	-0.845
ENSG00000178809.11.TRIM73.protein_coding	1.525	2.388	0.863	1.682	2.513	0.831	0.863	1.957	4.365	1.46E-03	2.75E-01	-0.845
ENSG00000106012.18.IQCE.protein_coding	3.930	3.529	-0.400	3.990	3.500	-0.490	-0.400	3.729	-4.360	1.47E-03	2.75E-01	-0.852
ENSG00000214827.11.MTCP1.protein_coding	0.101	0.649	0.548	0.017	0.522	0.505	0.548	0.375	4.356	1.48E-03	2.75E-01	-0.857
ENSG00000166348.18.USP54.protein_coding	2.272	2.941	0.670	2.206	2.926	0.720	0.670	2.607	4.346	1.50E-03	2.75E-01	-0.870
ENSG00000274114.2.ALOX15P1.transcribed_unprocessed	1.545	1.984	0.439	1.481	2.045	0.564	0.439	1.765	4.345	1.51E-03	2.75E-01	-0.871
ENSG00000181350.12.LRRK7A.protein_coding	2.172	2.480	0.308	2.120	2.495	0.375	0.308	2.326	4.338	1.52E-03	2.75E-01	-0.879
ENSG00000287387.1.ACO10883.												

Table S13. GSEA results

Formatted Name	MES (DMAM BCR02)	MES (Gene expression BCR02)	MES (CD4 - REDUC)	MES (PBMC - REDUC)	MES (DMAM BCR02)	MES (Gene expression BCR02)	MES (CD4 - REDUC)	MES (PBMC - REDUC)	MES (DMAM BCR02)	MES (Gene expression BCR02)	qual (CD4 - REDUC)	qual (PBMC - REDUC)
Cell cycle mitotic	-1.04	-2.41	2.80	-1.46	4.14E-01	0.00E+00	0.00E+00	9.72E-02	7.53E-01	7.05E-04	0.00E+00	2.88E-01
Metabolic disease	-1.00	-2.30	-3.03	-0.78	2.02E-01	0.00E+00	0.00E+00	7.46E-01	1.21E-01	1.20E-02	0.00E+00	7.96E-01
Cell cycle and mitosis	-1.00	-2.30	-3.03	-0.78	2.02E-01	0.00E+00	0.00E+00	7.46E-01	1.21E-01	1.20E-02	0.00E+00	7.96E-01
Enriched in myeloid cells and monocytes (M81)	-1.04	-2.41	2.80	-1.46	4.14E-01	0.00E+00	0.00E+00	9.72E-02	7.53E-01	7.05E-04	0.00E+00	2.88E-01
Rho GTPase effectors	-1.04	-2.41	2.80	-1.46	4.14E-01	0.00E+00	0.00E+00	9.72E-02	7.53E-01	7.05E-04	0.00E+00	2.88E-01
Activation of the mRNA upon binding of the cap-binding complex and eIFs, and subsequent binding to 43S	0.98	-2.45	-3.42	-1.76	1.88E-01	0.00E+00	0.00E+00	2.14E-02	6.91E-01	6.00E-04	0.00E+00	1.14E-01
Cell cycle checkpoints	1.18	-1.85	-3.42	-1.76	1.88E-01	0.00E+00	0.00E+00	2.14E-02	6.91E-01	6.00E-04	0.00E+00	1.14E-01
Cell cycle and mitosis	-1.10	-1.85	-3.42	-1.76	1.88E-01	0.00E+00	0.00E+00	2.14E-02	6.91E-01	6.00E-04	0.00E+00	1.14E-01
Post-transcriptional gene silencing by RNA	-0.98	-0.95	-2.81	1.51	3.86E-01	6.73E-01	0.00E+00	7.51E-02	7.13E-01	6.76E-04	0.00E+00	4.28E-01
Enriched in myeloid cells and monocytes (M81)	-0.94	-0.69	-2.81	1.51	3.86E-01	6.73E-01	0.00E+00	7.51E-02	7.13E-01	6.76E-04	0.00E+00	4.28E-01
PTEN regulation	-0.94	-0.69	-2.81	1.51	3.86E-01	6.73E-01	0.00E+00	7.51E-02	7.13E-01	6.76E-04	0.00E+00	4.28E-01
Mitochondrial protein import	-0.65	-0.50	-2.71	0.83E-01	9.83E-01	0.00E+00	0.00E+00	3.05E-02	4.09E-01	8.66E-01	4.35E-02	6.55E-01
Asymmetric localization of PCP proteins	-0.65	-0.50	-2.71	0.83E-01	9.83E-01	0.00E+00	0.00E+00	3.05E-02	4.09E-01	8.66E-01	4.35E-02	6.55E-01
SCF E3 ubiquitin ligase	-0.92	-1.04	-2.64	1.07	5.58E-01	3.98E-01	0.00E+00	3.71E-01	8.42E-01	1.00E-04	1.00E-04	1.00E-04
G2M checkpoints	1.87	-3.22	-2.64	1.07	5.58E-01	3.98E-01	0.00E+00	3.71E-01	8.42E-01	1.00E-04	1.00E-04	1.00E-04
Signaling pathway	-1.09	-0.67	-2.78	0.83E-01	9.83E-01	0.00E+00	0.00E+00	3.05E-02	4.09E-01	8.66E-01	4.35E-02	6.55E-01
Cytoskeleton	1.01	-1.68	-2.84	0.94E-01	9.49E-01	0.00E+00	0.00E+00	3.05E-02	4.09E-01	8.66E-01	4.35E-02	6.55E-01
Cellular assembly	1.01	-1.68	-2.84	0.94E-01	9.49E-01	0.00E+00	0.00E+00	3.05E-02	4.09E-01	8.66E-01	4.35E-02	6.55E-01
FCER mediated NF-kB activation	-1.15	-0.57	-2.84	0.94E-01	9.49E-01	0.00E+00	0.00E+00	3.05E-02	4.09E-01	8.66E-01	4.35E-02	6.55E-01
TNFR2 non-canonical NF-kB pathway	0.53	-0.60	-3.16	0.98E-01	9.88E-01	0.00E+00	0.00E+00	3.05E-02	4.09E-01	8.66E-01	4.35E-02	6.55E-01
Golgi-to-ER retrograde transport	1.15	-2.78	-2.13	2.84E-01	2.84E-01	0.00E+00	2.50E-03	2.50E-03	2.50E-03	2.07E-02	1.20E-03	2.07E-02
Enriched in monocytes (M11.0)	-0.90	-1.34	-2.25	2.11E-02	2.11E-02	1.70E-01	2.50E-03	2.50E-03	2.50E-03	2.07E-02	1.20E-03	2.07E-02
Transport to the Golgi and subsequent modification	-0.90	-1.34	-2.25	2.11E-02	2.11E-02	1.70E-01	2.50E-03	2.50E-03	2.50E-03	2.07E-02	1.20E-03	2.07E-02
Stabilization of p53	-0.65	-2.22	-2.99	0.00E+00	0.00E+00	3.20E-03	0.00E+00	0.00E+00	0.00E+00	4.05E-02	0.00E+00	4.05E-02
Stabilization of p53	-0.65	-2.22	-2.99	0.00E+00	0.00E+00	3.20E-03	0.00E+00	0.00E+00	0.00E+00	4.05E-02	0.00E+00	4.05E-02
Viral messenger RNA synthesis	1.70	-0.71	-1.78	1.54E-02	8.75E-01	0.00E+00	0.00E+00	0.00E+00	0.00E+00	9.73E-01	0.00E+00	9.73E-01
Diseases of signal transduction by growth factor receptors and second messengers	-1.06	-1.22	-2.84	0.83E-01	9.83E-01	0.00E+00	0.00E+00	3.05E-02	4.09E-01	8.66E-01	4.35E-02	6.55E-01
Programmed cell death	-1.09	-1.47	-1.85	0.71E-01	8.82E-02	2.68E-01	1.34E-03	4.29E-01	7.22E-01	1.39E-01	1.39E-01	1.39E-01
Immunoregulatory interactions between a lymphoid and a non-lymphoid cell	-0.85	-1.17	-2.85	0.64E-01	6.45E-01	2.68E-01	0.00E+00	0.00E+00	0.00E+00	8.88E-01	0.00E+00	8.88E-01
Regulation of P/TEFb stability and activity	1.19	-1.83	-1.99	2.02E-01	2.02E-01	2.90E-03	7.70E-03	7.70E-03	7.70E-03	2.71E-02	6.10E-03	2.71E-02
HIV lifecycle	1.72	-1.83	-1.99	2.02E-01	2.02E-01	2.90E-03	7.70E-03	7.70E-03	7.70E-03	2.71E-02	6.10E-03	2.71E-02
Signaling by GPCR in disease	2.28	-3.08	-2.73	-1.45	8.29E-01	0.00E+00	0.00E+00	0.00E+00	0.00E+00	4.19E-02	0.00E+00	4.19E-02
Olfactory signaling pathway	-0.72	0.54	-2.73	-1.45	8.29E-01	0.00E+00	0.00E+00	0.00E+00	0.00E+00	4.19E-02	0.00E+00	4.19E-02
PCP/CE pathway	-1.91	-0.25	-2.73	-1.45	8.29E-01	0.00E+00	0.00E+00	0.00E+00	0.00E+00	4.19E-02	0.00E+00	4.19E-02
Cell cycle and transcription (M4.0)	0.12	-2.09	-3.25	0.83E-01	9.83E-01	0.00E+00	0.00E+00	3.05E-02	4.09E-01	8.66E-01	4.35E-02	6.55E-01
Muscle contraction	-0.25	-2.09	-3.25	0.83E-01	9.83E-01	0.00E+00	0.00E+00	3.05E-02	4.09E-01	8.66E-01	4.35E-02	6.55E-01
Mitotic spindle assembly	-0.25	-2.09	-3.25	0.83E-01	9.83E-01	0.00E+00	0.00E+00	3.05E-02	4.09E-01	8.66E-01	4.35E-02	6.55E-01
GPCR ligand binding	1.78	-2.03	-2.13	1.71E-01	1.71E-01	1.76E-02	6.40E-03	9.22E-02	6.31E-01	9.20E-02	2.60E-02	2.95E-01
Mitotic prometaphase	-0.86	-2.19	-2.13	1.71E-01	1.71E-01	1.76E-02	6.40E-03	9.22E-02	6.31E-01	9.20E-02	2.60E-02	2.95E-01
ABC transporter disorders	-0.59	-3.01	-3.01	9.16E-01	9.16E-01	0.00E+00	0.00E+00	0.00E+00	0.00E+00	9.70E-01	0.00E+00	9.70E-01
Organelle biogenesis and maintenance	-0.64	-1.26	-1.87	9.28E-01	9.28E-01	1.94E-01	8.00E-03	8.00E-03	8.00E-03	3.14E-01	1.18E-02	3.14E-01
Metabolism of polyamines	0.89	-2.69	-2.69	5.43E-01	5.43E-01	1.94E-01	8.00E-03	8.00E-03	8.00E-03	3.14E-01	1.18E-02	3.14E-01
MAPK/MAPK signaling	-0.60	-3.47	-3.13	9.19E-01	9.19E-01	0.00E+00	0.00E+00	0.00E+00	0.00E+00	9.70E-01	0.00E+00	9.70E-01
MAPK/MAPK signaling	-0.60	-3.47	-3.13	9.19E-01	9.19E-01	0.00E+00	0.00E+00	0.00E+00	0.00E+00	9.70E-01	0.00E+00	9.70E-01
Mitotic G2/M phases	-0.71	-1.04	-2.47	7.85E-01	7.85E-01	3.80E-01	0.00E+00	0.00E+00	0.00E+00	9.70E-01	0.00E+00	9.70E-01
Mitotic G2/M phases	-0.71	-1.04	-2.47	7.85E-01	7.85E-01	3.80E-01	0.00E+00	0.00E+00	0.00E+00	9.70E-01	0.00E+00	9.70E-01
HCMV infection	1.35	-1.40	-2.47	7.44E-02	7.44E-02	1.07E-01	0.00E+00	0.00E+00	0.00E+00	4.03E-01	1.87E-01	4.03E-01
G-alpha 12/13 signaling events	-2.22	-0.96	-2.67	7.51E-01	7.51E-01	5.15E-01	0.00E+00	0.00E+00	0.00E+00	9.20E-01	1.00E-04	9.20E-01
Homology directed repair	1.51	-1.08	-2.06	8.64E-01	8.64E-01	3.61E-01	6.82E-02	6.82E-02	6.82E-02	5.70E-03	6.30E-02	5.70E-03
Chromosome maintenance	-0.67	-1.74	-1.71	2.90E-03	2.90E-03	3.42E-02	3.42E-02	3.42E-02	3.42E-02	7.40E-01	2.77E-02	7.40E-01
Telomere maintenance	0.95	-1.74	-1.74	8.70E-03	8.70E-03	2.27E-02	2.27E-02	2.27E-02	2.27E-02	7.40E-01	4.31E-02	7.40E-01
CD28 costimulation	-1.80	-2.61	-2.61	7.50E-01	7.50E-01	5.15E-01	0.00E+00	0.00E+00	0.00E+00	9.20E-01	1.00E-04	9.20E-01
Monocyte surface signature (S4)	-0.81	-1.55	-2.52	-1.25	7.51E-01	5.15E-01	0.00E+00	0.00E+00	0.00E+00	9.20E-01	1.00E-04	9.20E-01
Uls-specific processing proteases	-1.74	-2.04	-2.52	-1.25	7.51E-01	5.15E-01	0.00E+00	0.00E+00	0.00E+00	9.20E-01	1.00E-04	9.20E-01
RNA polymerase II transcription	-0.88	-1.86	-2.73	6.30E-01	6.30E-01	1.18E-02	0.00E+00	0.00E+00	0.00E+00	4.40E-03	2.36E-02	4.40E-03
Regulation of antigen presentation and immune responses (M5.0)	-0.66	-1.01	-2.73	4.29E-01	4.29E-01	1.18E-02	0.00E+00	0.00E+00	0.00E+00	4.40E-03	2.36E-02	4.40E-03
Blood coagulation (M11.1)	2.23	-1.79	-2.73	0.00E+00	0.00E+00	1.61E-02	0.00E+00	0.00E+00	0.00E+00	1.00E-01	1.00E-01	1.00E-01
Resolution of sister chromatid cohesion	1.56	-2.94	-2.94	3.33E-02	3.33E-02	0.00E+00	0.00E+00	0.00E+00	0.00E+00	2.50E-01	0.00E+00	2.50E-01
Cyclin A/Cdk2-associated events at S phase entry	-1.42	-1.65	-3.27	6.45E-02	6.45E-02	0.00E+00	0.00E+00	0.00E+00	0.00E+00	4.27E-01	1.59E-01	4.27E-01
Cellular interactions at the vascular wall	1.21	-1.68	-3.27	1.29E-01	1.29E-01	2.02E-02	0.00E+00	0.00E+00	0.00E+00	4.94E-01	5.86E-02	4.94E-01
G2/M DNA checkpoint	2.08	-2.92	-2.96	0.00E+00	0.00E+00	0.00E+00	0.00E+00	0.00E+00	0.00E+00	5.37E-02	0.00E+00	5.37E-02
Influenza infection	-1.80	-3.01	-3.01	5.06E-03	5.06E-03	0.00E+00	0.00E+00	0.00E+00	0.00E+00	1.22E-01	0.00E+00	1.22E-01
Phospholipid metabolism	-1.42	-1.68	-3.27	1.29E-01	1.29E-01	2.02E-02	0.00E+00	0.00E+00	0.00E+00	4.94E-01	5.86E-02	4.94E-01
Metabolism of amino acids and derivatives	2.08	-2.92	-2.96	0.00E+00	0.00E+00	0.00E+00	0.00E+00	0.00E+00	0.00E+00	5.37E-02	0.00E+00	5.37E-02
Eukaryotic translation initiation	-1.80	-3.01	-3.01	5.06E-03	5.06E-03	0.00E+00	0.00E+00	0.00E+00	0.00E+00	1.22E-01	0.00E+00	1.22E-01
Complex biogenesis	-0.82	-3.01	-3.01	7.06E-01	7.06E-01	0.00E+00	0.00E+00	0.00E+00	0.00E+00	9.16E-01	0.00E+00	9.16E-01
Enriched in B cells (M47.0)	-0.82	-3.01	-3.01	7.06E-01	7.06E-01	0.00E+00	0.00E+00	0.00E+00	0.00E+00	9.16E-01	0.00E+00	9.16E-01
Regulation of RUVBL1 expression and activity	-0.82	-3.01	-3.01	7.06E-01	7.06E-01	0.00E+00	0.00E+00	0.00E+00	0.00E+00	9.16E-01	0.00E+00	9.16E-01

TP53 Regulates metabolic genes	-1.31	-2.47	1.59E-03	0.00E+00	6.83E-01	5.66E-01	3.00E-04	
Parasite infection	-1.85	-3.19	3.70E-03	4.89E-02	8.99E-01	9.98E-02	0.00E-00	
Cellular responses to external stimuli	-0.73	-1.42	8.99E-01	0.00E+00	1.30E-03	9.50E-01	1.73E-01	
Antigen activated BCR leading to generation of second messengers	-2.00	1.58	1.30E-03	0.00E+00	6.61E-02	3.75E-02	0.00E-00	7.74E-01
Vesicle mediated transport	-1.30	-2.77	1.64E-02	0.00E+00	1.61E-01	5.83E-01	1.95E-01	
Interleukin-1 signaling	-1.30	-2.77	1.64E-02	0.00E+00	1.61E-01	5.83E-01	1.95E-01	
FL3 signaling	-0.89	-1.51	6.74E-01	4.92E-02	3.15E-01	8.74E-01	1.23E-01	
The citric acid (TCA) cycle and respiratory electron transport	-0.78	-1.72	3.15E-01	0.00E+00	7.53E-01	5.92E-01	4.69E-02	
Separation of sister chromatids	-1.75	-3.85	7.53E-01	2.30E-02	1.00E-00	9.41E-01	4.88E-02	
Signaling by integrins	-1.36	-2.86	5.03E-02	1.33E-02	1.00E-00	1.96E-01	0.00E-00	
P-75NTR receptor-mediated signaling	-1.15	-2.19	1.00E-00	0.00E+00	1.00E-00	1.00E-00	0.00E-00	
Regulation of transcription in non coding pre-mRNA	1.11	0.68	1.00E-00	0.00E+00	1.00E-00	1.00E-00	0.00E-00	
Metabolism of lipids	-1.64	-3.30	2.48E-01	7.09E-01	1.00E-00	2.55E-01	1.00E-00	1.00E-00
Autophagy	1.52	-2.73	2.04E-02	6.73E-01	0.00E+00	2.55E-01	1.00E-00	
NRAGE signals death through JNK	-2.25	0.81	0.00E+00	0.00E+00	0.00E+00	5.10E-03	0.00E-00	
Ion transport by P-type ATPases	-1.87	-2.58	3.70E-03	0.00E+00	0.00E+00	9.14E-02	0.00E-00	1.38E-03
Mitochondrial translation	1.86	-2.90	5.50E-03	0.00E+00	0.00E+00	1.12E-01	0.00E-00	
B cell surface signature (S2)	-0.73	-2.81	8.50E-01	0.00E+00	0.00E+00	9.50E-01	0.00E-00	
G1/S DNA Damage Checkpoints	-0.58	-2.81	9.18E-01	0.00E+00	0.00E+00	9.70E-01	0.00E-00	
mRNA splicing minor pathway	1.01	-2.10	4.44E-01	2.60E-03	0.00E+00	6.79E-01	0.00E-00	
Degradation of AXIN	-0.68	-3.01	8.33E-01	0.00E+00	0.00E+00	9.75E-01	0.00E-00	
Beta-catenin independent WNT signaling	-1.20	-2.86	2.33E-01	8.09E-01	0.00E+00	6.25E-01	0.00E-00	
Regulation of GLUT1 by the proteasome	-0.94	-2.49	9.64E-01	0.00E+00	0.00E+00	9.64E-01	0.00E-00	
Apoptosis	-0.81	-2.89	7.27E-01	0.00E+00	0.00E+00	9.18E-01	0.00E-00	
Extracellular matrix organization	-1.23	1.61	1.83E-01	4.28E-02	3.58E-01	6.33E-01	1.88E-01	9.27E-01
Switching of origins to a post-replicative state	-0.67	-2.86	8.69E-01	3.10E-01	0.00E+00	9.73E-01	0.00E-00	
AUF1 (hnRNP D0) binds and destabilizes mRNA	-0.64	-3.04	8.96E-01	0.00E+00	0.00E+00	9.77E-01	0.00E-00	
Ephrin signaling	-1.75	-3.04	1.35E-02	0.00E+00	0.00E+00	1.63E-01	0.00E-00	
RUNX1 regulates transcription of genes involved in differentiation of HSCs	-0.96	-2.53	5.23E-01	0.00E+00	0.00E+00	8.21E-01	3.00E-04	
DNA replication	-0.70	-3.14	8.53E-01	0.00E+00	0.00E+00	9.65E-01	0.00E-00	
The role of G1SE1 in G2/M progression after G2 checkpoint	0.77	-2.90	8.00E-01	0.00E+00	0.00E+00	8.98E-01	0.00E-00	
Regulation of lipid metabolism by PPAR-alpha	-1.73	0.62	6.70E-03	0.00E+00	0.00E+00	1.79E-01	0.00E-00	
Interleukin-1 family signaling	-1.23	-2.55	2.05E-01	8.90E-01	0.00E+00	6.34E-01	1.00E-00	
FCER mediated Ca2 mobilization	-1.79	-3.01	9.10E-03	0.00E+00	0.00E+00	1.27E-01	0.00E-00	
mRNA processing	-1.07	-1.55	3.15E-01	5.93E-02	0.00E+00	9.01E-01	1.31E-02	5.80E-02
Regulation of HIV factors	-0.56	-1.46	9.53E-01	8.09E-02	0.00E+00	9.01E-01	1.31E-02	0.00E-00
Nucleotide excision repair	-0.60	-2.27	9.05E-01	0.00E+00	0.00E+00	9.69E-01	2.74E-02	1.00E-03
Signaling by WNT	-1.04	-1.83	1.90E-02	0.00E+00	0.00E+00	1.90E-02	2.74E-02	1.00E-03
DNA double strand break repair	0.81	-1.93	4.22E-01	1.11E-02	0.00E+00	7.55E-01	9.18E-01	8.74E-02
Negative regulation of Notch4 signaling	-1.14	-1.55	3.11E-01	4.98E-02	0.00E+00	5.32E-01	1.08E-01	7.62E-02
rRNA modification in the nucleus and cytosol	-0.55	-3.07	9.48E-01	0.00E+00	0.00E+00	9.85E-01	0.00E-00	
Myeloid cell enriched receptors and transporters (M4.3)	-2.12	-2.54	1.30E-03	0.00E+00	0.00E+00	9.60E-03	0.00E-00	
Signaling by Notch	-0.98	-1.82	5.02E-01	7.89E-02	0.00E+00	8.15E-01	1.57E-02	
DNA repair	-0.58	-2.24	9.63E-01	0.00E+00	0.00E+00	9.69E-01	2.60E-03	1.00E-04
Transcriptional regulation by TP53	-1.10	-1.92	3.17E-01	7.50E-03	0.00E+00	7.07E-01	1.69E-02	5.00E-04
T cell activation (07.1)	1.67	-2.35	3.29E-02	0.00E+00	0.00E+00	2.03E-01	1.20E-03	
Desubiquitination	-1.05	-2.08	7.19E-01	7.04E-01	0.00E+00	7.47E-01	9.04E-01	3.80E-03
Transcriptional regulation by TP53	-1.88	-3.07	1.08E-02	4.08E-01	0.00E+00	1.08E-02	0.00E-00	
Regulation of mRNA stability by proteins that bind AU-rich elements	0.94	-1.01	5.31E-01	4.08E-01	0.00E+00	7.40E-01	5.88E-01	0.00E-00
rRNA processing	-1.83	-3.17	4.90E-03	0.00E+00	0.00E+00	1.05E-01	0.00E-00	0.00E-00
Cross-presentation of soluble exogenous antigens (endosomes)	-0.84	-2.80	3.88E-02	4.80E-03	0.00E+00	2.81E-01	5.60E-03	
Respiratory electron transport, ATP synthesis by chemiosmotic coupling, and heat production by uncoupling proteins	0.96	-2.21	6.62E-01	0.00E+00	0.00E+00	9.04E-01	0.00E-00	
FCGR2a mediated IL10 signaling	-1.73	-4.05	5.08E-01	0.00E+00	0.00E+00	7.28E-01	0.00E-00	
Disorders of transmembrane transporters	-0.45	-2.65	1.26E-02	1.41E-01	0.00E+00	1.74E-01	1.00E-04	
Antigen processing cross presentation	-0.66	-3.11	8.85E-01	0.00E+00	0.00E+00	9.95E-01	3.21E-01	
Decth-1 mediated noncanonical NF-kB signaling	-0.64	-3.18	8.89E-01	0.00E+00	0.00E+00	9.73E-01	0.00E-00	
Endoplasmic reticulum chaperone	0.14	-1.38	6.00E-01	5.14E-02	0.00E+00	9.76E-01	0.00E-00	
FCER1 signaling (07.7.3)	-1.33	-2.80	2.41E-01	0.00E+00	0.00E+00	5.23E-01	0.00E-00	
Rho GTPases activate formins	-1.15	-2.79	1.19E-01	5.13E-01	0.00E+00	5.54E-01	6.72E-01	1.00E-04
Ion channel transport	-0.65	-1.61	3.07E-01	7.89E-02	0.00E+00	1.68E-01	1.00E-04	
Signaling by Notch4	-0.85	-2.07	1.80E-02	2.40E-03	0.00E+00	1.76E-01	4.00E-03	
DNA replication pre-initiation	-0.62	-3.05	6.64E-01	9.97E-01	0.00E+00	8.89E-01	0.00E-00	
Aparagine N-linked glycosylation	-0.96	-1.06	5.46E-01	0.00E+00	0.00E+00	9.72E-01	0.00E-00	
Hedgehog on state	-0.97	-2.82	5.25E-01	0.00E+00	0.00E+00	8.20E-01	0.00E-00	
Neurotrophin system	-1.17	-1.69	2.08E-01	7.40E-03	8.62E-01	6.62E-01	0.00E-00	1.00E-00
Adaptive immune system	-1.32	-2.07	3.20E-02	2.73E-02	0.00E+00	5.61E-01	9.74E-02	
T cell activation (07.1)	-1.34	-2.64	1.26E-01	2.73E-01	0.00E+00	8.8E-01	3.80E-03	2.90E-01
Nuclear receptor transcription pathway	-1.90	-2.75	3.90E-03	0.00E+00	0.00E+00	9.00E-02	1.00E-04	
Regulation of cellular response and activity	-1.30	-2.38	1.07E-01	0.00E+00	0.00E+00	4.09E-01	0.00E-00	
Neuronal development	-1.32	-2.17	1.55E-01	0.00E+00	0.00E+00	5.59E-01	3.98E-03	
Mitotic spindle checkpoint	-1.36	-1.81	2.70E-02	1.09E-01	0.00E+00	5.00E-01	3.13E-01	1.00E-00
Signaling by GPCR	-0.78	-1.01	7.38E-01	4.24E-01	0.00E+00	9.43E-01	5.90E-01	
APC/C-mediated degradation of cell cycle proteins	-0.78	-2.77	0.00E+00	0.00E+00	0.00E+00	0.00E+00	0.00E-00	

Transcriptional regulation by RUNX3	-1.24	0.94	-2.65	2.24E-01	5.29E-01	0.00E+00	6.33E-01	8.43E-01	1.00E-04
Transcriptional regulation by RUNX2	-0.79	0.91	-2.16	1.53E-01	5.24E-01	0.00E+00	5.24E-01	8.43E-01	1.00E-04
Transcriptional regulation by RUNX1	-1.27	-0.53	-1.86	1.53E-01	9.69E-01	1.08E-02	6.09E-01	9.91E-01	1.21E-02
Translation	1.71	-3.21	-3.50	1.39E-02	0.00E+00	0.00E+00	1.88E-01	0.00E+00	0.00E+00
Regulation of expression of SUTs and ROBOs	1.30	-2.22	-2.83	1.44E-01	0.00E+00	0.00E+00	4.69E-01	2.90E-03	0.00E+00
Chromatin modifying enzymes	-1.05	-2.01	-1.01	3.97E-01	3.00E-03	4.24E-01	7.43E-01	1.03E-02	4.45E-01
Signaling by ROBO receptors	-1.15	-1.66	-2.25	2.59E-01	2.44E-02	0.00E+00	6.79E-01	6.26E-02	1.20E-03
Class II MHC mediated antigen processing & presentation	-0.79	1.46	-2.45	8.01E-02	8.04E-01	2.50E-03	9.31E-01	2.55E-01	4.00E-04
Degradation of DVL	-0.70	-1.50	-2.95	8.37E-01	6.08E-02	0.00E+00	9.64E-01	1.26E-01	4.69E-01
G-alpha 1 signaling events	-1.44	-1.14	-1.15	2.65E-02	9.28E-02	0.00E+00	7.95E-01	4.69E-01	0.00E+00
Regulation of integrin signaling	-1.24	-1.24	-3.12	9.09E-01	9.28E-02	0.00E+00	2.20E-03	6.00E-02	0.00E+00
Erbb3 in microvesicles (MVBs)	-2.57	-2.06	-2.58	9.22E-01	0.00E+00	0.00E+00	9.70E-01	7.20E-03	1.00E-04
Protein localization	-0.59	-0.84	-3.10	6.68E-01	0.00E+00	0.00E+00	9.00E-01	0.00E+00	0.00E+00
APC/Cdh1 mediated degradation of Cdc20 and other APC/Cdh1 targeted proteins in late mitosis/early G1	-0.84	-0.61	-2.99	9.18E-01	0.00E+00	0.00E+00	9.71E-01	0.00E+00	0.00E+00
Odc1 removal from chromatin	-0.61	-2.75	-3.61	0.00E+00	0.00E+00	0.00E+00	3.14E-02	2.00E-04	0.00E+00
SRP-dependent cotranslational protein targeting to membrane	2.22	-1.92	-1.92	1.00E+00	6.10E-03	0.00E+00	9.97E-01	1.66E-02	0.00E+00
HIV infection	-0.43	-1.15	-3.94	0.00E+00	2.85E-01	0.00E+00	6.30E-03	4.33E-01	0.00E+00
ILK and inflammatory signaling (M16)	-2.25	-1.15	-3.21	8.51E-01	0.00E+00	0.00E+00	9.33E-01	2.00E-04	0.00E+00
Cell cycle	-0.79	-2.64	-3.21	4.50E-03	0.00E+00	0.00E+00	1.20E-01	0.00E+00	1.00E-01
Integration of energy metabolism	1.80	-1.80	-3.21	4.00E-03	0.00E+00	0.00E+00	1.20E-01	0.00E+00	0.00E+00
Aggregopathy	1.95	-1.23	-1.31	4.00E-03	1.65E-01	1.44E-01	8.52E-02	3.44E-01	1.60E-01
Cytokines signaling in immune system	-1.18	-0.68	-4.18	1.52E-01	8.77E-01	0.00E+00	6.59E-01	9.37E-01	4.49E-01
Neutrophil degranulation	-2.17	-2.78	-2.78	2.02E-01	2.02E-01	0.00E+00	7.40E-03	6.03E-01	0.00E+00
Regulation of FAS by GAPS	-1.27	0.83	-2.61	3.42E-01	6.54E-01	0.00E+00	7.10E-01	9.23E-01	1.00E-04
UCH proteasomes	-1.11	-0.98	-4.61	1.20E-03	6.97E-01	0.00E+00	7.00E-01	0.00E+00	0.00E+00
Innate immune system	1.98	-0.98	-4.61	1.20E-03	6.97E-01	0.00E+00	7.00E-01	0.00E+00	0.00E+00
Immune regulation	-1.07	1.78	-3.09	3.89E-01	1.34E-02	0.00E+00	3.94E-02	0.00E+00	0.00E+00
SIC mediated membrane transport	-1.07	1.78	-3.09	3.89E-01	1.34E-02	0.00E+00	3.94E-02	0.00E+00	0.00E+00
EGFR (ErbB1) signaling	-1.47	0.70	-3.09	5.66E-02	8.18E-01	0.00E+00	4.00E-01	9.95E-01	0.00E+00
S-phase	-0.65	-1.81	-3.00	8.88E-01	8.30E-03	0.00E+00	9.77E-01	2.88E-02	0.00E+00
Response of EIF2AK4 (GCN2) to amino acid deficiency	1.96	-2.79	-1.59	1.69E-02	0.00E+00	4.00E-02	9.17E-02	2.00E-04	0.00E+00
MAPK family signaling cascades	-0.84	-1.23	-2.80	7.64E-01	2.27E-01	0.00E+00	9.02E-01	3.42E-01	4.87E-02
Cellular response to hypoxia	-0.95	-2.21	-2.80	5.34E-01	0.00E+00	0.00E+00	8.34E-01	0.00E+00	0.00E+00
HATs acetylate histones	-0.94	-2.21	-2.80	5.34E-01	0.00E+00	0.00E+00	8.34E-01	2.88E-03	0.00E+00
C-type lectin receptors	-1.60	-0.71	-3.16	1.47E-02	8.38E-01	0.00E+00	2.95E-01	9.28E-01	0.00E+00

Table S14. DMPs between Early and Late rebound

cg	Mean_Early	Mean_Late	DiffMean	Median_Early	Median_Late	DiffMedian	logFC	AveExpr	t	P.Value	adj.P.Val	B	chr	Relation_to_Isian	Gene	Heatmap	Common	CommonMAP	Increase_RMD
cg02585483	0.129	0.180	-0.051	0.128	0.179	-0.051	-0.581	-2.549	-5.166	5.54E-06	5.24E-02	3.218	chr5	Island	KIF2A	Yes	No	No	Yes
cg01758122	0.742	0.388	0.354	0.792	0.390	0.402	2.271	0.814	4.877	1.44E-05	9.20E-02	2.473	chr13	Island	RASA3	Yes	Yes	Yes	No
cg10919109	0.699	0.375	0.324	0.736	0.382	0.354	2.004	0.601	4.799	1.86E-05	1.00E-01	2.272	chr13	Island	RASA3	Yes	Yes	No	No
cg05052469	0.799	0.437	0.362	0.853	0.434	0.418	2.530	1.365	4.643	3.09E-05	1.17E-01	1.874	chr13	Island	RASA3	Yes	Yes	Yes	Yes
cg05598453	0.199	0.290	-0.091	0.197	0.289	-0.093	-0.723	-1.861	-4.414	6.47E-05	1.66E-01	1.293	chr17	Island	ACTG1	Yes	No	No	No
cg12532878	0.727	0.548	0.179	0.757	0.550	0.208	1.172	1.078	4.413	6.49E-05	1.66E-01	1.292	chr13	N_Shore	RASA3	Yes	Yes	Yes	No
cg03157226	0.184	0.253	-0.069	0.180	0.259	-0.079	-0.592	-2.039	-4.384	7.12E-05	1.66E-01	1.219	chr19	N_Shore	ATG4D	Yes	No	No	No
cg13281814	0.091	0.125	-0.034	0.092	0.129	-0.037	-0.517	-3.097	-4.256	1.07E-04	1.82E-01	0.898	chr8	Island	GDAP1	Yes	No	No	No
cg13921204	0.165	0.222	-0.058	0.163	0.223	-0.060	-0.536	-2.178	-4.219	1.20E-04	1.82E-01	0.805	chr10	Island	SEC61A2	Yes	No	No	No
cg03039398	0.337	0.232	0.105	0.347	0.236	0.111	0.749	-1.146	4.209	1.24E-04	1.82E-01	0.780	chr7	S_Shelf	WIP2	Yes	Yes	Yes	Yes
cg05835669	0.133	0.191	-0.058	0.133	0.197	-0.064	-0.631	-2.611	-4.115	1.67E-04	1.97E-01	0.548	chr22	Island	TUBA8	Yes	No	No	No
cg19693031	0.600	0.477	0.124	0.595	0.473	0.122	0.728	0.448	4.067	1.94E-04	2.11E-01	0.429	chr1	OpenSea	TXNIP	Yes	Yes	Yes	Yes
cg14701554	0.141	0.080	0.061	0.126	0.080	0.046	0.883	-2.971	4.022	2.23E-04	2.24E-01	0.320	chr11	OpenSea	NUMA1	Yes	Yes	Yes	Yes
cg12286158	0.197	0.142	0.055	0.205	0.139	0.067	0.560	-2.182	4.005	2.35E-04	2.25E-01	0.277	chr22	Island	DMIC1	Yes	No	No	No
cg03290131	0.186	0.252	-0.066	0.188	0.252	-0.064	-0.559	-1.868	-3.820	4.15E-04	2.66E-01	-0.171	chr10	OpenSea	DUSP5	Yes	Yes	Yes	Yes
cg00520378	0.311	0.482	-0.171	0.303	0.501	-0.198	-1.074	-0.869	-3.795	4.47E-04	2.66E-01	-0.230	chr16	S_Shore	PEX14	Yes	Yes	Yes	Yes
cg22715764	0.646	0.549	0.096	0.643	0.565	0.078	0.581	0.654	3.791	4.52E-04	2.66E-01	-0.238	chr1	OpenSea	CEU2_RNF166	Yes	No	No	No
cg26571870	0.627	0.720	-0.093	0.617	0.720	-0.103	-0.606	0.973	-3.642	7.08E-04	3.00E-01	-0.592	chr16	S_Shore	GINS2	Yes	Yes	Yes	Yes
cg26063719	0.376	0.467	-0.091	0.378	0.450	-0.071	-0.542	-0.542	-3.631	7.32E-04	3.08E-01	-0.618	chr10	S_Shore	VIM	Yes	No	No	No
cg05437132	0.666	0.570	0.096	0.680	0.567	0.113	0.597	0.868	3.596	8.12E-04	3.11E-01	-0.700	chr21	Island	TIPE	Yes	No	No	No
cg00240178	0.476	0.566	-0.089	0.478	0.552	-0.074	-0.521	-0.004	-3.587	8.34E-04	3.11E-01	-0.721	chr6	N_Shore	EEF1A1	Yes	No	No	No
cg00589617	0.719	0.621	0.098	0.721	0.612	0.108	0.652	1.129	3.578	8.56E-04	3.11E-01	-0.741	chr1	Island	GALNT2	Yes	Yes	Yes	Yes
cg05660312	0.453	0.327	0.126	0.451	0.329	0.123	0.768	-0.523	3.570	8.77E-04	3.11E-01	-0.760	chr7	S_Shelf	WIP2	Yes	Yes	Yes	Yes
cg24244444	0.629	0.708	-0.079	0.644	0.707	-0.062	-0.518	0.908	3.559	9.04E-04	3.13E-01	-0.785	chr7	Island	PRKAR1B	Yes	No	No	No
cg23215256	0.670	0.574	0.096	0.693	0.566	0.127	0.593	0.908	3.559	9.04E-04	3.13E-01	-0.785	chr7	Island	HLA-DQA	Yes	No	No	No
cg07173283	0.689	0.608	0.081	0.700	0.606	0.094	0.518	1.008	3.493	1.10E-03	3.28E-01	-0.938	chr6	N_Shore	ALDH3A2	Yes	No	No	No
cg14396505	0.074	0.104	-0.030	0.073	0.107	-0.034	-0.530	-3.557	-3.477	1.15E-03	3.31E-01	-0.974	chr17	Island	LOC255512_TOLUP	Yes	Yes	Yes	Yes
cg05157625	0.608	0.740	-0.132	0.623	0.733	-0.109	-0.883	0.930	-3.265	2.12E-03	3.73E-01	-1.454	chr14	Island	AFMID_TK1	Yes	Yes	Yes	Yes
cg00610021	0.508	0.418	0.090	0.505	0.436	0.069	0.535	-0.036	3.189	2.63E-03	3.87E-01	-1.622	chr22	Island	RIN3	Yes	Yes	Yes	Yes
cg16853860	0.319	0.423	-0.104	0.337	0.438	-0.101	-0.651	-1.016	-3.160	2.85E-03	3.93E-01	-1.685	chr6	S_Shore	SMC1B_RIBC2	Yes	Yes	Yes	Yes
cg24006662	0.370	0.457	-0.087	0.362	0.455	-0.093	-0.527	-0.601	-3.097	3.40E-03	4.13E-01	-1.823	chr1	N_Shore	PSMB9_TAP1	Yes	No	No	No
cg07582133	0.052	0.077	-0.025	0.050	0.077	-0.027	-0.592	-3.969	-3.085	3.51E-03	4.16E-01	-1.848	chr7	Island	ENO1	Yes	No	No	No
cg22731440	0.269	0.365	-0.096	0.280	0.369	-0.090	-0.679	-1.326	-3.034	4.04E-03	4.31E-01	-1.958	chr6	N_Shore	GROT_TP53TG1	Yes	No	No	No
cg24006662	0.105	0.145	-0.041	0.102	0.139	-0.037	-0.512	-2.923	-3.012	4.29E-03	4.32E-01	-2.004	chr6	Island	HLA-B	Yes	No	No	No
cg14048834	0.088	0.062	0.026	0.088	0.058	0.031	0.555	-3.500	2.977	4.71E-03	4.32E-01	-2.078	chr19	Island	TUBB2A	Yes	No	No	No
cg14227996	0.180	0.263	-0.083	0.173	0.266	-0.093	-0.644	-2.151	-2.976	4.72E-03	4.32E-01	-2.080	chr4	Island	MED28	Yes	No	No	No
cg24989962	0.332	0.254	0.078	0.324	0.256	0.069	0.545	-1.160	2.967	4.84E-03	4.33E-01	-2.098	chr14	Island	PTGDR	Yes	No	No	No
cg24337683	0.097	0.135	-0.038	0.092	0.130	-0.039	-0.561	-3.092	-2.916	5.56E-03	4.39E-01	-2.207	chr3	Island	CHMP2B	Yes	No	No	No
cg00945666	0.294	0.219	0.075	0.273	0.216	0.056	0.553	-1.393	2.888	5.99E-03	4.47E-01	-2.265	chr1	N_Shore	F11R	Yes	No	No	No
cg20770311	0.051	0.127	-0.076	0.054	0.052	0.002	-0.854	-4.147	-2.887	6.01E-03	4.47E-01	-2.267	chr11	Island	SMPD1	Yes	No	No	No
cg02464073	0.362	0.761	-0.399	0.406	0.769	-0.364	-2.885	-6.036	6.03E-03	4.47E-01	-2.270	chr21	N_Shore	ITGB2	Yes	Yes	Yes	Yes	
cg07156249	0.154	0.233	-0.079	0.151	0.236	-0.085	-0.804	-2.326	-2.871	6.27E-03	4.52E-01	-2.300	chr6	S_Shore	PSMB9_TAP1	Yes	Yes	Yes	Yes
cg00744866	0.421	0.338	0.083	0.408	0.333	0.075	0.506	-0.511	2.870	6.28E-03	4.52E-01	-2.301	chr3	OpenSea	CLASP2	Yes	No	No	No
cg05265849	0.344	0.268	0.076	0.346	0.262	0.085	0.521	-1.042	2.867	6.33E-03	4.53E-01	-2.307	chr7	OpenSea	IL6	Yes	Yes	Yes	Yes
cg27500148	0.822	0.730	0.091	0.812	0.731	0.081	0.744	1.948	2.867	6.33E-03	4.53E-01	-2.307	chr17	S_Shore	RPL23	Yes	Yes	Yes	Yes
cg09060608	0.157	0.312	-0.154	0.126	0.328	-0.201	-1.336	-2.115	-2.854	6.56E-03	4.54E-01	-2.334	chr5	Island	RUFY1	Yes	Yes	Yes	Yes
cg15755475	0.491	0.403	0.087	0.492	0.388	0.104	0.519	-0.286	2.823	7.11E-03	4.59E-01	-2.397	chr6	OpenSea	PPT2	Yes	No	No	No

cg18391757	0.119	0.180	-0.061	0.106	0.172	-0.066	-0.710	-2.753	-2.816	7.25E-03	4.59E-01	-2.412	chr11	Island	ATM1_NPAT	Yes	No	No	No
cg19518265	0.757	0.573	0.184	0.757	0.573	0.185	1.148	1.230	2.803	7.50E-03	4.59E-01	-2.439	chr3	S_Shore	IRAK2	Yes	Yes	Yes	No
cg00598125	0.196	0.299	-0.103	0.190	0.310	-0.120	-0.786	-1.814	-2.796	7.60E-03	4.59E-01	-2.453	chr6	S_Shelf	HLA-DRB1	Yes	Yes	Yes	No
cg09090440	0.669	0.446	0.223	0.773	0.451	0.322	1.428	0.651	2.786	7.83E-03	4.59E-01	-2.472	chr6	OpenSea	HLA-DPA1	Yes	No	No	Yes
cg25227170	0.858	0.742	0.116	0.857	0.852	0.005	0.820	2.412	2.778	8.01E-03	4.59E-01	-2.490	chr18	OpenSea	VPS4B	Yes	No	No	No
cg23285761	0.124	0.179	-0.055	0.111	0.168	-0.057	-0.638	-2.733	-2.767	8.23E-03	4.59E-01	-2.511	chr8	Island	DDHD2	Yes	No	No	No
cg24004745	0.097	0.133	-0.036	0.091	0.129	-0.038	-0.527	-3.202	-2.723	9.24E-03	4.67E-01	-2.600	chr3	Island	IL1RAP	Yes	No	No	No
cg14820908	0.177	0.366	-0.189	0.158	0.375	-0.217	-1.444	-1.872	-2.683	1.02E-02	4.73E-01	-2.678	chr5	N_Shore	RUFY1	Yes	Yes	Yes	Yes
cg19626725	0.420	0.554	-0.134	0.419	0.575	-0.156	-0.794	-2.026	-2.682	1.03E-02	4.73E-01	-2.680	chr5	N_Shore	RUFY1	Yes	Yes	Yes	No
cg06791592	0.405	0.493	-0.088	0.427	0.500	-0.072	-0.524	-0.465	-2.676	1.04E-02	4.76E-01	-2.692	chr6	S_Shore	PSMB9	Yes	No	No	No
cg11621667	0.140	0.204	-0.064	0.125	0.209	-0.084	-0.655	-2.502	-2.675	1.05E-02	4.76E-01	-2.695	chr7	Island	RALA	Yes	No	No	No
cg19242688	0.048	0.102	-0.054	0.049	0.050	-0.001	-0.728	-4.225	-2.638	1.18E-02	4.86E-01	-2.767	chr19	Island	SNRPB	Yes	No	No	No
cg05670953	0.146	0.194	-0.048	0.146	0.197	-0.051	-0.518	-2.397	-2.637	1.15E-02	4.86E-01	-2.769	chr3	N_Shore	MHL1_LPM2AIP1	Yes	No	No	No
cg19242688	0.525	0.439	0.086	0.519	0.444	0.075	0.503	0.052	2.634	1.16E-02	4.86E-01	-2.775	chr19	Island	GNGB	Yes	No	No	No
cg08928675	0.590	0.493	0.097	0.590	0.486	0.104	0.574	0.455	2.629	1.17E-02	4.86E-01	-2.784	chr7	Island	FBXL18	Yes	No	No	No
cg18854398	0.051	0.098	-0.047	0.048	0.072	-0.023	-0.837	-3.906	-2.627	1.18E-02	4.86E-01	-2.788	chr1	Island	C1orf166_LSG20L2	Yes	Yes	Yes	Yes
cg12226059	0.151	0.314	-0.163	0.126	0.321	-0.196	-1.475	-2.189	-2.626	1.18E-02	4.86E-01	-2.790	chr5	N_Shore	RUFY1	Yes	Yes	Yes	Yes
cg21893846	0.077	0.119	-0.042	0.074	0.082	-0.008	-0.509	-3.606	-2.619	1.20E-02	4.88E-01	-2.803	chr5	Island	LMBRD2_SKP2	Yes	No	No	No
cg14106680	0.770	0.664	0.106	0.781	0.722	0.059	0.732	1.532	2.602	1.26E-02	4.88E-01	-2.838	chr19	Island	MVH14	Yes	Yes	Yes	Yes
cg17984783	0.171	0.234	-0.062	0.167	0.221	-0.055	-0.543	-2.152	-2.613	1.22E-02	4.88E-01	-2.815	chr8	Island	SDCBP	Yes	No	No	No
cg01517384	0.232	0.304	-0.072	0.240	0.316	-0.077	-0.547	-1.581	-2.604	1.25E-02	4.88E-01	-2.832	chr6	N_Shore	HLA-B	Yes	No	No	Yes
cg06972019	0.103	0.156	-0.054	0.091	0.150	-0.059	-0.709	-2.946	-2.602	1.26E-02	4.88E-01	-2.836	chr1	N_Shore	ENO1	Yes	Yes	Yes	Yes
cg14106680	0.443	0.338	-0.046	0.443	0.338	0.059	0.732	1.532	2.602	1.26E-02	4.88E-01	-2.838	chr19	Island	MVH14	Yes	Yes	Yes	Yes
cg16431720	0.492	0.738	-0.246	0.443	0.719	-0.276	-1.546	0.524	-2.591	1.29E-02	4.90E-01	-2.858	chr6	OpenSea	HLA-DQA1	Yes	Yes	Yes	No
cg10409680	0.089	0.165	-0.076	0.081	0.163	-0.081	-0.945	-3.053	-2.590	1.30E-02	4.91E-01	-2.859	chr6	Island	HLA-C	Yes	No	No	No
cg04737361	0.148	0.202	-0.054	0.144	0.200	-0.056	-0.517	-2.443	-2.588	1.30E-02	4.91E-01	-2.864	chr2	Island	BAR1	Yes	No	No	No
cg22870256	0.075	0.116	-0.041	0.074	0.109	-0.034	-0.676	-3.424	-2.575	1.34E-02	4.94E-01	-2.888	chr8	Island	DFBT1	Yes	No	No	No
cg11229715	0.297	0.065	0.232	0.417	0.066	0.351	2.204	-2.291	2.561	1.39E-02	4.97E-01	-2.916	chr2	OpenSea	CUL3	Yes	Yes	Yes	Yes
cg23331433	0.260	0.170	0.089	0.251	0.194	0.068	0.921	-1.739	2.543	1.46E-02	5.00E-01	-2.951	chr6	OpenSea	HLA-DPA1	Yes	Yes	Yes	Yes
cg24089118	0.313	0.239	0.074	0.293	0.230	0.063	0.536	-1.293	2.541	1.47E-02	5.00E-01	-2.954	chr14	OpenSea	PIGDOR	Yes	No	No	No
cg00080972	0.170	0.298	-0.128	0.143	0.303	-0.160	-1.045	-1.968	-2.532	1.50E-02	5.01E-01	-2.971	chr5	N_Shore	RUFY1	Yes	Yes	Yes	Yes
cg16126286	0.250	0.189	0.061	0.245	0.205	0.040	0.548	-1.800	2.531	1.50E-02	5.01E-01	-2.972	chr1	N_Shore	SDCCAG8	Yes	No	No	No
cg07571734	0.076	0.105	-0.029	0.075	0.105	-0.030	-0.528	-3.441	-2.520	1.54E-02	5.04E-01	-2.994	chr7	N_Shore	PRKAG2	Yes	No	No	No
cg01055691	0.443	0.253	0.190	0.405	0.253	0.152	1.732	-0.911	2.510	1.58E-02	5.07E-01	-3.012	chr3	N_Shore	GAP43	Yes	Yes	Yes	Yes
cg26312542	0.858	0.804	0.054	0.857	0.811	0.046	0.530	2.462	2.498	1.63E-02	5.11E-01	-3.034	chr11	OpenSea	TEX12	Yes	Yes	Yes	No
cg03216697	0.193	0.633	-0.440	0.109	0.799	-0.690	-3.297	-1.506	-2.482	1.69E-02	5.11E-01	-3.064	chr6	Island	HLA-C	Yes	No	Yes	Yes
cg16200617	0.732	0.642	0.090	0.734	0.732	0.002	0.556	1.429	2.472	1.74E-02	5.14E-01	-3.083	chrX	N_Shore	BCYRN1_GIB1	Yes	No	No	No
cg08201700	0.183	0.112	0.071	0.181	0.111	0.071	0.756	-2.365	2.466	1.76E-02	5.15E-01	-3.094	chr7	Island	WDR60	Yes	No	No	No
cg24895834	0.184	0.242	-0.058	0.186	0.235	-0.049	-0.504	-2.045	-2.466	1.76E-02	5.15E-01	-3.094	chr10	Island	PRKCO	Yes	No	No	No
cg27541892	0.385	0.552	-0.167	0.394	0.500	-0.105	-1.051	-0.339	-2.462	1.78E-02	5.17E-01	-3.101	chr1	S_Shore	CDK11B	Yes	Yes	Yes	No
cg22037249	0.517	0.286	0.230	0.528	0.357	0.171	1.724	-0.449	2.454	1.81E-02	5.18E-01	-3.116	chr6	OpenSea	HLA-DPA1	Yes	Yes	Yes	Yes
cg24207068	0.336	0.421	-0.085	0.331	0.410	-0.079	-0.527	-0.878	-2.450	1.83E-02	5.18E-01	-3.125	chr17	S_Shore	RPTOR	Yes	No	No	No
cg01464730	0.779	0.696	0.083	0.803	0.680	0.124	0.623	1.688	2.433	1.91E-02	5.21E-01	-3.155	chr17	OpenSea	RPTOR	Yes	Yes	Yes	Yes
cg05457628	0.215	0.365	-0.151	0.185	0.386	-0.201	-1.183	-1.594	-2.433	1.91E-02	5.22E-01	-3.156	chr5	Island	RUFY1	Yes	No	No	No
cg27307781	0.048	0.079	-0.031	0.046	0.075	-0.029	-0.687	-4.119	-2.426	1.94E-02	5.24E-01	-3.168	chr21	Island	CBR1	Yes	Yes	Yes	Yes
cg22764044	0.173	0.291	-0.118	0.150	0.308	-0.158	-0.987	-2.037	-2.420	1.97E-02	5.24E-01	-3.179	chr5	Island	RUFY1	Yes	Yes	Yes	Yes
cg02788013	0.079	0.129	-0.050	0.080	0.100	-0.021	-0.697	-3.297	-2.406	2.04E-02	5.24E-01	-3.205	chr2	N_Shore	INPP5D	Yes	No	No	No
cg1992783	0.579	0.477	0.102	0.579	0.483	0.095	0.403	0.313	2.403	2.06E-02	5.24E-01	-3.210	chr19	Island	MVH14	Yes	No	No	Yes
cg02136620	0.230	0.365	-0.135	0.205	0.397	-0.192	-0.929	-1.484	-2.401	2.07E-02	5.24E-01	-3.215	chr5	Island	RUFY1	Yes	Yes	Yes	Yes
cg2352194	0.709	0.632	0.078	0.710	0.621	0.088	0.514	1.186	2.393	2.11E-02	5.26E-01	-3.229	chr19	Island	PLA2G4C	Yes	No	No	No
cg19311470	0.262	0.681	-0.419	0.059	0.684	-0.625	-3.769	-0.951	-2.382	2.16E-02	5.27E-01	-3.248	chr4	Island	RPL9_LUAS	Yes	Yes	Yes	Yes
cg25283336	0.689	0.445	0.244	0.691	0.553	0.138	1.819	0.718	2.376	2.19E-02	5.28E-01	-3.260	chr6	OpenSea	HLA-DPA1	Yes	Yes	Yes	Yes

cg14601097	0.123	0.170	-0.047	0.123	0.174	-0.050	-0.668	-2.749	-2.370	2.22E-02	5.28E-01	-3.271	chr12	Island	ANKLE2	No	No	No	No
cg13661648	0.584	0.406	0.178	0.592	0.469	0.123	1.127	0.093	2.361	2.27E-02	5.32E-01	-3.287	chr6	OpenSea	HLA-DPA1	Yes	Yes	Yes	Yes
cg27107292	0.507	0.292	0.215	0.461	0.256	0.205	1.617	-0.395	2.352	2.32E-02	5.35E-01	-3.303	chr6	OpenSea	HLA-DRB1	Yes	Yes	Yes	Yes
cg00786704	0.591	0.506	0.085	0.610	0.506	0.105	0.504	0.381	2.330	2.45E-02	5.42E-01	-3.342	chr15	Island	SNRPN	No	No	No	No
cg07325233	0.128	0.178	-0.050	0.110	0.138	-0.048	-0.566	-2.732	-2.328	2.46E-02	5.42E-01	-3.346	chr21	Island	IL10RB	Yes	Yes	Yes	Yes
cg21226754	0.824	0.546	0.278	0.822	0.624	0.198	2.029	1.485	2.317	2.52E-02	5.45E-01	-3.365	chr5	N_Shelf	RBM22	Yes	Yes	Yes	Yes
cg10890644	0.405	0.089	0.316	0.483	0.088	0.394	2.470	-1.702	2.317	2.52E-02	5.45E-01	-3.366	chr10	OpenSea	TUBAL3	Yes	Yes	Yes	Yes
cg27305029	0.475	0.371	0.104	0.484	0.332	0.153	0.635	-0.337	2.309	2.57E-02	5.45E-01	-3.380	chr13	S_Shelf	RAS3	Yes	Yes	Yes	Yes
cg12858166	0.432	0.267	0.165	0.433	0.336	0.097	1.385	-0.834	2.305	2.60E-02	5.45E-01	-3.387	chr6	OpenSea	HLA-DPA1	Yes	Yes	Yes	Yes
cg24113818	0.649	0.561	0.088	0.631	0.549	0.081	0.543	0.733	2.297	2.64E-02	5.46E-01	-3.401	chr13	Island	RAS3	Yes	No	No	No
cg15472574	0.146	0.198	-0.052	0.156	0.197	-0.042	-0.555	-2.468	-2.295	2.66E-02	5.46E-01	-3.404	chr1	Island	YBX1	Yes	No	No	No
cg14302130	0.679	0.445	0.234	0.684	0.556	0.128	1.835	0.599	2.295	2.66E-02	5.46E-01	-3.405	chr6	OpenSea	HLA-DPA1	Yes	No	No	No
cg20169779	0.703	0.622	0.281	0.701	0.628	0.072	0.503	1.141	2.275	2.78E-02	5.50E-01	-3.439	chr10	Island	SYCE1	Yes	No	No	No
cg00267207	0.571	0.345	0.226	0.641	0.340	0.301	1.644	-0.146	2.266	2.84E-02	5.54E-01	-3.455	chr12	OpenSea	GUCY2C	Yes	Yes	Yes	Yes
cg13019553	0.189	0.249	-0.060	0.189	0.243	-0.055	-0.504	-1.884	-2.254	2.92E-02	5.57E-01	-3.475	chr6	Island	HLA-B	Yes	No	No	No
cg03025850	0.614	0.526	0.088	0.611	0.525	0.086	0.534	0.671	2.239	3.02E-02	5.60E-01	-3.501	chr8	Island	FGF17	Yes	No	No	No
cg03502601	0.359	0.463	-0.104	0.342	0.438	-0.096	-0.638	-0.652	-2.231	3.08E-02	5.62E-01	-3.517	chr17	S_Shore	RPTOR	Yes	No	No	No
cg22466012	0.559	0.400	0.159	0.589	0.365	0.224	0.949	0.226	2.212	3.22E-02	5.64E-01	-3.549	chr3	OpenSea	PLD1	Yes	No	No	No
cg23815646	0.228	0.166	0.062	0.233	0.144	0.090	0.600	-1.967	2.183	3.44E-02	5.70E-01	-3.597	chr8	OpenSea	ADCY8	Yes	No	No	No
cg01188578	0.245	0.063	0.182	0.241	0.063	0.179	1.810	-2.657	2.181	3.46E-02	5.70E-01	-3.602	chr2	N_Shelf	HADHA	Yes	No	No	No
cg01815645	0.660	0.516	0.144	0.668	0.550	0.118	0.902	0.692	2.177	3.49E-02	5.71E-01	-3.609	chr6	N_Shelf	HLA-DRB1	Yes	Yes	Yes	Yes
cg09885502	0.301	0.623	-0.322	0.243	0.627	-0.384	-2.475	-0.753	-2.164	3.59E-02	5.74E-01	-3.630	chr20	Island	GNAS	Yes	Yes	Yes	Yes
cg20502501	0.647	0.410	0.237	0.690	0.308	0.382	1.441	0.423	2.143	3.77E-02	5.80E-01	-3.666	chr17	OpenSea	RPTOR	Yes	Yes	Yes	Yes
cg08812897	0.410	0.321	0.088	0.396	0.324	0.071	0.620	-0.655	2.142	3.78E-02	5.80E-01	-3.667	chrX	Island	RPS6KA3	Yes	No	No	No
cg00981070	0.611	0.523	0.088	0.615	0.511	0.104	0.528	0.488	2.134	3.84E-02	5.82E-01	-3.680	chr1	Island	PKCZ	Yes	No	No	No
cg04467659	0.363	0.176	0.187	0.386	0.107	0.279	1.560	-1.422	2.133	3.85E-02	5.82E-01	-3.682	chr11	OpenSea	COPB1	Yes	No	No	No
cg17806798	0.615	0.516	0.099	0.638	0.553	0.085	0.593	0.480	2.109	4.07E-02	5.87E-01	-3.722	chr1	OpenSea	NSUNA4	Yes	No	No	No
cg24470466	0.539	0.733	-0.194	0.504	0.844	-0.339	-1.433	0.768	-2.106	4.09E-02	5.88E-01	-3.727	chr6	OpenSea	HLA-DOA1	Yes	Yes	Yes	Yes
cg03959058	0.764	0.488	0.276	0.852	0.507	0.345	2.155	1.147	2.100	4.15E-02	5.89E-01	-3.737	chr10	OpenSea	PPP2R2D	Yes	Yes	Yes	Yes
cg21234082	0.533	0.413	0.120	0.546	0.375	0.171	0.712	0.006	2.088	4.26E-02	5.90E-01	-3.757	chr9	S_Shore	DAB2IP	Yes	Yes	Yes	Yes
cg02377073	0.193	0.249	-0.056	0.175	0.251	-0.076	-0.510	-2.108	-2.087	4.27E-02	5.91E-01	-3.764	chr8	Island	UBE2V2	Yes	No	No	No
cg19117186	0.619	0.533	0.087	0.639	0.535	0.104	0.524	0.656	2.083	4.31E-02	5.91E-01	-3.764	chr22	Island	CPT1B	Yes	No	No	No
cg19443786	0.332	0.581	-0.249	0.351	0.594	-0.243	-1.790	-0.787	-2.079	4.35E-02	5.92E-01	-3.772	chr17	S_Shelf	NGS2	Yes	Yes	Yes	Yes
cg04814784	0.181	0.456	-0.275	0.086	0.461	-0.376	-2.162	-1.870	-2.079	4.35E-02	5.92E-01	-3.772	chr3	N_Shore	VHL	Yes	Yes	Yes	Yes
cg12075498	0.259	0.184	0.075	0.261	0.204	0.057	0.618	-1.738	2.076	4.38E-02	5.92E-01	-3.776	chr1	N_Shelf	JAK1	Yes	Yes	Yes	Yes
cg11585022	0.407	0.631	-0.224	0.452	0.642	-0.191	-1.590	-0.166	-2.073	4.40E-02	5.93E-01	-3.781	chr5	N_Shore	WDR36	Yes	No	No	No
cg15571882	0.714	0.785	-0.072	0.703	0.793	-0.089	-0.531	1.511	-2.058	4.56E-02	5.95E-01	-3.806	chr1	N_Shore	SLC44A3	Yes	No	No	No
cg13679714	0.357	0.278	0.079	0.361	0.263	0.098	0.522	-0.962	2.054	4.60E-02	5.96E-01	-3.812	chr17	N_Shore	ENPP7	Yes	No	No	No
cg13573375	0.524	0.211	0.312	0.538	0.202	0.336	2.113	-0.533	2.049	4.64E-02	5.96E-01	-3.819	chr19	S_Shore	PASA4	Yes	No	No	No
cg24147543	0.191	0.298	-0.107	0.206	0.300	-0.094	-0.935	-1.878	-2.041	4.73E-02	5.97E-01	-3.833	chr6	S_Shelf	HLA-DRB1	Yes	No	No	No
cg26516362	0.889	0.398	-0.109	0.314	0.398	-0.084	-0.756	-1.051	-2.039	4.75E-02	5.98E-01	-3.836	chr5	Island	TRUF1	Yes	No	No	No
cg22686716	0.289	0.117	0.117	0.852	0.826	0.027	0.892	2.228	2.031	4.84E-02	6.00E-01	-3.850	chr1	OpenSea	TRIM33	Yes	No	No	No
cg24912473	0.845	0.751	0.094	0.848	0.815	0.032	0.716	2.219	2.028	4.86E-02	6.00E-01	-3.854	chr19	Island	SGTA	Yes	No	No	No
cg00670721	0.434	0.538	-0.104	0.459	0.533	-0.075	-0.624	-2.088	-2.025	4.90E-02	6.02E-01	-3.859	chr3	S_Shelf	SNORA63_MIR1248	Yes	No	No	No
cg11201654	0.150	0.235	-0.085	0.145	0.251	-0.107	-0.788	-2.318	-2.024	4.91E-02	6.02E-01	-3.860	chr6	N_Shore	HLA-F	Yes	No	No	No
cg15226348	0.534	0.449	0.086	0.532	0.478	0.054	0.519	0.048	2.021	4.94E-02	6.03E-01	-3.865	chr5	OpenSea	ADCY2	Yes	No	No	No
cg14655569	0.411	0.749	-0.338	0.458	0.833	-0.375	-2.596	0.013	-2.016	4.99E-02	6.05E-01	-3.873	chr9	N_Shelf	BICD2	Yes	No	No	No

Table S15. Correlation (Spearman Rho) of methylation levels in DMPs between Early and Late rebound at Vacc+RMD with viral, immunological and clinical variables (p-value < 0.05)

CpG Name	Gene	Clinical parameter	Rho	pval	Module
cg27500148	RPL23	Proviral	0.592	0.043	HIV
cg00267207	GUCY2C	Proviral	0.578	0.049	HIV
cg15416179	MAP2K3	SCA	-0.616	0.033	HIV
cg24337683	CHMP2B	CA_RNA	-0.725	0.008	HIV
cg19693031	TXNIP	CA_RNA	0.704	0.011	HIV
cg19311470	RPL9_LIAS	CA_RNA	-0.687	0.014	HIV
cg24006662	TUBB2A	CA_RNA	-0.673	0.017	HIV
cg24004745	IL1RAP	CA_RNA	-0.630	0.028	HIV
cg05265849	IL6	CA_RNA	0.630	0.028	HIV
cg12075498	JAK1	CA_RNA	0.606	0.037	HIV
cg19693031	TXNIP	Magnitude_HIVtotal	0.629	0.028	HIV
cg12075498	JAK1	Magnitude_HIVtotal	0.587	0.045	HIV
cg14048834	RPL13AP5_RPL13A	Breadth_HIVtotal	0.601	0.039	HIV
cg09513758	AHCYL1	time_MAP	-0.845	0.001	HIV
cg24989962	PTGDR	time_MAP	-0.824	0.001	HIV
cg05984533	ACTG1	time_MAP	0.711	0.009	HIV
cg14048834	RPL13AP5_RPL13A	time_MAP	-0.697	0.012	HIV
cg16853860	PSMB9_TAP1	time_MAP	0.634	0.027	HIV
cg23215256	PRKAR1B	time_MAP	-0.627	0.029	HIV
cg25835669	TUBA8	time_MAP	0.627	0.029	HIV
cg24089118	PTGDR	time_MAP	-0.627	0.029	HIV
cg10890644	TUBAL3	time_MAP	-0.620	0.032	HIV
cg19693031	TXNIP	time_MAP	-0.599	0.040	HIV
cg09885502	GNAS	time_MAP	0.585	0.046	HIV
cg15416179	MAP2K3	time_MAP	0.577	0.049	HIV
cg23815646	ADCY8	Time_on_cART_BCN02	-0.711	0.010	HIV
cg19242688	GNG8	Time_on_cART_BCN02	-0.616	0.033	HIV
cg15226348	ADCY2	VL_cART_initiation	0.734	0.007	HIV
cg04814784	VHL	VL_cART_initiation	-0.699	0.011	HIV
cg00267207	GUCY2C	VL_cART_initiation	0.608	0.036	HIV
cg15416179	MAP2K3	HIV_tocART	0.636	0.026	HIV
cg15416179	MAP2K3	UD_MAP	0.669	0.017	HIV
cg05265849	IL6	UD_MAP	-0.588	0.044	HIV
cg19443786	NOS2	UD_MAP	0.585	0.046	HIV
cg24895834	PRKCCQ	Proviral	-0.613	0.034	Immune
cg08812897	RPS6KA3	SCA	0.865	0.000	Immune
cg16431720	HLA-DQA1	SCA	-0.620	0.032	Immune
cg15416179	MAP2K3	SCA	-0.616	0.033	Immune
cg09900440	HLA-DPA1	SCA	0.609	0.035	Immune
cg17984783	SDCBP	SCA	-0.588	0.044	Immune
cg10409680	HLA-C	SCA	-0.588	0.044	Immune
cg02585483	KIF2A	CA_RNA	-0.767	0.004	Immune
cg24006662	TUBB2A	CA_RNA	-0.673	0.017	Immune
cg24004745	IL1RAP	CA_RNA	-0.630	0.028	Immune
cg05265849	IL6	CA_RNA	0.630	0.028	Immune

Chapter III

cg24895834	PRKCO	CA_RNA	-0.620	0.032	Immune
cg12075498	JAK1	CA_RNA	0.606	0.037	Immune
cg13921204	SEC61A2	CA_RNA	-0.585	0.046	Immune
cg07325233	IL10RB	Magnitude_HIVtotal	-0.608	0.036	Immune
cg12075498	JAK1	Magnitude_HIVtotal	0.587	0.045	Immune
cg11201654	HLA-F	VL_MAP	-0.630	0.028	Immune
cg13921204	SEC61A2	VL_MAP	-0.588	0.044	Immune
cg01815645	HLA-DRB1	time_MAP	-0.838	0.001	Immune
cg24147543	HLA-DRB1	time_MAP	0.775	0.003	Immune
cg02585483	KIF2A	time_MAP	0.725	0.008	Immune
cg09900440	HLA-DPA1	time_MAP	-0.725	0.008	Immune
cg07173283	HLA-DOA	time_MAP	-0.718	0.009	Immune
cg05984533	ACTG1	time_MAP	0.711	0.009	Immune
cg11992783	MYH14	time_MAP	-0.704	0.011	Immune
cg23331433	HLA-DPA1	time_MAP	-0.697	0.012	Immune
cg26063719	VIM	time_MAP	0.669	0.017	Immune
cg12858166	HLA-DPA1	time_MAP	-0.669	0.017	Immune
cg14302130	HLA-DPA1	time_MAP	-0.641	0.025	Immune
cg16853860	PSMB9_TAP1	time_MAP	0.634	0.027	Immune
cg25835669	TUBA8	time_MAP	0.627	0.029	Immune
cg01517384	HLA-B	time_MAP	0.627	0.029	Immune
cg22424444	LOC255512_TOLLIP	time_MAP	0.620	0.032	Immune
cg10890644	TUBAL3	time_MAP	-0.620	0.032	Immune
cg13921204	SEC61A2	time_MAP	0.613	0.034	Immune
cg13661648	HLA-DPA1	time_MAP	-0.599	0.040	Immune
cg16431720	HLA-DQA1	time_MAP	0.599	0.040	Immune
cg14106680	MYH14	time_MAP	-0.592	0.043	Immune
cg22037249	HLA-DPA1	time_MAP	-0.592	0.043	Immune
cg15416179	MAP2K3	time_MAP	0.577	0.049	Immune
cg22731440	HLA-B	time_MAP	0.577	0.049	Immune
cg27107292	HLA-DRB1	time_MAP	-0.577	0.049	Immune
cg00598125	HLA-DRB1	Time_on_cART_BCNO2	0.683	0.014	Immune
cg02788013	INPP5D	Time_on_cART_BCNO2	0.673	0.017	Immune
cg24470466	HLA-DQA1	VL_cART_initiation	-0.832	0.001	Immune
cg10982913	HLA-DQB1	VL_cART_initiation	-0.636	0.026	Immune
cg08812897	RPS6KA3	HIV_tocART	-0.692	0.013	Immune
cg15416179	MAP2K3	HIV_tocART	0.636	0.026	Immune
cg24470466	HLA-DQA1	HIV_tocART	0.608	0.036	Immune
cg16431720	HLA-DQA1	UD_MAP	0.879	0.000	Immune
cg13019553	HLA-B	UD_MAP	0.795	0.002	Immune
cg17984783	SDCBP	UD_MAP	0.781	0.003	Immune
cg27107292	HLA-DRB1	UD_MAP	-0.767	0.004	Immune
cg08812897	RPS6KA3	UD_MAP	-0.715	0.009	Immune
cg15416179	MAP2K3	UD_MAP	0.669	0.017	Immune
cg00598125	HLA-DRB1	UD_MAP	0.669	0.017	Immune
cg22731440	HLA-B	UD_MAP	0.658	0.020	Immune
cg05265849	IL6	UD_MAP	-0.588	0.044	Immune
cg19443786	NOS2	UD_MAP	0.585	0.046	Immune
cg26063719	VIM	UD_MAP	0.578	0.049	Immune

cg01815645	HLA-DRB1	UD_MAP	-0.578	0.049	Immune
cg21226754	RBM22	Proviral	0.799	0.002	Metabolism
cg27500148	RPL23	Proviral	0.592	0.043	Metabolism
cg07571734	PRKAG2	SCA	-0.722	0.008	Metabolism
cg00670721	SNORA63_MIR1248	SCA	-0.648	0.023	Metabolism
cg13679714	ENPP7	SCA	0.609	0.035	Metabolism
cg14227996	MED28	CA_RNA	-0.694	0.012	Metabolism
cg23285761	DDHD2	CA_RNA	-0.694	0.012	Metabolism
cg19311470	RPL9_LIAS	CA_RNA	-0.687	0.014	Metabolism
cg13573375	PIAS4	CA_RNA	0.683	0.014	Metabolism
cg23522194	PLA2G4C	CA_RNA	0.644	0.024	Metabolism
cg15755475	PPT2	CA_RNA	0.641	0.025	Metabolism
cg14396505	ALDH3A2	CA_RNA	-0.630	0.028	Metabolism
cg01188578	HADHA	CA_RNA	0.578	0.049	Metabolism
cg23285761	DDHD2	Magnitude_HIVconsv	-0.643	0.024	Metabolism
cg23285761	DDHD2	Magnitude_HIVtotal	-0.664	0.018	Metabolism
cg22870256	FDFT1	Breadth_HIVtotal	-0.640	0.025	Metabolism
cg14048834	RPL13AP5_RPL13A	Breadth_HIVtotal	0.601	0.039	Metabolism
cg23522194	PLA2G4C	VL_MAP	0.802	0.002	Metabolism
cg14227996	MED28	VL_MAP	-0.690	0.013	Metabolism
cg11585022	WDR36	VL_MAP	-0.655	0.021	Metabolism
cg01188578	HADHA	VL_MAP	0.609	0.035	Metabolism
cg01188578	HADHA	time_MAP	-0.796	0.002	Metabolism
cg07582133	CROT_TP53TG1	time_MAP	0.782	0.003	Metabolism
cg15472574	YBX1	time_MAP	0.704	0.011	Metabolism
cg14048834	RPL13AP5_RPL13A	time_MAP	-0.697	0.012	Metabolism
cg11585022	WDR36	time_MAP	0.676	0.016	Metabolism
cg13573375	PIAS4	time_MAP	-0.641	0.025	Metabolism
cg16853860	PSMB9_TAP1	time_MAP	0.634	0.027	Metabolism
cg00670721	SNORA63_MIR1248	time_MAP	0.634	0.027	Metabolism
cg01786704	SNRPN	time_MAP	-0.592	0.043	Metabolism
cg02136620	RUFY1	Time_on_cART_BCN02	0.690	0.013	Metabolism
cg14820908	RUFY1	Time_on_cART_BCN02	0.676	0.016	Metabolism
cg02788013	INPP5D	Time_on_cART_BCN02	0.673	0.017	Metabolism
cg26516362	RUFY1	Time_on_cART_BCN02	0.616	0.033	Metabolism
cg05457628	RUFY1	Time_on_cART_BCN02	0.616	0.033	Metabolism
cg21226059	RUFY1	Time_on_cART_BCN02	0.602	0.038	Metabolism
cg09060608	RUFY1	Time_on_cART_BCN02	0.581	0.047	Metabolism
cg21226754	RBM22	VL_cART_initiation	0.818	0.001	Metabolism
cg19112186	CPT1B_CHKB-CPT1B	HIV_tocART	-0.622	0.031	Metabolism
cg07571734	PRKAG2	UD_MAP	0.704	0.011	Metabolism
cg19112186	CPT1B_CHKB-CPT1B	UD_MAP	-0.630	0.028	Metabolism
cg00670721	SNORA63_MIR1248	UD_MAP	0.592	0.043	Metabolism
cg02136620	RUFY1	UD_MAP	0.588	0.044	Metabolism
cg00744866	CLASP2	SCA	0.662	0.019	cellcycle
cg02585483	KIF2A	CA_RNA	-0.767	0.004	cellcycle
cg05670953	MLH1_EPM2AIP1	CA_RNA	-0.746	0.005	cellcycle
cg24337683	CHMP2B	CA_RNA	-0.725	0.008	cellcycle
cg13573375	PIAS4	CA_RNA	0.683	0.014	cellcycle

cg24006662	TUBB2A	CA_RNA	-0.673	0.017	cellcycle
cg26571870	GINS2	CA_RNA	-0.627	0.029	cellcycle
cg26312542	TEX12	H3Ac	0.657	0.020	cellcycle
cg05670953	MLH1_EPM2AIP1	Magnitude_HIVconsV	-0.643	0.024	cellcycle
cg03958058	PPP2R2D	Breadth_HIVconsV	0.672	0.017	cellcycle
cg05670953	MLH1_EPM2AIP1	Magnitude_HIVtotal	-0.671	0.017	cellcycle
cg15075357	NPHP4	Magnitude_HIVtotal	0.636	0.026	cellcycle
cg03958058	PPP2R2D	Breadth_HIVtotal	0.643	0.024	cellcycle
cg12286158	DMC1	time_MAP	-0.789	0.002	cellcycle
cg26312542	TEX12	time_MAP	-0.782	0.003	cellcycle
cg02585483	KIF2A	time_MAP	0.725	0.008	cellcycle
cg14701554	NUMA1	time_MAP	-0.725	0.008	cellcycle
cg08201700	WDR60	time_MAP	-0.690	0.013	cellcycle
cg13573375	PIAS4	time_MAP	-0.641	0.025	cellcycle
cg16853860	PSMB9_TAP1	time_MAP	0.634	0.027	cellcycle
cg25835669	TUBA8	time_MAP	0.627	0.029	cellcycle
cg10890644	TUBAL3	time_MAP	-0.620	0.032	cellcycle
cg22061523	AFMID_TK	time_MAP	0.606	0.037	cellcycle
cg27541892	CDK11B	Time_on_cART_BCN02	0.767	0.004	cellcycle
cg00610021	SMC1B_RIBC2	Time_on_cART_BCN02	-0.662	0.019	cellcycle
cg00744866	CLASP2	UD_MAP	-0.718	0.009	cellcycle
cg22061523	AFMID_TK	UD_MAP	0.694	0.012	cellcycle
cg24895834	PRKCCQ	Proviral	-0.613	0.034	signaling
cg00502469	RASA3	Proviral	0.588	0.044	signaling
cg00502469	RASA3	CA_RNA	0.799	0.002	signaling
cg01758122	RASA3	CA_RNA	0.715	0.009	signaling
cg05265849	IL6	CA_RNA	0.630	0.028	signaling
cg22686716	TRIM33	CA_RNA	0.627	0.029	signaling
cg24895834	PRKCCQ	CA_RNA	-0.620	0.032	signaling
cg12532878	RASA3	CA_RNA	0.613	0.034	signaling
cg12075498	JAK1	CA_RNA	0.606	0.037	signaling
cg21234082	DAB2IP	H3Ac	0.860	0.000	signaling
cg00502469	RASA3	Magnitude_HIVconsV	0.657	0.020	signaling
cg12532878	RASA3	Magnitude_HIVconsV	0.615	0.033	signaling
cg10919109	RASA3	Magnitude_HIVconsV	0.580	0.048	signaling
cg12532878	RASA3	Magnitude_HIVtotal	0.762	0.004	signaling
cg27305029	RASA3	Magnitude_HIVtotal	0.706	0.010	signaling
cg10919109	RASA3	Magnitude_HIVtotal	0.664	0.018	signaling
cg00502469	RASA3	Magnitude_HIVtotal	0.594	0.042	signaling
cg12075498	JAK1	Magnitude_HIVtotal	0.587	0.045	signaling
cg27305029	RASA3	Breadth_HIVtotal	0.862	0.000	signaling
cg01758122	RASA3	Breadth_HIVtotal	0.657	0.020	signaling
cg12532878	RASA3	Breadth_HIVtotal	0.615	0.033	signaling
cg24113818	RASA3	Breadth_HIVtotal	0.590	0.043	signaling
cg03290131	DUSP5	time_MAP	0.866	0.000	signaling
cg05984533	ACTG1	time_MAP	0.711	0.009	signaling
cg00945666	F11R	time_MAP	-0.683	0.014	signaling
cg03025830	FGF17	time_MAP	-0.634	0.027	signaling
cg16853860	PSMB9_TAP1	time_MAP	0.634	0.027	signaling

cg01758122	RASA3	time_MAP	-0.599	0.040	signaling
cg24113818	RASA3	time_MAP	-0.585	0.046	signaling
cg11229715	CUL3	Time_on_cART_BCNO2	-0.581	0.047	signaling
cg05265849	IL6	UD_MAP	-0.588	0.044	signaling
cg07571734	PRKAG2	SCA	-0.722	0.008	transport
cg02585483	KIF2A	CA_RNA	-0.767	0.004	transport
cg24337683	CHMP2B	CA_RNA	-0.725	0.008	transport
cg03157226	ATG4D	CA_RNA	-0.697	0.012	transport
cg24006662	TUBB2A	CA_RNA	-0.673	0.017	transport
cg14396505	ALDH3A2	CA_RNA	-0.630	0.028	transport
cg26312542	TEX12	H3Ac	0.657	0.020	transport
cg16200617	BCYRN1_GJB1	Magnitude_HIVconsv	0.734	0.007	transport
cg04467639	COPB1	Breadth_HIVconsv	0.643	0.024	transport
cg16200617	BCYRN1_GJB1	Magnitude_HIVtotal	0.867	0.000	transport
cg14655569	BICD2	Magnitude_HIVtotal	-0.706	0.010	transport
cg04467639	COPB1	Breadth_HIVtotal	0.749	0.005	transport
cg16200617	BCYRN1_GJB1	Breadth_HIVtotal	0.671	0.017	transport
cg14655569	BICD2	Breadth_HIVtotal	-0.615	0.033	transport
cg07582133	CROT_TP53TG1	time_MAP	0.782	0.003	transport
cg13281814	GDAP1	time_MAP	0.775	0.003	transport
cg26660312	WIPI2	time_MAP	-0.761	0.004	transport
cg00393985	WIPI2	time_MAP	-0.739	0.006	transport
cg02585483	KIF2A	time_MAP	0.725	0.008	transport
cg05984533	ACTG1	time_MAP	0.711	0.009	transport
cg26063719	VIM	time_MAP	0.669	0.017	transport
cg25835669	TUBA8	time_MAP	0.627	0.029	transport
cg10890644	TUBAL3	time_MAP	-0.620	0.032	transport
cg00589617	GALNT2	time_MAP	-0.606	0.037	transport
cg24207068	RPTOR	Time_on_cART_BCNO2	0.753	0.005	transport
cg03502601	RPTOR	Time_on_cART_BCNO2	0.715	0.009	transport
cg26660312	WIPI2	VL_cART_initiation	0.594	0.042	transport
cg05157625	RIN3	UD_MAP	0.743	0.006	transport
cg07571734	PRKAG2	UD_MAP	0.704	0.011	transport
cg00240178	EEF1A1	UD_MAP	0.669	0.017	transport
cg22715764	PEX14	UD_MAP	-0.616	0.033	transport
cg26660312	WIPI2	UD_MAP	-0.613	0.034	transport
cg03502601	RPTOR	UD_MAP	0.595	0.041	transport
cg19443786	NOS2	UD_MAP	0.585	0.046	transport
cg26063719	VIM	UD_MAP	0.578	0.049	transport

Discussion

The use of systems biology analysis in immunology has led to a better understanding of the immune system's role in different disease settings and, has allowed for the identification of novel biomarkers of disease progression or of efficacy of therapeutic interventions [149,155,178]. In the present thesis, the main objective was the identification of novel biomarkers and mechanisms, especially at epigenetic level, associated with HIV-1 control in different clinical situations: in the context of natural HIV-1 infection or in the setting of a kick-and-kill therapeutic vaccination. To this end, integrated systems biology analyses, including the study of DNA methylation and gene expression levels in PBMC and soluble factors in plasma, were conducted in a cohort of chronically HIV-1 infected individuals with different levels of HIV-1 control in the absence of antiretroviral treatment, as well as in samples obtained from participants in the kick-and-kill clinical trial BCN02.

Specifically, in the cohort of chronically HIV-1 infected individuals without antiretroviral treatment, PBMC DNA methylation levels or the abundance of plasma soluble factors were compared between individuals with different levels of spontaneous HIV-1 viral control. On the one hand, a PBMC DNA methylation signature was identified that allowed the classification of individuals in relation to their virus burden in peripheral blood. In this setting, individuals with a better HIV-1 control, showed hypermethylation of antiviral genes, and hypomethylation of T-cell activation genes, which correlated with different virological and immune parameters, in particular, interferon regulated genes (ISGs) like PARP9, USP18 and MX1. These results were validated in unrelated cohorts of PLWH (untreated or under antiretroviral treatment) and a group of elite controllers, which confirmed that the silencing of these genes was indeed associated with an enhanced HIV-1 control. These results are in line with previous reports indicating that a strong interferon response during the chronic phase of the HIV-1 infection is associated with disease progression [36,39,179]. Interestingly, the epigenetic regulation of ISGs has been shown to be relevant in other diseases including autoimmune diseases such as Systemic Lupus Erythematosus (SLE) and Sjögren's syndrome, and in other viral infectious diseases including Covid-19 [180–183]. Overall, the data from this study demonstrate that DNA methylation contributes to the silencing of ISGs during the

Discussion

chronic phase of infection in individuals with a good control of the infection. This is supported by transcriptomics studies of PLWH with different rate of HIV-1 disease progression, where LTNPs and ECs showed low level of ISGs expression [153]. Longitudinal analysis of individuals sampled before and after HIV-1 infection will likely be necessary to understand to what extent acute HIV-1 infection impacts the epigenetic landscape and how pre-existing epigenetic signatures define the outcome of infection. These insights could add great value to our understanding of HIV-1 pathogenesis and guide future therapeutic interventions.

In the context of the BCN02 clinical trial that combined the latency reversing agent romidepsin with vaccination using the HIVconsv T-cell immunogen, DNA methylation profiling showed the potential to discriminate between individuals with an Early and Late viral rebound during ART treatment interruption. Interestingly, these differences were present at earlier time points, but were strongly accentuated by romidepsin treatment. This suggests that prior to the kick-and-kill intervention, specific epigenetic patterns may already predict response to the intervention and control the viral rebound in ATI. As the participants in BCN02 were rolled-over from BCN01, it however remains unclear whether there was a determining effect of previous vaccinations (in BCN01) and to what degree early antiretroviral treatment or a basal host epigenome prior to HIV-1 infection determined ATI outcome. In addition, the findings need to be translated into larger cohorts and clinical trials for validation. Still, considering the important role of DNA methylation as a regulator of T-cell immunity and its effect on the formation of memory-like phenotypes in innate immune cells [168,184–186], the inclusion of longitudinal DNA methylation assessments in future vaccine studies has the potential to identify new pathways and mechanisms of virus control. As there is a few data that have addressed the capacity of DNA methylation to predict vaccine efficacy [176,177], future studies have also the potential to identify early biomarkers of vaccine efficacy so that antiretroviral treatment is only stopped in individuals with high chances of virus control.

Of note, the most prominent DNA methylation marks of HIV-1 control observed in the cohort of chronically HIV-infected individuals, do not overlap with the ones observed in

the kick and kill approach, although some of the differentially methylated positions are located in common genes. This is the case of *NLR5* gene, which is hypomethylated in individuals with a poor spontaneous control of HIV-1 infection and in BCN02 participants with early rebound, and that has also been reported to be hypomethylated in HIV-1 infected individuals in contrast to uninfected ones [172]. In parallel, *ADARB1*, a gene that promotes HIV-1 replication, is hypermethylated in individuals with a better control of untreated infection and, in BCN02, in participants with a late viral rebound [187]. Finally, the DMPs hypomethylated in individuals with a delayed HIV-1 rebound (Chapter III) and in individuals with a better HIV-1 control (Chapter I) are enriched in repressed chromatin regions (ReprPC) based on the 18-chromatin states of PBMCs from Roadmap database (Figure 14)[188]. This enrichment of DMPs in repressed chromatin regions, suggest the basal host epigenetic landscape could be associated with HIV-1 control, both in chronic infection or after therapeutic interventions. However, the dissimilarities between the two studies presented in this dissertation could also reflect different mechanisms of viral control in the context of natural infection versus a therapeutic kick-and-kill strategy and post-treatment control. In fact, in the VISCONTI study, the post-treatment control after early and long-term antiretroviral treatment was not associated with the presence of protective HLA class I genotypes nor with the activation of HIV-specific CD8 T cells that is observed in chronically infected, untreated individuals with an elite controller phenotype. Instead, the main characteristic of post-treatment controllers (PTCs) was the capacity to maintain low-level blood reservoirs [87]. In this line, the differential epigenetic landscapes between individuals with an early and late rebound in the BCN02 could not only be related to the immune responses against HIV-1, but could also reflect differences in HIV-1 integration sites, which ultimately can as well impact viral rebound kinetics. Thus, future analyses, combining the study of chromatin accessibility, HIV-1 integration sites, immunogenicity and DNA methylation may help to identify markers that can predict control of viral rebound after treatment interruption and to design new strategies or combination approaches to achieve a functional cure for HIV-1.

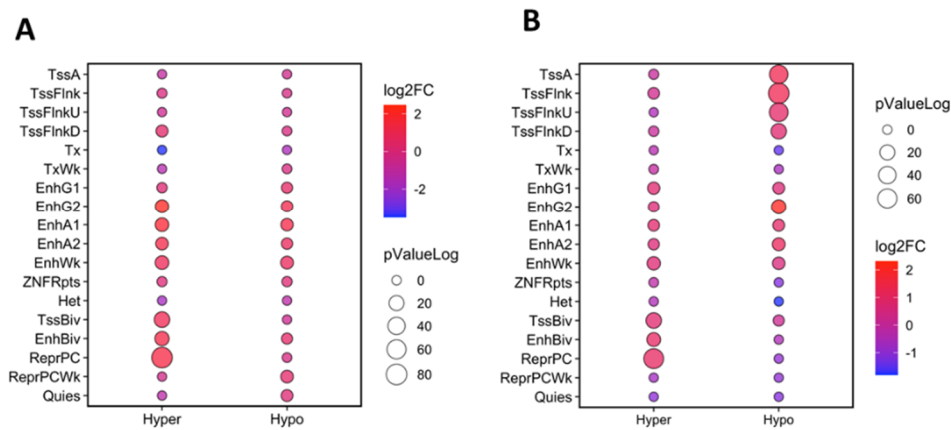


Figure 14. Chromatin state enrichment. (18-state ChromHMM in PBMCs). A. Chromatin state enrichment based on DMPs between individuals with different natural HIV-1 control (Chapter I). X-axis make reference to DMPs hypermethylated (Hyper) or hypomethylated (Hypo) in individuals with a poor natural HIV-1 control. B. Chromatin state enrichment based on DMPs between individuals with an early or late viral rebound after vaccination and romidepsin in the BCN02 study (Chapter III). X-axis make reference to DMPs hypermethylated (Hyper) or hypomethylated (Hypo) in individuals with a rapid viral load rebound (reaching 2,000 HIV-1 RNA copies/ml after 4 weeks of treatment interruption)

Aside from DNA methylation profiles, transcriptional changes were as well observed in the context of the BCN02 study. One week after vaccination, there was an increase in the expression of genes involved in Fc signaling, complement activation and BCR activation. Strikingly, although the HIVconsv immunogen was designed to elicit HIV-1 specific T-cell responses, no enrichment was observed in pathways associated with T-cell immunity when comparing post-vaccination time point versus baseline. This lack of T-cell signatures could be due to the select of the sampling time points for transcriptomic analysis, which was one week after vaccination and thus at a time when T-cell responses may have already contracted again. Another possibility is that gene expression changes induced in T-cells specifically were diluted in total PBMCs transcriptomics study. In parallel, after HIVconsv vaccination and the romidepsin infusion (Vacc+RMD), several gene expression changes associated with HIV-1 mobilization and immune activation, both at T cell and innate immunity level were observed. Interestingly, in some of these pathways (e.g. *HIV life cycle*, *Enriched in Monocytes* or *T-cell activation*) a possible epigenetic regulation was likely as the majority of the genes that were upregulated in transcriptomics analyses were hypomethylated, or vice versa. However, limited matches were identified between the two -omics datasets. Furthermore, the lack of a control placebo arm did not allow to fully

comprehend the net effect of vaccination and/or romidepsin on the two omics assessments.

To partially overcome this issue, a transcriptomics study in PBMCs and isolated CD4 T cells of individuals who had only been treated with RMD (part A REDUC clinical trial) was conducted. Strikingly, a high overlap was observed between BCN02 PBMCs and REDUC CD4 T cells, which suggest that many signals in the BCN02 study were indeed derived from CD4 T cells and that previous vaccination could account for these differences. Still, for a complete integrative analysis that allows to identify which longitudinal changes were due to which clinical intervention, a clinical study design with a larger sample size, a proper control arm and more regular analyses time points would be needed. Nevertheless, the current data in this exploratory clinical study highlight the feasibility and the potential scientific benefits that could be gained from applying genome-wide gene expression and DNA methylation analyses in future clinical trials. While samples from such clinical interventions will always be scarce, their adequate use could help identify beneficial/protective mechanisms triggered during the therapy and provide the scientific community with new hypothesis to be tested in iterative clinical trials towards an HIV cure.

Plasma proteomics studies have been widely applied in systems biology studies in different fields as it is an easy-accessible fluid which can reflect the differential biological processes between groups of individuals, or between different treatments applied [131,189,190]. In the present dissertation, a targeted protein array covering proteins involved in cell to cell communication was applied to evaluate plasma factors in a large cohort of chronically untreated HIV-infected individuals. These analyses identified the TL1A/DR3 axis as a potential therapeutic target to improve HIV-specific cellular immune responses. In particular, individuals with a better HIV-1 control in the absence of cART showed elevated levels of both sTL1A and sDR3, and high gene expression of DR3 in PBMCs. Correlation analyses showed that, while sTL1A was negatively correlated with pVL and positively with CD4 counts, interestingly positive correlations were identified between the levels of sDR3 and the magnitude and the breadth of the HIV-specific T-cell

response in these individuals. Additionally, in a cohort of cART treated individuals, sDR3 levels were correlated with the percentage of activated effector CD8 T cells, whereas sTL1A was correlated with the percentage of CD4 and CD8 regulatory T cells. These results point towards a possible dual role of the TL1A-DR3 axis where, on the one hand, CD8 T cells, in the presence of a cognate antigen express DR3 to stimulate antigen-specific responses [191–193], while on the other hand, sTL1A binds to constitutively expressed DR3 in Tregs to limit inflammation and prevent the damage to host tissues [194–196]. The latter is in line with the beneficial results seen with TL1A-Ig treatment in graft-versus-host disease [196]. In Chapter II, we also show that in mice previously vaccinated with HTI immunogen, the stimulation of splenocytes with HTI-peptides and an agonistic DR3 antibody (4C12) increased the percentage of HTI-specific T-cell responses *in ex-vivo* assays. To further validate these results, we also stimulated *ex vivo* PBMCs from untreated PLWH with a pool of HIV peptides, together with an antibody against DR3 (with no described agonistic or antagonistic function), which led to an increase in the magnitude of HIV-specific CD8 T cells. Therefore, these results suggest that the co-stimulation of TL1A/DR3 axis during HIV-1 vaccination could boost the specific cellular response *in vivo*. One of the major benefits of this strategy, would be that DR3 is only expressed on CD4 and CD8 T cells in the presence of a cognate antigen to stimulate TCR, so that it could be beneficial in the context of HIV-1 vaccination to enhance specifically the cellular response against HIV-1. Although no commercially available agonistic antibody was identified at the time when these experiments were conducted, a first phase I clinical trial using PTX-35 drug (a DR3 agonist monoclonal antibody) is ongoing in the cancer field (NCT04430348) to evaluate its safety profile. Of note, in the cancer immunotherapy field, agonistic effect of other costimulatory molecules (e.g. OX40, 4-1BB) are being tested clinically and could be translated to HIV-1 infection. In particular, previous data in HIV-1 vaccination in mice have proposed the stimulation of 4-1BB or OX40 to enhance HIV-specific T-cell responses [197,198]. As recent clinical trials using HIV-1 T-cell vaccination have yielded promising results and, in the context of the AELIX-002 trial, even showed a correlation between the magnitude of the immunogen-specific T-cell response and the time off ART during treatment

interruption, boosting these responses by agonistic antibodies may provide critical improvements [97,101].

Overall, the results in the present thesis have revealed that the epigenetic landscape can affect both, the spontaneous control of HIV-1 infection and the viral rebound kinetics after a kick-and-kill intervention (Chapter I and Chapter III). Additionally, the combined study of gene expression and DNA methylation (Chapter III) has identified the pathways that are modulated during the BCN02 intervention and identified potentially important pathways that could be epigenetically regulated. In parallel, these analyses also demonstrated that plasma-based proteomics not only provides biomarkers of HIV control, but also markers that may mirror the different immune mechanisms involved in the maintenance of a natural control of the HIV-1 infection, and which could be exploited therapeutically to improve current vaccine therapies (Chapter II).

The mechanisms suggested by our analyses need a cautious interpretation as the cellular origin of plasma factors signals, and DNA methylation and gene expression marks in total PBMCs remain unidentified. In the case of DNA methylation in PBMCs, this is especially critical as each cell type has a cell-specific DNA methylation pattern. Thus, identified differential methylation signatures between two groups or the association of a DNA methylation signature with a given variable, could reflect a different cell type composition rather than true functional relationships. Different methods have been proposed to correct for such variable cell type proportions, although there is no general consensus on how to deal best with this variability [199,200]. In Chapter I of this thesis, it was indeed necessary to take such adjustment into account since a pronounced bias in CD4 counts was present between individuals with differential HIV-1 natural control. To that end, the different PBMC cell type proportions were estimated based on DNA methylation using a previous reference dataset, and these variables were adjusted in the model [125,201]. In the BCN02 study, participants were more homogenous with regards to cell type proportions and such adjustment was not applied. Notwithstanding, to evaluate the cellular origin of the DNA methylation marks, the gene expression levels or the plasma levels of specific proteins, the results should be evaluated in individual,

isolated cell types. Interestingly, the epigenetic regulation of T-cell activation in Chapter I, is also observed in a study comparing the DNA methylation of isolated CD4 T cells from PLWH with differential HIV-1 disease progression, indicating that relevant CD4 methylation imprints can still be detected in total PBMCs. In contrast though, the hypermethylation of ISGs observed in our study (Chapter I) is not the most prominent signal in isolated CD4 T cells, although some genes, including *MX1* are as well hypermethylated in CD4 T cells of ECs [202]. This latter observation suggests that the epigenetic regulation of the antiviral response might be more relevant in other cell types, such as monocytes. This could also explain some recent findings in early HIV-1 infection where a demethylation of ISGs was observed and which could be driven by viremia [203]. Still, published and our own data indicated that the most pronounced signals in specific cell-types can still be detected in global PBMCs. While PBMCs use is especially appealing from a biomarker point of view, to identify therapeutic targets and design or refine clinical strategies, *in vitro* experiments in isolated cell types to validate the generated hypothesis and to describe the molecular mechanisms mediating the HIV-1 immune control would also be needed.

Beyond cellular heterogeneity, other limitations such as the limited sample size and the high variability between individuals need to be considered. In addition, in the comparisons applied in the different chapters of this thesis, all the individuals used in comparisons groups were HIV-1 infected, so the differences at DNA methylation, gene expression or proteomics level, may be less evident than in studies where HIV uninfected control individuals could be included. For the BCN02 study, were the sample size was especially limited, we opted to conduct the analysis from an exploratory perspective, interpreting the results at pathway rather than at single gene or CpG position level. Notwithstanding, the BCN02 results serve as a proof of concept that DNA methylation represents a stable mark, albeit affected by the environment, which should be further explored as a source of candidate biomarker in the context of HIV-1 clinical trials to predict virus rebound after treatment interruption or to identify individuals that can benefit from a specific treatment. This is supported by a recent study that has evaluated the longitudinal variability of different types of omics data and which has

shown that DNA methylation is the more stable mark between two different time-points, while gene expression profiles were more variable [167]. Thus, DNA methylation-derived profiles can possibly serve as useful biomarkers to compare groups of individuals at a single time point, while gene expression is more informative of longitudinal changes, especially when sampled close enough to a specific intervention. Importantly, the DNA methylation imprint reflect a complex epigenetic program which was not fully elucidated in the present analysis. Still, we showed a differential epigenetic landscape between individuals with different post treatment viral control that might affect the binding of transcription factors and, as suggested by correlation analysis, might impact the T-cell responses to vaccination. As such, epigenetic regulation studies might reveal important insights into host defense mechanisms in HIV infection and guide future cure and eradication strategies.

Finally, the biological mechanisms behind a phenotype of HIV-1 control are heterogenous and may involve molecular regulations at different levels. Thus, integration of multiple -omics datasets might be helpful to better characterize these individuals [204]. To this end, in the recent years several studies have integrated different types of -omics data with different analytical approaches. Some of them have analyzed separated datasets and then identified overlapping signatures, others have focused on pathways common to different datasets, while more recently, statistical methods to integrate both datasets have been applied [146]. In this sense, methods like DIABLO, an extension of Partial Least Square – Discriminant Analysis (PLS-DA), have been developed and their aim is to identify a multi-omic signatures with highly correlated features and with the capacity to discriminate individuals in two different groups [142,147]. Such analyses have the potential to identify targets regulated at different levels that could explain the differences between the two groups. Although this approach was applied in the BCN02 clinical trial, the low sample size precluded the identification of a reliable multi-omics biomarker of HIV-1 control.

The identification of candidate biomarkers of HIV control would greatly benefit the safety of conducting analytical treatment interruptions (ATIs). Current HIV cure clinical

trials include the use of ATIs, which requires intensive monitoring and have associated risks as well as ethical implications, so that a surrogate biomarker of such post-intervention control is urgently needed [205]. In addition, HIV-1 infection and the levels of spontaneous virus control are highly heterogeneous, possibly due to a combination of different factors determining final level of control. It is thus possible that there is no single HIV-1 cure that would be applicable to all individuals and it might be required to stratify individuals according to the capacity to respond to the different treatments (precision medicine). In order to build a reliable classification or to define predictive biomarkers that could be readily translated into clinics, it will certainly be necessary to base these analyses on cohorts of sufficient sample size, including training data sets and an external testing set to validate the results [143,183]. Ideally, subsequent steps would then also include the validation of resulting biomarkers with other techniques like pyrosequencing, MSP (methylation specific PCR) qRT-PCR, or ELISA, and, if possibly, by *in vitro* experimentation. Of course, if the biomarkers can be assessed by techniques used in routine clinical laboratory facilities, or can be easily adapted to its use (e.g. customized arrays), this would greatly facilitate their translation into the clinical practice [206].

Overall, systems biology has allowed and will continue to allow the gathering of highly valuable information from limited human samples, like the samples from the cohorts studied in chapter I and II and the samples from the clinical trial in chapter III. Such information will help to identify the biological processes dysregulated between different conditions and thereby lead to the discovery of new therapeutic targets. Similarly, these studies also point to possible candidate biomarkers that can serve as surrogates of viral control, either in a situation of natural control or in post-treatment control in the context of a clinical study. Therefore, systems biology in the HIV-1 field are highly useful to refine current therapeutically strategies or to design new ones, and to identify the groups of individuals that can benefit the most from each of such interventions.

Conclusions

1. DNA methylation profiling can provide biomarkers of viral control in situations of spontaneous and/or post-treatment virus control.
2. In a cohort of untreated chronically HIV-1 infected individuals, the individuals with a better HIV-1 control showed high methylation levels of ISGs while low methylation levels on genes involved in T-cell activation and differentiation. Therefore, the epigenetic regulation of these pathways, which are modulated by potential HIV-1 cure therapies involving kick-and-kill approaches, need to be considered in future HIV-1 cure strategies.
3. The TL1A-DR3 axis was associated with HIV-1 control in a targeted-plasma proteomics study in a cohort of untreated chronically HIV-1 infected individuals. *In silico* and *in vitro* validation analyses demonstrated that the stimulation of this axis improved HIV-1-specific T-cell responses. Additionally, studies in mice suggest that in vaccination strategies, DR3 agonistic stimulation can improve vaccine-elicited T-cell responses.
4. A systems biology analysis in the BCN02 clinical trial identified host transcriptional and DNA methylation programs that were impacted by the kick-and-kill intervention, including genes involved in HIV-1 infection, T-cell activation and innate immunity.
5. DNA methylation profiling has the potential to discriminate between individuals with an early or a late viral rebound after ART is stopped, even in samples tested before the actual treatment interruption phase.
6. Omics-based studies applied in HIV-1 infection can provide novel mechanisms and biomarkers that can be considered in future, refined HIV-1 cure strategies.

Publications

Articles published during the PhD

Oriol-Tordera B, Llano A, Ganoza C, Cate S, Hildebrand W, Sanchez J, Calle ML, Brander C, Olvera A. Impact of HLA-DRB1 allele polymorphisms on control of HIV infection in a Peruvian MSM cohort. *HLA*. 2017 Oct;90(4):234-237. doi: 10.1111/tan.13085. Epub 2017 Jul 5. PMID: 28677168.

Ruiz-Riol M, Berdnik D, Llano A, Mothe B, Gálvez C, Pérez-Álvarez S, **Oriol-Tordera B**, Olvera A, Silva-Arrieta S, Meulbroek M, Pujol F, Coll J, Martinez-Picado J, Ganoza C, Sanchez J, Gómez G, Wyss-Coray T, Brander C. Identification of Interleukin-27 (IL-27)/IL-27 Receptor Subunit Alpha as a Critical Immune Axis for In Vivo HIV Control. *J Virol*. 2017 Jul 27;91(16):e00441-17. doi: 10.1128/JVI.00441-17. PMID: 28592538; PMCID: PMC5533920.

Oriol-Tordera B, Berdasco M, Llano A, Mothe B, Gálvez C, Martinez-Picado J, Carrillo J, Blanco J, Duran-Castells C, Ganoza C, Sanchez J, Clotet B, Calle ML, Sánchez-Pla A, Esteller M, Brander C, Ruiz-Riol M. Methylation regulation of Antiviral host factors, Interferon Stimulated Genes (ISGs) and T-cell responses associated with natural HIV control. *PLoS Pathog*. 2020 Aug 6;16(8):e1008678. doi: 10.1371/journal.ppat.1008678. PMID: 32760119; PMCID: PMC7410168.

Oriol-Tordera B, Olvera A, Duran-Castells C, Llano A, Mothe B, Massanella M, Dalmau J, Ganoza C, Sanchez J, Calle ML, Clotet B, Martinez-Picado J, Negredo E, Blanco J, Hartigan-O'Connor D, Brander C, Ruiz-Riol M. TL1A-DR3 Plasma Levels Are Predictive of HIV-1 Disease Control, and DR3 Costimulation Boosts HIV-1-Specific T Cell Responses. *J Immunol*. 2020 Dec 15;205(12):3348-3357. doi: 10.4049/jimmunol.2000933. Epub 2020 Nov 11. PMID: 33177161; PMCID: PMC7725879.

Bibliography

1. Abbas A, Lichtman A, Pillai S. Cellular and Molecular Immunology (9th ed). Elseiver. 2016.
2. Barre-Sinoussi F, Chermann J, Rey F, Nugeyre M, Chamaret S, Gruest J, et al. Isolation of a T-lymphotropic retrovirus from a patient at risk for acquired immune deficiency syndrome (AIDS). *Science* (80-). 1983;220: 868–871. doi:10.1126/science.6189183
3. Gallo R, Salahuddin S, Popovic M, Shearer G, Kaplan M, Haynes B, et al. Frequent detection and isolation of cytopathic retroviruses (HTLV-III) from patients with AIDS and at risk for AIDS. *Science* (80-). 1984;224: 500–503. doi:10.1126/SCIENCE.6200936
4. Fauci AS, Lane HC. Four Decades of HIV/AIDS — Much Accomplished, Much to Do. *N Engl J Med*. 2020;383: 1–4. doi:10.1056/nejmp1916753
5. Deeks SG, Overbaugh J, Phillips A, Buchbinder S. HIV infection. *Nat Rev Dis Prim* 2015 11. 2015;1: 1–22. doi:10.1038/nrdp.2015.35
6. Maartens G, Celum C, Lewin SR. HIV infection: epidemiology, pathogenesis, treatment, and prevention. *Lancet*. 2014;384: 258–271. doi:10.1016/S0140-6736(14)60164-1
7. Malekinejad M, Parriott A, Blodgett JC, Horvath H, Shrestha RK, Hutchinson AB, et al. Effectiveness of community-based condom distribution interventions to prevent HIV in the United States: A systematic review and meta-analysis. Nikolopoulos GK, editor. *PLoS One*. 2017;12: e0180718. doi:10.1371/journal.pone.0180718
8. Faust L, Yaya S. The effect of HIV educational interventions on HIV-related knowledge, condom use, and HIV incidence in sub-Saharan Africa: a systematic review and meta-analysis. *BMC Public Health*. 2018;18: 1254. doi:10.1186/s12889-018-6178-y
9. Aspinall EJ, Nambiar D, Goldberg DJ, Hickman M, Weir A, Van Velzen E, et al. Are needle and syringe programmes associated with a reduction in HIV transmission among people who inject drugs: a systematic review and meta-analysis. *Int J Epidemiol*. 2014;43: 235–248. doi:10.1093/ije/dyt243
10. UNAIDS. Fact sheet - Latest global and regional statistics on the status of the AIDS

Bibliography

- epidemic. Unaided. 2017; 8. Available: https://www.unaids.org/en/resources/documents/2021/UNAIDS_FactSheet
11. Greene WC, Peterlin BM. Charting HIV's remarkable voyage through the cell: Basic science as a passport to future therapy. *Nature Medicine* Nature Publishing Group; 2002 pp. 673–680. doi:10.1038/nm0702-673
 12. González ME. Vpu protein: The viroporin encoded by HIV-1. *Viruses*. MDPI AG; 2015. pp. 4352–4368. doi:10.3390/v7082824
 13. Arts EJ, Hazuda DJ. HIV-1 antiretroviral drug therapy. *Cold Spring Harb Perspect Med*. 2012;2. doi:10.1101/cshperspect.a007161
 14. FDA-Approved HIV Medicines | NIH. [cited 24 May 2021]. Available: <https://hivinfo.nih.gov/understanding-hiv/fact-sheets/fda-approved-hiv-medicines>
 15. Mogensen TH, Melchjorsen J, Larsen CS, Paludan SR. Innate immune recognition and activation during HIV infection. *Retrovirology*. 2010;7: 54. doi:10.1186/1742-4690-7-54
 16. Altfeld M, Gale M. Innate immunity against HIV-1 infection. *Nature Immunology*. Nature Publishing Group; 2015. pp. 554–562. doi:10.1038/ni.3157
 17. Hendricks CM, Cordeiro T, Gomes AP, Stevenson M. The Interplay of HIV-1 and Macrophages in Viral Persistence. *Front Microbiol*. 2021;12: 646447. doi:10.3389/fmicb.2021.646447
 18. Colomer-Lluch M, Ruiz A, Moris A, Prado JG. Restriction Factors: From Intrinsic Viral Restriction to Shaping Cellular Immunity Against HIV-1. *Front Immunol*. 2018;9: 2876. doi:10.3389/FIMMU.2018.02876
 19. Kazer SW, Walker BD, Shalek AK. Evolution and Diversity of Immune Responses during Acute HIV Infection. *Immunity*. 2020;53: 908–924. doi:10.1016/J.IMMUNI.2020.10.015
 20. Collins DR, Gaiha GD, Walker BD. CD8 + T cells in HIV control, cure and prevention. *Nat Rev Immunol* 2020 208. 2020;20: 471–482. doi:10.1038/s41577-020-0274-9
 21. Chevalier MF, Didier C, Girard P-M, Manea ME, Campa P, Barré-Sinoussi F, et al. CD4 T-Cell Responses in Primary HIV Infection: Interrelationship with Immune Activation and Virus Burden. *Front Immunol*. 2016;7: 395.

- doi:10.3389/FIMMU.2016.00395
22. Overbaugh J, Morris L. The Antibody Response against HIV-1. *Cold Spring Harb Perspect Med.* 2012;2. doi:10.1101/CSHPERSPECT.A007039
 23. Carrillo J, Clotet B, Blanco J. Antibodies and Antibody Derivatives: New Partners in HIV Eradication Strategies. *Front Immunol.* 2018;9: 2429. doi:10.3389/FIMMU.2018.02429
 24. Moir S, Fauci AS. B cells in HIV infection and disease. NIH Public Access; Apr, 2009. Available: /pmc/articles/PMC2779527/
 25. Aasa-Chapman MM, Hayman A, Newton P, Cornforth D, Williams I, Borrow P, et al. Development of the antibody response in acute HIV-1 infection. *AIDS.* 2004;18: 371–381. doi:10.1097/00002030-200402200-00002
 26. Fryer HR, Frater J, Duda A, Roberts MG, Investigators TST, Phillips RE, et al. Modelling the Evolution and Spread of HIV Immune Escape Mutants. *PLoS Pathog.* 2010;6. doi:10.1371/JOURNAL.PPAT.1001196
 27. Cao J, McNevin J, Malhotra U, McElrath MJ. Evolution of CD8+ T Cell Immunity and Viral Escape Following Acute HIV-1 Infection. *J Immunol.* 2003;171: 3837–3846. doi:10.4049/JIMMUNOL.171.7.3837
 28. Kim J, De La Cruz J, Lam K, Ng H, Daar ES, Balamurugan A, et al. CD8 + Cytotoxic T Lymphocyte Responses and Viral Epitope Escape in Acute HIV-1 Infection. *Viral Immunol.* 2018;31: 525–536. doi:10.1089/vim.2018.0040
 29. Sunshine JE, Larsen BB, Maust B, Casey E, Deng W, Chen L, et al. Fitness-Balanced Escape Determines Resolution of Dynamic Founder Virus Escape Processes in HIV-1 Infection. Silvestri G, editor. *J Virol.* 2015;89: 10303–10318. doi:10.1128/JVI.01876-15
 30. Robb ML, Ananworanich J. Lessons from acute HIV infection. *Curr Opin HIV AIDS.* 2016;11: 555. doi:10.1097/COH.0000000000000316
 31. Moir S, Chun T-W, Fauci AS. Pathogenic Mechanisms of HIV Disease. *Annu Rev Pathol Mech Dis.* 2011;6: 223–248. doi:10.1146/annurev-pathol-011110-130254
 32. Lawn SD, Butera ST, Folks TM. Contribution of Immune Activation to the Pathogenesis and Transmission of Human Immunodeficiency Virus Type 1 Infection. *Clin Microbiol Rev.* 2001;14: 753. doi:10.1128/CMR.14.4.753-777.2001

Bibliography

33. Hazenberg MD, Otto SA, van Benthem BH, Roos MT, Coutinho RA, Lange JM, et al. Persistent immune activation in HIV-1 infection is associated with progression to AIDS. *AIDS*. 2003;17: 1881–1888. doi:10.1097/00002030-200309050-00006
34. Chan JK, Greene WC. Dynamic roles for NF- κ B in HTLV-I and HIV-1 retroviral pathogenesis. *Immunol Rev*. 2012;246: 286–310. doi:10.1111/j.1600-065X.2012.01094.x
35. Wong LM, Jiang G. NF- κ B sub-pathways and HIV cure: A revisit. *EBioMedicine*. Elsevier; 2021. p. 103159. doi:10.1016/j.ebiom.2020.103159
36. Soper A, Kimura I, Nagaoka S, Konno Y, Yamamoto K, Koyanagi Y, et al. Type I Interferon Responses by HIV-1 Infection: Association with Disease Progression and Control. *Front Immunol*. 2018;8: 1823. doi:10.3389/fimmu.2017.01823
37. Cheng L, Ma J, Li J, Li D, Li G, Li F, et al. Blocking type I interferon signaling enhances T cell recovery and reduces HIV-1 reservoirs. *J Clin Invest*. 2016;127: 269–279. doi:10.1172/JCI90745
38. Jacquelin B, Mayau V, Targat B, Liovat A-S, Kunkel D, Petitjean G, et al. Nonpathogenic SIV infection of African green monkeys induces a strong but rapidly controlled type I IFN response. *J Clin Invest*. 2009;119: 3544–3555. doi:10.1172/JCI40093
39. Bosinger SE, Li Q, Gordon SN, Klatt NR, Duan L, Xu L, et al. Global genomic analysis reveals rapid control of a robust innate response in SIV-infected sooty mangabeys. *J Clin Invest*. 2009;119: 3556–72. doi:10.1172/JCI40115
40. Ramendra R, Isnard S, Lin J, Fombuena B, Ouyang J, Mehraj V, et al. Cytomegalovirus Seropositivity Is Associated With Increased Microbial Translocation in People Living With Human Immunodeficiency Virus and Uninfected Controls. *Clin Infect Dis*. 2020;71: 1438–1446. doi:10.1093/cid/ciz1001
41. Brenchley JM, Price DA, Schacker TW, Asher TE, Silvestri G, Rao S, et al. Microbial translocation is a cause of systemic immune activation in chronic HIV infection. *Nat Med*. 2006;12: 1365–1371. doi:10.1038/nm1511
42. Wherry EJ, Ha S-J, Kaech SM, Haining WN, Sarkar S, Kalia V, et al. Molecular signature of CD8⁺ T cell exhaustion during chronic viral infection. *Immunity*.

- 2007;27: 670–84. doi:10.1016/j.immuni.2007.09.006
43. Virgin HW, Wherry EJ, Ahmed R. Redefining chronic viral infection. *Cell*. 2009;138: 30–50. doi:10.1016/j.cell.2009.06.036
 44. Abbar B, Baron M, Katlama C, Marcelin AG, Veyri M, Autran B, et al. Immune checkpoint inhibitors in people living with HIV: What about anti-HIV effects? *AIDS*. 2020;34: 167–175. doi:10.1097/QAD.0000000000002397
 45. Grabmeier-Pfistershammer K, Stecher C, Zettl M, Roskopf S, Rieger A, Zlabinger GJ, et al. Antibodies targeting BTLA or TIM-3 enhance HIV-1 specific T cell responses in combination with PD-1 blockade. *Clin Immunol*. 2017;183: 167–173. doi:10.1016/J.CLIM.2017.09.002
 46. Freeman GJ, Wherry EJ, Ahmed R, Sharpe AH. Reinvigorating exhausted HIV-specific T cells via PD-1-PD-1 ligand blockade. *J Exp Med*. 2006;203: 2223–7. doi:10.1084/jem.20061800
 47. Vanhamel J, Bruggemans A, Debyser Z. Establishment of latent HIV-1 reservoirs: what do we really know? *J Virus Erad*. 2019;5: 3. Available: /pmc/articles/PMC6362902/
 48. Chauveau M, Billaud E, Bonnet B, Merrien D, Hitoto H, Bouchez S, et al. Tenofovir DF/emtricitabine/rilpivirine as HIV post-exposure prophylaxis: results from a multicentre prospective study. *J Antimicrob Chemother*. 2019;74: 1021–1027. doi:10.1093/jac/dky547
 49. Grant RM, Lama JR, Anderson PL, McMahan V, Liu AY, Vargas L, et al. Preexposure Chemoprophylaxis for HIV Prevention in Men Who Have Sex with Men. <http://dx.doi.org/101056/NEJMoa1011205>. 2010;363: 2587–2599. doi:10.1056/NEJMOA1011205
 50. Molina J-M, Capitant C, Spire B, Pialoux G, Cotte L, Charreau I, et al. On-Demand Preexposure Prophylaxis in Men at High Risk for HIV-1 Infection. <http://dx.doi.org/101056/NEJMoa1506273>. 2015;373: 2237–2246. doi:10.1056/NEJMOA1506273
 51. Whitney JB, Hill AL, Sanisetty S, Penaloza-MacMaster P, Liu J, Shetty M, et al. Rapid seeding of the viral reservoir prior to SIV viraemia in rhesus monkeys. *Nature*. 2014;512: 74–77. doi:10.1038/nature13594

Bibliography

52. Colby DJ, Trautmann L, Pinyakorn S, Leyre L, Pagliuzza A, Kroon E, et al. Rapid HIV RNA rebound after antiretroviral treatment interruption in persons durably suppressed in Fiebig I acute HIV infection. *Nat Med*. 2018;24: 923–926. doi:10.1038/s41591-018-0026-6
53. Persaud D, Gay H, Ziemniak C, Chen YH, Piatak M, Chun T-W, et al. Absence of detectable HIV-1 viremia after treatment cessation in an infant. *N Engl J Med*. 2013;369: 1828–35. doi:10.1056/NEJMoa1302976
54. Chaillon A, Gianella S, Dellicour S, Rawlings SA, Schlub TE, De Oliveira MF, et al. HIV persists throughout deep tissues with repopulation from multiple anatomical sources. *J Clin Invest*. 2020;130: 1699–1712. doi:10.1172/JCI134815
55. Rothenberger MK, Keele BF, Wietgreffe SW, Fletcher C V., Beilman GJ, Chipman JG, et al. Large number of rebounding/founder HIV variants emerge from multifocal infection in lymphatic tissues after treatment interruption. *Proc Natl Acad Sci*. 2015;112: E1126–E1134. doi:10.1073/pnas.1414926112
56. Banga R, Procopio FA, Noto A, Pollakis G, Cavassini M, Ohmiti K, et al. PD-1(+) and follicular helper T cells are responsible for persistent HIV-1 transcription in treated aviremic individuals. *Nat Med*. 2016;22: 754–61. doi:10.1038/nm.4113
57. Andrade VM, Mavian C, Babic D, Cordeiro T, Sharkey M, Barrios L, et al. A minor population of macrophage-tropic HIV-1 variants is identified in recrudescing viremia following analytic treatment interruption. *Proc Natl Acad Sci*. 2020;117: 9981–9990. doi:10.1073/pnas.1917034117
58. Dufour C, Gantner P, Fromentin R, Chomont N. The multifaceted nature of HIV latency. *J Clin Invest*. 2020;130: 3381–3390. doi:10.1172/JCI136227
59. Jean MJ, Fiches G, Hayashi T, Zhu J. Current Strategies for Elimination of HIV-1 Latent Reservoirs Using Chemical Compounds Targeting Host and Viral Factors. *AIDS Res Hum Retroviruses*. 2019;35: 1–24. doi:10.1089/AID.2018.0153
60. Henderson LJ, Reoma LB, Kovacs JA, Nath A. Advances toward Curing HIV-1 Infection in Tissue Reservoirs. *J Virol*. 2020;94. Available: <https://doi.org/10.1128/JVI.00375-19>.
61. Chomont N, DaFonseca S, Vandergeeten C, Ancuta P, Sékaly R-P. Maintenance of CD4+ T-cell memory and HIV persistence: keeping memory, keeping HIV. *Curr*

- Opin HIV AIDS. 2011;6: 30–6. doi:10.1097/COH.0b013e3283413775
62. Cohn LB, Chomont N, Deeks SG. The Biology of the HIV-1 Latent Reservoir and Implications for Cure Strategies. *Cell Host Microbe*. 2020;27: 519–530. doi:10.1016/J.CHOM.2020.03.014
63. Castro-Gonzalez S, Colomer-Lluch M, Serra-Moreno R. Barriers for HIV Cure: The Latent Reservoir. *AIDS Res Hum Retroviruses*. 2018;34: 739–759. doi:10.1089/AID.2018.0118
64. Ait-Ammar A, Kula A, Darcis G, Verdikt R, De Wit S, Gautier V, et al. Current Status of Latency Reversing Agents Facing the Heterogeneity of HIV-1 Cellular and Tissue Reservoirs. *Front Microbiol*. 2020;10: 3060. doi:10.3389/fmicb.2019.03060
65. Coiras M, López-Huertas MR, Pérez-Olmeda M, Alcamí J. Understanding HIV-1 latency provides clues for the eradication of long-term reservoirs. *Nat Rev Microbiol*. 2009;7: 798–812. doi:10.1038/nrmicro2223
66. Chomont N, El-Far M, Ancuta P, Trautmann L, Procopio FA, Yassine-Diab B, et al. HIV reservoir size and persistence are driven by T cell survival and homeostatic proliferation. *Nat Med*. 2009;15: 893. doi:10.1038/NM.1972
67. Ndung'u T, McCune JM, Deeks SG. Why and where an HIV cure is needed and how it might be achieved. *Nature*. 2019;576: 397–405. doi:10.1038/s41586-019-1841-8
68. Bailon L, Mothe B, Berman L, Brander C. Novel Approaches Towards a Functional Cure of HIV/AIDS. *Drugs*. 2020. pp. 859–868. doi:10.1007/s40265-020-01322-y
69. Mothe B, Ibarondo J, Llano A, Brander C. Virological, immune and host genetics markers in the control of HIV infection. *Dis Markers*. 2009;27: 105–20. doi:10.3233/DMA-2009-0655
70. Sáez-Cirión A, Pancino G. HIV Controllers: A Genetically Determined Or Inducible Phenotype? *Immunol Rev*. 2013;254: 281–294. doi:10.1111/imr.12076
71. Woldemeskel BA, Kwaa AK, Blankson JN. Viral reservoirs in elite controllers of HIV-1 infection: Implications for HIV cure strategies-NC-ND license (<http://creativecommons.org/licenses/by-nc-nd/4.0/>). *EBioMedicine*. 2020;62: 103118. doi:10.1016/j.ebiom.2020.103118
72. Kawashima Y, Pfafferott K, Frater J, Matthews P, Payne R, Addo M, et al.

Bibliography

- Adaptation of HIV-1 to human leukocyte antigen class I. *Nature*. 2009;458: 641–5. doi:10.1038/nature07746
73. IPD-IMGT/HLA Database. [cited 14 Oct 2021]. Available: <https://www.ebi.ac.uk/ipd/imgt/hla/about/statistics/>
74. Pereyra F, Jia X, McLaren PJ, Telenti A, de Bakker PIWW, Walker BD, et al. The Major Genetic Determinants of HIV-1 Control Affect HLA Class I Peptide Presentation. *Science* (80-). 2010;330: 1551–1557. doi:10.1126/science.1195271
75. Oriol-Tordera B, Llano A, Ganoza C, Cate S, Hildebrand W, Sanchez J, et al. Impact of HLA-DRB1 allele polymorphisms on control of HIV infection in a Peruvian MSM cohort. *HLA*. 2017;90: 234–237. doi:10.1111/tan.13085
76. Olvera A, Pérez-Álvarez S, Ibarondo J, Ganoza C, Lama JR, Lucchetti A, et al. The HLA-C*04: 01/KIR2DS4 gene combination and human leukocyte antigen alleles with high population frequency drive rate of HIV disease progression. *AIDS*. 2015;29: 507–17. doi:10.1097/QAD.0000000000000574
77. Arellano ER de, Díez-Fuertes F, Aguilar F, Tarazona HE de la T, Sánchez-Lara S, Lao Y, et al. Novel association of five HLA alleles with HIV-1 progression in Spanish long-term non progressor patients. *PLoS One*. 2019;14. doi:10.1371/JOURNAL.PONE.0220459
78. Zuñiga R, Lucchetti A, Galvan P, Sanchez S, Sanchez C, Hernandez A, et al. Relative dominance of Gag p24-specific cytotoxic T lymphocytes is associated with human immunodeficiency virus control. *J Virol*. 2006;80: 3122–5. doi:10.1128/JVI.80.6.3122-3125.2006
79. Berger CT, Frahm N, Price DA, Mothe B, Ghebremichael M, Hartman KL, et al. High-Functional-Avidity Cytotoxic T Lymphocyte Responses to HLA-B-Restricted Gag-Derived Epitopes Associated with Relative HIV Control. *J Virol*. 2011;85: 9334–9345. doi:10.1128/JVI.00460-11
80. Mothe B, Llano A, Ibarondo J, Daniels M, Miranda C, Zamarreño J, et al. Definition of the viral targets of protective HIV-1-specific T cell responses. *J Transl Med*. 2011;9: 208. doi:10.1186/1479-5876-9-208
81. Pereyra F, Heckerman D, Carlson JM, Kadie C, Soghoian DZ, Karel D, et al. HIV Control Is Mediated in Part by CD8+ T-Cell Targeting of Specific Epitopes. *J Virol*.

- 2014;88: 12937–12948. doi:10.1128/JVI.01004-14
82. Noyan K, Nguyen S, Betts MR, Sönnnerborg A, Buggert M. Human Immunodeficiency Virus Type-1 Elite Controllers Maintain Low Co-Expression of Inhibitory Receptors on CD4+ T Cells. *Front Immunol.* 2018;9: 19. doi:10.3389/FIMMU.2018.00019
 83. Rosás-Umbert M, Llano A, Bellido R, Olvera A, Ruiz-Riol M, Rocafort M, et al. Mechanisms of Abrupt Loss of Virus Control in a Cohort of Previous HIV Controllers. Kirchhoff F, editor. *J Virol.* 2019;93: e01436-18. doi:10.1128/JVI.01436-18
 84. Rutishauser RL, Deguit CDT, Hiatt J, Blaeschke F, Roth TL, Wang L, et al. TCF-1 regulates HIV-specific CD8+ T cell expansion capacity. *JCI Insight.* 2021;6. doi:10.1172/JCI.INSIGHT.136648
 85. Abdel-Mohsen M, Raposo RAS, Deng X, Li M, Liegler T, Sinclair E, et al. Expression profile of host restriction factors in HIV-1 elite controllers. *Retrovirology* 2013 101. 2013;10: 1–13. doi:10.1186/1742-4690-10-106
 86. Riveira-Muñoz E, Ruiz A, Pauls E, Permanyer M, Badia R, Mothe B, et al. Increased expression of SAMHD1 in a subset of HIV-1 elite controllers. *J Antimicrob Chemother.* 2014;69: 3057–60. doi:10.1093/jac/dku276
 87. Sáez-Cirión A, Bacchus C, Hocqueloux L, Avettand-Fenoel V, Girault I, Lecuroux C, et al. Post-Treatment HIV-1 Controllers with a Long-Term Virological Remission after the Interruption of Early Initiated Antiretroviral Therapy ANRS VISCONTI Study. *PLoS Pathog.* 2013;9. doi:10.1371/journal.ppat.1003211
 88. Namazi G, Fajnzylber JM, Aga E, Bosch RJ, Acosta EP, Sharaf R, et al. The Control of HIV After Antiretroviral Medication Pause (CHAMP) Study: Posttreatment Controllers Identified From 14 Clinical Studies. *J Infect Dis.* 2018;218: 1954–1963. doi:10.1093/infdis/jiy479
 89. Ananworanich J, Dubé K, Chomont N. How does the timing of antiretroviral therapy initiation in acute infection affect HIV reservoirs? *Curr Opin HIV AIDS.* 2015;10: 18–28. doi:10.1097/COH.000000000000122
 90. Gupta RK, Peppas D, Hill AL, Gálvez C, Salgado M, Pace M, et al. Evidence for HIV-1 cure after CCR5Δ32/Δ32 allogeneic haemopoietic stem-cell transplantation 30

Bibliography

- months post analytical treatment interruption: a case report. *Lancet HIV*. 2020;7: e340–e347. doi:10.1016/S2352-3018(20)30069-2
91. Hütter G, Nowak D, Mossner M, Ganepola S, Müßig A, Allers K, et al. Long-Term Control of HIV by CCR5 Delta32/Delta32 Stem-Cell Transplantation. <http://dx.doi.org/101056/NEJMoa0802905>. 2009;360: 692–698. doi:10.1056/NEJMOA0802905
 92. Létourneau S, Im E-J, Mashishi T, Brereton C, Bridgeman A, Yang H, et al. Design and pre-clinical evaluation of a universal HIV-1 vaccine. Nixon D, editor. *PLoS One*. 2007;2: e984. doi:10.1371/journal.pone.0000984
 93. Hu X, Lu Z, Valentin A, Rosati M, Broderick KE, Sardesai NY, et al. Gag and env conserved element CE DNA vaccines elicit broad cytotoxic T cell responses targeting subdominant epitopes of HIV and SIV Able to recognize virus-infected cells in macaques. *Hum Vaccin Immunother*. 2018;14: 2163–2177. doi:10.1080/21645515.2018.1489949
 94. Mothe B, Rosás-Umbert M, Coll P, Manzardo C, Puertas MC, Morón-López S, et al. HIVconsv Vaccines and Romidepsin in Early-Treated HIV-1-Infected Individuals: Safety, Immunogenicity and Effect on the Viral Reservoir (Study BCN02). *Front Immunol*. 2020;11: 823. doi:10.3389/fimmu.2020.00823
 95. Mothe B, Manzardo C, Sanchez-Bernabeu A, Coll P, Morón-López S, Puertas MC, et al. Therapeutic Vaccination Refocuses T-cell Responses Towards Conserved Regions of HIV-1 in Early Treated Individuals (BCN 01 study). *EClinicalMedicine*. 2019;11: 65–80. doi:10.1016/j.eclinm.2019.05.009
 96. Létourneau S, Im E-J, Mashishi T, Brereton C, Bridgeman A, Yang H, et al. Design and Pre-Clinical Evaluation of a Universal HIV-1 Vaccine. *PLoS One*. 2007;2: e984. doi:10.1371/JOURNAL.PONE.0000984
 97. Colby DJ, Sarnecki M, Barouch DH, Tipsuk S, Stieh DJ, Kroon E, et al. Safety and immunogenicity of Ad26 and MVA vaccines in acutely treated HIV and effect on viral rebound after antiretroviral therapy interruption. *Nat Med* 2020 264. 2020;26: 498–501. doi:10.1038/s41591-020-0774-y
 98. Mothe B, Brander C. Small steps forward for HIV vaccine development. *Nat Med* 2020 264. 2020;26: 466–467. doi:10.1038/s41591-020-0837-0

99. Mothe B, Hu X, Llano A, Rosati M, Olvera A, Kulkarni V, et al. A human immune data-informed vaccine concept elicits strong and broad T-cell specificities associated with HIV-1 control in mice and macaques. *J Transl Med.* 2015;13: 60. doi:10.1186/s12967-015-0392-5
100. Kiepiela P, Ngumbela K, Thobakgale C, Ramduth D, Honeyborne I, Moodley E, et al. CD8+ T-cell responses to different HIV proteins have discordant associations with viral load. *Nat Med.* 2007;13: 46–53. doi:10.1038/nm1520
101. Bailon L, Llano A, Cedeño S, Lopez MB, Alarcon Y, Coll P, et al. A placebo-controlled trial of HTI vaccines in early treated HIV infection. CROI Conference. 2021. Available: <https://www.croiconference.org/abstract/a-placebo-controlled-trial-of-hti-vaccines-in-early-treated-hiv-infection/>
102. Gay CL, Bosch RJ, Ritz J, Hataye JM, Aga E, Tressler RL, et al. Clinical Trial of the Anti-PD-L1 Antibody BMS-936559 in HIV-1 Infected Participants on Suppressive Antiretroviral Therapy. *J Infect Dis.* 2017;215: 1725–1733. doi:10.1093/infdis/jix191
103. Martinsen JT, Gunst JD, Højen JF, Tolstrup M, Søgaard OS. The Use of Toll-Like Receptor Agonists in HIV-1 Cure Strategies. *Front Immunol.* 2020;11: 1112. doi:10.3389/fimmu.2020.01112
104. Rerks-Ngarm S, Pitisuttithum P, Nitayaphan S, Kaewkungwal J, Chiu J, Paris R, et al. Vaccination with ALVAC and AIDSVAX to Prevent HIV-1 Infection in Thailand. <http://dx.doi.org/101056/NEJMoa0908492>. 2009;361: 2209–2220. doi:10.1056/NEJMOA0908492
105. Fourati S, Ribeiro SP, Blasco Tavares Pereira Lopes F, Talla A, Lefebvre F, Cameron M, et al. Integrated systems approach defines the antiviral pathways conferring protection by the RV144 HIV vaccine. *Nat Commun.* 2019;10: 863. doi:10.1038/s41467-019-08854-2
106. del Moral-Sánchez I, Sliепен K. Strategies for inducing effective neutralizing antibody responses against HIV-1. *Expert Review of Vaccines.* Taylor and Francis Ltd; 2019. pp. 1127–1143. doi:10.1080/14760584.2019.1690458
107. Deeks SG. Shock and kill. *Nature.* 2012;487: 439–440. doi:10.1038/487439a
108. Kim Y, Anderson JL, Lewin SR. Getting the “Kill” into “Shock and Kill”: Strategies

Bibliography

- to Eliminate Latent HIV. *Cell Host and Microbe*. Cell Press; 2018. pp. 14–26. doi:10.1016/j.chom.2017.12.004
109. Abner E, Jordan A. HIV “shock and kill” therapy: In need of revision. *Antiviral Res.* 2019;166: 19–34. doi:10.1016/j.antiviral.2019.03.008
110. Delagrèverie HM, Delaugerre C, Lewin SR, Deeks SG, Li JZ. Ongoing Clinical Trials of Human Immunodeficiency Virus Latency-Reversing and Immunomodulatory Agents. *Open Forum Infect Dis.* 2016;3. doi:10.1093/ofid/ofw189
111. Søgaaard OS, Graversen ME, Leth S, Olesen R, Brinkmann CR, Nissen SK, et al. The Depsipeptide Romidepsin Reverses HIV-1 Latency In Vivo. Siliciano RF, editor. *PLOS Pathog.* 2015;11: e1005142. doi:10.1371/journal.ppat.1005142
112. Archin NM, Liberty AL, Kashuba AD, Choudhary SK, Kuruc JD, Crooks AM, et al. Administration of vorinostat disrupts HIV-1 latency in patients on antiretroviral therapy. *Nature.* 2012;487: 482–5. doi:10.1038/nature11286
113. Rasmussen TA, Tolstrup M, Brinkmann CR, Olesen R, Erikstrup C, Solomon A, et al. Panobinostat, a histone deacetylase inhibitor, for latent-virus reactivation in HIV-infected patients on suppressive antiretroviral therapy: a phase 1/2, single group, clinical trial. *lancet HIV.* 2014;1: e13-21. doi:10.1016/S2352-3018(14)70014-1
114. Leth S, Schleimann MH, Nissen SK, Højen JF, Olesen R, Graversen ME, et al. Combined effect of Vacc-4x, recombinant human granulocyte macrophage colony-stimulating factor vaccination, and romidepsin on the HIV-1 reservoir (REDUC): a single-arm, phase 1B/2A trial. *Lancet HIV.* 2016;3: e463–e472. doi:10.1016/S2352-3018(16)30055-8
115. Fidler S, Stöhr W, Pace M, Dorrell L, Lever A, Pett S, et al. Antiretroviral therapy alone versus antiretroviral therapy with a kick and kill approach, on measures of the HIV reservoir in participants with recent HIV infection (the RIVER trial): a phase 2, randomised trial. *Lancet.* 2020;395: 888–898. doi:10.1016/S0140-6736(19)32990-3
116. Elsheikh MM, Tang Y, Li D, Jiang G. Deep latency: A new insight into a functional HIV cure. *EBioMedicine.* 2019;45: 624–629. doi:10.1016/j.ebiom.2019.06.020
117. Sun Y V, Hu Y-J. Integrative Analysis of Multi-omics Data for Discovery and

- Functional Studies of Complex Human Diseases. *Adv Genet.* 2016;93: 147–90. doi:10.1016/bs.adgen.2015.11.004
118. Poetz O, Schwenk JM, Kramer S, Stoll D, Templin MF, Joos TO. Protein microarrays: catching the proteome. *Mech Ageing Dev.* 2005;126: 161–70. doi:10.1016/j.mad.2004.09.030
119. Gonzalo Sanz R, Sánchez-Pla A. Statistical Analysis of Microarray Data. Bolón-Canedo V, Alonso-Betanzos A, editors. *Methods Mol Biol.* 2019;1986: 87–121. doi:10.1007/978-1-4939-9442-7_5
120. Schulze A, Downward J. Navigating gene expression using microarrays - A technology review. *Nat Cell Biol.* 2001;3. doi:10.1038/35087138
121. Eyster KM. Protocol for DNA Microarrays on Glass Slides. *Methods Mol Biol.* 2019;1986: 17–33. doi:10.1007/978-1-4939-9442-7_2
122. Ritchie ME, Phipson B, Wu D, Hu Y, Law CW, Shi W, et al. limma powers differential expression analyses for RNA-sequencing and microarray studies. *Nucleic Acids Res.* 2015;43: e47. doi:10.1093/nar/gkv007
123. Smyth GK, Ritchie M, Thorne N, Wettenhall J, Shi W, Hu Y. limma: Linear Models for Microarray and RNA-Seq Data User's Guide.
124. Bibikova M, Barnes B, Tsan C, Ho V, Klotzle B, Le JM, et al. High density DNA methylation array with single CpG site resolution. *Genomics.* 2011;98: 288–295. doi:10.1016/J.YGENO.2011.07.007
125. Aryee MJ, Jaffe AE, Corrada-Bravo H, Ladd-Acosta C, Feinberg AP, Hansen KD, et al. Minfi: a flexible and comprehensive Bioconductor package for the analysis of Infinium DNA methylation microarrays. *Bioinformatics.* 2014;30: 1363–1369. doi:10.1093/bioinformatics/btu049
126. Sutandy FXR, Qian J, Chen C, Zhu H. Overview of Protein Microarrays. *Curr Protoc Protein Sci.* 2013;72: 2711. doi:10.1002/0471140864.PS2701S72
127. Assarsson E, Lundberg M, Holmquist G, Björkesten J, Thorsen SB, Ekman D, et al. Homogenous 96-Plex PEA Immunoassay Exhibiting High Sensitivity, Specificity, and Excellent Scalability. *PLoS One.* 2014;9: e95192. doi:10.1371/JOURNAL.PONE.0095192
128. Filbin MR, Mehta A, Schneider AM, Kays KR, Guess JR, Gentili M, et al. Longitudinal

Bibliography

- proteomic analysis of severe COVID-19 reveals survival-associated signatures, tissue-specific cell death, and cell-cell interactions. *Cell reports Med.* 2021;2: 100287. doi:10.1016/j.xcrm.2021.100287
129. Bhardwaj M, Terzer T, Schrotz-King P, Brenner H. Comparison of Proteomic Technologies for Blood-Based Detection of Colorectal Cancer. *Int J Mol Sci* 2021, Vol 22, Page 1189. 2021;22: 1189. doi:10.3390/IJMS22031189
130. Ruiz-Riol M, Berdnik D, Llano A, Mothe B, Gálvez C, Pérez-Álvarez S, et al. Identification of Interleukin-27 (IL-27)/IL-27 Receptor Subunit Alpha as a Critical Immune Axis for In Vivo HIV Control. *J Virol.* 2017;91: JVI.00441-17. doi:10.1128/JVI.00441-17
131. Ray S, Britschgi M, Herbert C, Takeda-Uchimura Y, Boxer A, Blennow K, et al. Classification and prediction of clinical Alzheimer's diagnosis based on plasma signaling proteins. *Nat Med.* 2007;13: 1359–62. doi:10.1038/nm1653
132. Wang Z, Gerstein M, Snyder M. RNA-Seq: a revolutionary tool for transcriptomics. *Nat Rev Genet.* 2009;10: 57. doi:10.1038/NRG2484
133. Lowe R, Shirley N, Bleackley M, Dolan S, Shafee T. Transcriptomics technologies. *PLOS Comput Biol.* 2017;13: e1005457. doi:10.1371/JOURNAL.PCBI.1005457
134. Berge K Van den, Hembach KM, Sonesson C, Tiberi S, Clement L, Love MI, et al. RNA Sequencing Data: Hitchhiker's Guide to Expression Analysis. <https://doi.org/10.1146/annurev-biodatasci-072018-021255>. 2019;2: 139–173. doi:10.1146/ANNUREV-BIODATASCI-072018-021255
135. Leek JT, Scharpf RB, Bravo HC, Simcha D, Langmead B, Johnson WE, et al. Tackling the widespread and critical impact of batch effects in high-throughput data. *Nat Rev Genet* 2010 1110. 2010;11: 733–739. doi:10.1038/nrg2825
136. Morris TJ, Butcher LM, Feber A, Teschendorff AE, Chakravarthy AR, Wojdacz TK, et al. ChAMP: 450k Chip Analysis Methylation Pipeline. *Bioinformatics.* 2014;30: 428–430. doi:10.1093/bioinformatics/btt684
137. Ruiz-Riol M, Berdnik D, Llano A, Mothe B, Gálvez C, Pérez-Álvarez S, et al. Identification of IL-27/IL-27RA as a critical immune axis for in vivo HIV control. *J Virol.* 2017; JVI.00441-17. doi:10.1128/JVI.00441-17
138. Robinson MD, McCarthy DJ, Smyth GK. edgeR: A Bioconductor package for

- differential expression analysis of digital gene expression data. *Bioinformatics*. 2009;26: 139–140. doi:10.1093/bioinformatics/btp616
139. Love MI, Huber W, Anders S. Moderated estimation of fold change and dispersion for RNA-seq data with DESeq2. *Genome Biol* 2014 1512. 2014;15: 1–21. doi:10.1186/S13059-014-0550-8
140. Reimand J, Isserlin R, Voisin V, Kucera M, Tannus-Lopes C, Rostamianfar A, et al. Pathway enrichment analysis and visualization of omics data using g:Profiler, GSEA, Cytoscape and EnrichmentMap. *Nat Protoc*. 2019;14: 482–517. doi:10.1038/s41596-018-0103-9
141. Adam L, Rosenbaum P, Bonduelle O, Combadière B. Strategies for immunomonitoring after vaccination and during infection. *Vaccines*. *Vaccines* (Basel); 2021. doi:10.3390/vaccines9040365
142. Rohart F, Gautier B, Singh A, Lê Cao K-A. mixOmics: An R package for 'omics feature selection and multiple data integration. Schneidman D, editor. *PLoS Comput Biol*. 2017;13: e1005752. doi:10.1371/journal.pcbi.1005752
143. Slawski M, Daumer M, Boulesteix A-L. CMA: a comprehensive Bioconductor package for supervised classification with high dimensional data. *BMC Bioinformatics*. 2008;9: 439. doi:10.1186/1471-2105-9-439
144. Hastie T, Tibshirani R, Friedman J. *The Elements of Statistical Learning*. 2009 [cited 26 Jul 2021]. doi:10.1007/978-0-387-84858-7
145. Kuhn M, Wing J, Weston S, Williams A, Keefer C, Engelhardt A, et al. Package "caret" Title Classification and Regression Training. 2021. Available: <https://cran.r-project.org/web/packages/caret/caret.pdf>
146. Cavill R, Jennen D, Kleinjans J, Briedé JJ. Transcriptomic and metabolomic data integration. *Brief Bioinform*. 2016;17: 891–901. doi:10.1093/BIB/BBV090
147. Singh A, Shannon CP, Gautier B, Rohart F, Vacher M, Tebbutt SJ, et al. DIABLO: an integrative approach for identifying key molecular drivers from multi-omics assays. *Bioinformatics*. 2019;35: 3055–3062. doi:10.1093/bioinformatics/bty1054
148. López de Maturana E, Alonso L, Alarcón P, Martín-Antoniano IA, Pineda S, Piorno L, et al. Challenges in the Integration of Omics and Non-Omics Data. *Genes* (Basel).

Bibliography

- 2019;10. doi:10.3390/genes10030238
149. Pulendran B, Davis MM. The science and medicine of human immunology. *Science* (80-). 2020;369. doi:10.1126/SCIENCE.AAY4014
 150. Reichmann MT, Tezera LB, Vallejo AF, Vukmirovic M, Xiao R, Reynolds J, et al. Integrated transcriptomic analysis of human tuberculosis granulomas and a biomimetic model identifies therapeutic targets. *J Clin Invest*. 2021;131. doi:10.1172/JCI148136
 151. Oh JZ, Ravindran R, Chassaing B, Carvalho FA, Maddur MS, Bower M, et al. TLR5-mediated sensing of gut microbiota is necessary for antibody responses to seasonal influenza vaccination. *Immunity*. 2014;41: 478–492. doi:10.1016/j.immuni.2014.08.009
 152. Salgado M, López-Romero P, Callejas S, López M, Labarga P, Dopazo A, et al. Characterization of host genetic expression patterns in HIV-infected individuals with divergent disease progression. *Virology*. 2011;411: 103–112. doi:10.1016/J.VIROL.2010.12.037
 153. Díez-Fuertes F, De La Torre-Tarazona HE, Calonge E, Pernas M, Alonso-Socas MDM, Capa L, et al. Transcriptome Sequencing of Peripheral Blood Mononuclear Cells from Elite Controller-Long Term Non Progressors. *Sci Rep*. 2019;9: 14265. doi:10.1038/s41598-019-50642-x
 154. Zhang W, Ambikan AT, Sperk M, van Domselaar R, Nowak P, Noyan K, et al. Transcriptomics and Targeted Proteomics Analysis to Gain Insights Into the Immune-control Mechanisms of HIV-1 Infected Elite Controllers. *EBioMedicine*. 2018;27: 40–50. doi:10.1016/j.ebiom.2017.11.031
 155. Gaucher D, Therrien R, Kettaf N, Angermann BR, Boucher G, Filali-Mouhim A, et al. Yellow fever vaccine induces integrated multilineage and polyfunctional immune responses. *J Exp Med*. 2008;205: 3119–3131. doi:10.1084/JEM.20082292
 156. Querec TD, Akondy RS, Lee EK, Cao W, Nakaya HI, Teuwen D, et al. Systems biology approach predicts immunogenicity of the yellow fever vaccine in humans. *Nat Immunol* 2008 101. 2008;10: 116–125. doi:10.1038/ni.1688
 157. Ovsyannikova IG, Salk HM, Kennedy RB, Haralambieva IH, Zimmermann MT, Grill

- DE, et al. Gene signatures associated with adaptive humoral immunity following seasonal influenza A/H1N1 vaccination. *Genes Immun* 2016 177. 2016;17: 371–379. doi:10.1038/gene.2016.34
158. Gonçalves E, Bonduelle O, Soria A, Loulergue P, Rousseau A, Cachanado M, et al. Innate gene signature distinguishes humoral versus cytotoxic responses to influenza vaccination. *J Clin Invest*. 2019;129: 1960–1971. doi:10.1172/JCI125372
159. Kazmin D, Nakaya HI, Lee EK, Johnson MJ, van der Most R, van den Berg RA, et al. Systems analysis of protective immune responses to RTS,S malaria vaccination in humans. *Proc Natl Acad Sci U S A*. 2017;114: 2425–2430. doi:10.1073/pnas.1621489114
160. Anderson J, Olafsdottir TA, Kratochvil S, McKay PF, Östensson M, Persson J, et al. Molecular Signatures of a TLR4 Agonist-Adjuvanted HIV-1 Vaccine Candidate in Humans. *Front Immunol*. 2018;9: 301. doi:10.3389/fimmu.2018.00301
161. Fourati S, Ribeiro SP, Lopes FBTP, Talla A, Lefebvre F, Cameron M, et al. Integrated systems approach defines the antiviral pathways conferring protection by the RV144 HIV vaccine. *Nat Commun* 2019 101. 2019;10: 1–12. doi:10.1038/s41467-019-08854-2
162. Sanchez J, Gonçalves E, Llano A, Gonzáles P, Fernández-Maldonado M, Vogt A, et al. Immune Profiles Identification by Vaccinomics After MVA Immunization in Randomized Clinical Study. *Front Immunol*. 2020;11: 586124. doi:10.3389/fimmu.2020.586124
163. Gonçalves E, Guillén Y, Lama JR, Sanchez J, Brander C, Paredes R, et al. Host Transcriptome and Microbiota Signatures Prior to Immunization Profile Vaccine Humoral Responsiveness. *Front Immunol*. 2021;0: 1552. doi:10.3389/FIMMU.2021.657162
164. Berdasco M, Esteller M. Clinical epigenetics: seizing opportunities for translation. *Nat Rev Genet*. 2019;20: 109–127. doi:10.1038/s41576-018-0074-2
165. Portela A, Esteller M. Epigenetic modifications and human disease. *Nat Biotechnol*. 2010;28: 1057–1068. doi:10.1038/nbt.1685
166. Hofmeister BT, Lee K, Rohr NA, Hall DW, Schmitz RJ. Stable inheritance of DNA methylation allows creation of epigenotype maps and the study of epiallele

- inheritance patterns in the absence of genetic variation. *Genome Biol.* 2017;18: 155. doi:10.1186/s13059-017-1288-x
167. Gallego-Paüls M, Hernández-Ferrer C, Bustamante M, Basagaña X, Barrera-Gómez J, Lau C-HE, et al. Variability of multi-omics profiles in a population-based child cohort. *BMC Med* 2021 191. 2021;19: 1–16. doi:10.1186/S12916-021-02027-Z
168. Suarez-Alvarez B, Rodriguez RM, Fraga MF, López-Larrea C. DNA methylation: a promising landscape for immune system-related diseases. *Trends Genet.* 2012;28: 506–514. doi:10.1016/J.TIG.2012.06.005
169. Fang J-Y, Mikovits JA, Bagni R, Petrow-Sadowski CL, Ruscetti FW. Infection of Lymphoid Cells by Integration-Defective Human Immunodeficiency Virus Type 1 Increases De Novo Methylation. *J Virol.* 2001;75: 9753–9761. doi:10.1128/jvi.75.20.9753-9761.2001
170. Youngblood B, Reich NO. The early expressed HIV-1 genes regulate DNMT1 expression. *Epigenetics.* 2008;3: 149–56. doi:10.4161/epi.3.3.6372
171. Luzzi A, Morettini F, Gazaneo S, Mundo L, Onnis A, Mannucci S, et al. HIV-1 Tat induces DNMT over-expression through microRNA dysregulation in HIV-related non Hodgkin lymphomas. *Infect Agent Cancer.* 2014;9. doi:10.1186/1750-9378-9-41
172. Zhang X, Justice AC, Hu Y, Wang Z, Zhao H, Wang G, et al. Epigenome-wide differential DNA methylation between HIV-infected and uninfected individuals. *Epigenetics.* 2016;11: 750–760. doi:10.1080/15592294.2016.1221569
173. Shu C, Justice AC, Zhang X, Marconi VC, Hancock DB, Johnson EO, et al. DNA methylation biomarker selected by an ensemble machine learning approach predicts mortality risk in an HIV-positive veteran population. *Epigenetics.* 2021;16: 741–753. doi:10.1080/15592294.2020.1824097
174. Gross AM, Jaeger PA, Kreisberg JF, Licon K, Jepsen KL, Khosroheidari M, et al. Methylome-wide Analysis of Chronic HIV Infection Reveals Five-Year Increase in Biological Age and Epigenetic Targeting of HLA. *Mol Cell.* 2016;62: 157–168. doi:10.1016/j.molcel.2016.03.019
175. Zhang Y, Li S-K, Yi Yang K, Liu M, Lee N, Tang X, et al. Whole genome methylation

- array reveals the down-regulation of IGFBP6 and SATB2 by HIV-1. *Sci Rep.* 2015;5: 10806. doi:10.1038/srep10806
176. Zimmermann MT, Oberg AL, Grill DE, Ovsyannikova IG, Haralambieva IH, Kennedy RB, et al. System-wide associations between DNA-methylation, gene expression, and humoral immune response to influenza vaccination. *PLoS One.* 2016;11: e0152034. doi:10.1371/journal.pone.0152034
177. Das J, Verma D, Gustafsson M, Lerm M. Identification of DNA methylation patterns predisposing for an efficient response to BCG vaccination in healthy BCG-naïve subjects. <https://doi.org/10.1080/1559229420191603963>. 2019;14: 589–601. doi:10.1080/15592294.2019.1603963
178. Ewing E, Kular L, Fernandes SJ, Karathanasis N, Lagani V, Ruhrmann S, et al. Combining evidence from four immune cell types identifies DNA methylation patterns that implicate functionally distinct pathways during Multiple Sclerosis progression. *EBioMedicine.* 2019;43: 411–423. doi:10.1016/J.EBIOM.2019.04.042
179. Sandstrom TS, Ranganath N, Angel JB. Impairment of the type I interferon response by HIV-1: Potential targets for HIV eradication. *Cytokine Growth Factor Rev.* 2017;37: 1–16. doi:10.1016/j.cytogfr.2017.04.004
180. Imgenberg-Kreuz J, Sandling JK, Almlöf JC, Nordlund J, Signér L, Norheim KB, et al. Genome-wide DNA methylation analysis in multiple tissues in primary Sjögren's syndrome reveals regulatory effects at interferon-induced genes. *Ann Rheum Dis.* 2016;75: 2029–2036. doi:10.1136/annrheumdis-2015-208659
181. Absher DM, Li X, Waite LL, Gibson A, Roberts K, Edberg J, et al. Genome-Wide DNA Methylation Analysis of Systemic Lupus Erythematosus Reveals Persistent Hypomethylation of Interferon Genes and Compositional Changes to CD4+ T-cell Populations. *PLoS Genet.* 2013;9: 1003678. doi:10.1371/JOURNAL.PGEN.1003678
182. Corley MJ, Pang APS, Dody K, Mudd PA, Patterson BK, Seethamraju H, et al. Genome-wide DNA methylation profiling of peripheral blood reveals an epigenetic signature associated with severe COVID-19. *J Leukoc Biol.* 2021;110: 21–26. doi:10.1002/JLB.5HI0720-466R

Bibliography

183. Castro de Moura M, Davalos V, Planas-Serra L, Alvarez-Errico D, Arribas C, Ruiz M, et al. Epigenome-wide association study of COVID-19 severity with respiratory failure. *EBioMedicine*. 2021;66: 103339. doi:10.1016/j.ebiom.2021.103339
184. Fanucchi S, Domínguez-Andrés J, Joosten LAB, Netea MG, Mhlanga MM. The Intersection of Epigenetics and Metabolism in Trained Immunity. *Immunity*. 2021;54: 32–43. doi:10.1016/J.IMMUNI.2020.10.011
185. Calle-Fabregat C de la, Morante-Palacios O, Ballestar E. Understanding the Relevance of DNA Methylation Changes in Immune Differentiation and Disease. *Genes (Basel)*. 2020;11. doi:10.3390/GENES11010110
186. Schmidl C, Klug M, Boeld TJ, Andreesen R, Hoffmann P, Edinger M, et al. Lineage-specific DNA methylation in T cells correlates with histone methylation and enhancer activity. *Genome Res*. 2009;19: 1165. doi:10.1101/GR.091470.109
187. Doria M, Tomaselli S, Neri F, Ciafrè SA, Farace MG, Michienzi A, et al. ADAR2 editing enzyme is a novel human immunodeficiency virus-1 proviral factor. *J Gen Virol*. 2011;92: 1228–1232. doi:10.1099/vir.0.028043-0
188. Roadmap database E062 Collection. [cited 14 Oct 2021]. Available: https://egg2.wustl.edu/roadmap/data/byFileType/chromhmmSegmentations/ChmmModels/coreMarks/indivModels/default_init/E062/
189. Eltahir M, Fletcher E, Dynesius L, Jarblad JL, Lord M, Laurén I, et al. Profiling of donor-specific immune effector signatures in response to rituximab in a human whole blood loop assay using blood from CLL patients. *Int Immunopharmacol*. 2021;90: 107226. doi:10.1016/J.INTIMP.2020.107226
190. Berbers R-M, Drylewicz J, Ellerbroek PM, van Montfrans JM, Dalm VASH, van Hagen PM, et al. Targeted Proteomics Reveals Inflammatory Pathways that Classify Immune Dysregulation in Common Variable Immunodeficiency. *J Clin Immunol* 2020 412. 2020;41: 362–373. doi:10.1007/S10875-020-00908-1
191. Twohig JP, Marsden M, Cuff SM, Ferdinand JR, Gallimore AM, Perks W V, et al. The death receptor 3/TL1A pathway is essential for efficient development of antiviral CD4⁺ and CD8⁺ T-cell immunity. *FASEB J*. 2012;26: 3575–86. doi:10.1096/fj.11-200618
192. Schreiber TH, Podack ER. Immunobiology of TNFSF15 and TNFRSF25. *Immunol*

- Res. 2013;57: 3–11. doi:10.1007/s12026-013-8465-0
193. Slebioda TJ, Rowley TF, Ferdinand JR, Willoughby JE, Buchan SL, Taraban VY, et al. Triggering of TNFRSF25 promotes CD8+ T-cell responses and anti-tumor immunity. *Eur J Immunol*. 2011;41: 2606–2611. doi:10.1002/EJL.201141477
194. Mavers M, Simonetta F, Nishikii H, Ribado J V., Maas-Bauer K, Alvarez M, et al. Activation of the DR3-TL1A Axis in Donor Mice Leads to Regulatory T Cell Expansion and Activation With Reduction in Graft-Versus-Host Disease. *Front Immunol*. 2019;0: 1624. doi:10.3389/FIMMU.2019.01624
195. Khan SQ, Tsai MS, Schreiber TH, Wolf D, Deyev V V, Podack ER. Cloning, expression, and functional characterization of TL1A-Ig. *J Immunol*. 2013;190: 1540–50. doi:10.4049/jimmunol.1201908
196. Wolf D, Barreras H, Bader CS, Copsel S, Lightbourn CO, Pfeiffer BJ, et al. Marked in Vivo Donor Regulatory T Cell Expansion via Interleukin-2 and TL1A-Ig Stimulation Ameliorates Graft-versus-Host Disease but Preserves Graft-versus-Leukemia in Recipients after Hematopoietic Stem Cell Transplantation. *Biol Blood Marrow Transplant*. 2017;23: 757–766. doi:10.1016/j.bbmt.2017.02.013
197. Ganguly S, Liu J, Pillai VB, Mittler RS, Amara RR. Adjuvantive effects of anti-4-1BB agonist Ab and 4-1BBL DNA for a HIV-1 Gag DNA vaccine: Different effects on cellular and humoral immunity. *Vaccine*. 2010;28: 1300–1309. doi:10.1016/J.VACCINE.2009.11.020
198. Liu J, Ngai N, Stone GW, Yue FY, Ostrowski MA. The adjuvancy of OX40 ligand (CD252) on an HIV-1 canarypox vaccine. *Vaccine*. 2009;27: 5077–5084. doi:10.1016/J.VACCINE.2009.06.046
199. Titus AJ, Gallimore RM, Salas LA, Christensen BC. Cell-type deconvolution from DNA methylation: a review of recent applications. *Hum Mol Genet*. 2017;26: R216–R224. doi:10.1093/HMG/DDX275
200. Jaffe AE, Irizarry RA. Accounting for cellular heterogeneity is critical in epigenome-wide association studies. *Genome Biol* 2014 152. 2014;15: 1–9. doi:10.1186/GB-2014-15-2-R31
201. Houseman EA, Accomando WP, Koestler DC, Christensen BC, Marsit CJ, Nelson HH, et al. DNA methylation arrays as surrogate measures of cell mixture

Bibliography

- distribution. *BMC Bioinformatics*. 2012;13: 86. doi:10.1186/1471-2105-13-86
202. Moron-Lopez S, Urrea V, Dalmau J, Lopez M, Puertas MC, Ouchi D, et al. The Genome-wide Methylation Profile of CD4+ T Cells From Individuals With Human Immunodeficiency Virus (HIV) Identifies Distinct Patterns Associated With Disease Progression. *Clin Infect Dis*. 2020 [cited 30 Apr 2021]. doi:10.1093/cid/ciaa1047
203. Corley MJ, Sacdalan C, Pang APS, Chomchey N, Ratnaratorn N, Valcour V, et al. Abrupt and altered cell-type specific DNA methylation profiles in blood during acute HIV infection persists despite prompt initiation of ART. *PLOS Pathog*. 2021;17: e1009785. doi:10.1371/JOURNAL.PPAT.1009785
204. Ruiz-Riol M, Brander C. Can we just kick-and-kill HIV: possible challenges posed by the epigenetically controlled interplay between HIV and host immunity. *Immunotherapy*. 2019;11: 931–935. doi:10.2217/imt-2019-0092
205. Julg B, Dee L, Ananworanich J, Barouch DH, Bar K, Caskey M, et al. Recommendations for analytical antiretroviral treatment interruptions in HIV research trials-report of a consensus meeting. *lancet HIV*. 2019;6: e259–e268. doi:10.1016/S2352-3018(19)30052-9
206. Quezada H, Guzmán-Ortiz AL, Díaz-Sánchez H, Valle-Rios R, Aguirre-Hernández J. Omics-based biomarkers: current status and potential use in the clinic. *Boletín Médico Del Hosp Infant México (English Ed)*. 2017;74: 219–226. doi:10.1016/J.BMHIME.2017.11.030